Expanding the Knowledge on Oocyst Molecules of *Toxoplasma gondii*

Inaugural-Dissertation to obtain the academic degree
Doctor rerum naturalium (Dr. rer. nat.)

submitted to the Department of Biology, Chemistry, Pharmacy of
Freie Universität Berlin

by

Benedikt Fabian

2021

The presented work was performed at the

Robert Koch-Institut in

Unit 16: Mycotic and Parasitic Agents and Mycobacteria

under the supervision of

Prof. Dr. Frank Seeber

and at Freie Universität Berlin

in the Department of Biology, Chemistry and Pharmacy

between August 2017 and November 2021

1st Reviewer:	Prof. Dr. Frank Seeber
2nd Reviewer:	Prof. Dr. Monika Hilker
Date of Defense:	February 28, 2022

Acid-fast lipids,
Fibrils of beta-glucan,
Dityrosine glows.

—Anonymous
Haiku of the oocyst wall

Table of contents

Abbreviations

°C	Degrees Celsius
(µ/m)M	(micro-/milli-) mole per liter
(k)Da	(kilo) Dalton
(m)Ab	(monoclonal) antibody
(q/RT-)PCR	(quantitative/Reverse transcriptase) Polymerase chain reaction
3D	Three-dimensional
A	absorbance
a. dest.	Distilled water
AEO	Agarose embedded oocysts
APAD	Acetylpyridine adenine dinucleotide
BLAST	Basic Local Alignment Search Tool
bp	Base pairs
BSA	Bovine serum albumin
CD	Circular dichroism
cDNA	(complementary) deoxyribonucleic acid
cGy	Centigray (absorbed dose of ionizing radiation)
CIDER	Classification of Intrinsically Disordered Ensemble Regions
CLR	C-type lectin receptor
cm	centimeters
CSA	Chicken serum albumin
Cy5	Indodicarbocyanine
CheZOD	Chemical shift Z-score for quantitative protein Order and Disorder assessment
d	Day(s)
DAPI	4′,6-diamidino-2-phenylindole
DMEM	Dulbecco‘s modified eagles medium
DMSO	Dimethyl sulfoxide
dNTP	Deoxyribonucleotide triphosphate

dpi	Days post infection
ECL	Enhanced chemiluminescence
EDC	1-ethyl-3-(3-dimethylaminopropyl)carbodiimide hydrochloride
EDTA	Ethylenediaminetetraacetate
ELISA	Enzyme-linked immunosorbent assay
EM	Electron microscopy
FAGLA	FA-glycyl-L-leucine amide
FITC	Fluorescein isothiocyanate
FPLC	Fast protein liquid chromatography
fwd	forward
g	Gravitational force equivalent (g-force)
GalNac	N-acetyl-galactosamine
GlcNac	N-acetyl-D-glucosamine
GPI	glycosylphosphatidylinositol
GRAVY	Grand average of hydropathy
h	Hour(s)
hFc	Constant region of human IgG1
hCD1	human calpastatin domain I
HEPES	4-(2-hydroxyethyl)-1-piperazineethanesulfonic acid
HFF	Human foreskin fibroblasts
IDP(R)	Intrinsically disordered protein (region)
IFA	Immunofluorescence assay
Ig(G/M/Y)	Immunoglobulin (G/M/Y)
IPTG	Isopropyl-β-D-thiogalacto-pyranoside
LB	lysogeny broth
(p/Tg)LDH(1)	(porcine/*T. gondii*) Lactate dehydrogenase (isoform 1)
LEA	Late embryogenesis abundant
MAT	Modified agglutination test
MFI	Median fluorescence intensity
min	Minute(s)

mm	millimeters
mol	Mole(s)
MPA	*Maclura pomifera* agglutinin
MPA-FITC	FITC conjugated MPA
MW	Molecular weight
NAD^+/NADH	Oxidized/reduced form of nicotinamide adenine dinucleotide
nm	nanometers
NMR	Nuclear magnetic resonance spectroscopy
$OD_{(600)}$	Optical density (at 600 nm)
P/S	Penicillin/streptomycin
PBMCs	Peripheral blood monocytes
PBS	Phosphate buffered saline
pH	Negative decimal logarithm of hydrogen ion concentration
pn	Personal notice
PO	(horseradish) peroxidase
PRR	Pattern recognition receptor
rev	reverse
RH	Denominator given to a type I strain of *T. gondii* that was initially isolated from a six year old boy, only known as R. H.
RIN	RNA integrity number
RKI	Robert Koch-Institut
(m)RNA	(messenger) ribonucleic acid
rpm	Revolutions per minute
RT	Room temperature
RTase	Reverse transcriptase
s	seconds
$SAG1_{(bio)}$	(biotinylated) Surface antigen 1
SDS-PAGE	Sodium dodecyl sulfate polyacrylamide gelelectrophoresis
SEC	Size exclusion chromatography

SLiCE	Seamless ligation cloning extract
SOC	Super optimal broth with catabolite repression
Sulfo-NHS	N-hydroxysulfosuccinimide
TAE	Tris-acetate-EDTA
Taq	*Thermus aquaticus*
TEDs	Transepithelial dendrites
TFE	Trifluoroethanol
Tg	*Toxoplasma gondii*
T_m	Melting temperature
TSA	Thermal shift assay
TTC	Triphenyl tetrazolium chloride
U	Units
UK	United Kingdom
US	United States
V	Volt(s)
v/v and w/v	Volume and weight per volume, respectively
VHH	Variable fragment of the heavy chain of a heavy chain-only antibody
WGA	Wheat germ agglutinin
WHO	World Health Organization

Chapter 1: Introduction

1.1 Toxoplasmosis

Toxoplasmosis, the disease caused by the obligate intracellular parasite *Toxoplasma gondii*, is a disease of high public health concern. Nearly a third of the world's population is infected by the parasite (Montoya and Liesenfeld, 2004). As of 2017, toxoplasmosis is among the three most relevant foodborne diseases in the European Union (EU). It is estimated that the disease is responsible for up to 17 % of all foodborne disease cases in the EU and *T. gondii* is considered to infect approx. one million people per year in the EU (WHO, 2017). The seroprevalence in individual countries is highly variable, however. The Netherlands, for example, report a low prevalence of *T. gondii* infections in the population (Hofhuis et al., 2011). Similarly, in France, where the seroprevalence among pregnant women used to be relatively high at 83 % in the 1960s, due to implementation of stricter prevention methods in recent years, these numbers continuously decreased to 37 % (Nogareda et al., 2014). In contrast, in Germany, infection numbers have consistently been higher than in both neighboring countries with around 50 % of the population being infected by the parasite (Wilking et al., 2016).

While infections with the parasite only seldom result in acute illness and mostly go unnoticed, certain groups of people are at great risk in the case of a *T. gondii* infection. Namely, patients with a weaker immune system, such as AIDS patients or organ transplant recipients, are more likely to develop severe cases of toxoplasmosis that could lead to damages of important tissues (Schmidt et al., 2013). Moreover, in pregnant women that do not have antibodies against *T. gondii* due to a previous infection, the unborn child could suffer lasting damages to the brain or the retina or an infection could even lead to death of the unborn child (Remington et al., 2011).

1.2 *Toxoplasma gondii*

1.2.1 The parasite's life cycle

T. gondii is a unicellular obligate intracellular apicomplexan parasite. Discovered in the early years of the 20th century (Nicolle and Manceaux, 1908), it wasn't until the late 1960s that the full lifecycle of the parasite was discovered. At that time it was already known that a form of *T. gondii* could be transmitted via ingestion of meat from infected animals. Surprisingly though, the parasite had also been found in herbivore animals and strictly vegetarian human populations, strongly suggesting a more complex life cycle. Only when Hutchison conducted infection experiments with cats, the oocyst stage as a result of sexual replication of *T. gondii* could be observed for the first time (Hutchison, 1965). Since then, the understanding of the parasite has greatly improved. *T. gondii* does not have a specific host species, rather it could be shown to infect virtually any warm-blooded animal and some publications even report infection of fish (Sanders et al., 2015; Marino et al., 2019; Yoshida et al., 2020). However, to

complete its life cycle, it is now well understood that *T. gondii* requires infection of the feline small intestine. Only there differentiation into so called merozoites is initiated which in turn differentiate into macro- and microgametes. These fuse to form what will later become the oocyst, *T. gondii's* environmental form. These oocysts are shed into the environment by an infected felid to the millions and could be shown to stay infective in the environment for up to two years. Since *T. gondii* exhibits no strict host specificity, these oocysts likely play an important role in the parasite's widespread distribution, as they can be dispersed in the environment via water, wind, or other means, stay viable for prolonged time and can infect many different intermediate and definite hosts (see Figure 1).

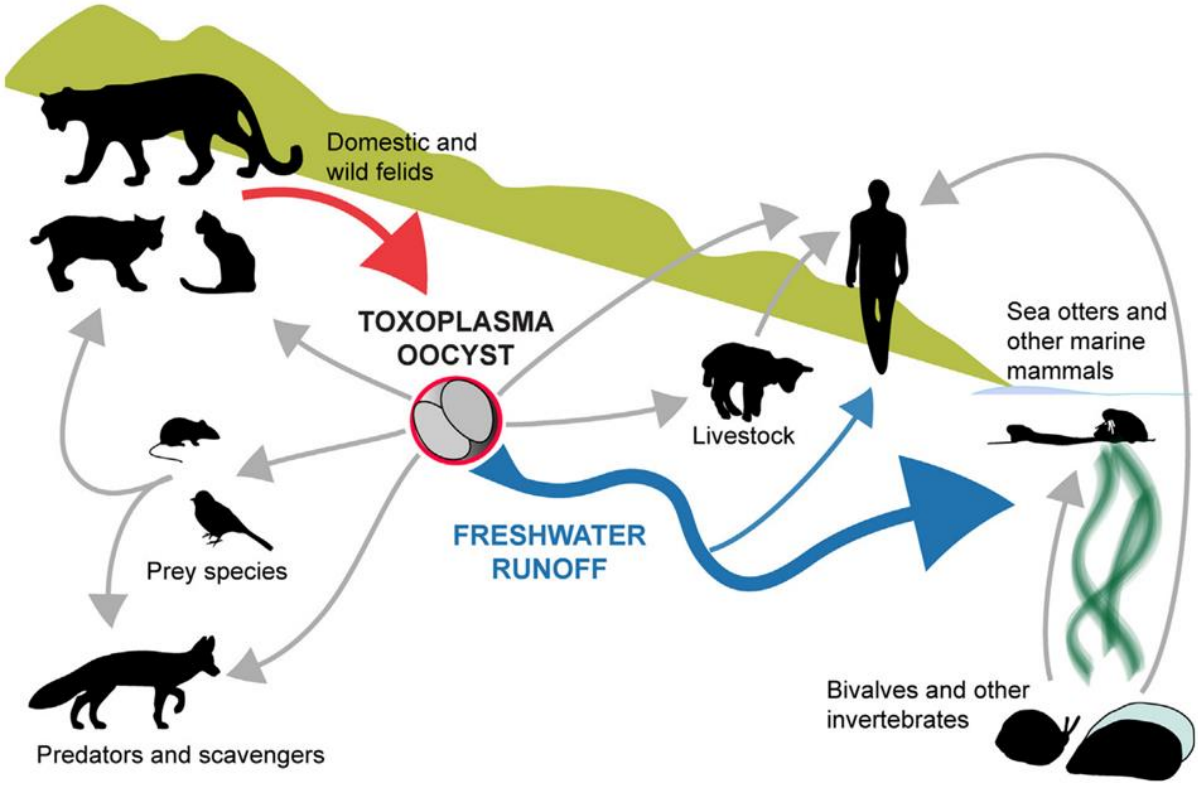

Figure 1: Life cycle of Toxoplasma gondii. The oocyst plays a vital role in the parasite's spread especially into other habitats but is vastly understudied. Adapted from VanWormer (VanWormer et al., 2013).

The oocyst harbors eight sporozoites. Upon ingestion by another felid or any other intermediate host, the sporozoites excyst once they passed the stomach and reach the intestine, although other possible ways for oocysts to enter the body, for example via the lung when inhaled, are being proposed (Freppel et al., 2016). Once excysted, the sporozoites start invading surrounding epithelial cells where they soon differentiate into the fast-replicating form, the tachyzoites (Delgado Betancourt et al., 2019). The tachyzoites allow the parasite to quickly disseminate throughout the body of its host until after some time they differentiate into the slow replicating and more dormant form, the bradyzoites. These bradyzoites form cysts in various tissues of the host, preferably in muscle or brain tissue or in the retinal tissue. However, cysts

have also been observed in other organs such as the liver, kidney or the heart, amongst others (Dubey, 2016). While the tachyzoites are somewhat easy for the hosts immune system to control, the host cannot really do anything against the bradyzoite cysts. These cysts allow *T. gondii* to chronically infect and persist within a host, increasing the chances of infecting a new host, when the current one is preyed upon. Then, the bradyzoites can revert to the tachyzoite stage and start infecting new surrounding tissue. Transmission of *T. gondii* to another intermediate host or a definitive host can occur vertically by transmission of tachyzoites from mother to offspring either via milk or in the placenta (Remington and Klein, 1983; Jackson and Hutchison, 1989). Horizontal transmission can occur either via ingestion of tissue cysts or via ingestion of oocysts (Dubey et al., 1996; Dubey, 2001; Dubey, 2006; Dubey, 2016).

1.2.2 The oocyst

Oocyst formation upon sexual reproduction is a key characteristic of all members of the subclass coccidia (Dubey, 1993; Lindsay and Todd, 1993). Therefore, a lot of knowledge on *T. gondii* oocysts is derived from studies on more readily available *Eimeria* and *Cryptosporidium* oocysts (Belli et al., 2006). Still, while the oocyst stage of *T. gondii's* is vital to its life cycle, it is vastly understudied (Djurkovic-Djakovic et al., 2019; Shapiro et al., 2019). One reason for this is the limited access to oocysts for studying (Wadman, 2019). Generally, an infected felid sheds oocyst for roughly a week, after which the infected felid is considered to have developed sufficient immunity to the parasite and will not shed oocysts again (Dubey and Frenkel, 1974). Since then, more and more evidence has been gathered indicating a chance of repeated shedding of oocysts, depending on several factors such as *T. gondii* strain, number of ingested bradyzoites, nutritional status or age of the cat (Dubey, 1995; Zulpo et al., 2018).

Oocysts are ovoid in shape and measure approx. 10 x 12 µm. When shed with the feces, oocysts contain cytoplasmic mass, lipid droplets and polysaccharide granules. Only after incubation under aerobic conditions for several days oocysts become fully sporulated and infective. Sporulated oocysts contain two sporocysts, each containing four sporozoites, totaling eight sporozoites per oocyst (see Figure 2, right sporocyst). Each Sporocyst is surrounded by a wall similar to that of the oocyst, ensuring increased protection to the fragile sporozoites. The wall of each sporocyst is made from four curved plate-like structures that form the also ovoid shaped sporocyst. These plates are held together at the edges by sutures (see Figure 2, left sporocyst) (Ferguson et al., 1982; Speer et al., 1998; Freppel et al., 2019). Ultrastructural observations hint at a predominantly staggered orientation of these sutures (Ferguson et al., 1982), although, in other instances a more uniform arrangement of the sutures was observed as well (Ferguson et al., 1979). Once shed from the felid host, the sporozoites within the oocyst have no access to external nutrients, fully relying on all metabolites provided and stored in the

oocyst once shed. This causes limited viability of oocysts after residing in the environment outside of possible hosts for prolonged time. However, studies indicate that oocysts can remain viable in the environment for several years (Lélu et al., 2012; Shapiro et al., 2019).

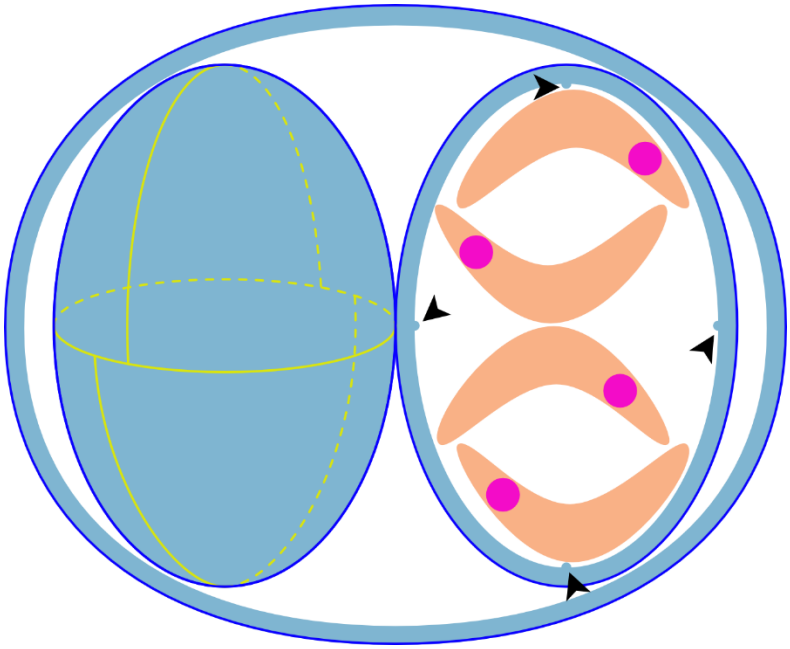

Figure 2: Schematic representation of a sporulated T. gondii *oocyst. The oocyst is surrounded by the bilayered wall consisting of the thin outer layer (blue) and the thicker inner layer (light blue). The sporocyst wall is similarly bilayered and each sporocyst is formed from four plates that are cojoined at the so-called sutures (left sporocyst, yellow). Each sporocyst harbors four sporozoites (orange, right sporocyst) who possess one nucleus each (magenta). The sutures result in thickened areas in the sporocyst wall (black arrowheads).*

The contribution of oocysts to the worldwide spread of toxoplasmosis is currently unknown although the relevance of oocyst-induced infections is increasingly recognized, not least due to seemingly more severe disease outcomes (Jones and Dubey, 2010; Dattoli et al., 2011; VanWormer et al., 2013). Mostly this is due to lack of reliable methods to differentiate sources of infection in serological tests. Additionally, the lack of robust methods to determine oocyst contamination in the environment further prevents estimations about oocysts relevance in the spread of *T. gondii.* But since oocysts are shed to the millions to the environment by an individual cat and one oocyst is shown to be sufficient to cause an infection (Dubey et al., 1996), there is no doubt, the oocyst plays a key role in the parasites life cycle. Therefore, it is worthwhile to further study this life stage of *T. gondii*, as expanded knowledge for example on the molecular composition of oocysts could allow development of better methods for oocyst detection in the environment or determination of infections caused by oocysts. In addition, it could help to develop methods for prevention of oocyst infections for example through more efficient eradication measures.

1.3 Molecules binding to the oocyst wall

1.3.1 Oocyst wall structure and composition

Although electron microscopic evidence suggests that during its development within the host, the oocyst wall appears to be a multi-layered structure (Ferguson et al., 1975), recent publications suggest to view walls of mature, sporulated oocysts as two-layered structures, as some of the layers only occur during development or are shed prior to fecal excretion (Belli et al., 2006; Weiss and Kim, 2020). The outer of those two layers is 20 nm thin and electron-dense. The inner wall layer forms after the outer layer is formed, is thicker at 30 to 70 nm and electron-lucent (Freppel et al., 2019). Remarkably, the two layers are not tightly connected and can be separated by certain methods. For example, incubation with sodium hypochlorite removes the outer layer of the oocyst wall, while the inner layer remains intact (Dumètre et al., 2013). This is further evidence to distinct differences in the composition of the two layers. The main building blocks of the oocyst wall are beta-1,3-glucan fibrils, acid-fast lipids and glycoproteins. However, the distribution varies between the two layers. Proteins, especially those rich in tyrosine and cysteine, make up approx. 90 % of the oocyst wall (Possenti et al., 2010; Dumètre et al., 2013) and are present in both layers. Additionally, those tyrosine-rich proteins are cross-linked, leading to high content of dityrosines, resulting in the oocysts characteristic blue autofluorescence under UV-light (Belli et al., 2006; Mai et al., 2009). This process is accompanied by quinone tanning and dehydration events (Dumètre et al., 2013). Since sporocysts exhibit similar autofluorescence under UV-light, the presence of similar cross-linked, tyrosine-rich proteins in the sporocyst wall is safe to assume. But since the oocyst and the sporocyst wall are difficult to separate in fractionation experiments, there is no definite indication for this (Freppel et al., 2019). In addition to glycoproteins, the outer wall layer is rich in acid-fast lipids, as indicated by staining with the diarylmethane dye Auramine O and the abundance of polyketide synthases in *T. gondii* oocysts, a class of synthases also found in mycobacteria which are known to incorporate mycolic acids as lipids in their cell walls (Bushkin et al., 2013). The structure of the inner wall is reinforced by a scaffold of beta-1,3-glucan fibrils, likely contributing to the high rigidity of the oocyst wall. Inhibitor studies in *Eimeria* underlined the importance of glucan scaffold, as chickens treated with micafungin and anidulafungin did not release oocysts (Bushkin et al., 2012). As with acid-fast lipids, the glucan fibril scaffold seems to be absent in sporocyst walls, indicating role-specific composition variations between the two different walls. For the sporocyst wall, there seem to be yet-to-be discovered structural components that could be more important to survive the environment of the digestive tract, such as low pH and digestive proteases. A proteomic screening of fractionated oocysts identified approx. 225 different proteins present in the oocyst wall (Fritz et al., 2012), of which some were shown to be differentially expressed in oocysts of different *T. gondii* strains with proposed implications regarding virulence and environmental resistance (Zhou et al., 2017). But due to the limited availability of oocysts for such large-scale studies, these numbers cannot

be considered reliable and warrant further investigations. Additionally, the function of a large part of these wall proteins is unknown and must be characterized still (Possenti et al., 2010). Identification of new proteins only present in the oocyst wall could aid in the development of new methods to detect oocysts in the environment or lead to insights into oocyst eradication methods.

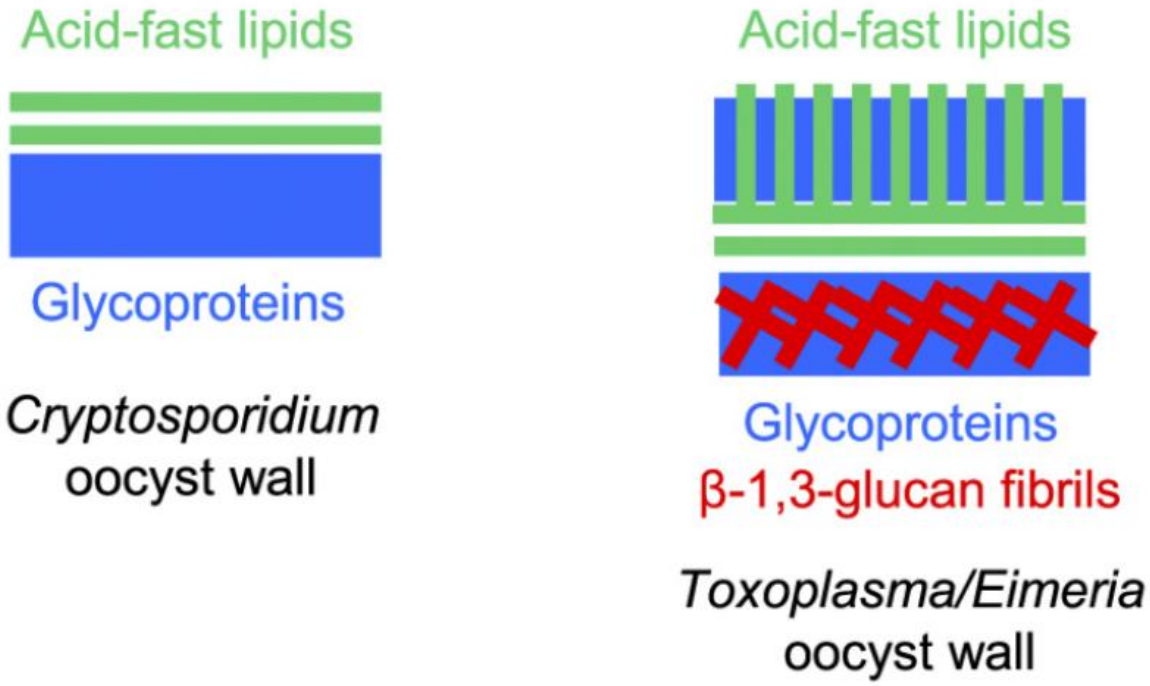

Figure 3: Composition of the wall of coccidian oocysts. Oocyst walls are bilayered, however, in Cryptosporidium *oocysts (left), the outer wall layer is only comprised of acid-fast lipids, while the inner layer is exclusively made up from glycoproteins. In contrast,* T. gondii *and* Eimeria *oocysts (right) have glycoproteins in both wall layers. The inner layer is reinforced by a scaffold of beta-1,3-glucan fibrils, while the outer layer incorporates acid-fast lipids. Adapted from Bushkin (Bushkin et al., 2013).*

1.3.2 Conventional methods for oocyst purification from environmental samples

Over the years, several methods haven been proposed and applied to detect oocysts in environmental samples. A common feature of most is that a purification step is followed by a characterization step, e.g., via qPCR. The characterization by qPCR is a necessary step to unequivocally confirm the presence of viable *T. gondii* oocysts in the sample. Purification prior to the qPCR is needed as the effectiveness of the very sensitive qPCR is easily affected by inhibiting contaminants present in the environmental sample. Therefore, published methods to detect oocysts recommend purification of oocysts either by magnetic beads coated with a ligand molecule that binds oocysts or by usage of filter columns to isolate oocysts (Dumètre and Dardé, 2005; Shapiro et al., 2010; Harito et al., 2017; Harito et al., 2017). All these methods, however, bear certain disadvantages. For one, the use of specific ligands to enrich oocysts could lead to preferred selection of oocysts from a certain strain or genotype, as

studies could show that there are translational differences between various *T. gondii* strains (Zhou et al., 2017). In contrast, a filter column-based approach would allow isolation of oocysts regardless of genotype or strain. However, it is not known, how efficient this technique would eradicate factors that might influence subsequent qPCR analyses, as indicated by the observation that microscopic analysis was more sensitive than PCR analysis after filtration of the sample (Shapiro et al., 2010). Moreover, the recovery of oocysts stuck to the filter might be impaired, resulting in reduced numbers of oocysts after filtration. This could lead to non-representative assumptions about the presence of oocysts in the sample prior to filtration. Lastly, none of these techniques can be easily adapted to varying environmental conditions that might for example hamper ligand-receptor interactions.

1.3.3 Nanobodies

By accident it was discovered that members of the Camelidae family have a special type of heavy chain-only antibodies in addition to regular antibodies found in most warm blooded species (Hamers-Casterman et al., 1993). These antibodies are devoid of light chains as opposed to prevalent antibodies. In addition, it could be shown that the variable fragment of these antibodies exhibits sufficiently high affinity to possible ligands. These variable fragments of the heavy chain of heavy chain-only antibodies (VHH) can therefore be used as a highly affine molecule for all kinds of ligand based interactions such as affinity-based purification, conjugate-mediated labeling or ligand-based inhibition (Revets et al., 2005; Vanlandschoot et al., 2011; Schoonooghe et al., 2012; Muyldermans, 2013). Partly due to their relatively small size of 15 kDa, the commonly used term for VHHs is Nanobody. Nanobodies bring several advantages that make them well suited candidates for purification by affinity chromatography of particles from environmental samples. They can be easily produced in bulk by recombinant expression in bacteria or yeast and during the selection process of suitable nanobodies future sample conditions can already be simulated to find a candidate that works well under such conditions. Moreover, Nanobodies can be constructed as dimeric molecules to increase affinity (Fridy et al., 2014). Thus, nanobodies are prime candidates for development of new methods to enrich oocysts from the environment, as they can be selected to withstand the harsh experimental conditions environmental samples usually present, such as samples collected from especially alkaline soil areas. Their much lower size in comparison to conventional antibodies could allow access to previously unavailable epitopes on the oocyst surface and their potential for highly affine interactions could contribute to more reliable results due to reduced loss of oocysts during enrichment. Their ability for dimerization opens up the potential to use different targets in the oocyst wall for increased purification success.

There are several methods to generate specific nanobodies, with the most commonly used technique relying on the usage of phage display (Smith, 1985; Pardon et al., 2014). In short, a

serologically naïve camelid is immunized with the target molecule, for example a recombinant protein. After several rounds of immunization, peripheral blood monocytes (PBMCs) are isolated. MRNA is extracted from the PBMCs and converted to cDNA via rtPCR. From the cDNA, using specific primers, the VHH coding sequence is amplified and subsequently cloned into phages to generate a nanobody expressing phage library. This library is then selected against the target molecule in several panning rounds. For this, the target molecule can for example be coated on the surface of an ELISA plate and incubated with the phage library. After a washing step, only bound phages remain then are retained during a cleavage step to detach the phage from the bound nanobody. Caught phages are enriched and incubated again with the target molecule to increase enrichment. After several rounds of panning, few nanobody candidate expressing phages remain that are used to generate bacteria that express the candidate nanobodies for further characterization studies. More recently, it has been proposed to harness the advantages modern bioinformatic methods provide to make this process more feasible, for example by transcriptomic analyses of naïve and immunized camelids to immediately detect enriched nanobody sequences and reduce the need for phage panning (Deschaght et al., 2017).

1.3.4 Molecules known to bind to oocysts

Several different molecules binding to the oocyst surface have been discovered, such as lectins and C-type lectin receptors (CLRs). Lectins are proteins that exhibit high affinity towards sugar groups. Due to their widely known effect on cell-cell adhesion they are implied to play an important role in the innate immune system (Rutishauser and Sachs, 1975; Walker, 1985; Brudner et al., 2013). The lectin wheat germ agglutinin (WGA) specifically binds to N-acetyl-D-glucosamine (GlcNAC). Harito et al. reported observation of WGA binding to walls of aged oocysts (several years old), while fresh oocysts were unlabeled by the lectin (Harito et al., 2016). Interestingly, upon treatment with acidified pepsin, WGA also bound to fresh oocysts. It is possible, the acid-pepsin treatment simulated age-related degradation of parts of the oocyst wall, allowing access for WGA to the parts where GlcNAC molecules are present. Another lectin binding to oocyst structures is *Maclura pomifera* agglutinin (MPA). MPA is specific for N-acetyl-galactosamine (GalNAC) (Huang et al., 2010) and is known to bind to the walls of sporocysts and oocysts (Chatterjee et al., 2010; Bushkin et al., 2012). Often the discovery of molecules binding to the oocyst wall or of dyes staining oocyst structures leads to new insights into the oocyst wall composition (Bushkin et al., 2012; Bushkin et al., 2013). The presence of acid-fast lipids in the oocyst wall or the trabecular scaffold formed by beta-1,3-glucans in the inner wall layer were discovered via Auramine-O staining and through binding of the CLR Dectin-1 (CLEC7A), respectively (see section 1.3.1). The binding of CLRs to the oocyst wall in particular presents an interesting aspect with immunity related implications.

1.3.5 CLRs of the Dectin-1 cluster

CLRs are receptor molecules expressed on the surface of several cell types. Their name is derived from their carbohydrate-binding lectin domain that is stabilized by two disulfide bonds, providing high variability in carbohydrate binding. This binding activity requires calcium, hence the term C-type (Murphy and Weaver, 2018). Some CLRs can act as pattern recognition receptors (PRRs) and are thus known to play roles in the adaptive and innate immune response. CLRs are involved in antigen presentation upon pathogen detection but also in cross-presentation of antigen for example of detected necrotic cells (Bermejo-Jambrina et al., 2018). CLEC7A belongs and gave name to a cluster of CLRs, the Dectin-1 cluster (Tone et al., 2019), that is part of the so-called mammalian natural killer gene complex and is present on a variety of immune cells. The cluster is comprised of receptors that detect a diverse array of ligands, resulting in involvement in several different innate immune responses (Plato et al., 2013). Among the CLRs in this cluster are CLEC1B (CLEC-2), CLEC7A (Dectin-1), CLEC9A (DNGR1), CLEC12A (MICL), and CLEC12B (macrophage antigen H [MAH]) (Tone et al., 2019). CLEC7A can bind to fungal structures (see above) and is furthermore involved in the detection of apoptotic cells. Other members of the Dectin-1 cluster lack detailed characterization, resulting in limited knowledge of the ligands of CLEC1B, CLEC9A, CLEC12A, and CLEC12B (see Table 1). A cause for this is the promiscuous and flexible nature of the CLR binding sites, as exemplified by two of the known ligands of CLEC1B, the glycoprotein podoplanin which is expressed in diverse human tissues and the non-glycosylated snake venom toxin rhodocytin. Upon binding to CLEC1B, both can cause platelet aggregation, although binding is mediated differently, as discovered by three-dimensional (3D) structural analyses (Nagae et al., 2014).

To investigate if CLRs of the Dectin-1 cluster other than CLEC7A also bind to oocyst structures of *T. gondii*, a library of fusion proteins consisting of the extracellular part of murine CLRs, covering the carbohydrate recognition domain, and the constant region of human IgG1 (hFc) will be used. These fusion proteins have been constructed by cloning of the individual cDNA sequences of the respective extracellular CLR domains into the pFuse-hIgG1-Fc vector that already contains the hFc cDNA sequence (see Figure 4). This yields a molecule that carries two CLR recognition sites and the constant region of human antibody molecules that can easily be detected by immunofluorescence using conjugated antibodies that specifically bind to the heavy chain of human IgG1 constant region. The resulting CLR-hFc-fusion protein-library has been constructed and published earlier (Maglinao et al., 2014) and was kindly gifted by Prof. Bernd Lepenies of the Tierärztliche Hochschule Hannover, Germany. The library comprises almost all members of the Dectin-1 cluster except for CLEC8A (see Table 1).

Table 1: CLRs from the Dectin-1 cluster that were assessed in this thesis. Table adapted from Tone (Tone et al., 2019).

CLR	**Known ligands**
CLEC1B	Rhodocytin (Watson et al., 2008) Podoplanin (Nagae et al., 2014) Fucoidan Diesel exhaust particles
CLEC7A	β-glucan Tropomyosin Mycobacterium (Wagener et al., 2018) Leishmania (Lima-Junior et al., 2017) Galectin Galactosylated immunoglobulin
CLEC9A	Dead cells (F-actin, myosin II) (Hanc et al., 2015)
CLEC12A	Dead cells (Neumann et al., 2014) Hemozoin (Raulf et al., 2019) Uric acid (Neumann et al., 2014; Raulf et al., 2019)
CLEC12B	Unknown

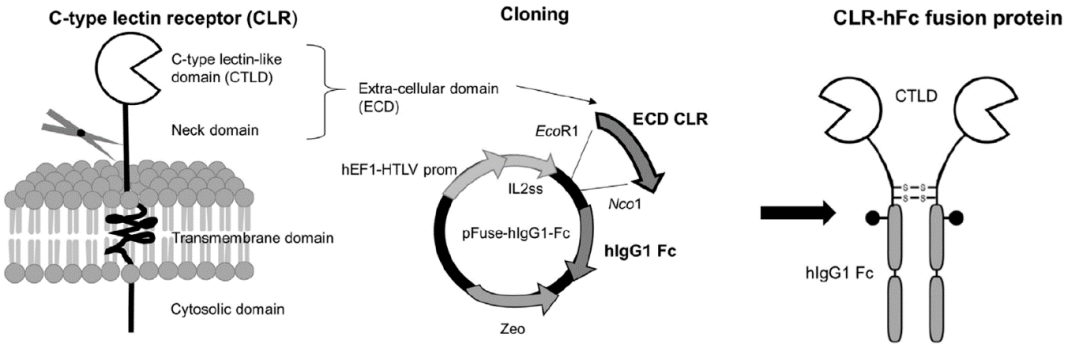

Figure 4: Scheme of the construction of the used CLR-hFc-fusion protein library. CDNA encoding for the carbohydrate recognition domain of the CLRs was cloned into the expression vector and thus fused to the cDNA fragment encoding for hFc, resulting in a fusion protein that carries two CLR recognition domains and is detectable via conjugated anti-human antibodies. Adapted from Mayer (Mayer et al., 2018).

1.4 Molecules contributing to stress tolerance inside the oocyst

1.4.1 Oocyst resilience in the environment

As an obligate intracellular parasite, *T. gondii* tachyzoites rapidly die when exposed to the extracellular environment for prolonged amounts of time, as they rely on the hosts metabolic pathways. Although tachyzoite survival for up to 11 days extracellularly has been reported, these experiments demonstrated survival under non-physiological conditions (Kalani et al., 2016). The dormant tissue cyst form, housing the bradyzoite stage, can stay infective for longer periods, posing high risk of infection in contaminated meat from infected animals (Dubey, 2016). Measures to minimize the risk of infection include heating of the meat to above 50 °C for 10 minutes or freezing at -20 °C for 2 days (El-Nawawi et al., 2008). In contrast, the oocyst stage of *T. gondii* has been shown to survive for as long as 24 months under optimal conditions and remain infective (Lindsay and Dubey, 2009). This, together with studies on oocyst survival under different conditions (Yilmaz and Hopkins, 1972; Lélu et al., 2012) indicates specific oocyst characteristics that increase resistance to environmental stressors. The oocyst wall with its many different components is proposed to be the main contributor to the oocyst's resilience (Dumètre et al., 2013). Together with the sporocyst wall, the fragile sporozoites are assumed to be well shielded from adverse events. This is corroborated by the lack of efficacy of many commonly used disinfection methods on oocysts (Frenkel and Dubey, 1973; Dubey et al., 1998; Dumetre et al., 2008; Dumètre et al., 2013) that would kill any other form of the parasite. However, the presence of other molecular factors contributing to environmental resistance of oocysts is a possibility that warrants further research as identification of such factors would allow more efficient removal of oocysts from the environment to prevent the parasite's spread (Yan et al., 2016).

1.4.2 Intrinsically Disordered Proteins

Intrinsically disordered proteins (IDPs) and hybrid proteins carrying intrinsically disordered regions (IDPRs) as well as structured domains have been discovered in organisms from all domains of life as well as in viruses (Uversky, 2019). The proportion of IDPs and IDPRs of an organisms proteome vary greatly, although a correlation between the percentage of IDPs and IDPRs in the proteome and an organisms complexity as well as the habitat have been observed (Xue et al., 2012), indicating that multicellular organisms possess a greater number of IDPs and IDPRs. A key characteristic of IDPs is their lack of a defined structure. This results in them exhibiting aberrant molecular weight in chromatography experiments such as size exclusion chromatography (SEC) as well as resistance to high temperatures where globular proteins usually denature and aggregate (Receveur-Brechot et al., 2006). The latter can be exploited for easy purification of IDPs. As compared to globular proteins, IDPs are not folded after translation. Hence, their relevance for biological processes was mostly disregarded and neglected, due to the long lasting structure-function paradigm, stating that a proteins particular biological function is derived from its specific defined structure (Fischer, 1894). However, in recent years, evidence that IDPs play important physiological roles in several different kinds of processes has been collected. For one, it has been proposed that due to their flexible nature, IDPs can serve as regulator molecules of cellular processes. In yeast, the IDP Pab1 is known to bind mRNA under physiological conditions thus repressing translation. In response to thermal or pH stress, Pab1 dislocates from mRNA and forms hydrogel structures, enabling mRNA translation (Chavali et al., 2017). Another proposed mechanism is that IDPs are disordered under certain conditions but if these conditions change, for example due to increase in temperature or loss of water, IDPs change from a disordered state to a more ordered one to protect certain cellular structures from damage induced by the stressing conditions (van der Lee et al., 2014). Such effects have since been observed in small invertebrates like the *Tardigrada* (Boothby et al., 2017).

1.4.3 Late embryogenesis abundant proteins

Late embryogenesis abundant (LEA) proteins are a specific class of IDPs that has been discovered in the 1980s in late-stage plant embryonic tissue (Dure et al., 1981). The term LEAs was first used in 1986, when several mRNA transcripts were detected to be most abundant during late stage embryogenesis of cotton seeds as compared to earlier or germinating stages (Galau et al., 1986). The knowledge on LEA proteins has since steadily increased. They have been discovered in a wide variety of other plant embryos as well as microorganisms and invertebrates. Since their discovery, several different classification formats have been proposed for LEA proteins, based on motifs in their peptide sequence. The two most recent considerations are that LEA proteins either include eight groups (LEA_1 to 6, dehydrins and seed maturation proteins (Nagaraju et al., 2019) or that they are divided into classes 1 to 12

(Jaspard et al., 2012)). For consistency purposes, this thesis adheres to the latter classification. The individual LEA groups have been linked to different functions within the plant embryo, as expression of LEA proteins from different groups in *Saccharomyces cerevisiae* revealed differences in their function (Zhang et al., 2000). In particular, class 6 (group 3 at that time) LEA proteins are proposed to form structures similar to cytoskeletal filaments (Wise and Tunnacliffe, 2004). Moreover, proteins that bear high similarity to class 6 LEA proteins have been discovered in nematodes (Browne et al., 2002). For some time it has been proposed that LEA proteins act as cellular protectors through their IDP characteristic, i.e. through conformational changes induced by changes on a molecular level (Hincha and Thalhammer, 2012). In addition to dividing LEA proteins in different classes, some researchers consider LEA proteins to be part of a larger group of proteins called “hydrophilins” (Battaglia et al., 2008). Characteristic for hydrophilins is a glycine content above 6 % and a grand average of hydropathy (GRAVY; (Kyte and Doolittle, 1982)) score below 1, indicating a hydrophilicity score of greater than 1 (Garay-Arroyo et al., 2000; Dang and Hincha, 2011). These characteristics show to be a unifying factor between all LEA classes, as most LEA proteins exhibit these characteristics.

1.4.4 LEAs in *T. gondii*

Transcriptomic and proteomic scans of *T. gondii* sporozoite fractions revealed abundant expression of four proteins specific to the oocyst stage that were previously unknown (Fritz et al., 2012; Fritz et al., 2012). Namely, the genes coding for these proteins are TGME49_276850 (acc. Number XM_002370392), TGME49_276860 (acc. Number XM_018781754), TGME49_276870 (acc. Number XM_002370394) and TGME49_276880 (acc. Number XM_018781755). While further analysis regarding LEA protein classification using the protein family data base (PFAM; (Mistry et al., 2020)) only classified TGME49_276860 as a class 6 LEA protein (PFAM: PF02987), amino acid sequence analysis via the Basic Local Alignment Search Tool (BLASTp; (Altschul et al., 1997)) against an online database of LEA proteins revealed close homology to predominantly class 6 LEA proteins for all four candidate proteins, among them Ce-LEA from *C. elegans*. Thus, in this thesis, the four proteins will be referred to as “TgLEA-850”, TgLEA-860”, “TgLEA-870” and “TgLEA-880”, respectively. Remarkably, the genes are located on the same chromosome, adjacent to each other. Assuming similar functions of the proteins, this is an uncommon occurrence, since functionally related genes are not necessarily located in close proximity in the genomes of eucaryotes (Lee and Sonnhammer, 2003), although polycistronic mRNAs have been reported in *Trypanosoma* and *Caenorhabditis elegans* (Blumenthal, 1998; Blumenthal et al., 2002). In addition, analysis and comparison of genomic sequences using the free online tool ToxoDB (Harb and Roos, 2020), reveals homolog sequences for all TgLEAs in other closely related coccidian parasites to

T. gondii, such as *Besnoitia besnoiti, Hammondia hammondi* and *Neospora caninum* (see Figure 5).

Moreover, these homolog sequences are similarly arranged in the respective genomic regions, suggesting shared synteny between the genomic regions of these proteins between all four parasites. This preservation of the genomic region would also support the assumption that TgLEAs play an important role during the oocyst stage, as functionally related genes from transcription clusters have been shown to be more conserved over several species than unrelated genes (Amores et al., 1998; Moreno-Hagelsieb et al., 2001).

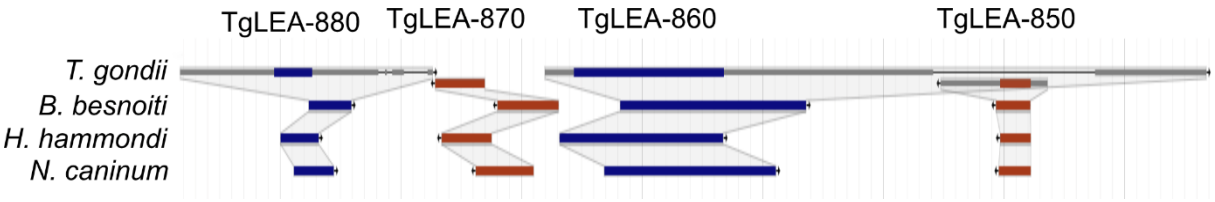

Figure 5: Synteny in the genomic region of TgLEAs with closely related species. The figure shows the alignment of coding sequences in the genomic locus of TgLEAs in T. gondii *to coding sequences in the coccidia* B. besnoiti, H hammondi *and* N. caninum. *All four TgLEAs are shown to have homolog sequences in these related parasites that are similarly arranged on the genome, indicating synteny between the species.*

Initial confirmation of IDP characteristics of the TgLEAs, acquired through disorder prediction using the online tool MobiDB 4.0 ((Piovesan et al., 2021), see Table 2) indicates that all TgLEAs contain disordered regions to a varying extend, while the globular control protein TgSAG1 contains no disordered regions and domain I of human calpastatin (hCD1), a known unfolded peptide (Uemori et al., 1990), is predicted to contain 96.33 % of disordered regions. Further, all TgLEAs have a GRAVY score below 1, like hCD1, while TgSAG1 has a positive GRAVY score. Lastly, all TgLEAs and hCD1 have a glycin content of 6 % or higher, while TgSAG1 only contains 5 % glycin.

Table 2: In silico predictions for TgLEAs and control proteins.

Protein	MobiDB disordered consensus	GRAVY score	Glycin content [%]
TgLEA-850	54.81 %	- 0.672	9
TgLEA-860	25.15 %	-0.824	7
TgLEA-870	33.33 %	-0.481	6
TgLEA-880	60 %	-0.596	8
TgSAG1	0 %	0.132	5
hCD1	96.33 %	-1.193	9

Using the online tool Classification of Intrinsically Disordered Ensemble Regions (CIDER (Holehouse et al., 2015)) to characterize the TgLEAs' structure further, all four TgLEAs are sorted into the category of so-called "Janus sequences", meaning they predominantly possess regions that are folded or unfolded depending on the surrounding environment (see Figure 6). In contrast, the control protein TgSAG1, a known globular protein, is sorted into the group of weak polyampholytes or globular proteins while hCD1, a known IDP, is classified as a strong polyampholyte. This observation yields more evidence to the assumption that TgLEAs are IDPs or at least possess IDPRs. Moreover, the categorization as Janus sequences could also hint at LEA characteristics, suggesting conformational changes upon stress induction.

These preliminary findings suggest interesting aspects regarding the involvement of these four proteins in oocyst viability. As stated above, *T. gondii* oocysts, like all coccidian oocysts, are known to withstand harsh environmental conditions and survive many routinely used disinfectants (Ito et al., 1975; Kuticic and Wikerhauser, 1996; Dubey et al., 1998). Mostly, this stress tolerance has been attributed mainly to the thick oocyst and sporocyst walls, as it is assumed they shield sensitive cellular components from most stressors (Dumètre et al., 2003; Dumètre et al., 2013). The only methods to reliably kill oocysts that have been confirmed experimentally are incubation at temperatures above 58 °C for at least 15 minutes and freezing at -20 °C for 21 days, while drying of oocysts for extended times did not reliably kill significant numbers (Kuticic and Wikerhauser, 1996).

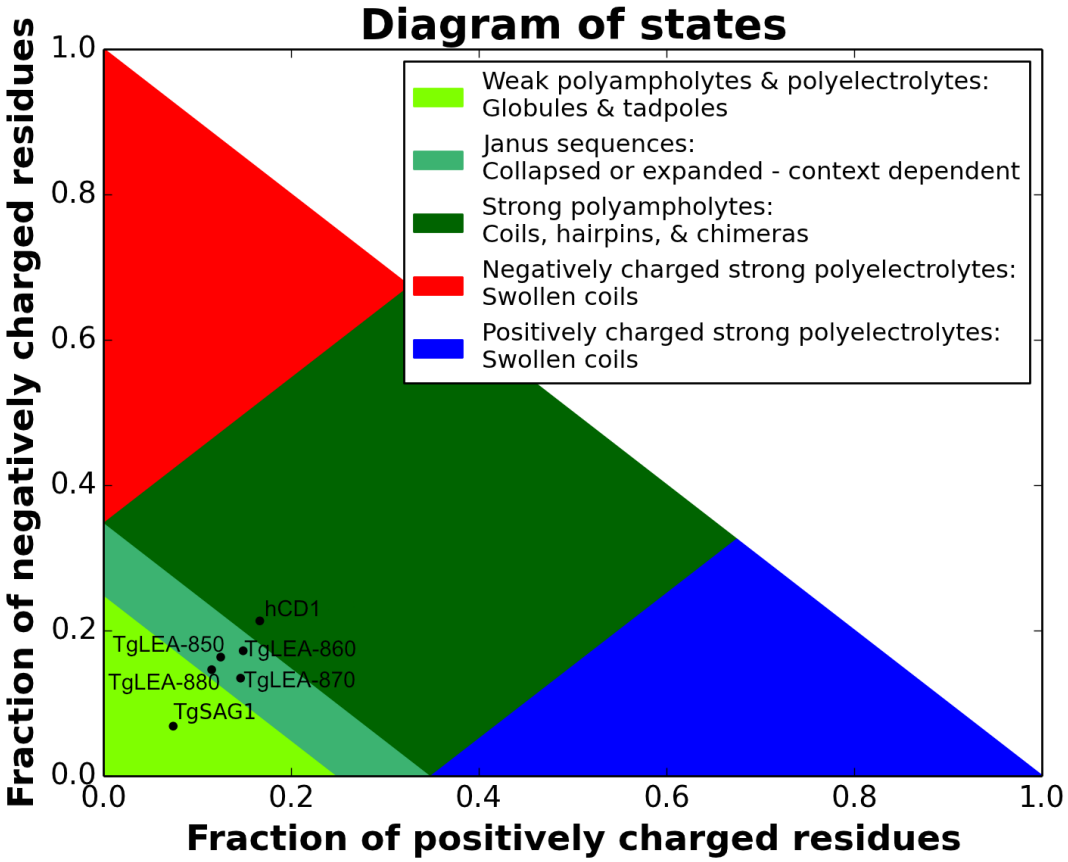

Figure 6: CIDER analysis of TgLEAs indicates they exhibit context dependent structure. The image shows categorization of all four TgLEAs as group 2 proteins (light green) by the CIDER algorithm while SAG1 is sorted into group 1 (bright green) as a globular protein and hCD1 as a highly disordered protein is sorted into group 3 (dark green) of strong polyampholytes.

Interestingly, Frenkel and Dubey observed that while freezing oocysts greatly influenced their viability, a constant temperature below the freezing point was much more deleterious than repeated freezing and thawing (Frenkel and Dubey, 1973). Additionally, it was observed that sporulated oocysts were more resistant to freezing damage than unsporulated oocysts. Since there is only a small difference in the wall composition of sporulated and unsporulated coccidian oocysts reported, which could also be due to contaminating sporocyst wall fragments during analysis (Mai et al., 2009), these observations give reason to assume, that sporulated oocysts could harbor molecules that aid in protection against freezing stress. This is also corroborated by the upregulated expression of all four TgLEAs in sporulating oocysts as compared to unsporulated oocysts (Fritz et al., 2012). Finally, TgLEA-860's classification as a class 6 LEA protein and close homology to a class 6 LEA protein from *C. elegans* that was found to provide stress resistance (Gal et al., 2004) further underlines the need for characterization of the TgLEAs to assess their disorder state and investigate whether they are contributing factors to the increased oocysts resilience. Of particular interest would be analyses of their effect on cellular survival upon freezing and desiccation but also on growth

under osmotic stress and high temperatures, as other LEA proteins have been shown to protect against such stresses (Zhang et al., 2000; Li et al., 2012; Gao and Lan, 2016).

1.4.5 The role of lactate dehydrogenase (LDH)

The enzyme LDH provides an easy and reproducible experimental setup to assess the protective effects of candidate proteins on protein stability under different physiological conditions of interest, as it allows for a fast analysis of effects on aggregation as well as activity. Thus, assays including citrate synthase and LDH are often used in the assessment of possible LEA proteins (Goyal et al., 2005; Thalhammer et al., 2014; Boothby et al., 2017).

T. gondii possesses two isoforms of LDH, LDH1 and LDH2. While LDH2 is predominantly expressed in the bradyzoite stage, LDH1 is the predominant isoform in tachyzoites and sporozoites (Yang and Parmley, 1997). Proteomics show that LDH1 is among the five most abundant proteins in the oocyst stage (Fritz et al., 2012). Recent studies have demonstrated that LDH is an important pathogenesis factor of *T. gondii*, since deletion mutants were not able to reproduce in host cells and in addition were lacking the ability for stage conversion (Xia et al., 2018; Xia et al., 2018). While LDH catalyzes the reversible reaction of pyruvate to lactate using nicotinamide adenine dinucleotide bonded with hydrogen (NADH) as co-factor (Figure 7A), *T. gondii* LDH isoform 1 (TgLDH1) was shown to utilize the NAD analogue 3-acetylpyridine adenine dinucleotide (APAD) more efficiently than NADH, resulting in preference for lactate as substrate (Figure 7B; (Dando et al., 2001)).

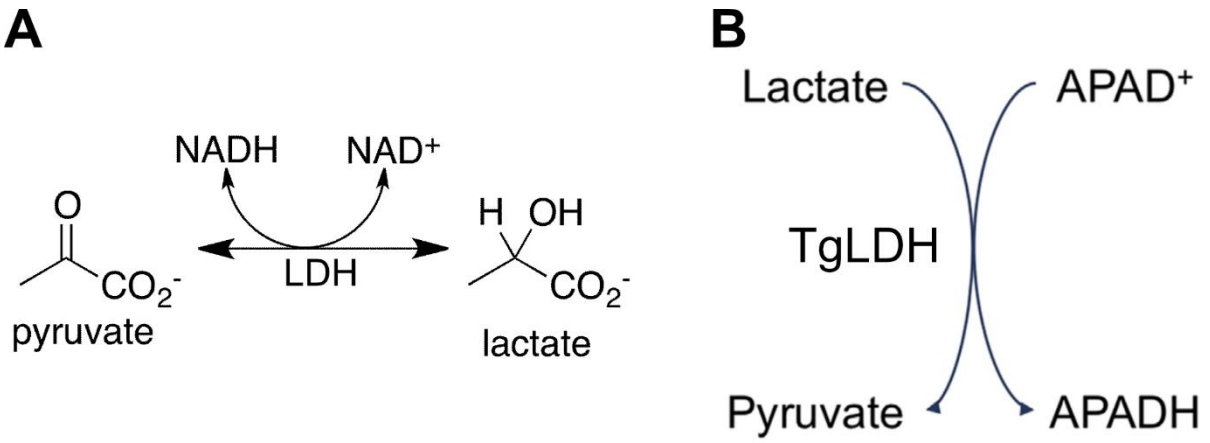

Figure 7: Reaction catalyzed by LDH. (A) LDH catalyzes the reaction from pyruvate to lactate and the reverse reaction under usage of NADH and NAD+, respectively. (B) In T. gondii, like in P. falciparum, LDH tends to favor APAD as co-factor. Adapted from (Markwalter et al., 2016).

1.5 Molecules as antigens for identification of oocyst-mediated infections

1.5.1 Conventional serological test methods for *T. gondii*

Since *T. gondii* undergoes several equally infective developmental stages, a key part in effective prevention of the parasites' spread is the ability to differentiate infection routes, e.g., the ability to determine if an infection was caused through tachyzoites, bradyzoites or oocysts. Test methods enabling identification of infection clusters resulting from environmental oocysts could aid in the early prevention of the parasite's spread by taking appropriate measures to prevent further infections (Opsteegh et al., 2014). Established serological test methods for *T. gondii* infections today, however, do not allow such a discrimination and only give a quantitative answer concerning an infection in general, irrespective of the source. Such test methods include the Sabin-Feldman dye test (DT), modified agglutination test (MAT), enzyme-linked immunosorbent assays (ELISA) and western blot analyses. The DT is still considered to be the definitive method with regards to confirmation of infections in humans (Dubey, 2016). Generally, the DT is assumed to be very sensitive and specific with no reports of false results in humans. Also, it allows for detection of IgG as well as IgM antibodies. However, sera from other animals may need to be heat inactivated prior to testing, as is the case for some ruminant species (Havakhah et al., 2014), or might not work at all in the DT, as demonstrated for some avian species (Frenkel, 1981). As a cost and material saving, low risk alternative to the DT with similar titer results, the MAT has been extensively used in serological analyses of humans and animals (Desmonts and Remington, 1980) and has been improved and adapted over time (Dubey and Desmonts, 1987). One Drawback of the MAT as opposed to the DT is that IgM are not detected due to pre-treatment of sera with 2-mercaptoethanol which removes IgM from the samples. Therefore, the risk of a false negative result in the MAT in the case of an early infection is elevated (Dubey and Crutchley, 2008). In contrast to DT and MAT, the ELISA test for *T. gondii* infections relies on recombinantly expressed antigens. Thus, its main advantage over those tests is the possibility to use stage specific antigens or antigens that are recognized by a specific type of immunoglobulin. More specifically, it has been shown previously that certain proteins of *T. gondii* were only detected by antibodies from sera of acutely infected patients and vice versa (Erlich et al., 1983). Therefore, as opposed to DT and MAT, ELISA tests would allow for differentiation of infection acquisition as well as determination whether an infection is acute or chronic (Naot and Remington, 1980; Naot et al., 1981). Moreover, ELISA tests allow for higher sample throughput than MAT and DT and are more material saving and thus cost-efficient. Additionally, if used in combination with a plate reading machine and standard serum, ELISA results can be quantified, allowing a more detailed insight into the antibody titer.

1.5.2 The Luminex technology as a multiplexing serological test method

An even further improvement over ELISA tests present multiplexing techniques like the Luminex technology. Thus, although most serological testing for *T. gondii* infections is already routinely done with ELISA, development of Luminex assays to determine *T. gondii* infections using different antigens has steadily increased in recent years (Griffin et al., 2011; Priest et al., 2015; Priest et al., 2016; Wang et al., 2016; Brenner et al., 2019; Klein et al., 2020).

The Luminex technology relies on the use of magnetic polystyrene beads that are coated with the desired antigen. These beads contain two distinct dyes that allow specific identification of 100 individual bead sets, thus enabling parallel use of different antigens and controls. Serum antibodies bound to the antigen coated beads after incubation are detected via a secondary antibody that is conjugated with phycoerythrin (PE). The analysis is done in a plate reader equipped with two lasers of specific wavelengths. One determines the specific type of bead that is analyzed and thus the used antigen, while the second laser detects fluorescent signal of the secondary antibody thus determining presence or absence of serum antibodies in the sample (Graham et al., 2019).

One main drawback of conventional serological test methods is the limited availability of sample material. This in turn limits the number of analyses that can be conducted on one sample. Although ELISA tests, for example, allow relatively easy parallel testing of many samples, the amount of sample material needed is still high. This is an important factor to take into consideration when conducting large scale serological surveys, since especially studies that are conducted in areas with limited access to resources would benefit from multiplexing opportunities (Jani et al., 2002; Priest et al., 2015; Metcalf et al., 2016). Multiplexing techniques, while higher in initial costs, allow simultaneous tests on the same sample, maximizing the number of analyses that can be done on one sample, thus rendering such studies much more efficient. Thus, with an increasing sample size, the high initial costs of multiplexing technologies like Luminex are overcome by the clear advantages of reduced sample material and processing time (Boonham et al., 2014).

1.5.3 Serological markers for infections caused by oocysts

The term serological marker in the context of this thesis is used similarly to previous publications (Kerkhof et al., 2016; Hachim et al., 2020) and refers to antibodies present in a host against certain *T. gondii* antigens that allow identification of an existing or past infection. The most prominent antigen used in serological tests to detect antibodies against *T. gondii* is the SAG1 protein present on the surface of the tachyzoite stage of the parasite (Lekutis et al., 2001). However, since SAG1 seems to be specific for the tachyzoite stage and infections are mainly caused bradyzoites or sporozoites (Pinto-Ferreira et al., 2019), tests relying on SAG1 for antibody detection are only able to determine infections in general as they only indicate

presence of antibodies against tachyzoites, which are occurring with every *T. gondii* infection. Serological tests that allow the differentiation of sources that caused *T. gondii* infections would be highly beneficial to public health agencies for example to prevent spread of the disease.

Hill et al. proposed antibodies against one of the previously mentioned TgLEA proteins (TgLEA-850 in this thesis, TgERP in the original publication) as serological markers for *T. gondii* infections caused by oocysts (Hill et al., 2011). In sera from pigs and mice that were either infected with tissue cysts or oocysts of *T. gondii*, usage of TgLEA-850 as antigen in serological analyses showed great promise as a specific marker for oocyst-caused infections. Up to eight months post infection, serum samples from oocyst infected animals were reacting to the antigen. In addition, sera from participants of several different study populations from outbreaks of unknown infection sources were investigated, using TgLEA-850 in ELISA and Western Blot tests. These analyses also showed promising results, with detectable antibodies up to eight months post infection.

However, the oocyst and more specifically the sporozoite stage, are not very long-lived in the body of the host once taken up. While the cause for excystation remains unclear (Freyre and Falcón, 2004; Freppel et al., 2019), it is known that excystation events occur early after oocysts are introduced into the intestine and the excysted sporozoites begin invading the surrounding epithelium as early as 30 minutes post infection (Dubey, 1998). At 6 hours after the infection, most sporozoites occur in the lamina propria, where they undergo endodyogenie and by 12 hours post infection almost all sporozoites have differentiated into tachyzoites (Dubey et al., 1997; Speer and Dubey, 1998). Thus, the mounting of an effective immune response resulting in generation of antibodies that last for prolonged amounts of time against such a short-lived life-stage seems unlikely.

In addition to TgLEA-850, other proposed oocyst specific markers include members of a family of oocyst wall proteins (TgOWPs; (Possenti et al., 2010; Sousa et al., 2020)) and CCp5A (Santana et al., 2015). However, looking at the literature, there are only few publications using TgLEA-850 to study oocyst infections (Vieira et al., 2015; Burrells et al., 2016; Mangiavacchi et al., 2016; Milne et al., 2020). Only one publication included CCp5A in their experiments (Liu et al., 2019) and no publications were found investigating TgOWPs. This lack of studies on potential oocyst specific infection markers highlights the need for further investigation and in-depth characterization of these and other potential infection markers. Such tools are crucial to advance public health efforts in infection prevention (Milne et al., 2020). Therefore, in addition to further investigation of the proposed marker TgLEA-850, all previously mentioned TgLEA-proteins were analyzed regarding their suitability to elicit antibodies that can serve as accurate serological markers, since all four TgLEAs are specific to the oocyst stage of *T. gondii* (Fritz et al., 2012).

1.5.4 Antigenicity of TgLEAs

Since TgLEAs are predicted to contain disordered regions and thus do not necessarily exhibit secondary structures under physiological conditions (see chapter 1.4.4), it is questionable whether TgLEAs are suitable candidates for proteins that elicit a strong immune response in infected hosts that can be detected by serological tests. The ability of IDPs to form high affinity interactions with antibodies has long been doubted, since the IDPs flexible nature would counteract such strong, long lasting bonds (Dunker et al., 2002). Accordingly, it seems that many IDPs are, due to their characteristic flexibility, predominantly involved in signal transduction processes in many organisms that require a possible ligand to bind several different interaction partners, a process that would be facilitated by weak receptor ligand interactions (Wright and Dyson, 2015). Still, as the TgLEAs are predicted to be less disordered than known IDPs, they could potentially cause an antibody response targeting their structured regions, due to their increased abundance in the oocyst. In addition, IDPs flexible nature is also theorized to effectuate the formation of high-affinity antibodies through their disordered nature that allows deeper binding of a disordered region in an antibodies paratope (MacRaild et al., 2016). In contrast, some publications showed that functionally important domains of proteins from pathogenic organisms are either of flexible nature or at least flanked by flexible regions. This characteristic is assumed to serve the purpose of “masking” these conserved domains by reducing the immunogenic pressure (Colman, 1997; Kwong et al., 2002; MacRaild et al., 2011). In this context it is even more important to further assess the antigenic potential of TgLEA-850 and the closely related other TgLEAs.

1.6 Aims of this work

As has been established in the introduction, oocysts are a vital stage in the parasite's life cycle as they are the product of sexual reproduction. The relevance of oocysts in *T. gondii's* distribution is still unclear due to lack of reliable methods to quantify the prevalence of oocysts in the environment. Furthermore, oocysts have been shown to be resilient to environmental stress factors, likely increasing their contribution to the parasite's epidemiology. Lastly, knowledge on the oocyst's role in the high worldwide seroprevalence of *T. gondii* is insufficient, as reliable and robust serological test methods to clearly identify oocyst caused infections are lacking.

Thus, the goal of this thesis is to shed more light on the oocyst stage of *T. gondii* regarding several key aspects such as possible new molecules in the oocyst wall that can be harnessed for ligand-based methods for detection, molecules inside the oocyst that contribute to the increased stress resistance and molecules that can be used in serological detection methods. To this end, the project is split into three parts. The first part, detailed in chapters 3.1 and 4.1, aims to lay the groundwork for establishment of new methods for oocyst enrichment in environmental samples by identifying new molecules binding to the oocyst wall. As a basis for further experiments, a method for robust immunofluorescence experiments using only small numbers of oocysts is developed. Using this method, molecules binding to the oocyst wall can be identified and their binding characteristics further analyzed. The generation of nanobodies targeting the oocyst wall is explored. Also, members from the Dectin-1 CLR cluster are investigated with special focus on their binding to the oocyst wall. Results from these experiments will also contribute to new insights into the molecular composition of the oocyst wall.

In the second part, detailed in chapters 3.2 and 4.2, factors contributing to the oocysts resilience to environmental stress are investigated. Oocysts are known to stay viable in the environment under varying conditions, relatively untouched by environmental factors. This is often attributed to the rigidity of the bilayered walls that protect the oocyst and the sporocysts. However, the presence of so-called LEA proteins inside the oocyst that contribute to protection against damage induced by certain stress factors has been hypothesized. These LEA proteins are known to confer stress resistance in plants and invertebrates through their disordered structure. Through *in silico, in vitro* and *in vivo* characterization of the TgLEAs, more in depth knowledge will be acquired, collecting predictions and findings regarding their IDP characteristics, their biochemical properties as well as their effect on bacterial growth upon several stresses. The *in vitro* analyses will investigate the LEA protein's potential to protect an important *T. gondii* pathogenesis factor from stress induced damage. The findings from these experiments will lead to a better understanding of oocyst physiology as well as opening up

more possibilities to develop methods to eradicate oocysts from the environment in a targeted and more efficient manner and prevent parasite spread.

Lastly, chapter 3.3 and 4.3 analyze the oocyst specific TgLEAs regarding their putative role as antigens that can elicit a specific antibody response, serving as infection marker. Such a serological tool would be highly beneficial in early identification of infection clusters and efficient mounting of counter measures to prevent further spread. First, antibodies against two most promising LEA proteins will be generated by immunization of two rabbits to serve as additional controls in future experiments as well as proof of basic antigenicity of TgLEAs. Subsequently, the Luminex technology will be shortly introduced and adapted to allow feasible analyses of large numbers of chicken sera for *T. gondii* infections. ELISA tests will assess the TgLEAs' antigenic potential by analysis of sera from experimentally infected chickens. Lastly, the Luminex technology will be employed to corroborate the ELISA findings and investigate on a large-scale different serum dilutions to confirm if TgLEAs are suitable antigens to differentiate different *T. gondii* infection routes, i.e. tachyzoite, bradyzoite or oocyst.

In summary, this project will expand the knowledge on molecules (1) binding to the oocyst wall, (2) contributing to stress tolerance inside the oocyst and (3) as antigens for identification of oocyst-mediated infections.

Chapter 2: Material and methods

2.1 Material

2.1.1 Laboratory equipment

Device	Manufacturer
2100 Bioanalyzer	Agilent, US
Äkta Purifier FPLC system	GE Healthcare, US
Analog-digital converter	DataQ, US
Automatic plate washer	Tecan, Austria
Axioskop 2 microscope	Zeiss, Germany
AxioVert 25 microscope	Zeiss, Germany
Bio-plex 200 analyzer	BioRad, US
Blotting chamber	BioRad, US
Centrifuges	Thermo Fisher, US; Eppendorf, Germany
CFX96 Touch Real-Time PCR reader	BioRad, US
EM-1 Econo UV monitor	Bio-Rad, US
Fusion FX luminescence image detector	Vilber, France
Gammacell 40 Exactor	MDS Nordion, US
Gel documentation	Serva, Germany
Gelelectrophoresis equipement	BioRad, US
GenePix 4300A microarray scanner	Molecular Devices, US
Incubator bacterial plates	Heraeus Instruments, Germany
Incubator *T. gondii* cell culture	Binder, Germany
Infinite M200 pro plate reader	Tecan, Austria
Lightpad A930	Artograph Inc., US
LSM 780 confocal microskope	Zeiss, Germany
Observer Z1	Zeiss, Germany
Peristaltic pump	GE Healthcare, US
pH meter PB-11	Sartorius, Germany
Pipettes	Gilson, France; Eppendorf, Germany

Device	Manufacturer
Power supply	BioRad, US
Qubit Fluorometer	Thermo Fisher Scientific, US
SDS-PAGE equipment	BioRad, US
Shaking incubators bacteria cultures	New Brunswick, US
Shaking tube heating block	Eppendorf, US
Sonoplus HD70 Sonicator	Bandelin, Germany
Spectrophotometer Ultrospec 10	GE Healthcare, US
Te-Inject-reagent injectors	Tecan, Austria
VacuSafe pump	Integra, Switzerland
VacuSip pump	Integra, Switzerland
Water bath	GFL, Germany

2.1.2 Chemicals and consumables

Material	Manufacturer
12 mm round cover slips	Paul Marienfeld, Germany
64-well incubation chambers	Grace Bio-Laboratories, US
96 well plates for ELISA	Thermo Fisher, US
96 well plates for Luminex	Greiner Bio-One, Austria
Acetic acid	Merck KGaA, Germany
Acetone	Carl Roth, Germany
Acrylamide 30 %	Carl Roth, Germany
Agar	Carl Roth, Germany
ATP	Carl Roth, Germany
Bacto tryptone	Carl Roth, Germany
Beta-Mercaptoethanol	Carl Roth, Germany
Bio-Plex Pro Magnetic COOH *beads*	Bio-Rad, US
Bromphenol blue	Merck KGaA, Germany
BSA	Carl Roth, Germany
$CaCl_2$	Carl Roth, Germany
Citric acid	Carl Roth, Germany
Counting chamber	PAA Laboratories, US

Material	Manufacturer
CSA	Sigma-Aldrich, Germany
DAPI	Sigma-Aldrich, Germany
DB71	Sigma-Aldrich, Germany
DMEM	Capricorn Scientific GmbH, Germany
DMSO	Sigma-Aldrich, Germany
dNTPS	Carl Roth, Germany
Dream*Taq* DNA polymerase	Thermo Fisher Scientific, US
DTT	Carl Roth, Germany
ECL substrate	Self-made
EDC	Thermo Fisher Scientific, US
EDTA	Carl Roth, Germany
Ethanol	Carl Roth, Germany
FAGLA	Alfa Aesar, Germany
FCS	Sigma-Aldrich, Germany
Fluoromount	Sigma-Aldrich, Germany
GeneRuler 1 kb Plus DNA Ladder	Thermo Fisher Scientifc, US
Glycerol	Carl Roth, Germany
hCD1	Merck, Germany,
HCl	Carl Roth, Germany
HEPES	Carl Roth, Germany
HisTrap HP 1 ml column	GE Healthcare, US
HiTrap Protein A HP antibody purification column, 1 ml	GE Healthcare, US
Imidazol	Fluka, Germany
Inoculation loops, 10 µl	VWR, Germany
IPTG	PEQLAB Biotechnologie GmbH, Germany
Isopropanol	Carl Roth, Germany
KCl	Carl Roth, Germany
Low-bind reaction tubes	Corning Costar, US
Low-melt agarose	Carl Roth, Germany
Lymphoprep	Stemcell, US
MES	Carl Roth, Germany
$MgCl_2$	Carl Roth, Germany

Material	Manufacturer
Midori green direct nucleic acid stain	Nippon Genetics Europe, Germany
Mowiol	Sigma-Aldrich, Germany
NaCl	Carl Roth, Germany
NADH	Carl Roth, Germany
NaH_2PO_4	Carl Roth, Germany
$NaHCO_3$	Carl Roth, Germany
NanoQuant quartz plate	Tecan, Austria
Natriumazide	Carl Roth, Germany
Nitrocellulose membrane	GE Healthcare, US
PageRuler™ Prestained Protein Ladder	Thermo Fisher Scientific, US
Parafilm	Pechiney plastic packaging, US
Penicillin-Streptomycin (100 units/ml)	Biochrom AG, Germany
Porcine LDH	Carl Roth, Germany
Protease inhibitor c0mplete EDTA-free	Roche, Switzerland
Q5® High-Fidelity DNA Polymerase	New England Biolabs, US
qPCR plate and cover strips	Thermo Fisher Scientific, US
Quartz plate	Hellma, Germany
Reaction tubes, 0.5 – 2 ml	Neolab, Germany
Reaction tubes, 15 & 50 ml	TPP, Switzerland
Restriction enzymes	New England Biolabs, US
RNA Later	Qiagen, Germany
SDS	Carl Roth, Germany
Sephadex columns	GE HEalthcare, US
SepMate-50 tubes	Stemcell, US
Six-well glass microscopic slides	Paul Marienfeld, Germany
Skimmed milk powder	Carl Roth, Germany
Sodium pyruvate	Biochrom AG, Germany
StabilGuard®	Surmodics, US
Sterile filter 0.45 µm	TPP, Switzerland
Sulfo-NHS	Thermo Fisher Scientific, US
Sulfuric acid	Carl Roth, Germany
T. gondii strain ME49 oocysts	JP Dubey, US
TEMED	Carl Roth, Germany

Material	Manufacturer
TFE	Carl Roth, Germany
$TgSAG1_{bio}$	(Klein et al., 2020)
Thermolysin	Promega, US
Tris-glycine	Merck KGaA, Germany
Tris-HCl	Carl Roth, Germany
Trypsin/EDTA solution (10x)	Biochrom AG, Germany
Tween-20	Merck, Germany
Uric acid crystals	Sigma-Aldrich, Germany
Uricase	Sigma-Aldrich, Germany
Vivaspin 2, 10,000 MWCO PES	Sartorius, Germany
Whatman paper	Carl Roth, Germany
Yeast extract	Carl Roth, Germany
Yellow fluorescent polystyrene beads	Spherotech, US

2.1.3 Bacteria strains

Name	Description	Antibiotic resistance	References
BW25113	Used for TgLEA expression and growth assays; Δ(araD-araB)567, ΔlacZ4787(::rrnB-3), λ-, rph-1, Δ(rhaD-rhaB)568, hsdR514	-	(Datsenko and Wanner, 2000)
JW5312-3	"cold sensitive"; ∆(araD-araB)567, ∆lacZ4787(::rrnB-3), λ-, ∆otsA747 ::kan, rph-1, ∆(rhaD-rhaB)568, hsdR514	Kanamycin	(Baba et al., 2006)
LOBSTR	Reduces contamination with unwanted proteins during purification; Used for TgLDH1 expression; gifted by Furio Spano	-	(Andersen et al., 2013)
OmniMAX 2T1R	Sensitive to ccdB toxin, used for positive selection of cloned genes via SLiCE; Thermo Fisher, US; F′[proAB+ $lacI^q$ lacZΔM15 $Tn10(Tet^R)$ Δ(ccdAB)] mcrA Δ(mrr-hsdRMS-mcrBC) φ80(lacZ)ΔM15 Δ(lacZYA-argF)U169 endA1 recA1 glnV44 thi-1 gyrA96(NalR) relA1 tonA panD	Tetracyclin	proprietary

2.1.4 *T. gondii* strain and host cells

Name	Description
BJ-5ta	HFF cells for maintenance of *T. gondii* strains. Cells were immortalized after transfection with human telomerase reverse transcriptase (hTERT); LGC Standards GmbH, Germany
RhßGFPmt	*T. gondii* strain expressing a green fluorescence protein in the mitochondria and the β-galactosidase enzyme

2.1.5 Solid and liquid growth media

Name	Composition
E. coli freezing medium	700 µl LB medium + 300 µl sterile glycerol = 15 % glycerol (v/v)
HFF growth medium	DMEM high glucose (4.5 g/l) with sodium pyruvate and stable glutamine containing 10 % heat-inactivated FCS and 100 µg/ml Penicillin-Streptomycin
Hypertonic growth agar	LB agar containing 342 mM NaCl (2x)
Hypotonic growth agar	LB agar without NaCl
LB agar / isotonic growth agar	LB medium + 20 % (w/v) agar
LB Medium	10 g/l Bacto-Tryptone; 5 g/l yeast extract; 171 mM NaCl (pH 7.0)
SOC medium	20 g/l Bacto Tryptone; 5 g/l yeast extract; 0.5 g/l NaCl; 2.5 mM KCl; 10 mM MgCl2 (pH 7.0)
T. gondii growth medium	DMEM high glucose (4.5 g/l) with sodium pyruvate and stable glutamine containing 2 % heat-inactivated FCS and 100 µg/ml Penicillin-Streptomycin
T. gondii freezing medium	90 % (v/v) of HFF growth medium + 10 % of DMSO

2.1.6 Buffers and solutions

Name	Composition
10x SLiCE buffer	500 mM Tris-HCl (pH 7.5), 100 mM $MgCl_2$*6 H_2O, 10 mM ATP, 10 mM DTT
AEO-IFA blocking buffer	PBS, 3 % (w/v) BSA
Binding buffer	50 mM NaH_2PO_4, 500 mM NaCl, 20 mM Imidazol (pH 8)
DB71 destaining solution	50 % (v/v) absolute ethanol, 15 % (v/v) 1M $NaHCO_3$, in a. dest.
Direct Blue 71 (DB71) whole protein staining	8 % (v/v) of 0.1 % DB71 stock solution in 40 % ethanol / 10% acetic acid solution
ELISA BSA blocking buffer	PBS, 0.1 % (v/v) tween-20, 3 % (w/v) BSA
ELISA milk blocking buffer	PBS, 0.1 % (v/v) tween-20, 5 % (w/v) skimmed milk powder
Elution buffer	50 mM NaH_2PO_4, 500 mM NaCl, 500 mM Imidazol (pH 8)
IgG neutralizing buffer	1 M Tris-HCl in a. dest. (pH 9)
IgG purification binding buffer	20 mM NaH_2PO_4 in a. dest.
IgG purification elution buffer	0.1 M citric acid in a. dest (pH 3 to 6).
Inoue transformation buffer	55 mM $MnCl_2$*$4H_2O$; 15 mM $CaCl_2$·$2H_2O$; 250 mM KCl; 10 mM PIPES (pH 6.7)
Laemmli buffer	250 mM Tris, 25 % (v/v) glycerol, 7.5 % (w/v) SDS, 0.25 mg/ml bromphenol blue, 12.5 % (v/v) ß-mercaptoethanol in a. dest.
LDH activity assay buffer	100 mM NaH_2PO_4, 100 µM NADH, 2 mM pyruvate (pH 8)
Lectin binding buffer	50 mM HEPES, 5 mM $MgCl_2$, 5 mM $CaCl_2$
Luminex assay buffer	PBS, 1 % (w/v) BSA
Lysis buffer	50 mM NaH_2PO_4, 300 mM NaCl, 10 mM Imidazol (pH 8)
PBS	13.7 mM NaCl; 8.0 mM Na_2HPO_4; 2.7 mM KCl; 1.5 mM KH_2PO_4 (pH 7.4)
TAE electrophoresis buffer	40 mM Tris; 20 mM acetic acid; 1 mM EDTA
Thermolysin resuspension buffer	50 mM Tris-HCl, 0.5 mM $CaCl_2$ (pH 8)
Western blot / ELISA / Luminex washing buffer	PBS, 0.1 % tween-20
Western blot blocking buffer	PBS, 0.1 % (v/v) tween-20, 5 % (w/v) skimmed milk powder

Name	Composition
Western blot transfer buffer	20 % (v/v) ethanol, 10 % (v/v) Tris-Glycine. 70 % a. dest.

2.1.7 Antibiotics

Name	Working concentration [µg/ml]
Kanamycin	50
Tetracyclin	50
Timentin	25

2.1.8 Antibodies, lectins & CLRs

Name	Origin	Dilution
3B11	Furio Spano, Italy	IFA: 1:500
3G4	Aurélien Dumétre, France	IFA: 1:25
Anti-6His-tag	Linaris, Germany	WB: 1:2,000
Anti-chicken IgY PE	Rockland Immunochemicals, US	Luminex: 1:333
Anti-chicken IgY PO	Dianova, Germany	ELISA: 1:5,000
Anti-human IgG Fc DyLight-650	Dianova, Germany	IFA: 1:500
Anti-Lama-DyLight-650	Dianova, Germany	IFA: 1:500
Anti-mouse IgG PO	Dianova GmbH, Germany	WB: 1:5,000
Anti-mouse IgM Cy5	Dianova, Germany	IFA: 1:500
Anti-rabbit IgG PO	Dianova, Germany	ELISA: 1:5,000 WB: 1:3,000
Anti-TgLEA-850 & -860	Preclinics, Germany	ELISA, LX: 1:2,000
CLR-hFc-fusion protein-library	Bernd Lepenies (Mayer et al., 2018)	IFA: 2.5 ng/µl
MPA-FITC	Vector Laboratories, US	IFA: 1:100
Anti-llama secondary antibody	Invitrogen, US	Microarray: 1:400

2.1.9 Plasmids

Name (length)	Details	Resistance marker
pQE90S_TgLEA-850	Obtained from GenExpressGmbH, Germany; proprietary plasmid, full sequence not known, IPTG inducible expression of codon adapted TgLEA-850 with C-terminal 6His-tag	Amp
pQE90S_TgLEA-860	Self-cloned, proprietary plasmid from GenExpress GmbH as backbone, full sequence not known, IPTG inducible expression of TgLEA-860 isolated from *T. gondii* RH-strain without signal peptide in frame with a C-terminal 6His-tag	Amp
pQE90S_TgLEA-870	Obtained from GenExpressGmbH, Germany; proprietary plasmid, full sequence not known, IPTG inducible expression of codon adapted TgLEA-870 with C-terminal 6His-tag	Amp
pQE90S_TgLEA-880	Obtained from GenExpressGmbH, Germany; proprietary plasmid, full sequence not known, IPTG inducible expression of codon adapted TgLEA-880 with C-terminal 6His-tag	Amp
pAviTag_TgLEA-LDH1 (3,343 bp)	Self-cloned, backbone from Expresso Biotin Cloning and Expression System, Lucigen; IPTG inducible expression of TgLDH1 isolated from tachyzoites of the RH strain (see Figure 56: Plasmid map of pAviTag_TgLDH1	Kan

2.1.10 Oligos

Name	Sequence (5‘ → 3‘)
LDH-1_SL-fwd	AAGAAGGAGATATACATATGGCACCCGCACTTGTGCAGAG
LDH-1_SL-rev	GTCGGCGGGGTGGATAAGCTCGCCTGAAGAGCAGCAACCG
LEA_860_SLiC_fwd	ATTCATTAAAGAGGAGAAATTACATATGGAAACAGCCGGACAAAA
LEA_860_SLiC_rev	TTAAGCATTCTGCCGACATGGAAGCTTAATGGTGATGGTGATGGTGCTCC TCCCGTTTTTTTT

Nslic-AlpVh-F1	CCAGCCGGCCATGGCCCAGGTGCAGCTGCAGKTGCAGCTCGTGGAGTCNGGNGG
Nslic-F4-rev	CGTAGTCCGGAACGTCGTACGGGTAGCGGCCGCTTGAGGAGACRGTGACCTGGGT
pEtite-rev	CCTCAAGACCCGTTTAGAGGC
pQE90S_col_PCR-rev	AATTACGCCCCGCCCTGCCA
pRham-fwd	GCTTTTTAGACTGGTCGTAGGGAGA
T7_prom_fwd	TAATACGACTCACTATAGGG

2.1.11 Commercial kits

Name	Manufacturer
1-Step Ultra TMB-ELISA Substrate Solution	Thermo Fisher Scientific, US
Agilent RNA 6000 Nano Kit	Agilent, US
BigDye Terminator v3.1 Cycle Sequencing Kit	Applied Biosystems, US
DNA Clean & Concentrator	Zymo Research Europe, Germany
GloMelt Thermal Shift Protein Stability Kit	Biotium, US
InstantBlue Coomassie Protein Stain	Abcam, US
Pierce 660nm Protein Assay Reagent	Thermo Fisher Scientific GmbH, US
PrimeScript RT-PCR Kit	Takara Bio Inc., Japan
PureLink HiPure Plasmid Midiprep Kit	Life Technologies GmbH, Germany
QIAshredder spin column	Qiagen, Germany
Qubit Protein Assay Kit	Thermo Fisher Scientific, US
RNeasy Plus Mini Kit	Qiagen, Germany
Zyppy Plasmid Miniprep Kit	Zymo Research Europe, Germany

2.1.12 Software & databases

Name	Source
Affinity Suite	Serif, UK

AxioVision Rel. 4.8	Zeiss, Germany
BLAST	blast.ncbi.nlm.nih.gov/Blast.cgi
CFX Maestro	Bio-Rad, US
Creative Suite 6	Adobe, US
E. coli genotypes	openwetware.org/wiki/Escherichia_coli
Geneious 11.1.5	Biomatters Ltd., New Zealand
Graphpad Prism 8	GraphPad, US
i-control 1.10	Tecan, Austria
ImageJ 1.51g	National Institute of Health, US
MobiDB 4.0	mobidb.bio.unipd.it/
ODiNPred	st-protein.chem.au.dk/odinpred
Office Professional	Microsoft, US
PS Remote	Breeze Systems, UK
Pubmed	National Center for Biotechnology Information (NCBI)
ToxoDB	toxodb.org/toxo
WinDaq	DataQ, US
ZEN 2012	Zeiss, Germany

2.2 Methods

2.2.1 Oocyst inactivation and treatment

For the first immunization, whole oocysts were divided into two batches. One batch was inactivated via incubation for 1 min at 60 °C. The other group was inactivated via repeated freezing in an ethanol-dry ice bath and subsequently thawing at room temperature. This process was repeated in total three times. Oocysts from both groups were tested in mouse bioassay for infectivity. No cyst formation was observed four weeks after infection and oocysts were thus assumed to be inactivated. Mouse bioassays were performed by the group of Gereon Schares, FLI, Greifswald, Germany. Oocysts from both groups were pooled 1:1 prior to alpaca immunization.

For the second, intramuscular immunization, oocysts were shredded using a sonicator and successful shredding was confirmed microscopically. In addition to inactivation, oocysts were radiated with a dosage of 40,093.7 cGy to remove microbial contamination.

2.2.2 Alpaca Immunization

The first immunization scheme included 7 weekly subcutaneous injections of 10^6 whole inactivated oocysts and GERBU adjuvans 1:1 with final extraction of approx. 100 ml blood 3 d after the last immunization.

For the second immunization, $7 * 10^6$ fractionated, irradiated inactivated oocysts and Freud adjuvant in a ratio 1:1 were applied intramuscular over 12 weeks in monthly intervals. Again, approx. 100 ml of final blood were extracted 3 d after the final immunization. In both cases, the blood was immediately processed to PBMC isolation.

All immunization procedures were conducted by animal facility personnel of the FLI, Greifswald, Germany, and were ethically approved by the “Landesamt für Landwirtschaft, Lebensmittelsicherheit und Fischerei” of the German Federal State of Mecklenburg-Western Pomerania. Care and maintenance of the animal were in accordance with governmental and institutional guidelines.

2.2.3 PBMC isolation

PBMCs were isolated using Stemcell SepMate-50 tubes and Lymphoprep according to the manufacturer’s instructions. In brief, blood was diluted with PBS 1:1 and tubes were prefilled with 15 ml Lymphoprep. Diluted blood was pipetted above Lymphoprep. Tubes were than centrifuged at 1,200 g for 10 min and separated plasma containing PBMCs transferred to a new tube. PBMCs were than washed twice with PBS at 300 g for 8 min and afterwards stored in RNA later until further use.

2.2.4 RNA extraction and cDNA reverse transcription

RNA was extracted form cells using the RNeasy Plus kit in combination with QIAshredder and gDNA elimination columns, all from Qiagen, according to the manufacturer's instructions. Cells were counted using Neubauer improved counting chambers and 10^7 Cells were used per reaction. RNA was eluted from the column in 30 µl RNase-free water. RNA quality was assessed using the Agilent 2100 Bionalyzer system and the RNA 6000 Nano kit.

cDNA reverse transcription was carried out using Primescript RT-PCR kit from Takara according to the manufacturer's instructions. Briefly, 4 µl template RNA were mixed with 1 µl provided dNTPs, 1 µ provided random 6-mer primers and 4 µl of RNase-free a. dest. And placed in a thermal cycler at 65 °C for 7 min for RNA denaturation and to facilitate primer annealing. Subsequently, 4 µl 5x PrimeScript buffer, 20 units of RNase inhibitor, 0.5 µl of PrimeScript RTase and 5 µl of RNase-free a. dest. were added to the mix. Tubes were again placed in thermal cycler under the following protocol: 30 °C for 10 min, 42 °C for 1 h, 72 °C for 15 min. Afterwards, cDNA was stored at -80 °C until further use.

2.2.5 PCR

PCR was routinely used to isolate genetic sequences for subsequent cloning and to confirm successful transformation of bacteria. If high sequence accuracy was not required, e.g., for sequence confirmation, DreamTaq polymerase was used. In these cases, composition of 25 µl reaction mixtures was as follows: 2.5 µl 10x *DreamTaq*™ buffer, 0.2 mM of each dNTP, 1.25 units polymerase, approx. 100 ng DNA and 0.2 µM of each fwd and rev oligonucleotide contained in nuclease-free a. dest. General PCR protocol was as follows: 95 °C for 2 min, 95 °C for 30 s, T_m-5 for 30 s where T_m is the melting point of the individual oligonucleotide pairs, 72 °C for 1 min. The last three steps were repeated for a total of 30 cycles, followed by 72 °C for 7 min and subsequent incubation at 4 °C until further processing.

In cases where high sequence accuracy was required, e.g., for cloning of *T. gondii* sequences into *E. coli*, Q5 polymerase was used and the PCR protocol adjusted as follows: 25 µl reaction mixtures consisted of 5 µl 5x Q5 reaction buffer, 0.2 mM of each dNTP, 0.5 units of Q5 polymerase, approx. 100 ng template DNA 0.2 µM of each fwd and rev primer were contained in 25 µl a. dest. The PCR protocol was as follows: 98 °C for 30 s, 98 °C for 10, T_m-5 for 20 s, 72 °C for 25 s. The last three steps were repeated for a total of 30 cycles, followed by 72 °C for 2 min and subsequent incubation at 4 °C until further processing.

Colony PCR to facilitate easy processing of high numbers of possible clones were done mostly like general DreamTaq PCR. Instead of 100 ng DNA, cellular material of 1 individual colony was transferred to the DNA mixture using a 200 µl sterile pipette tip and the initial denaturation step of the protocol was extended to 3 min at 95 °C.

2.2.6 Agarose gelelectrophoresis

For electrophoretic analysis, PCR products were mixed with 1:10 *Midori Green Direct* DNA dye and applied to 0.8 % agarose gel in 1x TAE buffer. The electrophoretic separation was then carried out after applying a voltage of 100 V in a horizontal gel chamber for 45 min. Separation of the DNA bands was visualized using a blue light transilluminator, detecting Midori green mediated fluorescence at approx. 500 nm. Size of observed bands was determined with the DNA size standard GeneRuler 1 kb Plus DNA Ladder. Desired DNA fragments were isolated by excision for downstream applications. DNA was purified from the agarose gel for downstream processing using the Zymoclean Gel DNA Recovery Kit according to the manufacturer's instructions. Concentration of DNA was assessed at the Inifinite M200 Tecan plate reader using a NanoQuant quartz plate.

2.2.7 Glycan microarray analysis for epitope mapping

Alpaca sera from different timepoints during the immunization procedure were characterized on the glycan microarray at the Max Planck Institute of colloids and interfaces, Berlin, Germany. Microarray slides displaying *T. gondii* specific GPI structures were blocked with 1 % (w/v) BSA in PBS for 1 h at RT, rinsed with ultrapure water and dried by centrifugation. 64-well incubation chambers were applied to the microarray slides. 25 µL of sera diluted 1:50 in PBS were added to each well for incubation overnight at 4 °C in a humidified chamber. Following incubation, sera were discarded and the wells rinsed with 0.05 % (v/v) Tween-20 in PBS. Anti-llama secondary antibodies were added to each well, diluted 1:400 with 1 % (w/v) BSA, 0.05 % (v/v) Tween-20 in PBS and incubated on the microarray slides for 1 h at RT. Microarray slides were rinsed repeatedly first with 0.1% (v/v) Tween-20 in PBS, then PBS only, finally with ultrapure water, and then dried by centrifugation. Microarray slides were scanned with a GenePix 4300A microarray scanner. Background-subtracted MFI values reflected the antibody titer present in the sera.

2.2.8 AEO-IFA

Individual wells of six-well glass microscopic slides were coated with 10 ml of 1 % (wt/vol) low-melt agarose dissolved in a. dest. and air-dried, after which they were stored at 4 °C until use. Inactivated oocysts in PBS ($2.5 * 10^5$/ml) and 1 % low-melt agarose were mixed 1:1 (vol/vol) prior to being loaded onto the microscopic slide. A total of 3-ml drops of the resulting oocyst-agarose suspension were rapidly dispensed onto the prepared wells of the slide and distributed evenly using a pipette tip. For blocking, 20 ml of blocking buffer was dispensed onto each well, and slides were incubated overnight at room temperature in a humidified chamber with slight agitation. For acetone permeabilization, slides were placed in a vertical microscopic slide holder filled with ice-cold acetone and incubated at -20°C for 30 min. The slides were then removed from the holder, and acetone was evaporated on air at room temperature. Then, either 7.5 µl of CLR binding buffer and 2.5 µl of CLR, 10 µl of a 1:25 dilution of 3G4 antibody,

10 µl of a 1:500 dilution of 3B11 antibody, 10 µl of a 1:10 dilution of alpaca serum, or 10 µl of a 2-mg/ml MPA-FITC solution were added to each well. The slides were incubated in a humidified chamber at room temperature for 2 h without agitation and then washed three times with 20 µl PBS per well before 10 µl of secondary antibody in blocking buffer was pipetted onto each well. Slides were again incubated for 2 h at room temperature in a humidified chamber. After washing as described above, 1.5 µl Fluoromount or Mowiol was pipetted into each well, which then was individually covered with a 12-mm round coverslip, and light pressure was applied and left for 10 min at room temperature for the mounting medium to harden. For color-blind-friendly visualization, colors of the fluorescent channels were adjusted as follows: blue to cyan, red to magenta, and green to yellow (Wong, 2011).

2.2.9 *In silico* analyses

CIDER analysis was performed using version 1.7[Full] at http://pappulab.wustl.edu/CIDER/analysis/ in April 2021. Disorder prediction via MobiDB was performed using version 4.0 at: https://mobidb.bio.unipd.it/ in April 2021. Blastp analysis against the LEA protein data base was performed at http://forge.info.univ-angers.fr/~gh/Leadb/index.php?action=2&mode=5&viewseq=3 in April 2021. GRAVY scores were calculated using the Sequence Manipulation Suite at https://www.bioinformatics.org/sms2/protein_gravy.html in April 2021. Sequence synteny was assessed using Release 53 of Toxodb at https://toxodb.org in July 2021 and PFAM classification of TgLEAs was performed using Motif Scan at https://myhits.sib.swiss/cgi-bin/motif_scan in July 2021.

2.2.10 Cloning and Transformation

Plasmid DNA was introduced into bacteria by heat shock and bacteria were prepared for heat shock mediated DNA uptake (made “chemically competent”) according to the method published by Inoue et al. (Inoue et al., 1990). The OmniMAX2T1 *E. coli* strain was used for transformation of DNA constructs. Briefly, bacteria were transferred to 25 ml liquid LB medium with appropriate antibiotic and incubated at 37 °C and 250 rpm for 6-8 h at 225 rpm. Three 1 L flasks filled with 250 ml each of antibiotic supplemented medium were inoculated with 2, 4 or 10 ml of the preculture. The subsequent overnight incubation at 18 °C at 225 rpm was stopped after one culture reached an OD_{600} of 0.5. The respective culture was chilled on ice for 10 min prior to centrifugation at 4°C for 10 min at 2,500 g. The supernatant was discarded, and the cells gently resuspended in 40 ml of ice-cold Inoue transformation buffer and afterwards centrifuged as described above. The buffer was removed, and the pellet was resuspended in 10 ml of ice-cold Inoue transformation buffer, supplemented with 750 µl DMSO. After incubation on ice for 10 min, the suspension was divided into 100 µl aliquots and snap-frozen in liquid nitrogen. The chemically competent cells were immediately transferred to -70°C for storage.

Plasmids were constructed following the SLiCE cloning method published by Zhang et al. (Zhang et al., 2014). The method enables single-step cloning. A prerequisite is the amplification of the gene of interest with very long oligonucleotides encoding for recombinase sites in their overhangs, that are present in the cloning site of the recipient plasmid. Incubation of plasmid, PCR product and recombinase together leads to facile gene insertion in the vector. SLiCE buffer and extract were prepared following the published protocol, aliquoted and stored at -80 °C until use. In general, SLiCE reaction mixture was as follows: 100 ng of vector, 1 µl of SLiCE extract, 1 µl SLiCE buffer and an insert:vector ratio of 6:1. Total reaction volume was adjusted to 10 µl with a. dest. The reaction mixture was incubated at 37 °C for 1 h and afterwards transformed into chemically competent OmniMAX2T1.

For transformation via heat shock, 1 aliquot of chemically competent OmniMAX2T1 was thawed on ice and subsequently incubated on ice for 30 min with 5 µl of the SLiCE reaction mixture. Additionally, cells were incubated with a. dest. as a negative control and 5 ng of pUC19 plasmid DNA as a positive control. After incubation on ice, cells were exposed to 42 °C in a water bath for 1 min. Immediately afterwards, 500 µl SOC medium was added to the cells and they were incubated at 37 °C and 200 rpm for 1 h. Positive clones were selected by plating 200 µl of the transformation mixture on solid LB agar plates supplemented with the respective antibiotic and grown overnight at 37 °C.

Transformation efficiency for newly prepared chemically competent *E. coli* was determined following this formula:

$$Transformants\ per\ \mu g\ DNA\ = \frac{colonies\ \times total\ V\ (\mu l)}{plated\ V\ (\mu l) \times dilution\ factor\ \times \mu g\ DNA}$$

Grown colonies were used to inoculate 5 ml cultures that were grown at 37 °C and 225 rpm overnight for storage and colony PCR was conducted in parallel to confirm successful cloning.

2.2.11 Cultivation of host cells and *T. gondii strains*

Adherently growing HFF cells were cultured in HFF growth medium under 5 % CO_2 at 37 °C and transferred to a new culture when confluency was reached. For this purpose, the medium contained in the cell culture flasks was aspirated and cells were washed twice with 10 ml of PBS. Cells were detached by adding 1 ml of trypsin / EDTA solution (1x), followed by 5 min incubation at 37 °C. Afterwards, cells were resuspended in 10 ml of HFF growth medium and transferred to a 15 ml centrifuge tube and centrifuged for 4 min at 300 g. After discarding the supernatant, the pelleted cells were resuspended in an appropriate volume of HFF growth medium and distributed into new culture flasks.

T. gondii tachyzoites were cultured on HFF cells in *T. gondii* growth medium under 5 % CO_2 and at 37 °C. Every other day ~ 0.5 ml of a freshly lysed tachyzoite suspension was transferred to an uninfected cell culture flask with confluent HFF cells with a Pasteur pipette.

2.2.12 Cloning of TgLEA-860

The coding sequence of TgLEA-860 was isolated from DNA of *in vitro* grown tachyzoites of the RH strain of *T. gondii*, using primers LEA_860_SLiC_fwd and LEA_860_SLiC_rev. These primers were designed to remove the signal peptide of 25 aa at the N-terminus from the isolated sequence as well as allow SLiCE cloning of the sequence into the same vector used for expression of the other TgLEA-proteins (pQE90S). Linearized pQE90S vector and TgLEA-860 PCR fragment were SLiCE cloned into chemically competent Omnimax *E. coli* cells and isolated plasmid DNA from positively identified clones was subsequently transformed into chemically competent *E. coli* cells of the same strain as for the other TgLEA proteins (BW25113, JW5312-3).

2.2.13 Culturing of *E. coli*

The cultivation of the different *E. coli* strains was mostly carried out at 37 °C and 225 rpm in liquid LB medium or on LB agar plates with addition of the appropriate antibiotics. For the permanent storage of the strains, 700 µl of an overnight liquid culture were mixed with 300 µl of 50 % sterile glycerol, immediately snap-frozen in liquid nitrogen and stored at -80 °C.

2.2.14 Bacterial growth assays

E. coli strains expressing one TgLEA or a non-functional peptide were streaked out from cryo stocks on LB agar containing the appropriate antibiotics for selection of plasmid containing bacteria and incubated overnight at 37 °C. Material from one singular colony was used to inoculate 5 ml liquid LB medium containing appropriate antibiotics, using a sterile pipette tip. The inoculated culture was grown at 37 °C at 225 rpm until an OD_{600} of 0.5, at which point protein expression was induced by addition of IPTG or simulated by addition of the same volume of PBS. Cultures were allowed to grow for 3 h after induction. Afterwards, the final OD_{600} was determined, and the cultures were divided into three 1.5 ml aliquots in 2 ml reaction tubes and the cells were pelleted by centrifugation at 4,000 rpm for 5 min at 4 °C. The pelleted cells were washed two times with ice-cold PBS. Washed cells were either stored at -20 °C for later confirmation of protein expression via western blot or immediately resuspended in PBS. For resuspension, the number of cells per tube was calculated from the final OD_{600} and the volume of PBS for resuspension was adjusted to a final concentration of 10^9 cells per ml. Cells were either exposed to incubation at -20 °C for 1 d or 4 °C for 7 d (cold temperature stress), incubation at 50 °C for 30 or 60 min, respectively (high temperature stress), or processed immediately as follows (no stress). 10^8 cells were transferred to the first column of a 96-well plate, where ten-fold serial dilutions were performed in PBS using a multi-channel pipette ranging from 10^{-1} to 10^{-7}. 10 µl drops of 10^{-2} to 10^{-7} dilutions were transferred in triplicates to

LB agar plates containing appropriate antibiotics in hyper- and hypoosmotic growth medium, respectively (osmotic stress), or regular LB agar supplemented with appropriate antibiotics (no stress). Cells exposed to high and low temperature stress were processed similarly. LB agar plates were left to dry for 10 min and then incubated overnight at 37 °C or in an exsiccator at RT for 7 d and then at 37 °C overnight (desiccation stress). Afterwards, cells were counted, the number of surviving cells after stress determined and normalized to growth without stress. For easy detectability to facilitate colony counting, 1 % triphenyl tetrazolium chloride was added to the LB agar, resulting in red strained *E. coli* colonies.

2.2.15 Recombinant expression and purification of TgLEAs

E. coli expressing the desired protein were streaked out from cryo stocks on LB agar containing timentin for selection of plasmid containing bacteria and incubated overnight at 37 °C to isolate singular colonies. A 5 ml liquid LB culture supplemented with timentin was inoculated with material from one individual colony by sterile pipette tip and again incubated overnight at 37 °C and 225 rpm. This constituted the pre-culture. For protein expression, 500 ml of liquid LB medium supplemented with timentin was inoculated with the pre-culture and grown at 37 °C and 225 rpm until OD_{600} reached 0.5, at which point the expression was induced with 500 µM IPTG and the culture was grown for 3 h under the same conditions. After incubation, bacterial cultures were spun down for 20 min at 4,000 rpm and 4 °C. The supernatant was discarded and the pelleted cells were resuspended in 10 ml ice-cold lysis buffer supplemented with c0mplete protease inhibitor. The cell lysate was sonicated on ice in a Sonoplus HD70 sonicator for a total of six bursts à 30 s. In general, after sonication, the cell lysate was incubated for 10 min in a boiling water bath. For comparison, in heat sensitivity experiments, a portion of cell lysate was not incubated in a boiling water batch and processed immediately. Prior to filtration, the cell lysate was spun down for 10 min at 10,000 g and 4 °C and the resulting supernatant was sterile filtered using 10 ml syringes and filters of 0.45 µm pore size. Filtered lysate was stored at -20 °C until further use.

Proteins were purified using HisTrap HP or FF 1 ml columns, prepacked with precharged Ni-Sepharose for affinity chromatography of histidine-tagged proteins. The columns were loaded using a peristaltic pump with a flow rate of 1 ml/min and connected to a EM-1 Econo UV monitor to observe protein concentration in eluted fractions. The signal from the UV monitor was transferred to an analog-digital converter connected to a computer and visualized in software. Prior to loading of lysate on the columns, they were washed with 5 ml of a. dest. and equilibrated with 5 ml of binding buffer. During equilibration, the absorbance measurement of the UV monitor was calibrated and defined as the baseline. Filtered lysate was run through the column and the flow-through was caught for later analysis. Columns were washed with at least 15 ml of washing buffer until the observed absorbance reached a steady baseline and washing

fractions were caught for later analysis. Tagged proteins bound to the column were eluted with 5 ml of elution and collected in 1 ml fractions when absorbance peaks were observed. Afterwards, columns were washed again with 5 ml of a. dest. and then 5 ml of 20 % ethanol before storage.

Buffer exchange of purified proteins was performed by washing three times with PBS using Vivaspin 2, 10,000 MWCO, PES columns according to the manufacturer's instructions. Protein concentration was determined using a Qubit Fluorometer and the Qubit Protein Assay Kit according to the manufacturer's instructions. Proteins were divided into aliquots and stored at -20 °C until further use.

2.2.16 SDS-PAGE and western blot

SDS-PAGE gel composition is detailed in Table 3 and Table 4. SDS-PAGE was run at 80 V until the sample front left reached the end of the stacking gel at which point voltage was increased to 120 V until the sample front reached the end of the resolving gel. Separated proteins were transferred from the gel to nitrocellulose membrane using a semidry blotting chamber and the manufacturer's pre-set parameters.

Table 3: Resolving gel composition.

	12 %	15 %
a. dest.	3.3 ml	2.3 ml
30 % Acrylamid	4 ml	5 ml
1.5 M Tris-HCl (pH 8.8)	2.5 ml	2.5 ml
10 % SDS	100 µl	100 µl
10 % APS	100 µl	100 µl
TEMED	10 µl	10 µl

Table 4: Stacking gel composition.

	5 %
a. dest.	1.7 ml
30 % Acrylamid	415 µl

	5 %
0.5 M Tris-HCl (pH 6.8)	315 µl
10 % SDS	25 µl
10 % APS	25 µl
TEMED	2.5 µl

Total protein stain as loading control was done via DB71 staining according to the protocol of Hong et al. (Hong et al., 2000) was performed. After the stain was completely washed off, non-specific binding sites were blocked overnight with blocking buffer. Subsequently, blocked membranes were incubated with desired primary antibody diluted in blocking buffer for 1 h at RT. After three washes with washing buffer, the membrane was incubated with horseradish peroxidase (PO)-conjugated secondary antibody diluted in blocking buffer. The membrane was afterwards again washed three times with washing buffer. Enhanced chemiluminescent PO substrate (ECL) was added and the signal detected in a Fusion FX luminescent image analyzer.

2.2.17 Protease sensitivity assay

Trypsin was dissolved in PBS to a final concentration of 0.2 ng/µl. For the assay, mixes of TgLEAs or control proteins with TFE concentrations of 10, 20 and 30 % (v/v) were prepared and the final mix volume was adjusted to 25 µl with PBS. Mixes were left to settle for 5 min, before 12.5 µl of trypsin (or PBS for the no trypsin control) were added to each mix for a final protein:thermolysin ratio of 10,000:1. The mixes were incubated at 25 °C for 1 h. After incubation, 8 µl of each mix were added to 2 µl of 5x Laemmli buffer and boiled for 5 min to inactivate the protease. Afterwards, the samples were analyzed by SDS-PAGE and Coomassie stain.

1 mg of thermolysin was dissolved in 1 ml of thermolysin resuspension buffer and subsequently diluted 1:10 in the same buffer for a final concentration of 0.1 µg/µl. For the assay, Mixes of TgLEAs or control proteins with TFE concentrations of 10, 15, 20, and 25 % (v/v) were prepared and the final mix volume was adjusted to 23.5 µl with a. dest. Mixes were left to settle for 5 min, before 1.5 µl of thermolysin (or a. dest. for the no thermolysin control) were added to each mix for a final protein:thermolysin ratio of 100:1. The mixes were incubated at 25 °C for 1 h. After incubation, 8 µl of each mix were added to 2 µl of 5x Laemmli buffer and boiled for 5 min to inactivate the protease. Afterwards, the samples were analyzed by SDS-PAGE and western blot.

2.2.18 Thermolysin susceptibility to TFE

Thermolysin was prepared as described above. Master mixes of FAGLA or PBS as control in thermolysin resuspension buffer and the same TFE concentrations as described above were prepared and preloaded in 198.5 µl triplicates in a 96-well quartz plate. The mixes were left to settle for 5 min, before 1.5 µl thermolysin (or a. dest. for the no thermolysin control) was added to the wells for a final protein:thermolysin ratio of 100:1. Absorbance at 345 nm was observed for 30 min at 25 °C and read in 1 min intervals using an Infinite M200 plate reader.

2.2.19 Thermal Shift Assay

Thermal shift assays (TSAs) were performed using the GloMelt Thermal Shift Protein Stability Kit. A working solution was prepared according to the manufacturer's instructions. Master mixes containing 9 µl of the GloMelt working solution and TgLEAs at a final concentration of 15 µM or the IgG control included with the kit at the proposed final concentration of 0.5 µg/ml were prepared on ice and the volume adjusted to 90 µl with HEPES buffer. Four 20 µl replicates were transferred to a 96-well qPCR plate, covered with corresponding strips and stored on ice. The plate was quickly spun down for 1 min at 1,000 rpm, and immediately transferred to a CFX96 Touch Real-Time PCR reader for analysis. The following melting curve parameters were applied: preincubation = 2 min at 0 °C; range = 0 – 99 °C; increments = 0.5 °C/min; read interval = 1 min. The data was exported to .txt format and analyzed using GraphPad Prism software.

2.2.20 Size exclusion chromatography (SEC)

SEC was performed by Frank Seeber and Sandra Klein, RKI, Germany, using an Äkta Purifier FPLC system and Sephadex columns following the manufacturer's instructions.

2.2.21 Circular dichroism spectroscopy

Circular dichroism (CD) spectroscopy was conducted by the group of Andreas Rummel at the Medizinische Hochschule Hannover, Germany. Briefly, CD data was collected with a Jasco J-810 spectropolarimeter in a 1 mm path length cuvette with a concentration of 2 µM respective protein in PBS pH 7.4. Spectra were recorded at 22 °C from 195 to 250 nm with 100 nm/min, response of 1 s, standard sensitivity, bandwidth of 1 nm and five accumulations. The spectra were analyzed, processed, and visualized using Spectra Manager II software (JASCO International Co. Ltd., Japan). Secondary structure estimation was conducted using the SSE module of Spectra Manager II applying Yang reference.

2.2.22 Cloning of TgLDH1

RNA was isolated from three tachyzoite cultures of the RH strain of *T. gondii* using the RNeasy Plus kit. Subsequently, RNA was reverse transcribed to cDNA using the PrimeScript RT-PCR kit. TgLDH1 sequence was amplified and prepared for SLiCE cloning via PCR using Q5 polymerase from cDNA using primers LDH-1_SL-fwd and LDH-1_SL-rev. Afterwards, the PCR

reaction was analyzed on an agarose gel and desired fragments were excised from the gel and purified using the Zymoclean Gel DNA Recovery kit. The PCR TgLDH1 fragment was SLiCE cloned into linearized pAviTag vector and subsequently transformed into chemically competent OmniMAX *E. coli.* Positive clones were selected on LB agar supplemented with kanamycin and tested for correct insertion by PCR using DreamTaq polymerase and primers pRham-fwd and pEtite-rev. The correct sequence was confirmed via sequencing of the plasmid using the same primers. For recombinant expression of TgLDH1, the plasmid was transformed into *E. coli* of the LOBSTR strain.

2.2.23 Recombinant expression and purification of TgLDH1

Recombinant expression of TgLDH1 in *E. coli* of the LOBSTR strain was mostly similar to TgLEA purification with minor adjustments. Precultures and expressing cultures were incubated at 15 °C and 200 rpm. Expression was induced with rhamnose at a final concentration of 0.2 %. Expression was allowed to proceed for 24 h. Cells were harvested and processed as described above, except that no incubation in a boiling water bath was performed. Successful TgLDH1purification was confirmed via SDS-PAGE and subsequent Coomassie staining using InstantBlue Coomassie Protein Stain according to the manufacturer's instructions. The stained gel was documented using a Fusion FX visualizer.

2.2.24 LDH aggregation assay

600 µl mixes of pLDH or TgLDH1 (final concentration: 12.5 µM) alone or with TgLEA or control protein (final concentration 25 µM) were prepared in PBS in 1.5 ml reaction tubes. The samples were left to settle for 5 min before 100 µl were transferred to a 96-well quartz plate for analysis in an Infinite M200 plate reader. This constituted aggregation before freeze-thawing. The samples were then submerged in liquid nitrogen for 30 s and then left to thaw at room temperature. Once completely thawed, 100 µl were taken off and transferred to the 96-well quartz plate and the absorbance at 280 nm and 340 nm was detected. This was repeated for a total of four times. The aggregation index for each sample after each freeze-thaw cycle was calculated with the following formula:

$$\frac{A_{340}}{(A_{280} - A_{340})}$$

Statistical significance was determined by multiple t test analysis.

2.2.25 LDH activity assay

60 µl master mixes of pLDH or TgLDH1 alone (final concentration: 0.5 µM) or with TgLEAs or control proteins in ratios of 1:25, 1:50 or 1:100 were prepared in 0.5 ml reaction tubes. The mixes were left to settle for 5 min, before three 3 µl replicates were transferred to a 96-well quartz plate for analysis in an Infinite M200 plate reader combined with Te-Inject-reagent injectors. 297 µl of LDH activity assay buffer were dispensed into each well and absorbance

at 340 nm was immediately observed for 1 min in 10 s intervals. This constituted activity without freeze-thawing. The LDH-protein mixes were submerged in liquid nitrogen for 30 s and then completely thawed at room temperature. Once thawed, 3 µl were transferred to the 96-well quartz plate in triplicates and analyzed as described above. This was repeated for a total of four freeze-thaw cycles. Enzyme activity was calculated following the Beer-Lambert law:

$$\frac{\Delta_A}{\varepsilon_{NADH} \times l} = \Delta_{c_{NADH}}$$

Where Δ_A is the difference in absorbance per minute, ε_{NADH} is the absorptivity of NADH ($\frac{6.2 \times 10^3}{M \times cm}$), l is the optical path length (approx. 0.8 cm) and $\Delta_{c_{NADH}}$ is the concentration of NADH processed per minute. Enzyme activity values determined this way were then normalized using the "normalize" function of GraphPad Prism software, where the largest mean of each individual dataset was defined as 100 % activity. Statistical significance was determined by multiple t test analysis.

2.2.26 Rabbit immunization and IgG purification

Rabbits were immunized with recombinantly expressed TgLEA-850 or -860 proteins by Preclinics, Germany. Extracted serum was confirmed in western blot for reactivity to TgLEA-850 or -860 proteins. IgG from serum were purified over Protein A columns from GE Healthcare, following the manufacturer's instructions.

2.2.27 Chicken sera

Sera from experimentally infected chickens (breed ISA JA 757) were provided by Dr. Berit Bangoura and Dr. Martin Köthe of the Veterinary Institute at Leipzig University, Leipzig, Germany and sera from naturally infected chickens were provided by Dr. Gereon Schares from the Friedrich Loeffler Institut, Greifswald, Germany. Experiments in chickens had been approved by the responsible authority (Landesdirektion Leipzig, Germany). Care and maintenance of animals were in accordance with governmental and institutional guidelines.

2.2.28 ELISA

96-well polystyrene plates were coated with 100 ng of TgLEA-850, -870 or -880 or $TgSAG1_{bio}$ or 200 ng TgLEA-860 per well by incubation with the required amount of protein diluted in blocking buffer at RT for 1 h. In experiments that required optimal presentation of possible epitopes to the interior of the well, wells were precoated with 100 µl of anti-histidine tag antibody at a concentration of 5 µg/ml by incubation overnight at 4 °C. After binding of the protein to the well wall, unbound protein was washed of three times with PBS, before blocking for 1 h at RT with 200 µl blocking buffer. After the blocking buffer was aspirated, wells were incubated with 100 µl of undiluted hybridoma supernatant against TgLEA-880, chicken or mouse sera diluted 1:200 in blocking buffer, purified anti TgLEA-850 and -860 rabbit IgG

diluted 1:2,000 in blocking buffer, or blocking buffer as secondary antibody control for 1 h at RT. Afterwards, wells were washed three times with 200 µl washing buffer and then incubated with 100 µl of appropriate PO-conjugated secondary antibody for 1 h at RT. Unbound secondary antibody was washed off three times with washing buffer before bound antibody was visualized by using 1-Step Ultra TMB-ELISA Substrate Solution according to the manufacturer's instructions. Reaction was stopped by addition of 50 µl 1 M sulfuric acid to each well. The plates were then analyzed using an Infinite M200 pro plate reader to measure absorbance at 450 nm. Uncoated wells that were only incubated with PBS were measured as blank values and used for correction of measured samples as were secondary antibody only controls. Purified rabbit IgG on uncoated wells were performed as controls to exclude unspecific antibody binding (data not shown).

2.2.29 Luminex

The chemical coupling of either recombinant streptavidin (16.67 µg/10^6 MagPlex beads, region 33), TgLEA-850 (16.67 µg/10^6 MagPlex beads, region 36), TgLEA-860 (66.67 µg/10^6 MagPlex beads, region 42), TgLEA-870 (16.67 µg/10^6 MagPlex beads, region 48), TgLEA-880 (16.67 µg/10^6 MagPlex beads, region 89), CSA (12 µg/10^6 MagPlex beads, region 52) as a negative control, or chicken IgY (6.67 µg/10^6 MagPlex beads, region 54) as a positive control followed the instructions of the xMAP® Cookbook (Angeloni et al., 2016). Prior to coupling, bead stocks were vortexed for 30 s and sonicated for 30 s in a water-bath. Beads (1.5×10^6) were transferred from the stock to individual low-binding reaction tubes for each bead region, i.e. dye signatures, washed with a. dest., vortexed and sonicated for 10 s and incubated in 80 µl 0.1 M NaH_2PO_4, pH 6.2 per tube. The tubes were again vortexed and sonicated for 10 s prior to addition of 500 µg Sulfo-NHS and EDC. The beads were then incubated for 20 min on a horizontal shaker at 300 rpm and vortexed briefly after 10 min. After incubation, the tubes were again placed in a magnetic separator for 2 min and the supernatant removed. The beads were washed twice with 250 µl of 0.05 M MES before addition of conjugates, and each tube was adjusted to 500 µl by adding 0.05 M MES. Tubes were briefly vortexed and then incubated for 2 h on a horizontal shaker at 300 rpm, with an intermittent brief vortexing step after 1 h. The tubes were again placed in a magnetic separator for 2 min and the supernatant removed. 500 µl of PBS containing 0.02 % Tween-20, 0.1 % BSA and 0.05 % sodium azide were added and the beads incubated for 30 min on a horizontal shaker at 300 rpm, before the samples were placed in a magnetic separator for 2 min to remove the supernatant. The beads were washed twice with 1 ml PBS containing 0.02 % Tween-20, 0.1 % BSA and 0.05 % sodium azide without sonication. For storage, the beads were resuspended in 500 µl Stabilguard. $TgSAG1_{bio}$ (10 ng/1,500 beads) was added to the streptavidin-coated beads as described previously (Klein et al., 2020).

For testing of sera by Luminex, the bead mixes were adjusted to 1,000 beads per sample in assay buffer. 20 µl of each region were added to 100 µl of sera diluted 1:200 or 1:25 in assay buffer in a 96-well plate. The plate, protected from light, was shaken at room temperature for 1 h. Beads were then washed twice with washing buffer using a magnetic plate washer. 100 µl of rabbit-F(ab')2 anti-chicken IgG-PE was added to each sample and the plate shaken at room temperature for 30 min, protected from light. Beads were again washed twice, resuspended in 125 µl assay buffer and analyzed with a Bio-Plex 200 reader. The readout was set to 50 beads per region and the reading timeout was set to 90 s. The High RP1 target option was activated (i.e. increasing the voltage on the photomultiplier tube) for increased sensitivity, allowing quantification of lower concentrations of analytes and three wells containing only beads and assay buffer were set as blank samples.

2.2.30 Sequencing

Generated plasmid DNA or PCR products were checked for correctness by sequencing. Prior to sequencing, DNA was purified using DNA Clean & Concentrator kit according to manufacturer's instructions. Samples were sequenced with the BigDye Terminator 3.1 Cycle Sequencing Kit, which is based on the Sanger method. After a PCR reaction of the desired DNA with only one oligonucleotide per sample, the sequencing was carried out in the in-house facility. A 10 µl sequencing reaction contained 1x ABI buffer (5x), 0.5 µl BigDye 3.1, DNA and 0.5 mM of the oligonucleotide in nuclease free a. dest. The DNA amount varied according to the template length following the facility's guidelines, i.e. 10 to 20 ng for 500 to 1000 bp long PCR products or 150 to 300 ng for plasmids. The following PCR program was used: 96 °C for 120 s; 96 °C for 10 s, T_m - 5 °C for 240 s. The last two steps were repeated for a total of 25 times, after which they were stored at 4 °C until analyzed. Sequencing results were evaluated using Geneious software.

Chapter 3: Results

3.1 Molecules binding to the oocyst wall

3.1.1 Development of a material saving immunofluorescence method to analyze molecules binding to oocysts

To find molecules that interact with the oocyst surface, in a first step it was necessary to develop a method to reliably conduct immunofluorescence experiments (IFAs) on whole oocysts without wasting too much precious material. In order to do so, a previously described method, based on the embedding of particles in agarose (Vartdal et al., 1986), was adapted to oocysts. For validation purposes and to save material, fluorescent biotinylated beads were used as an oocyst surrogate. Table 5 shows a comparison of the conventional tube-based IFA method and the adapted agarose-based method.

Table 5: Comparison of tube-based and agarose-based IFA methods with regards to important assay parameters.

	Before incubation [total # of beads]	**After 2 hours incubation and two washing steps [% of beads lost]**	**Assay volume [µl]**
Centrifuge tube	6,750	56.8 % (n = 3; SD = 6.3 %)	100
Agarose-embedded	100	9.7 % (n = 6; SD = 8.3 %)	10

Low-melt agarose at a concentration of 0.5 % provided a suitable matrix for successful embedding of as few as 100 oocysts (Agarose Embedded Oocysts – AEO) on a slide precoated with 1 % low-melting agarose. Precoating of the slides proved necessary to prevent the embedded oocysts from washing off the slide. 3 µl drops of a 1:1 oocysts:agarose mixture was sufficient for even distribution of oocysts in microscope slid well (diameter = 8 mm). For comparison of IFA techniques, the numbers of fluorescent beads before and after performing the centrifuge tube-based method versus embedded in agarose on a microscopic slide were compared. Using the agarose-embedded method, only a 10 % loss of particles was observed, while the centrifuge tube-based method including washing steps by centrifugation and pipetting resulted in a loss of more than 55 % of beads (see Table 5). Additionally, the number of beads needed to acquire robust results was much lower in the slide-based method than that in the tube-based method. Also, the volumes required for washing steps or antibody incubation steps could be reduced ten-fold using the AEO-IFA as opposed to the tube-based procedure.

3.1.2 AEO-IFA allows observation of antibody binding to the oocyst wall

To confirm the suitability of the AEO-IFA to detect antibodies binding to the oocyst wall, a murine monoclonal IgM (3G4), known to bind to the oocyst wall and sporocysts but not sporozoites (Dumètre and Dardé, 2005) was used. The autofluorescence of *T. gondii* oocysts marked the oocyst wall as well as the outline of the sporocysts. Immunofluorescence of intact oocysts confirmed the specific binding of mAb 3G4 to the oocyst wall (Figure 8, top), indicating unlimited access of molecules through the agarose. No unspecific background signals due to insufficient removal of unbound large IgM antibodies could be observed (Figure 8, bottom).

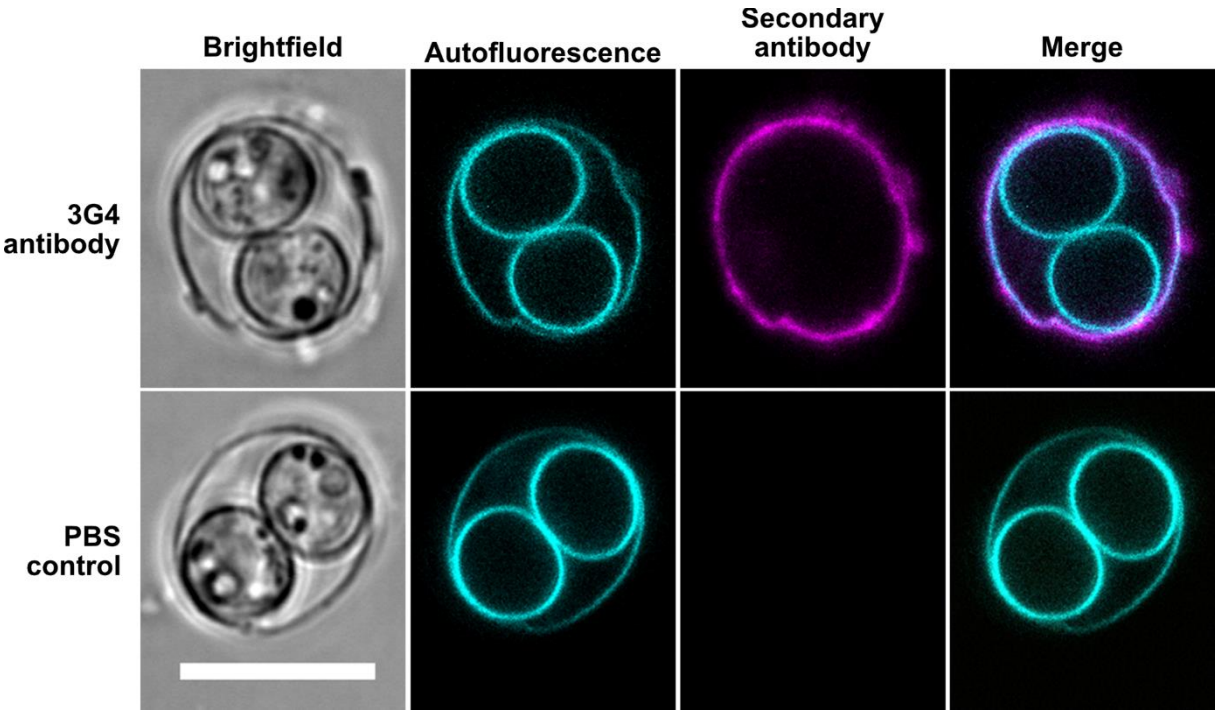

Figure 8: Oocysts can be labeled with 3G4 antibody known to bind to the oocyst wall using AEO-IFA. Autofluorescent oocyst and sporocyst walls are apparent in both experimental setups, whereas detection of bound 3G4 antibody with Cy5-labeled secondary antibody only localizes on the oocyst wall. Scale bar = 10 µm.

3.1.3 Alpaca immunization for nanobody production

To generate nanobody candidates against the oocyst wall, an immunization scheme for a 15-month-old alpaca was designed. The alpaca was immunized with inactivated oocysts weekly over a period of 49 days. However, serological analysis after completion of immunization via IFA did not detect measurable antibodies against whole oocysts. Thus, the immunization scheme was revised and conducted again. After the second immunization round, antibodies binding to the oocyst wall could be observed in the alpaca's serum via IFA, albeit only at a low dilution of 1:10.

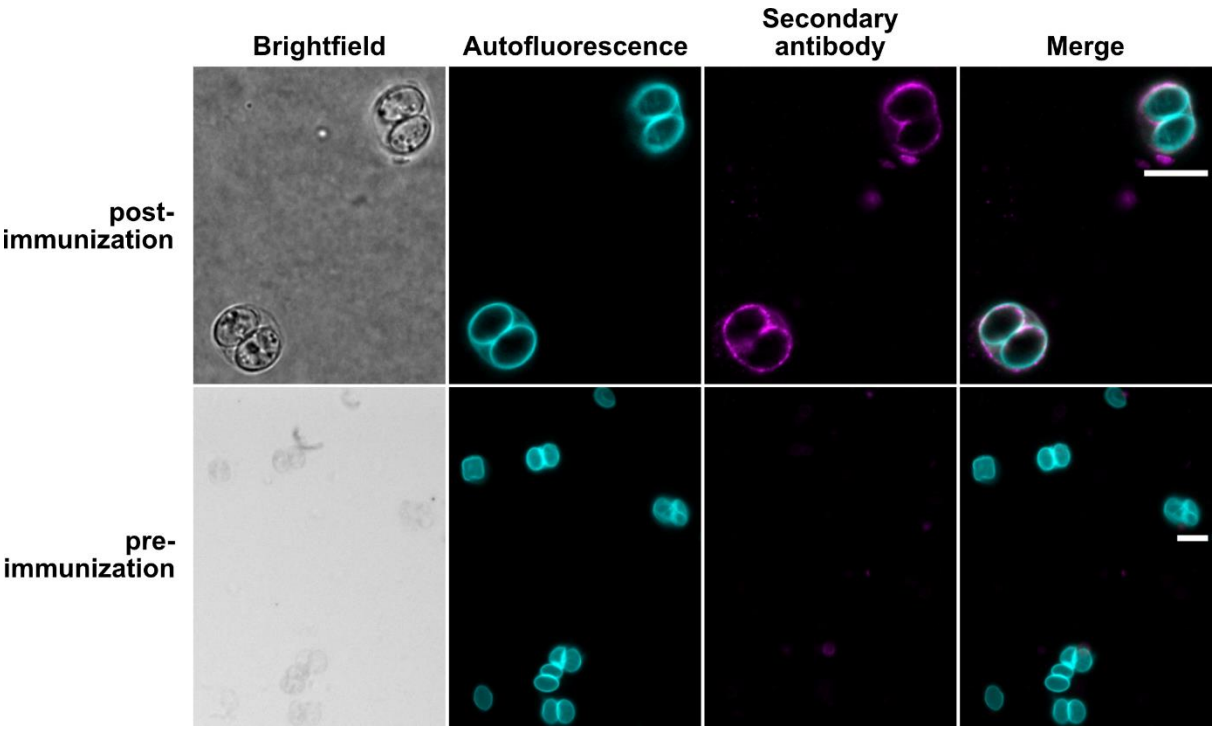

Figure 9: Detectable antibodies against the oocyst surface in an immunized alpaca. Incubating oocysts with serum of the immunized alpaca diluted 1:10 and using an anti-alpaca Cy5 labeled IgG (magenta) reveals co-localization of alpaca antibodies to the autofluorescent oocyst wall (cyan) while no such co-localization is observed in serum of the same alpaca before immunization. Scale bars = 10 µm.

To confirm the IFA findings, alpaca serum from before the start of the immunization and after completion of the second immunization was analyzed via glycan array in cooperation with Dr. Jonnel Jaurigue from the Max Planck Institute of colloids and surfaces (see Figure 10). The glycan array tested the alpaca serum for antibodies against the full side chain and two of its fragments of a *T. gondii* specific glycosylphosphatidylinositol (GPI). This experiment confirmed seroconversion of the alpaca after immunization, as the high signal indicates presence of antibodies against these *T. gondii* specific glycan structures.

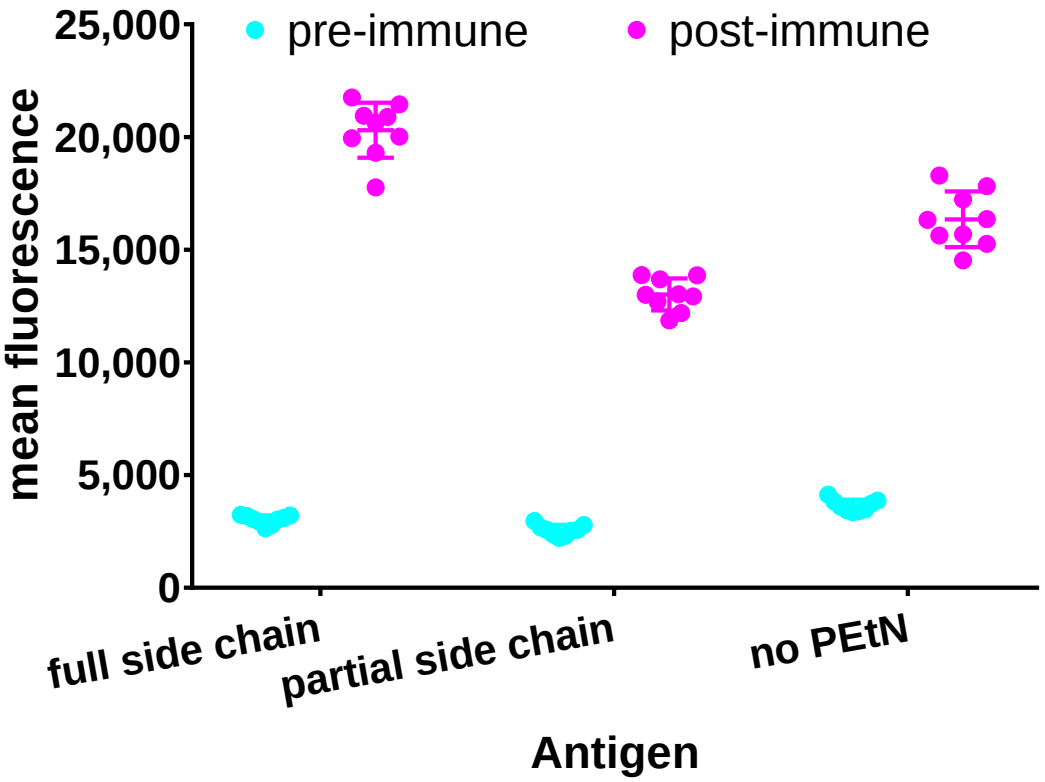

Figure 10: Successful immunization of alpaca with inactivated oocysts. Glycan array data reveals seroconversion of the alpaca as indicated by increased signal when serum is exposed to T. gondii-specific glycan structures. Prior to immunization the serum resulted in low fluorescence against all tested glycans (cyan) while after immunization, high fluorescence was observed for all three tested glycan structures (magenta).

After isolation of PBMCs, the RNA was extracted, and the quality assessed via Bioanalyzer (see Figure 11A). High RNA integrity number (RIN) values in this analysis warranted good suitability for subsequent cDNA conversion. However, after cDNA conversion, no VHH sequences could be successfully isolated via PCR (see Figure 11B). Amplicons of alpaca VHH sequences would be expected to exhibit sizes of 700 bp and 1,000 bp. Although different amounts of cDNA template were tested for optimal conditions, no bands were observed. The control reactions using different amounts of cDNA and primers provided by the kit used for reverse transcription, resulted in distinct bands at the expected size of 462 bp. A repeated PCR using previously isolated cDNA of a different alpaca as positive control did also not result in successful amplification of VHH sequences (data not shown). At this point, the project was put on hold to focus on other aspects of this thesis.

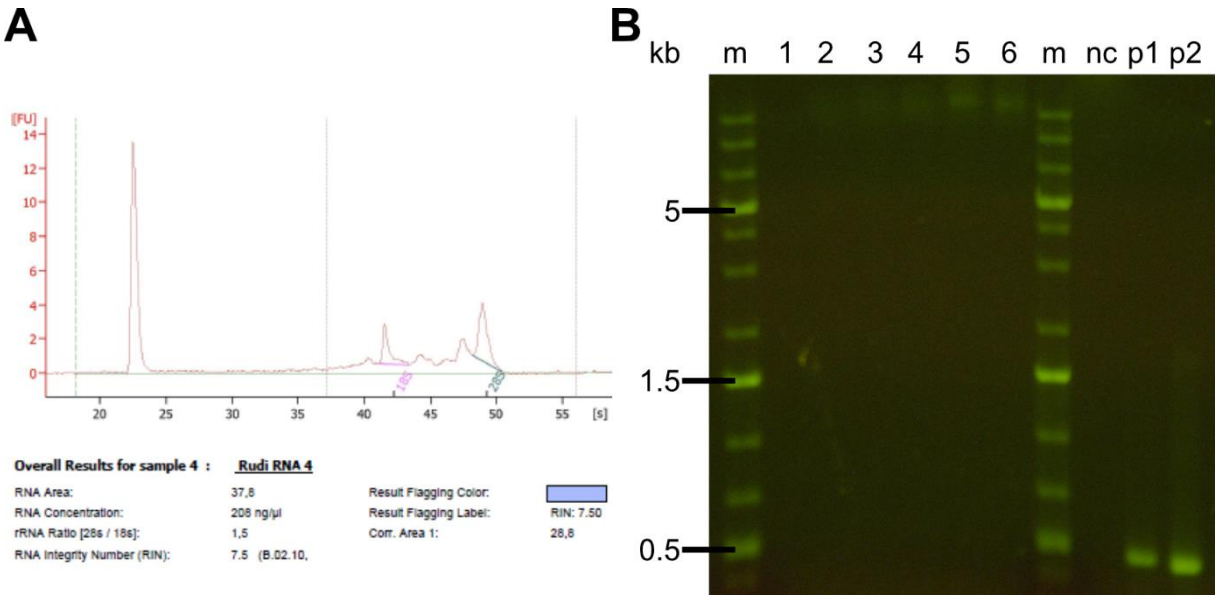

Figure 11: Unsuccessful amplification of VHH sequences from cDNA of the immunized alpaca. (A) Exemplary graph of isolated RNA in bioanalyzer. The alpaca RNA promised suitable for reverse transcription to cDNA as indicated by RIN values > 7. (B) Gelelectrophoresis shows that increasing cDNA amount in the PCR assay (1: 0 µl cDNA; 6: 5 µl cDNA) had no effect on successful amplification of VHH sequences. Bands of VHH sequence fragments should appear at 700 and 1,000 bp. m = marker; nc = no template control; p1 = 1 µl control template; p2 = 2 µl control template.

3.1.4 AEO-IFA enables visualization of molecules binding to inner oocyst structures

The oocysts that were available for experiments had been inactivated either by heat treatment or repeated freeze-thaw cycles (see chapter 2.2.1) and were thus assumed to be at least partially permeable to larger molecules. Therefore, the possibility to stain internal oocyst structures using the AEO-IFA was investigated. Embedded oocysts were incubated with fluorescein isothiocyanate (FITC)-conjugated MPA (Figure 12). Sporocysts were outlined by MPA-FITC with clear emphasis on the sutures and the connecting points where the four plates making up the sporocyst wall meet (Figure 12A, b, arrowheads, j). It appears these structures have not been documented in previous observations of MPA-labeled oocysts (Bushkin et al., 2012), underscoring an advantage of the AEO-IFA. To increase the walls' permeabilization, oocysts were incubated with ice-cold acetone before binding of MPA-FITC (Figure 12B). Slightly enhanced suture staining was observed as indicated by requiring only half of the laser intensity to obtain similar signal to that shown in Figure 12A, indicating increased permeabilization. The effect of acetone treatment was not always uniform and predictable, as illustrated by differences in antibody binding after acetone treatment. Incubation of oocysts with acetone resulted in the loss of the distinct surface staining by the 3G4 antibody. Instead, an intense, uneven, and spotty signal within the sporocysts (Figure 13A, top) was observed. Using another antibody, 3B11 (provided by Furio Spano), targeting the outer wall protein 3 of *T. gondii* (TgOWP3) which is known to be located in the oocyst wall (Possenti et al., 2010), it was observed that acetone treatment did not generally inhibit the binding of 3B11 antibody to

TgOWP3, but, not all walls were consistently stained, and weak reactivity of 3B11 with the sporocyst sutures could be observed in those oocysts where MPA-FITC staining indicated successful permeabilization (see Figure 13A, bottom). In addition to staining of oocyst and sporocyst wall components, successful staining of nuclei in the sporozoites after acetone permeabilization was tested (see Figure 13B). As described above, inconsistent nuclei staining was frequently observed, even within one well on the microscopy slide. In some cases, only nuclei in one sporocyst were stained. The reasons for this heterogeneity within the oocyst population are currently unknown.

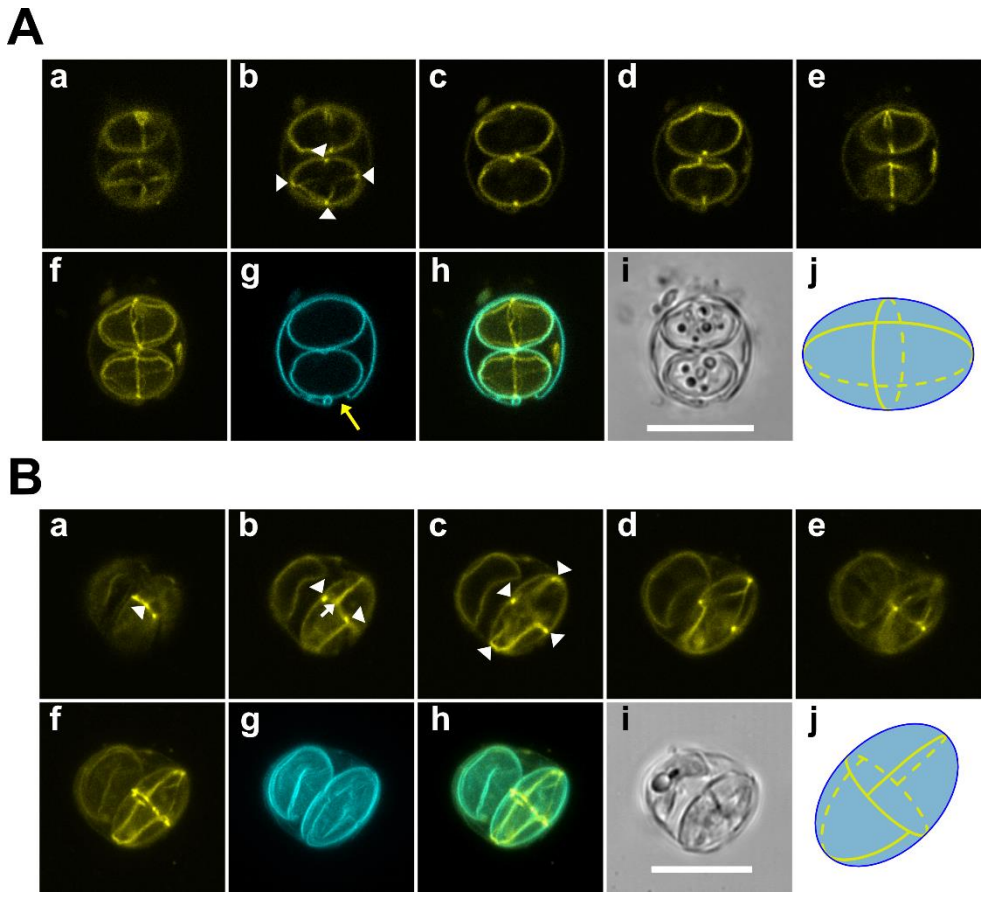

Figure 12: AEO-IFA allows for high-resolution immunofluorescence microscopy images of oocyst inner structures using MPA-FITC. The images show binding of MPA-FITC (yellow) to autofluorescent oocysts (cyan) incubated without (A) or with (B) acetone before the IFA procedure. Arrowheads indicate the increased MPA-FITC staining of sutures formed by the sporocyst wall plates that is present in all images. A possible rupture in the wall of the oocyst is indicated by the yellow arrow in Ag. Images a to e represent individual images from a stack of images along the z-axis (z-stack), f is a projection of the same stack. Image g in (A) is from a singular plane to emphasize the wall rupture, image g in (B) is projection of the same z-stack. Image h is a merged image of images f and g, image i shows a focus-stacked brightfield image and j proposes a scheme of the plates' orientation with regards to the sutures' arrangement (yellow), as deduced from the MPA-FITC staining. Scale bars = 10 µm.

Apart from the oocyst age, the dehydrating effect of acetone, which can cause the collapse of sporocysts and oocysts, as has been observed previously by EM (Birch-Andersen et al., 1976),

could be an explanation. Subsequently, aberrant signals might be a result of this loss of structural integrity.

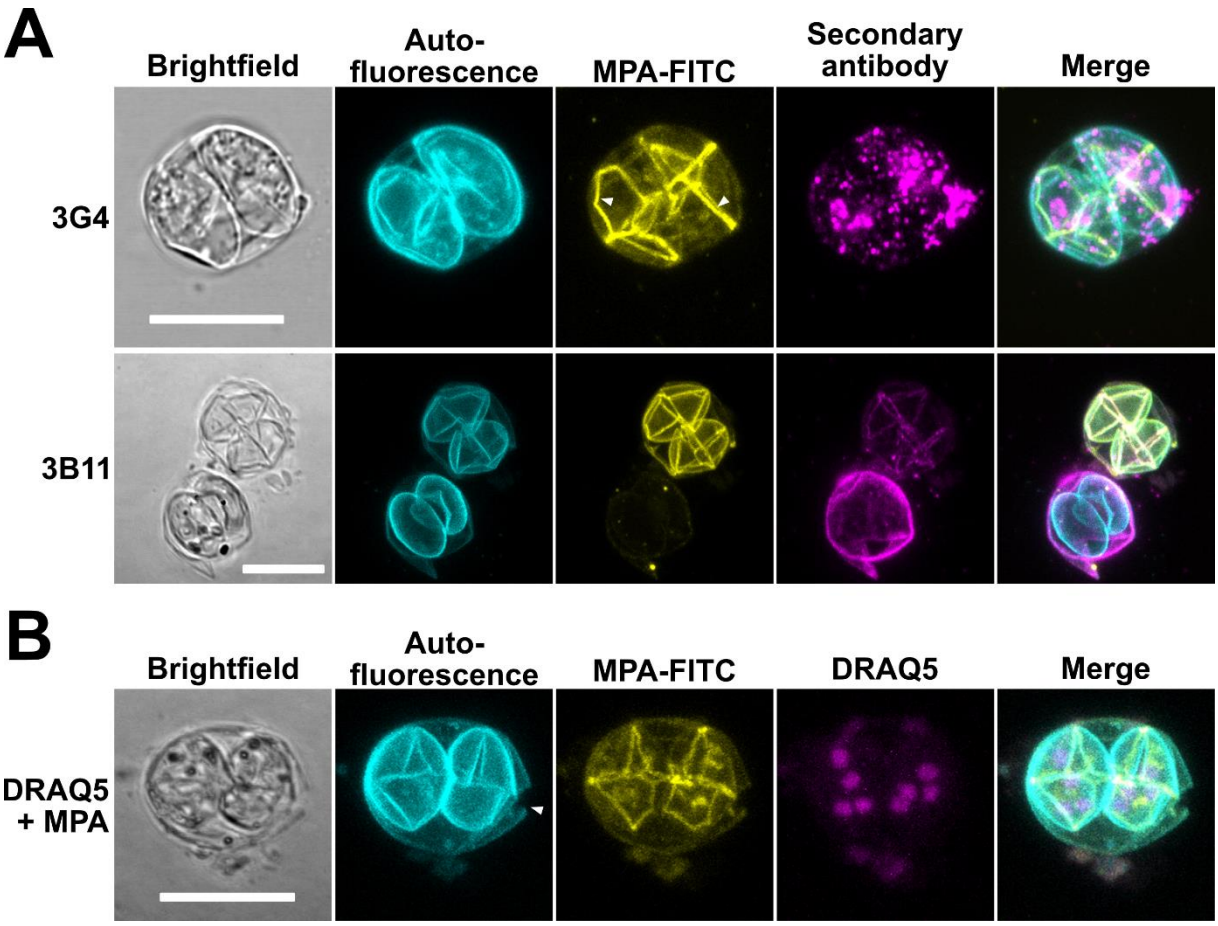

Figure 13: AEO-IFA shows acetone treatment of oocysts differently affecting binding of antibodies targeting the oocyst wall (A) and reveals staining of nuclei within the sporocysts (B). (A) Loss of signal was observed when trying to bind 3G4 antibody (magenta) to acetone treated oocysts (cyan) as compared to Figure 8, while the signal of 3B11 antibody targeting OWP3 was less affected. (B) DRAQ5 (magenta) visualizes four nuclei per sporocyst. Note the possible rupture in the oocyst wall (arrowhead). MPA-FITC staining indicates oocyst permeabilization. Scale bars = 10 µm.

3.1.5 Discovery of new oocyst-binding CLRs.

Prior description of CLEC7A binding to the oocyst wall (Bushkin et al., 2012) warranted the screening of a murine CLR-hFc fusion protein library comprising several CLRs from the same cluster (see Table 1 and Figure 4) which was kindly provided by Prof. Bernd Lepenies from the Tierärztliche Hochschule Hannover, Germany. As a control, a CLR from outside the Dectin-1 cluster, DCAR, was included. The hFc fragment without the extracellular CLR domains was used as a negative control in all assays.

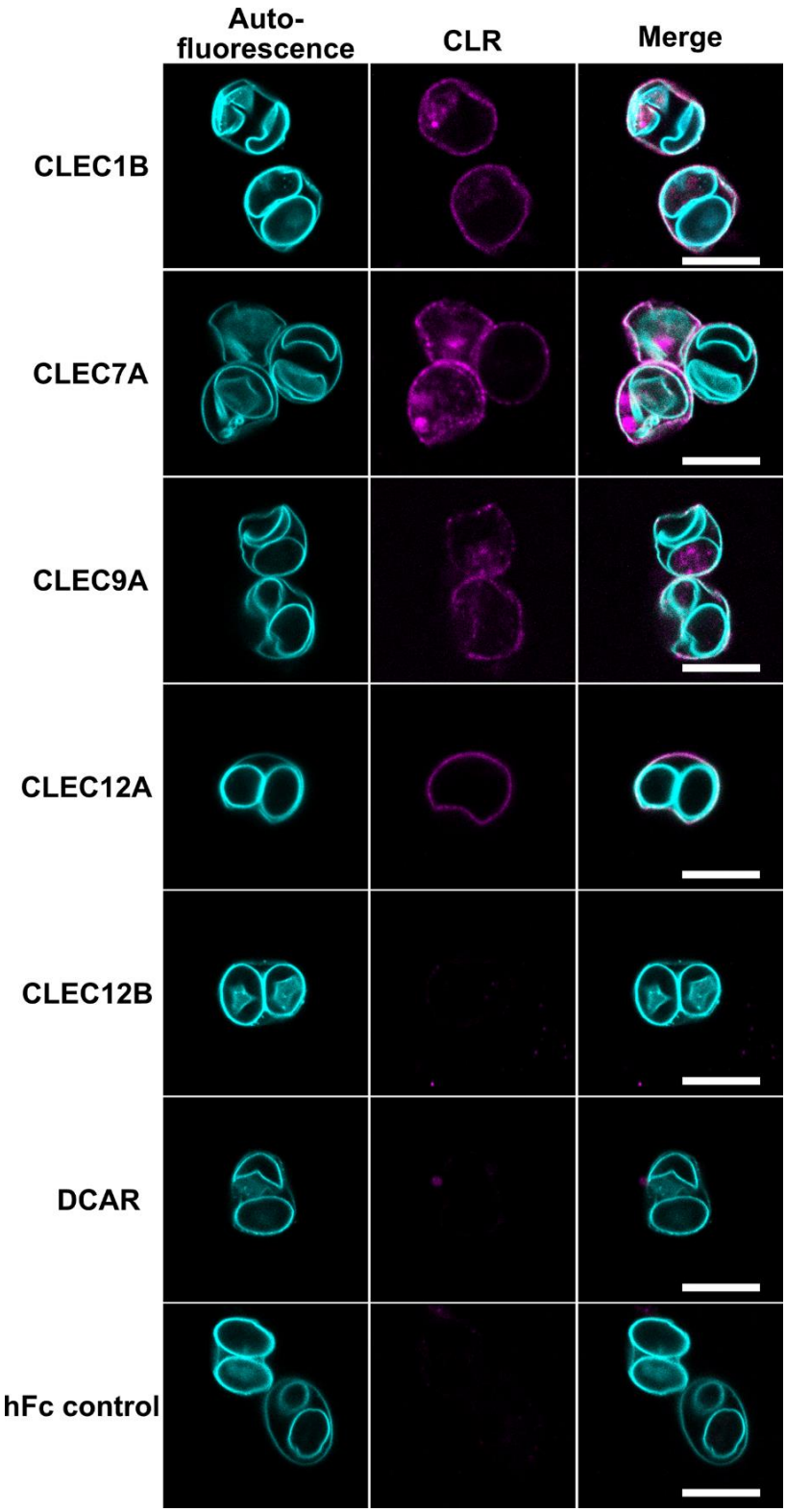

Figure 14: Screen of CLRs of the Dectin-1 cluster identifies new CLRs binding to oocysts. The left column shows autofluorescent oocysts (cyan), the center column shows the signal of DyLight-650-labeled anti-human IgG antibody (magenta) in case of bound CLRs and the right column shows merged images of the previous columns. CLEC12B, DCAR, and the hFC control did not bind to oocysts. Pictured are cut-outs from larger images for better visibility (originals are presented in Figure 43 in the appendix). Brightness and contrast in merged images were adjusted equally for better visibility. Scale bar = 10 µm.

Binding of CLEC7A to the oocyst wall could be observed and proved the suitability of the AEO-IFA to assess CLR binding to oocysts. Binding to the oocyst wall was observed for CLEC1B, CLEC9A and CLEC12A (see Figure 14). The hFc control ruled out unspecific signal, as no binding was detected. Corroborating this, DCAR as an unrelated CLR and CLEC12B from within the Dectin-1 cluster exhibited no binding to oocysts.

3.1.6 The newly discovered CLRs do not bind to sporocysts but to unsporulated oocysts

For further characterization of the newly identified CLRs, binding variability was examined. All CLRs were discovered to decorate the wall of sporulated and unsporulated oocysts equally well (see Figure 15A, C, D). Furthermore, in cases where oocysts were disrupted and singular sporocysts could be seen in the AEO-IFA, no binding of any of the three CLRs to sporocyst structures could be observed (see Figure 15B, D, F).

3.1.7 CLEC12A ligand on *T. gondii* oocysts is not uric acid.

Previously, CLEC12A was shown to bind uric acid crystals (Neumann et al., 2014). Since oocysts are shed via the fecal route, it was necessary to rule out possible contamination of oocysts with urine-derived uric acid. Oocysts were treated with uricase prior to incubation with CLEC12A. This pretreatment did not result in loss of secondary antibody signal and thus of CLEC12A binding to the oocyst surface (see Figure 16, upper panels). As a control, fluorescent polystyrene beads (see section 3.1.1) were coated with uric acid crystals and subsequently treated with uricase prior to incubation with CLEC12A. In these beads, no binding of CLEC12A could be observed. In comparison, in uric acid coated beads treated with PBS instead of uricase, CLEC12A decorated the uric acid crystals present on the bead surface (see Figure 15, lower panels). This indicates the presence of a ligand other than uric acid crystals on the oocyst surface that remains so far unknown.

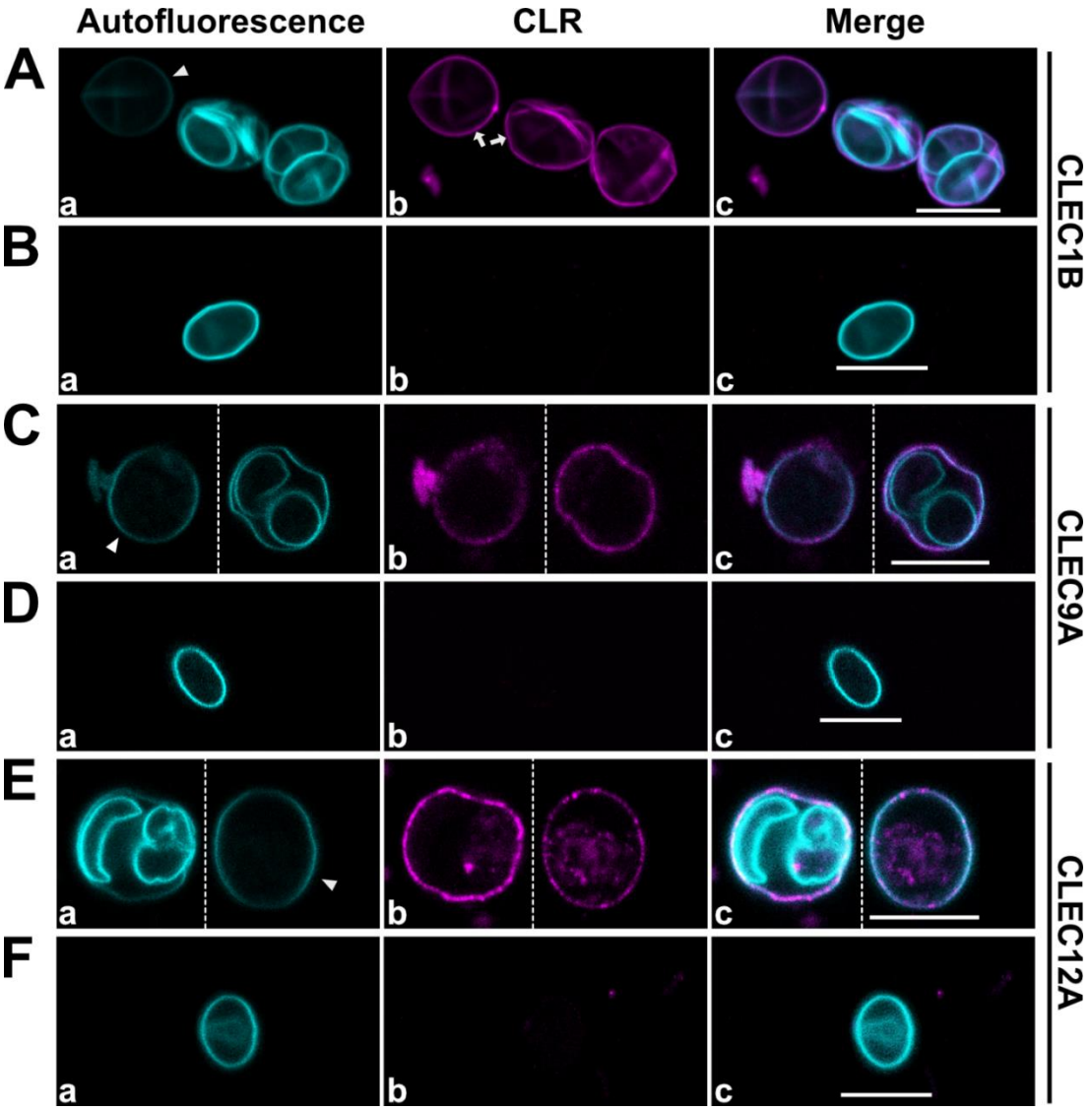

Figure 15: Assessment of binding of newly identified CLRs to sporulated and unsporulated oocysts and sporocysts. (A, C, E) The CLRs bind both sporulated and unsporulated oocysts equally well. The decreased autofluorescence (cyan) of unsporulated oocysts (arrowheads, a) is apparent compared to the stronger autofluorescent sporulated oocysts. The DyLight-650 signal of the secondary antibody (magenta) does not differ between the oocysts (arrows, b). (B, D, F) The CLRs do not bind to the walls of sporocysts, as confirmed by absence of DyLight-650 signal in images b and c. For better visibility, oocysts from the same field of view in the original image have been cropped and placed next to each other to allow image enlargement (indicated by stippled lines; see Figure 44 in the appendix for original images of (C) and (E)). Also, brightness of b and c in E has been slightly increased. Scale bars = 10 µm.

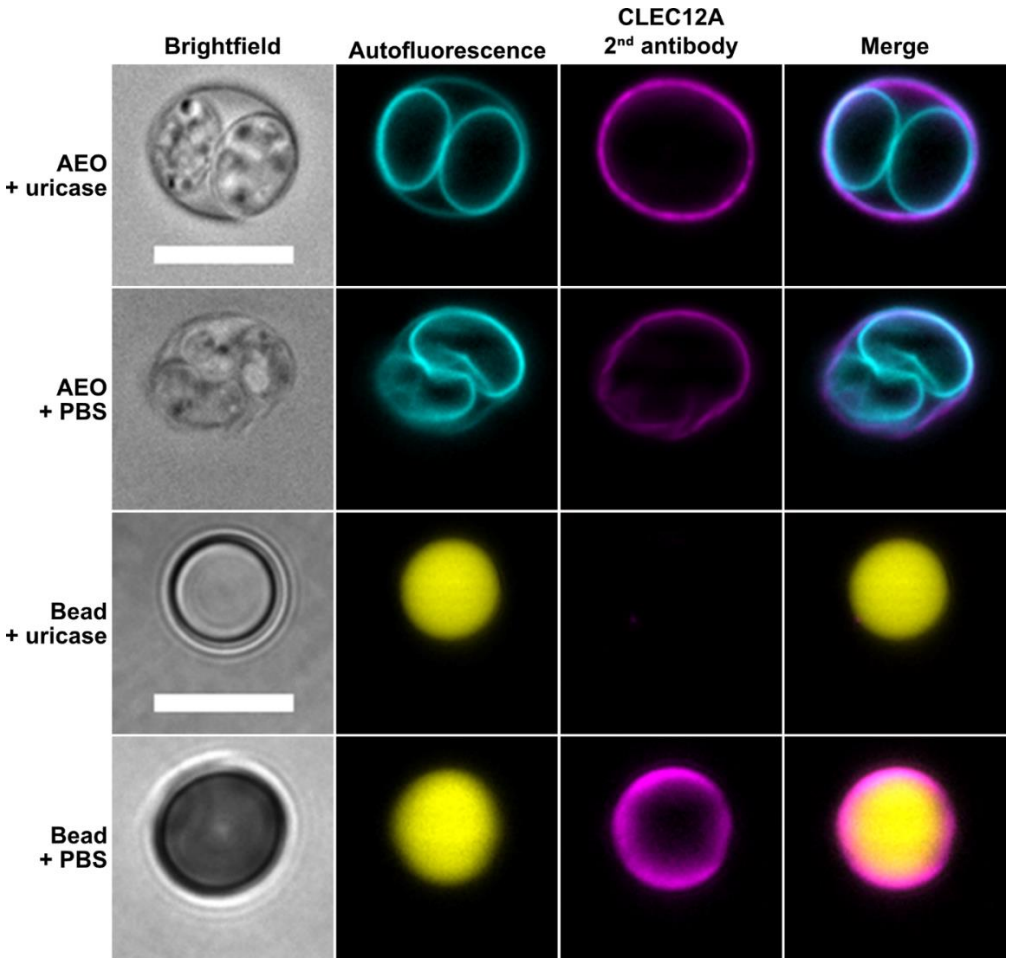

Figure 16: Incubation with uricase prior to CLEC12A rules out contamination with uric acid crystals on oocysts. The two upper rows detail binding of CLEC12A to oocysts (cyan) treated and not treated with uricase prior to the IFA. Signal of the secondary DyLight650 labeled antibody (magenta) is not reduced upon uricase treatment. The bottom rows depict fluorescent beads (yellow) coated with uric acid crystals and incubated with uricase or PBS prior to the IFA, causing loss of DyLight-650 signal upon uricase treatment. Scale bars = 10 µm.

3.2 Molecules contributing to stress tolerance inside the oocyst

3.2.1 Optimal protocol for expression of TgLEAs in *E. coli*

In a first step, optimal induction conditions for expression of recombinant TgLEA proteins in *E. coli* were tested. Protein expression was induced with varying amounts of isopropyl β-d-1-thiogalactopyranoside (IPTG) and the bacteria were incubated for 2 hours. Subsequently, the bacteria, expressing one of the four TgLEA proteins were exposed to desiccating conditions for 7 days. Afterwards, colonies were counted, showing that induction with 500 mM IPTG resulted in the most substantial effect as indicated by improved growth after 7 days of desiccation stress for the bacteria that expressed TgLEA-850. Other TgLEAs did not positively influence growth under stress.

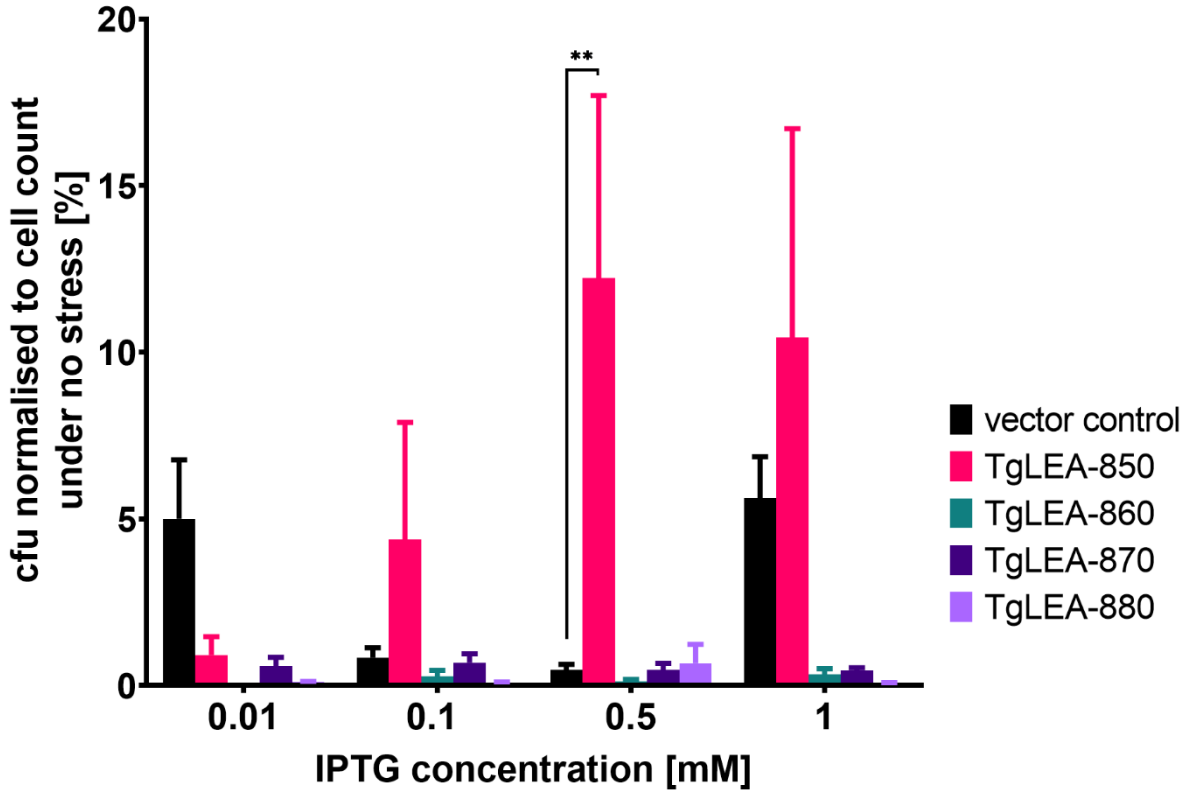

*Figure 17: 0.5 mM IPTG shown to be the optimal concentration for induction of expression. The graph depicts the percentage of E. coli colonies that were able to grow after exposure to stress, in relation to the concentration of IPTG used for induction of TgLEA expression. The number of colonies formed after stress exposure increased with the increased expression of TgLEA-850, maxing out at 0.5 mM IPTG. ** = P < 0.005 indicates a colony count significantly different from that of the vector control. Shown is the result of one representative experiment of three individually repeated experiments, each consisting of three technical replicates.*

3.2.2 TgLEAs do not protect *E. coli* against osmotic stress

E. coli strains which recombinantly expressed one of the four TgLEA proteins were exposed to different salt concentrations (0 mM, 171 mM, 342 mM) in the growth medium to induce osmotic stress on the bacteria. Counting colonies after growth on these media, none of the bacteria showed better growth as compared to the control strain expressing a non-functional

peptide (see Figure 18). Strikingly, bacteria transformed with TgLEA-860 seemed to grow worse under hyper- and hypoosmotic conditions when TgLEA-860 expression was not induced (Figure 18A). Upon induction, TgLEA-860 seems to confer resistance to hyperosmotic conditions (Figure 18B), although the high variance in colony counts does not allow an unequivocal determination of such an effect. Moreover, induction of TgLEA-850 caused reduced growth under hypoosmotic conditions compared to bacteria where TgLEA-850 expression was not induced. Since bacteria transformed with a plasmid which mediated the expression of a non-functional peptide of similar length as TgLEA-850 as transformation control exhibited less growth inhibition by osmotic stress than the majority of TgLEA expressing bacteria, involvement of TgLEAs in osmotic stress resistance is unlikely.

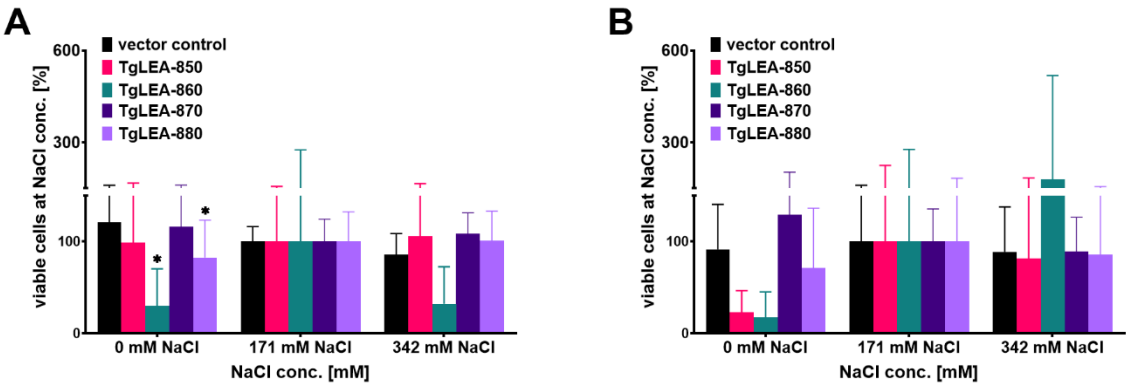

*Figure 18: TgLEAs do not increase resistance to osmotic stress in E. coli. Bacterial growth assays showed no clear benefit of induced expression of TgLEAs (B) over not-induced expression (A) on resistance to osmotic stress. Analyzed was the number of colonies formed after exposure to hyper- (0 mM NaCl; black), iso- (171 mM NaCl; magenta) and hypotonic (342 mM NaCl; green) growth media with and without expression of TgLEAs. (A) Bacteria grew equally well on all media except when expressing TgLEA-860 which reduced the number of formed colonies under osmotic stress to around 20 %. (B) Colony formation is not significantly inhibited in absence of TgLEAs as is indicated by high variability in colony numbers. The Graphs show mean and standard deviation values of three individual experiments. * = P < 0.05 shown above the bar indicate results significantly different from those for the vector control.*

3.2.3 TgLEAs do not protect *E. coli* against heat stress

The same *E. coli* strains were exposed to 0, 30 or 60 minutes of 50 °C, a temperature shown to be lethal to *E. coli* (Ezemaduka et al., 2014). Observing colony growth after the stress induction did not indicate any substantial protection by TgLEAs against heat stress (see Figure 19). Overall, a heat shock for 60 minutes resulted in growth reduction by approx. 75 % or almost 100 % in case of TgLEA-850 expressing bacteria, with no pronounced effect upon expression of TgLEAs (Figure 19B). A heat shock for 30 minutes resulted in 50 % growth reduction in bacteria transformed with the vector control, whereas TgLEAs expression caused growth reduction by 70 to 80 % in the case of TgLEAs-850 and -860. Expression of TgLEAs-

870 and -880 seemed to cause a lower growth reduction although the observed standard deviations complicate the determination of a distinct effect. In bacteria where protein expression was not induced (Figure 19A), the number of viable cells after stress was overall increased, especially in the case of TgLEA-850 transformed bacteria, and more uniform across all TgLEA transformed strains. Only in the case of TgLEA-880 transformed bacteria no difference between induced and not-induced was observed. While these findings suggest that TgLEA expression is somewhat restraining to bacterial growth rather than conferring resistance to heat induced stress, observation of bacterial growth after inoculation disproves this, as the measured OD did not vary substantially between individual strains or induction state, except for bacteria expressing TgLEA-860, where growth was slower than in other bacteria after induction of protein expression (see Figure 48 in the appendix).

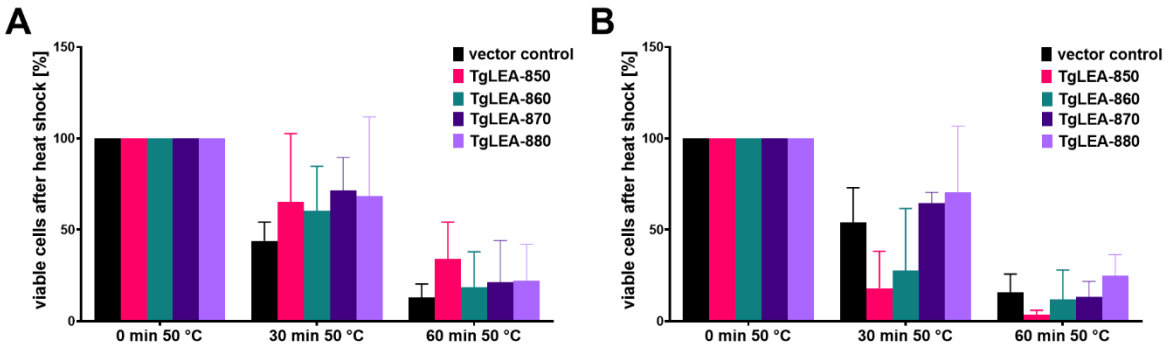

Figure 19: TgLEAs do not increase resistance to heat induced stress in E. coli. Bacterial growth assays showed no clear benefit of induced expression of TgLEAs (B) over not-induced expression (A) on resistance to heat-shock. Analyzed was the number of colonies formed after a heat shock for 0 (black), 30 (magenta) or 60 (green) minutes with and without expression of TgLEAs. (A) Bacterial growth was inhibited by 40 to 60 % after 30 minute heat shock and 60 to 80 % after a 60 minute heat shock with no significant difference between the individual groups. (B) Induction of TgLEA expression resulted in a lower number of viable cells of bacteria transformed with TgLEA-850 or -860 while no clear difference was observed in bacteria expressing TgLEA-870 or -880. The Graphs show mean and standard deviation values of three individual experiments.

3.2.4 TgLEAs do not protect *E. coli* against freezing stress

E. coli expressing one of the four TgLEA proteins were exposed to cold induced stress (24 hours at -20 °C or 7 days at 4 °C) and subsequently plated on growth medium to assess the TgLEAs' potential to confer resistance to cold temperature stress (see Figure 20). However, compared to strains where protein expression was not induced (Figure 20A), bacteria that expressed TgLEAs exhibited greater sensitivity to stress induced by cold temperatures (Figure 20B). After 24 hours at -20 °C, bacteria expressing TgLEA-880 were least affected, still, growth was reduced by approx. 60 %. While incubation for 7 days at 4 °C

did not seem to impact growth in absence of TgLEAs, in bacteria expressing TgLEAs, growth after stress was reduced by between 40 and 80 %.

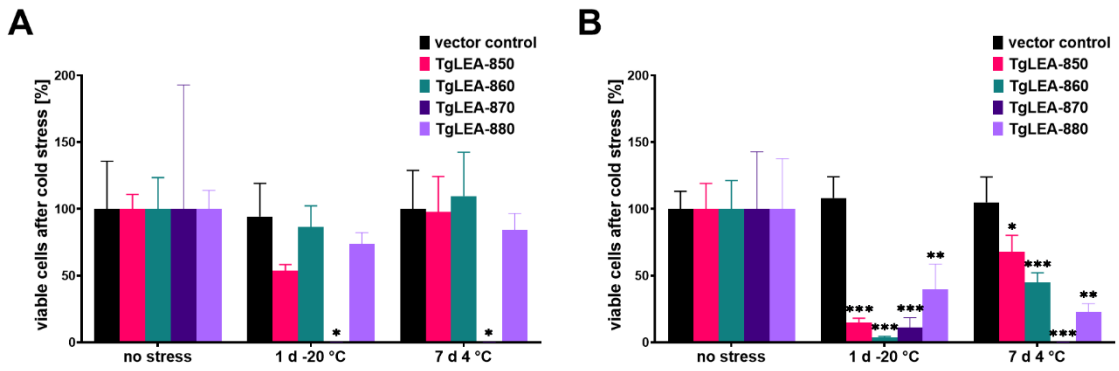

*Figure 20: TgLEAs do not increase resistance to cold induced stress in E. coli. Bacterial growth assays showed reduced growth after cold temperature stress when expression of TgLEAs was induced (B) as compared to not-induced expression (A). Analyzed was the number of colonies formed after no stress (black), incubation at -20 °C for 24 hours (magenta) or incubation at 4 °C for 7 days (green) with and without expression of TgLEAs. (A) High standard deviation under no stress and no observable growth after any stress in the TgLEA-870 strain indicate fundamental problems in this experimental context. Growth was inhibited by 50 % after 1 day at -20 °C in bacteria transformed with TgLEA-850 but not after 7 days at 4 °C. The remaining TgLEA strains and the control strain showed only slightly reduced growth after stressing. (B) Induction of protein expression caused reduced colony formation in all TgLEA strains while the control strain was unaffected. The Graphs show mean and standard deviation values of three technical replicates. * = P < 0.05, ** = P < 0.01 and *** = P < 0.001 shown above the bar indicate results significantly different from those for the vector control.*

In addition, possible beneficial effects of TgLEAs on cold resistance in the cold sensitive *E. coli* strain JW5132-3 that lacks a trehalose synthase gene were investigated (see Figure 21). In contrast to the parental strain, incubation for 24 hours at -20 °C reduced growth of the control strain by over 90 %, regardless if protein expression was induced (Figure 21B) or not (Figure 21A), confirming the sensitivity of the JW strain to damage upon freezing. Remarkably, growth was only reduced by 50 % in the TgLEA-860 strain when expression was not induced and even improved in the TgLEA-850 strain. The TgLEA-870 and -880 strains were similarly affected as the control strain after 24 hours at -20 °C. As in the parental strain, growth after 7 days at 4 °C was only marginally reduced. Interestingly, when TgLEA expression was induced, TgLEAs-850 and -860 seemed to impose a detrimental effect on bacterial growth, regardless of the stress, while expression of TgLEA-870 or -880 prevented growth inhibition upon freezing stress compared to the same strains without induction of protein expression. Similarly, growth after 7 days at 4 °C was not inhibited.

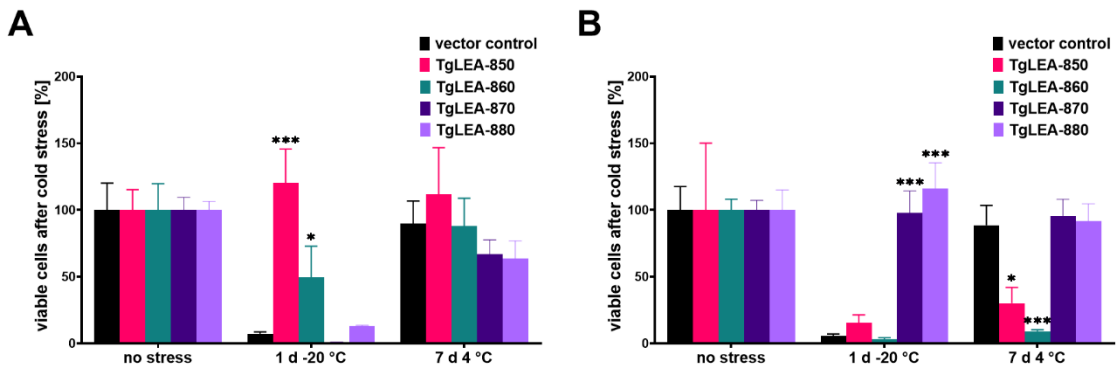

Figure 21: Some TgLEAs increase resistance to cold induced stress to cold sensitive E. coli. Bacterial growth assays showed reduced growth after cold temperature stress when expression of TgLEAs was induced (B) as compared to not-induced expression (A). Analyzed was the number of colonies formed after no stress (black), incubation at -20 °C for 24 hours (magenta) or incubation at 4 °C for 7 days (green) with and without expression of TgLEAs. (A) Without induced protein expression, the control strain shows almost no growth after freezing stress, while the TgLEA-850 strain formed even more colonies than without stress. At the same time, growth of the TgLEA-860 strain is only reduced by 50 %. Other TgLEAs show no beneficial effect on growth in this context and stress of 7 days at 4 °C only marginally affected bacterial growth, even in the control strain. (B) Induction of TgLEA expression caused the TgLEA-850 and -860 strain to exhibit growth reduction between 70 and 90 %, even after 7 days at 4 °C. In contrast, expression of TgLEA-870 or -880 lead to complete growth restoration after 1 day at -20 °C. The control strain showed no growth improvement after freezing stress. The Graphs show mean and standard deviation values of three individual experiments.

3.2.5 Recombinant expression and purification of TgLEAs

In order to test effects of TgLEAs on viability upon stress *in vitro* and *in vivo*, successful recombinant expression in *E. coli* needed to be confirmed prior to the bacterial growth assays. To this purpose, all TgLEAs were his-tagged for purification and easy detectability. After induction and protein expression, *E. coli* were harvested and lysed. Subsequently, two different lysate treatments prior to protein purification were compared, one involving an additional 10 minute incubation at 100 °C step, to assess the TgLEAs resistance to heat-induced denaturation and subsequent aggregation, as has been observed for IDPs (Receveur-Brechot et al., 2006). Secondly, if the TgLEAs proved resistant to such aggregation, this additional incubation step followed by centrifugation would aid in TgLEA purification, as more globular proteins are removed from the lysate (Kalthoff, 2003).

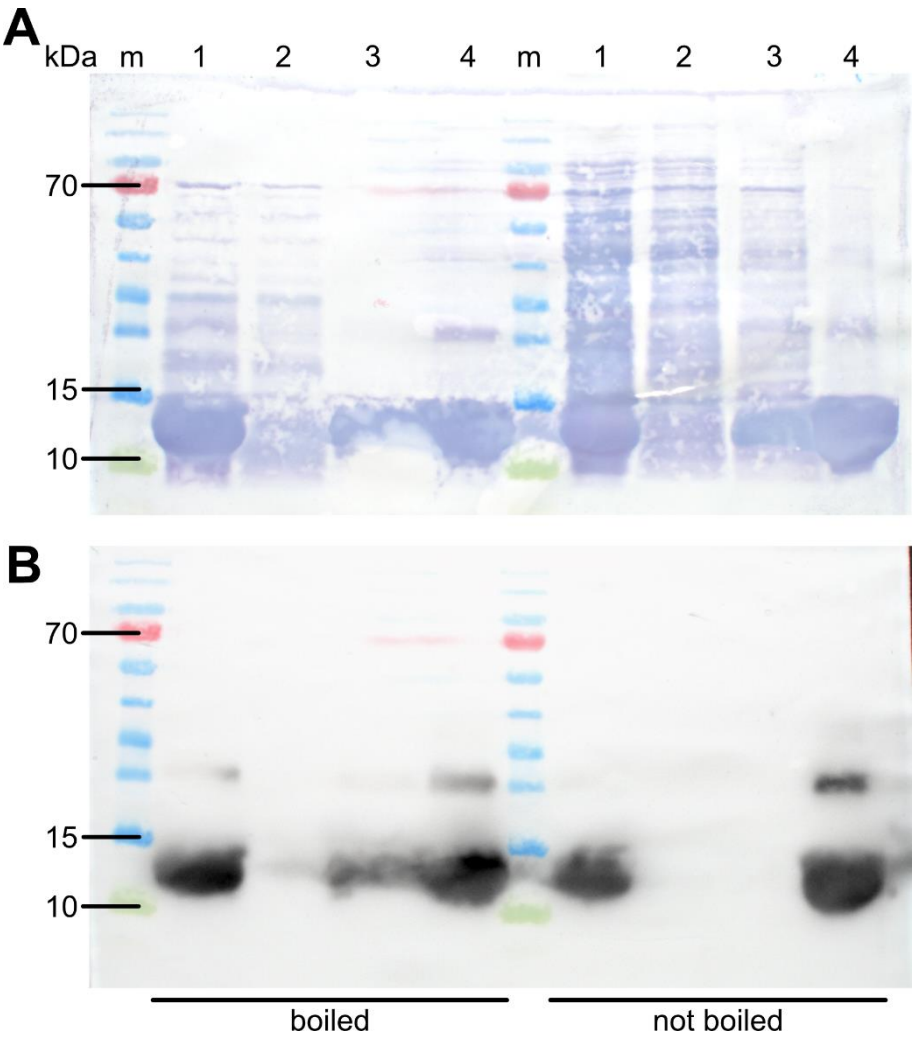

Figure 22: Western blot analysis of recombinantly expressed TgLEA-850. Pictured are total protein staining via DB71 (A) and ECL detection of his-tagged TgLEA-850 (B) of the same western blot membrane, comparing two protein preparation procedures (boiled vs. not boiled). (A) The total protein stain reveals that boiling the bacterial lysate prior to loading onto the column for purification reduces contamination with unwanted globular proteins during purification as indicated by overall reduction of signal in all fractions. (B) Specific ECL detection of his-tagged TgLEA-850 shows no difference with regards to concentration of the purified protein as there is no obvious signal difference in the eluate fractions. M = molecular marker, 1 = lysate prior to loading, 2 = lysate after running over column, 3 = washing fraction, 4 = pool of eluted fractions.

After purification of the TgLEAs over a Ni-Sepharose column, all fractions and the lysate prior to loading were analyzed via western blot. This confirmed successful recombinant expression of all TgLEAs (see Figure 22 for result of TgLEA-850 analysis and Figure 45 to Figure 47 for results of remaining TgLEAs). For TgLEA-850, a pronounced band appeared after detection with anti-his antibody representing the predicted molecular weight of approx. 11 kDa. A weaker band was also observed at 25 kDa. Similar aberrant bands were observed in the other TgLEA blots as well, especially in the case of TgLEA-860. This mirrors observations in other publications where similar aberrant bands were observed during recombinant LEA-protein

expression (Boswell et al., 2014; Warner et al., 2016) and could therefore be resulting from intrinsic disorder characteristics of the TgLEAs.

3.2.6 Analyzing IDP characteristics of TgLEAs *in vitro*

As many IDPs are extremely susceptible to protease digestion due to exposed binding sites for proteolytic enzymes, testing the TgLEAs susceptibility to digestion by proteases provides a feasible approach to test for IDP characteristics. Incubation with the protease trypsin revealed that TgLEAs are highly susceptible to proteolytic digestion and are rapidly degraded even at such low protease concentrations, similar to other IDPs such as casein (see Figure 49 in the appendix). Still, casein proved an unreliable control IDP as it produced no clear signal throughout the assay. Therefore, hCD1 was used as control IDP going forward. Furthermore, the susceptibility to trypsin was remedied by a concentration of approx. 20 % of trifluoroethanol (TFE) in TgLEAs and hCD1. TFE is a widely used organic solvent in IDP characterization experiments as it is known to simulate water loss on a molecular level, imitating the effects of desiccation on protein structure. The fact that TFE makes TgLEAs and an IDP control resistant to proteolysis hints at the IDP characteristic of the TgLEAs since it indicates structural reorganization upon changing physiological conditions. Although some publications reported an improved trypsin activity at TFE concentration of 5 % (Proc et al., 2010; Dickhut et al., 2014), it could not be ruled out that the structural changes mediated by higher TFE concentrations also affected trypsin reactivity, resulting in reduced proteolysis, as has been shown elsewhere (Ataei and Hosseinkhani, 2015). Thus, additional proteolysis experiments with thermolysin, a protease supposedly resistant to the effects of TFE (Receveur-Brechot et al., 2006), were conducted. As with trypsin, TgLEAs and hCD1 were highly sensitive to proteolytic digestion under similar conditions, while lysozyme remained unaffected. In addition, TFE again mediated resistance to protease digestion at a concentration of approx. 20 % (see Figure 50 in the appendix).

However, subsequent control experiments to assess the direct effects of TFE on thermolysin revealed that TFE negatively affects the activity of thermolysin. Using FA-glycyl-L-leucine amide (FAGLA), a substrate whose hydrolysis is catalyzed by thermolysin resulting in a decrease of absorbance at 345 nm (Feder, 1968), the effect of different TFE concentrations on enzyme activity was analyzed. Only in absence of TFE could a thermolysin mediated decrease of A_{345} be observed. Even a TFE concentration of 10 % was sufficient to completely inhibit thermolysin activity. (see Figure 23). Taken together, these findings confirm that like other IDPs, TgLEAs are highly susceptible to proteolytic digestion, strengthening the assumption that they are IDPs, although the resistance to proteases mediated by TFE cannot serve as an indicator of structural changes, as TFE also seems to adversely influence protease activity.

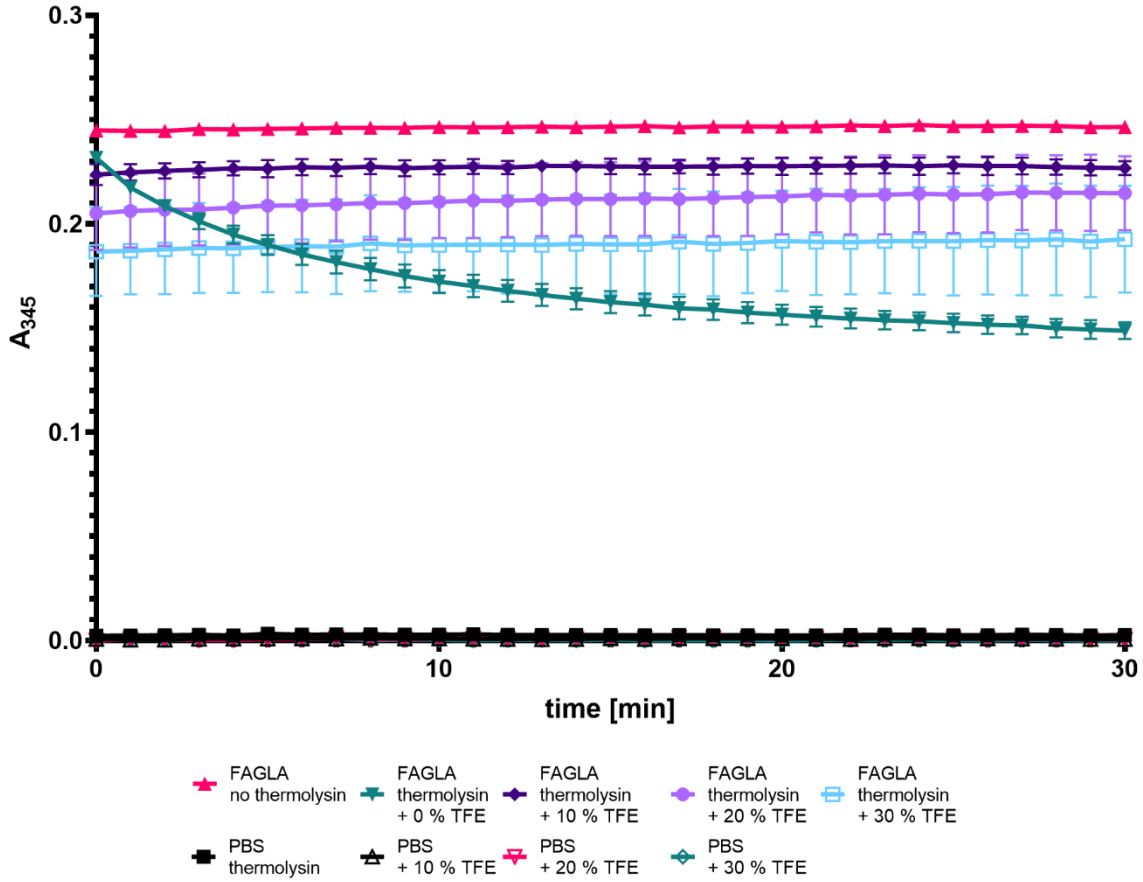

Figure 23: Spectral analysis reveals thermolysin inhibition even at low TFE concentrations. The graph depicts absorption of FAGLA at 345 nm over time in presence of thermolysin and TFE. Only when incubated solely with thermolysin the absorption of FAGLA decreased over time (green triangles). Any concentration of TFE resulted in stagnating absorbance values similar to absence of thermolysin albeit lower. Controls with PBS instead of FAGLA showed very low A_{345} values for all TFE concentrations.

An indirect approach to easily assess intrinsic disorder of candidate proteins presents SEC. SEC is applied to separate proteins in solution based on their size, rather than their molecular weight. This is performed by applying the sample to a stationary phase of porous polymers. The larger a molecule is, the less time it needs for diffusion through such a matrix, while exceptionally small molecules, that can fit into many of the pores, need significantly longer to diffuse through the matrix (Lathe and Ruthven, 1955). More specifically, SEC allows determination of a proteins hydrodynamic size (or its Stokes Radius) rather than the molecular weight, a principle still not fully understood (Sun et al., 2004). As IDPs exhibit a more extended conformation than globular proteins, they are predicted to exhibit an aberrant size in SEC experiments as opposed to the size derived from sequence data (Receveur-Brechot et al., 2006). Accordingly, the TgLEAs were analyzed in SEC experiments by Prof. Frank Seeber (FG16, RKI, Berlin) and appeared in fractions of much larger molecules than their sequence would lead to assume (see Figure 24), serving as further indication for their IDP characteristics.

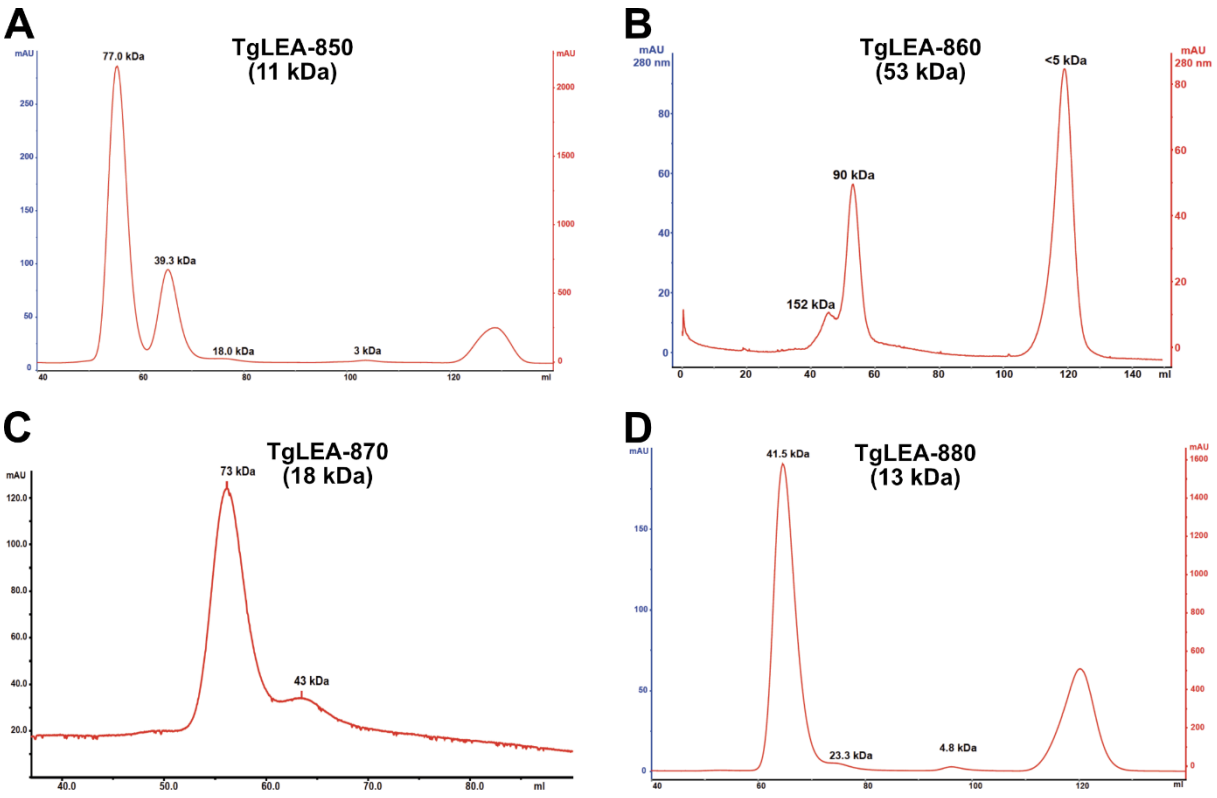

Figure 24: TgLEAs exhibit aberrant size in SEC. The graphs indicate fractionated molecules of different sizes that were separated from purified TgLEAs -850(A), -860 (B), -870 (C) and -880 (D) during SEC. The observed signals occurred in fractions of distinctly different sizes than the approx. molecular weight predicted for the TgLEAs (in brackets), based on their sequence.

Another approach to assess IDP characteristics of TgLEAs was the observation of their behavior in TSAs. Using a fluorescent dye that binds to hydrophobic sites on an unfolded protein the thermal stability of a protein can easily be assessed. A globular protein such as an IgG has a certain melting point at which the protein's structure denatures and it unfolds, allowing the dye to bind to more sites resulting in an increase in fluorescence. With an increasing amount of denatured proteins, the formation of protein aggregates increases as well, thus blocking binding sites for the dye resulting in a reduction of fluorescence. Opposed to that, TgLEAs did not exhibit clear peaks in TSAs (see Figure 26). Analyzed were several different batches of TgLEAs in TSAs. The first observation was the occurrence of differences in previously boiled and not-boiled protein preparations. With preparations of TgLEA-850 and -860 that were not boiled prior to loading on the column, there were peaks observable in the melting curves whereas with preparations of the same proteins that were boiled prior to loading on the column, those peaks were not observed (see Figure 25).

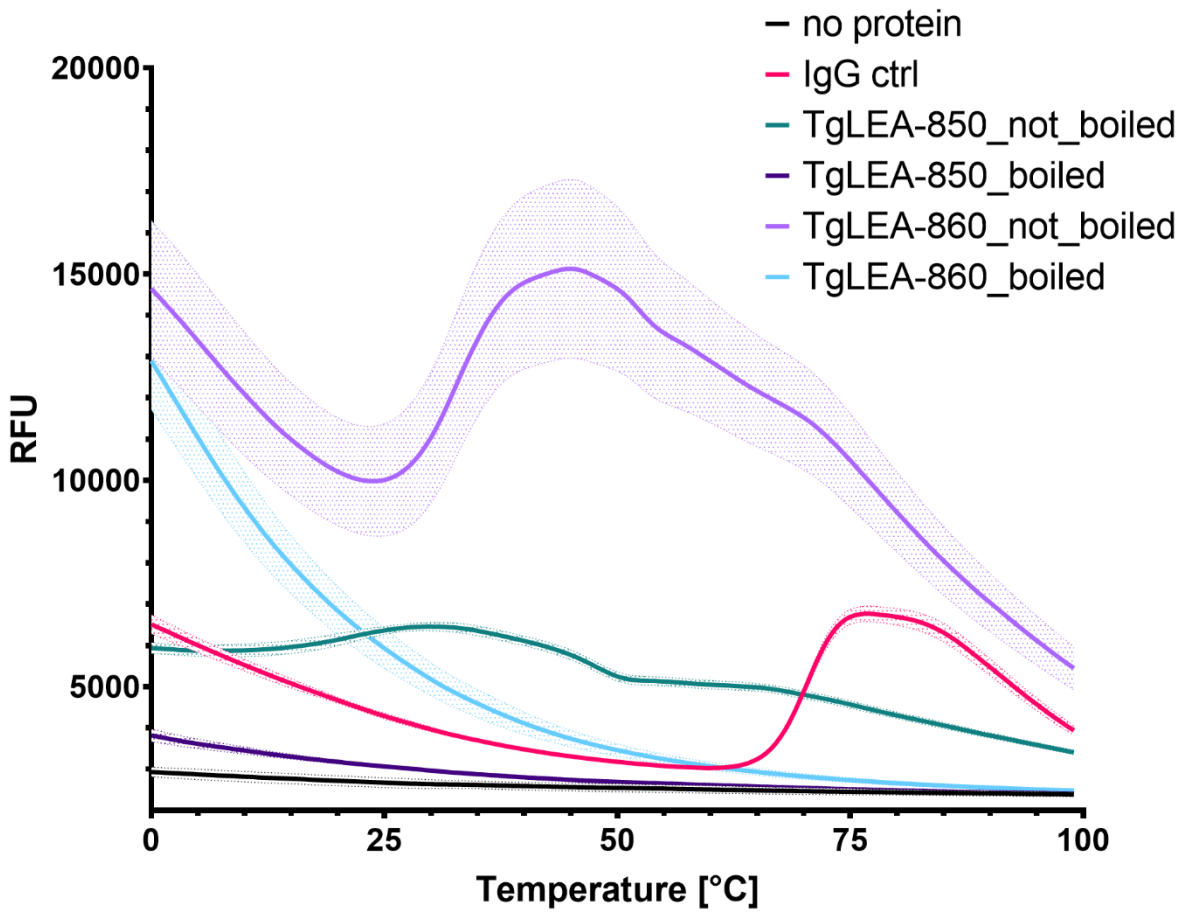

Figure 25: Effect of boiling on TgLEA preparation confirmed by TSA. The graph shows melting curves of recombinant TgLEA-850 and -860 that were prepared differently (boiled vs. unboiled) prior to purification. Melting curves of boiled preparations (dark violet and light blue) exhibit no clear peak and behave similar to the no protein control (black), while preparations of unboiled TgLEAs (green and light violet) exhibit varying melting points in a similar manner to the globular IgG control (magenta). n = 4 replicates; shaded areas indicate SD.

Similar to TgLEAs-850 and -860, preparations of TgLEAs-870 and -880 that were boiled for 10 minutes prior to loading on the Ni-sepharose column exhibited no peak in the TSA indicating no clear melting point (see Figure 26). An additional observation was that TgLEA-860 shows increased initial fluorescence around 0 °C that decreases over time with increasing temperature, indicating a possible change in conformation with increasing temperatures.

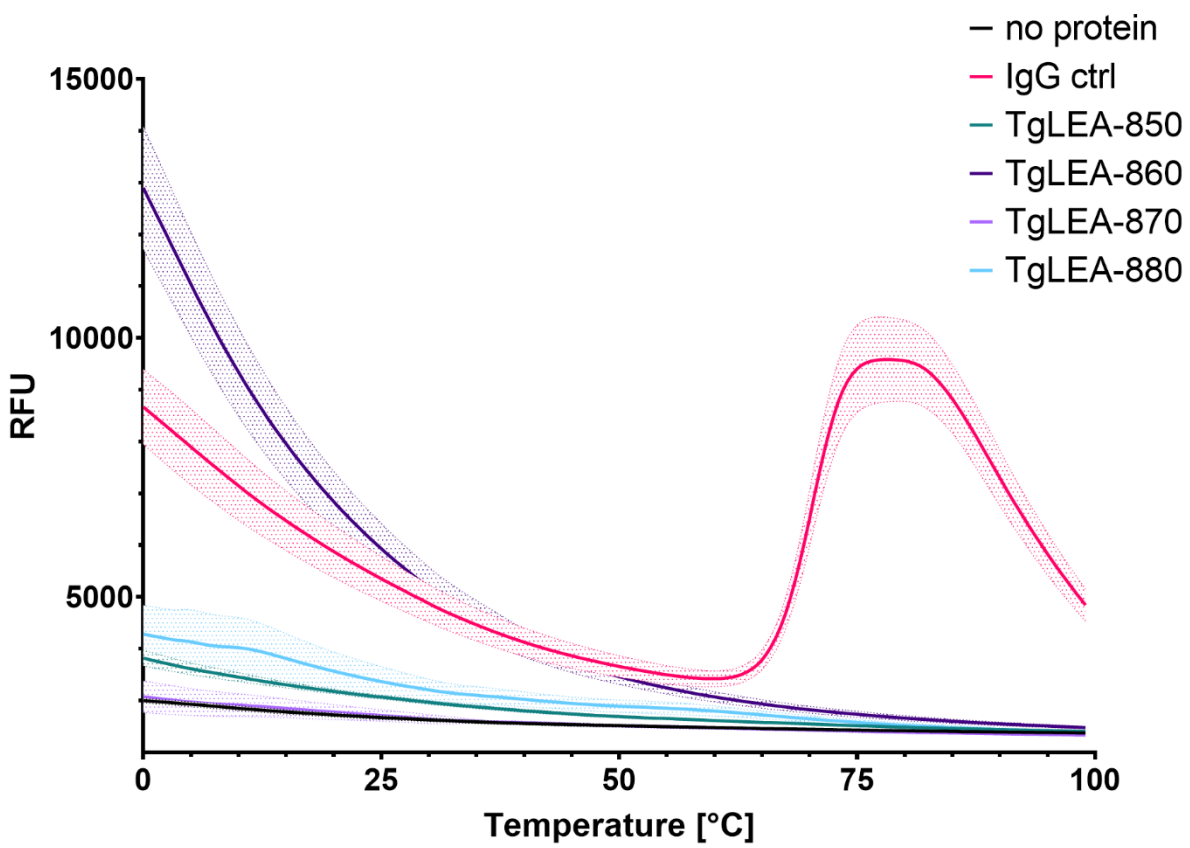

Figure 26: TgLEAs behave unlike globular proteins in TSA. The graph shows melting curves of all four recombinant TgLEAs. Despite TgLEA-860's high initial fluorescence, no TgLEA exhibits a fluorescent peak indicative of a conformational change, as observed in the IgG control. n = 4 replicates; shaded areas indicate SD.

The final confirmation of the TgLEAs' IDP characteristic was looked for via Circular dichroism spectroscopy in cooperation with the group of Dr. Andreas Rummel from the Medizinische Hochschule Hannover. This experiment revealed for all four TgLEAs a high content in disordered regions that raged between 30 to 50 % (see Figure 27). The highest structural component in all four TgLEAs were beta-sheet formations, that made up between 40 and 60 % of the proteins' structure. Random coils were found to be the second most dominant structural component, while alpha-helices and turns were only found to a small extend in three and two of the TgLEAs, respectively. These findings suggest that the TgLEAs are less likely to be IDPs but could rather be hybrid proteins carrying IDPRs (Uversky, 2019).

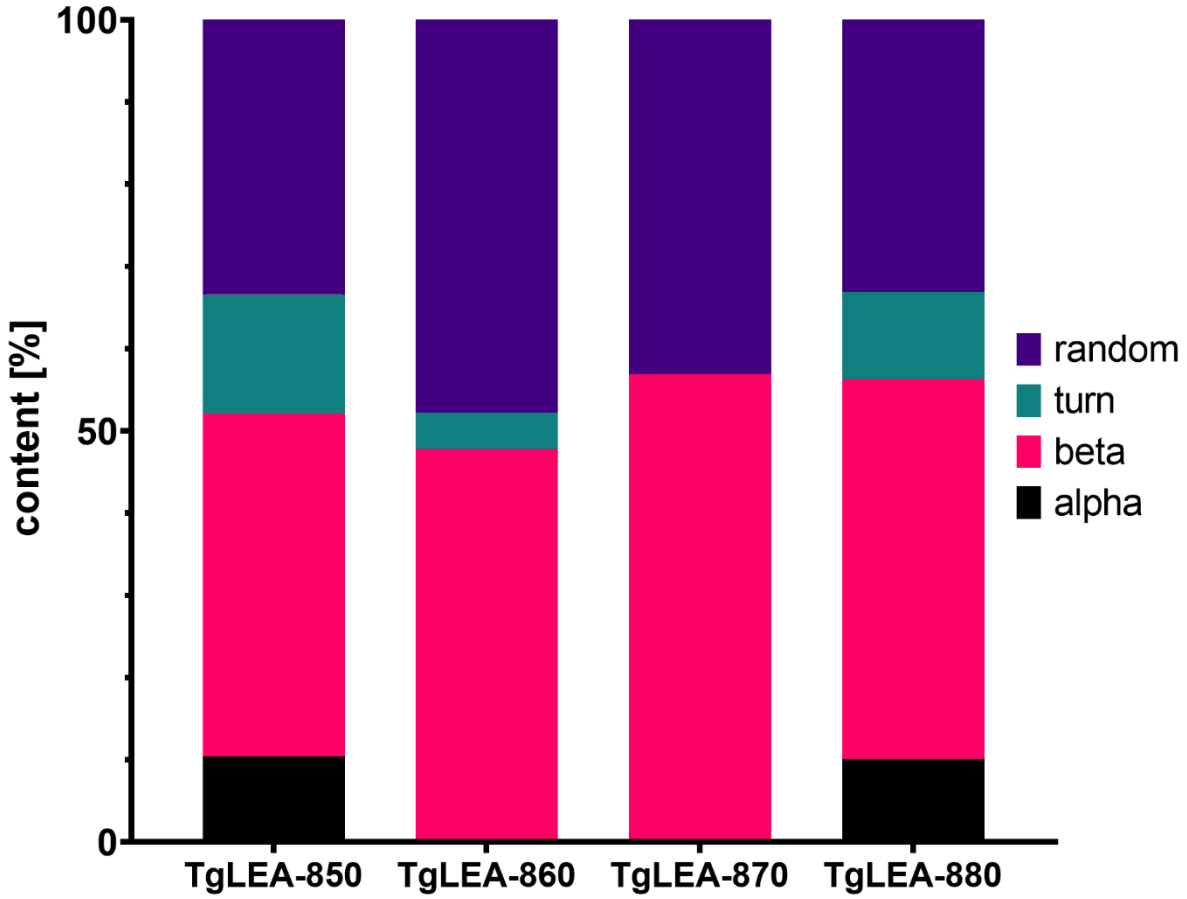

Figure 27: CD spectroscopy reveals high content of disordered regions for all four TgLEAs. The graph depicts the proportion of structures observed in all TgLEAs. The highest structural proportion for all TgLEAs are beta-sheets (magenta) followed by random coils (violet). Turns (green) and alpha helices (black) are only present in small amounts and not in all TgLEAs.

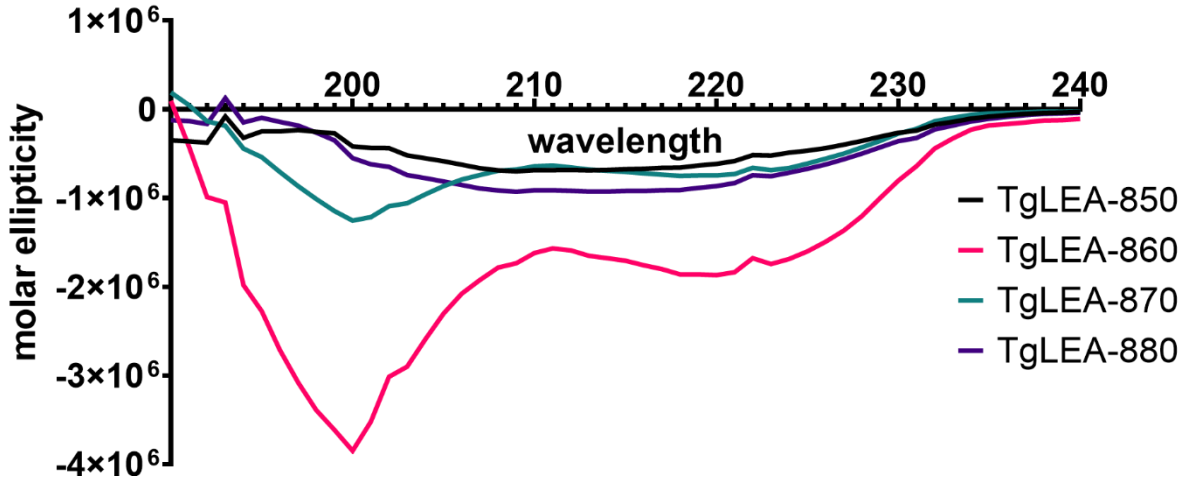

Figure 28: CD spectra of TgLEAs, depicted as molar ellipticity at different wavelengths. TgLEAs are characterized by highly negative molar ellipticity around the 200 nm wavelength, that extends to a drawn-out negative band until approx. 220 nm until negligible molar ellipticity is reached between 230 and 240 nm.

3.2.7 TgLEAs prevent aggregation of porcine LDH (pLDH) upon stress *in vitro*

Since the experimental approach to test a protective effect of TgLEAs on the growth of bacteria and yeast (data not shown) under stressing conditions yielded equivocal results, further tests were conducted *in vitro*. In a first experiment, the potential to prevent protein aggregation upon low temperatures was analyzed. The increase in aggregate formation of porcine LDH (pLDH) upon repeated freeze-thaw cycles was assessed, with and without TgLEAs, BSA and trehalose, tested in molar ratios of 1:100, 1:50 and 1:25. This experiment revealed that even at a molar ratio of 1:25, three of the four TgLEAs drastically reduced the amount of aggregate formation, while TgLEA-870 contributed to a reduction of aggregate formation to the same degree trehalose did (see Figure 30).

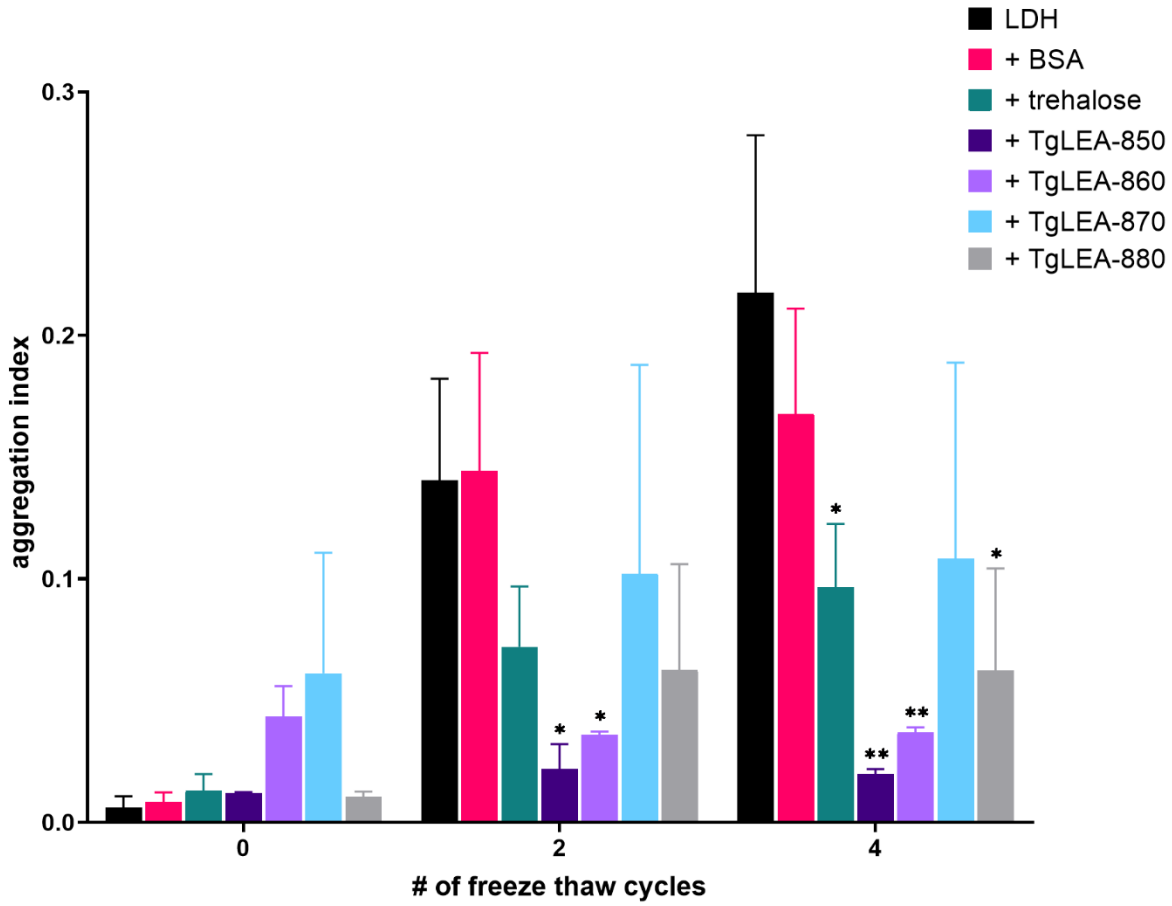

*Figure 29: Prevention of pLDH aggregation upon freeze-thaw-stress through TgLEAs. The graph shows the development of aggregate formation of LDH in presence of TgLEAs and cryoprotectants after repeated freeze-thawing. In presence of TgLEAs or trehalose maximal observed aggregate formation after four cycles is limited to approx. half of that of LDH alone and significantly reduced in all other TgLEAs in comparison to LDH alone. * = P < 0.05 and ** = P < 0.01 shown above the bar indicate results significantly different from those for LDH alone. n = two replicates.*

3.2.8 TgLEAs preserve activity of pLDH upon stress *in vitro*

After discovering that TgLEAs can protect pLDH from low-temperature-induced aggregation, their potential to preserve the enzymatic activity upon the same stress was investigated.

Several molar ratios of LDH and the respective TgLEA were tested, including ratios of 1:100 (0.5 µM pLDH and 50 µM TgLEA/control), 1:50 (0.5 µM pLDH and 25 µM TgLEA/control) and 1:25 (0.5 µM pLDH and 12.5 µM TgLEA/control). In general, the TgLEAs showed a protective effect even after 4 freeze-thaw-cycles at high molar ratio (0.5 µM LDH to 50 µM or 25 µM TgLEA; see Figure 52 and Figure 53 in the appendix). The lower the molar ratio was, the weaker the effect of TgLEA-850 on pLDH became. At a molar ratio of 1:25, the effect of TgLEA-850 on pLDH was not better than that of BSA, a known cryoprotectant, at the same ratio. By contrast, at the same molar ratio, TgLEA-860 still preserved nearly 100 % of the pLDH activity after four freeze-thaw-cycles.

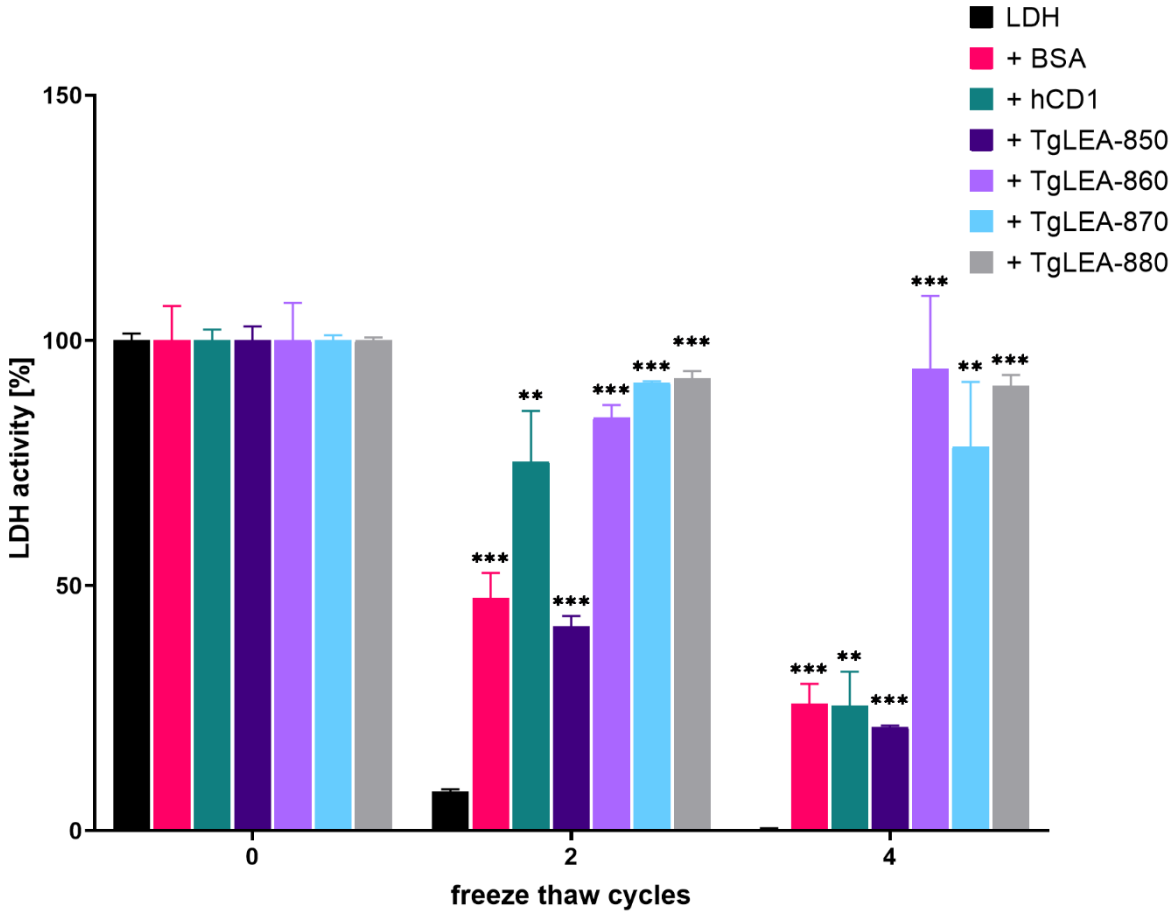

*Figure 30: Preservation of pLDH activity upon freeze-thaw-stress by TgLEAs. Depicted is relative pLDH activity in presence of TgLEAs and control proteins after repeated freeze-thawing. Alone, pLDH activity is reduced to almost 0 % after four freeze-thaw-cycles. BSA, hCD1 and TgLEA-850 preserve approx. 25 % of the initial pLDH activity, while the remaining TgLEAs preserve between 80 and 100 % of pLDH activity after four cycles. * = P < 0.05, ** = P < 0.01 and *** = P < 0.001 shown above the bar indicate results significantly different from those for LDH alone. n = three replicates.*

Moreover, TgLEAs-870 & -880 also still exhibited a preserving effect on LDH activity as both maintained pLDH activity at between 80 and 100 % even after four freeze-thaw- cycles (see Figure 30).

3.2.9 Cloning and recombinant expression of TgLDH1

In addition to demonstrating the protective properties of TgLEAs on pLDH, an assessment of similar function on TgLDH1 was conducted. Other than pLDH, TgLDH1 is not commercially available, thus a system for recombinant expression of TgLDH1 in *E. coli* was designed. *T. gondii* possesses two differentially expressed genes, each coding for one LDH isoform, LDH1 and LDH2, that are exclusive to tachyzoites and bradyzoites, respectively. In case of sporozoites, transcriptomic analysis revealed high expression levels of LDH1, similar to those found in tachyzoites, while transcripts of LDH2 showed low abundance, indicating a prevalence of LDH1 also in oocysts (Fritz et al., 2012). This allowed isolation of the TgLDH1 (acc. Number: XM_002368064) sequence from cDNA derived from *in vitro* cultured tachyzoites (see chapter 2.2.22) with primers that were designed to enable cloning into the pAviTag vector, in frame with a C-terminal 6His-tag for purification by immobilized metal affinity chromatography (see chapter 2.2.23). The resulting plasmid was named pAviTag-TgLDH1 (see Figure 56 in the appendix) and allowed selection using the antibiotic Kanamycin as well as induction of expression by IPTG, yielding > 10 mg/l of bacterial culture. Analysis of bacterial lysate after expression, the intermediate and final purification fractions via SDS-PAGE and subsequent Coomassie staining revealed a substantial band at the desired size of TgLDH1 (approx. 35 kDa; see Figure 31), indicating good suitability of the designed system for production of recombinant TgLDH1 for *in vitro* experiments.

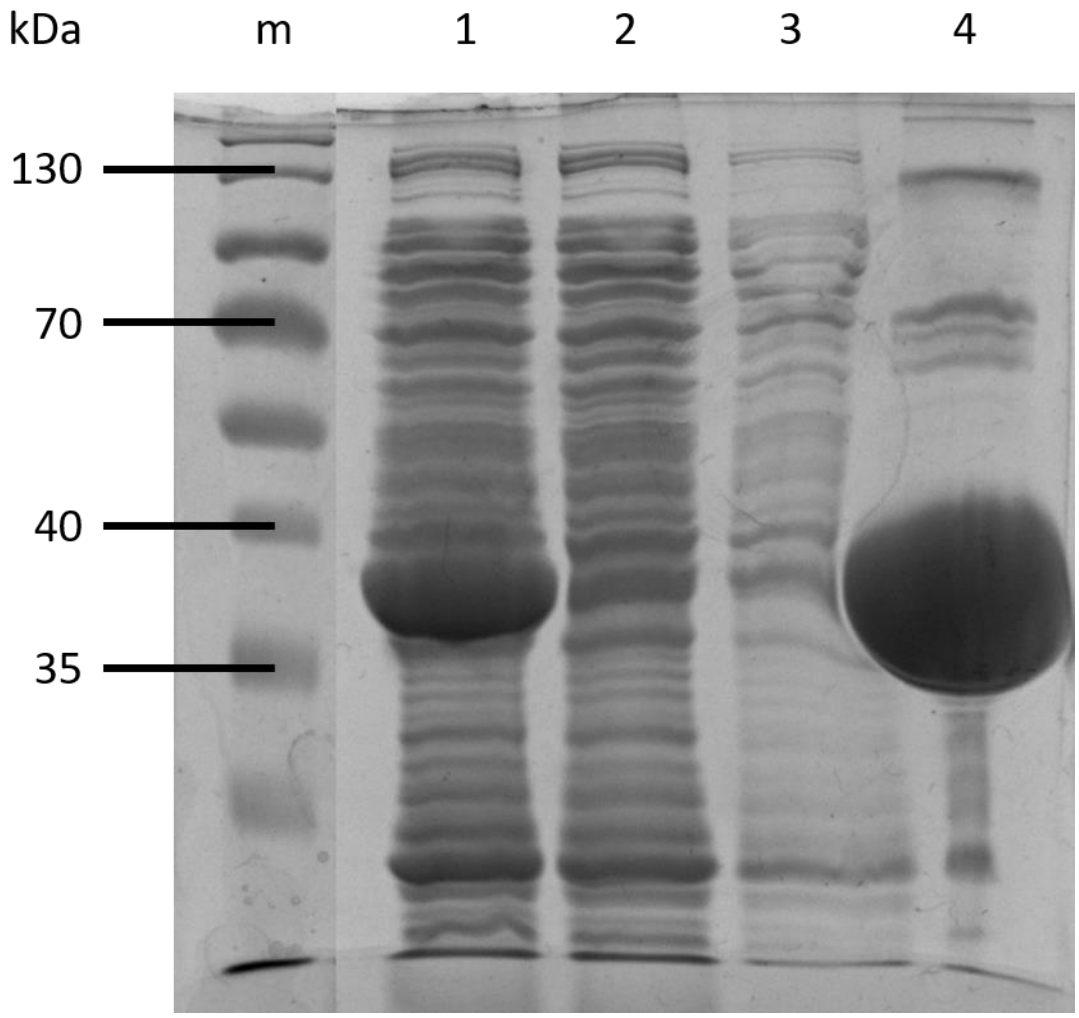

Figure 31: Confirmation of purified TgLDH1 via coomassie protein stain. The intense band in lane 4 indicates successful purification of TgLDH1 (molecular weight: 35.55 kDa). 1 = lysate prior to loading, 2 = lysate after running over column, 3 = washing fraction, 4 = pool of eluted fractions. Parts of the image were omitted for improved clarity, hence the fragment between lanes m and 1.

3.2.10 TgLEAs prevent aggregation of recombinantly expressed TgLDH1 upon stress

Since a molar ratio of 1:25 (0.5 µM LDH with 12.5 µM TgLEA/control) revealed an observable effect for all TgLEAs, these ratios were also applied for experiments with TgLDH1. Repeating the same assay as before but using TgLDH1 instead showed similar protective effects of TgLEAs on aggregate formation of TgLDH1 when exposed to repeated freeze-thawing.

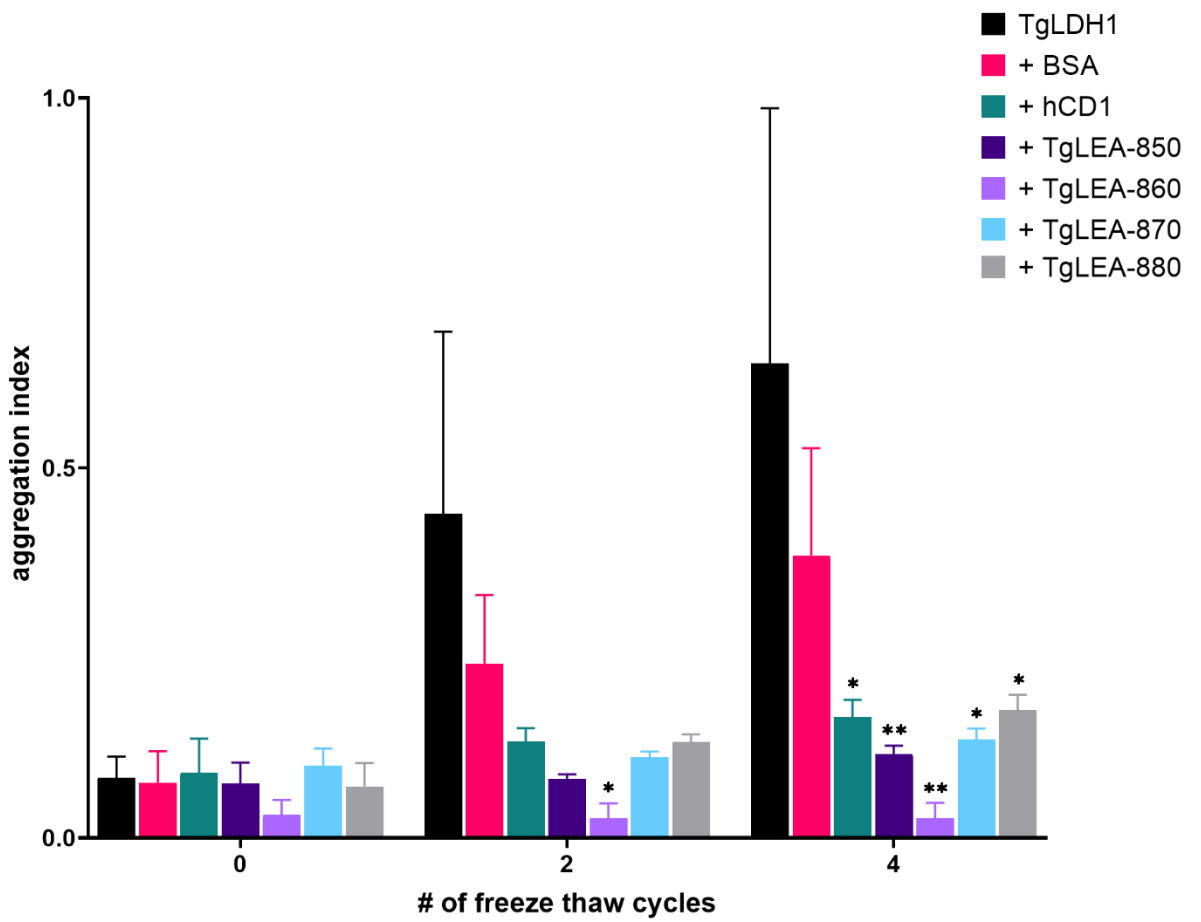

*Figure 32: Prevention of TgLDH1 aggregation upon freeze-thaw-stress through TgLEAs. The graph shows the increase in aggregate formation of TgLDH1 alone or in presence of TgLEAs and control proteins after repeated freeze-thawing. In presence of TgLEAs or hCD1, aggregate formation is significantly reduced after four cycles as compared to the cumulation of formed aggregates over four cycles in TgLDH1 alone (black) or in presence of BSA (magenta). * = P < 0.05 and ** = P < 0.01 shown above the bar indicate results significantly different from those for LDH alone. n = three replicates.*

Without any protectants, aggregation of TgLDH1 steadily increased over 4 freeze-thaw-cycles, while addition of BSA resulted in a reduction of aggregate formation by approx. 50 %. Presence of TgLEAs or hCD1 as IDP control resulted in virtually no observable aggregate formation even after 4 freeze-thaw-cycles.

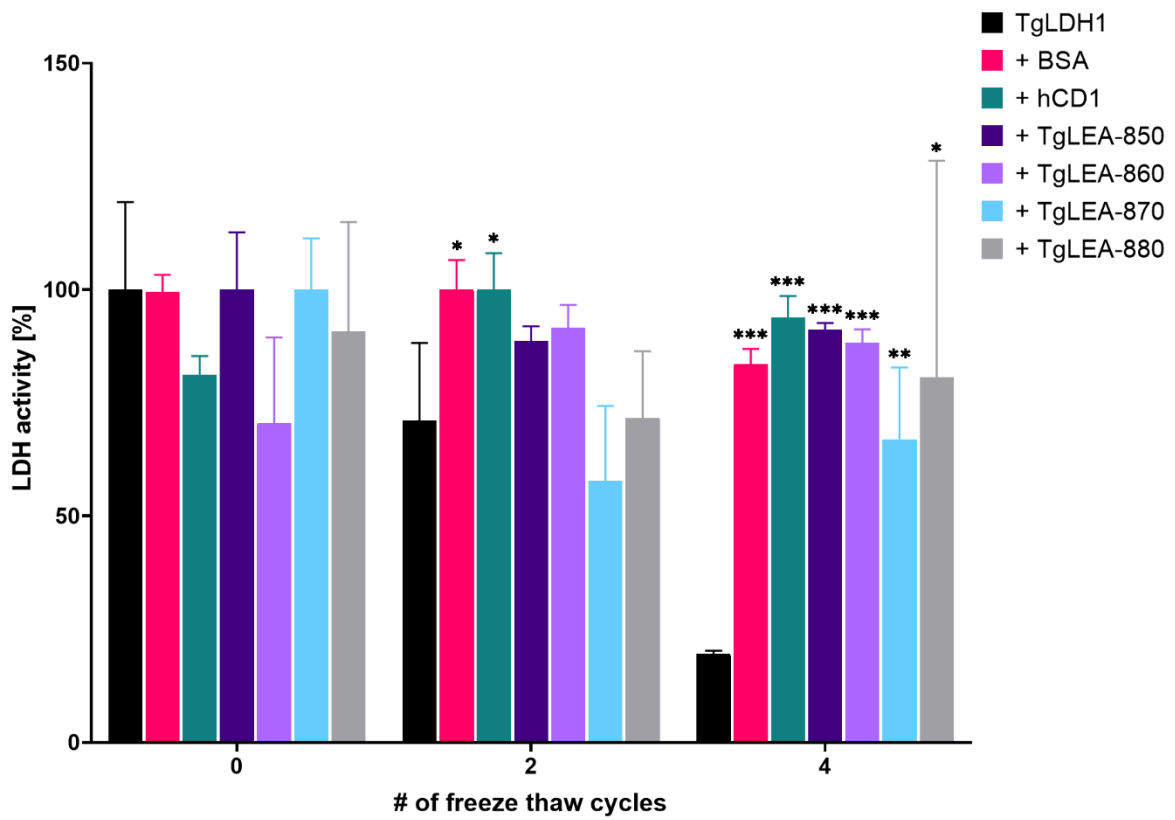

*Figure 33: TgLEAs preserve activity of TgLDH1 upon freeze thaw stress. Depicted is relative TgLDH1 activity in presence of TgLEAs and control proteins after repeated freeze-thawing. Alone, TgLDH1 activity is reduced by approx. 75 % after four freeze-thaw-cycles. TgLEAs-880 (gray) and -870 (blue) limit this loss to 50 %, while BSA, hCD1, TgLEA-860 and -850 limit the activity loss to between 5 and 20 %. * = P < 0.05, ** = P < 0.01 and *** = P < 0.001 shown above the bar indicate results significantly different from those for LDH alone. n = three replicates.*

3.2.11 TgLEAs preserve activity of TgLDH1 upon stress *in vitro*

Finally, it was also assessed, if recombinantly expressed TgLEAs preserve enzymatic activity of recombinantly expressed TgLDH1 when exposed to repeated freeze-thaw cycles and at the same molar ratio of 1:25 as before. Similar to the findings from the aggregation assay, TgLDH1 activity was reduced by 75 % after 4 freeze-thaw-cycles. In contrast, TgLEAs-870 and -880 mediated a slight stress resistance, as activity was only reduced by 50 to 40 %, respectively. Interestingly, BSA seemed to be as well suited as other TgLEAs and hCD1 in conferring stress resistance in this experimental setup, as the reduction of activity was limited to only 10 % at maximum after 4 freeze-thaw-cycles.

3.3 Molecules as antigens for identification of oocyst-mediated infections

3.3.1 Testing plate material and blocking protocols for ELISAs

Because of the TgLEAs assumed IDP characteristics, a more careful approach was necessary in testing the antigen suitability. In a first step, the optimal type of multi-well plate for ELISA testing as well as the preferred blocking reagent (BSA vs milk) was determined. ELISA tests were performed on TgLEA-880, as supernatant from hybridoma cell cultures expressing antibodies against this TgLEA was available, and biotinylated SAG1 ($TgSAG1_{bio}$) as antigens. Five different plate types were tested. MediSorp plates appeared to be best suited for ELISA tests using disordered proteins (see Figure 54 and Figure 55 in the appendix). Since both tested antigens, TgLEA-880 and $TgSAG1_{bio}$, carry a his-tag, anti-his antibody was used as coating control to confirm antigen presence. In all tested plate types, this control resulted in high signal, indicating successful coating for both antigens. Overall, the hybridoma supernatant against TgLEA-880 resulted in much lower signal than the anti-his antibody with 0.35 being the highest observed value for hybridoma supernatant compared to 4 for anti-his antibody. MediSorp plates exhibited slightly higher values for the TgLEA-880 antibody control. MediSorp plates gave much lower signal for the mice sera control, however, $TgSAG1_{bio}$ as antigen resulted in slightly elevated values. When blocking with milk, MaxiSorp and MediSorp plates performed similarly well. Both plate types exhibited very low signal for the negative mice sera controls, higher vlaues for TgLEA-880 when testing the hybridoma supernatant and very low background signal for all other controls over all. MediSorp plates however exhibited slightly higher values for the TgLEA-880 antibody control and MaxiSorp plates had lightly higher background signal in some uncoated wells. Therefore, all future ELISA tests were performed on MediSorp plates.

3.3.2 Establishing a Luminex assay to test chickens for *T. gondii* infections

Although several Luminex based serological tests for *T. gondii* infections have been published previously, those tests focus on human infections. Here, the aim was to establish a Luminex based assay to assess infections in chicken sera. This was done to facilitate the in-depth characterization of TgLEAs with regards to their potential to serve as antigen in serological surveys, as the multiplexing capabilities allow inclusion of more controls in the assays without having to reduce the number of tested samples. The possibility to test chicken sera using the Luminex technique was analyzed by using a biotinylated version of the known working antigen SAG1 (Klein et al., 2020), which was provided by Sandra Klein (FG16, RKI, Berlin). $TgSAG1_{bio}$ was specifically designed to enable optimal presentation of the epitopes. Thus, the mature $TgSAG1_{bio}$ protein can be bound to any surface coated with streptavidin in a targeted way, allowing uninhibited access to the N-terminal epitopes. Sera collected from 90 experimentally infected chickens were used. They had been collected from 23 noninfected and 67 infected

chickens that had either been orally inoculated with different numbers of oocysts (17 chickens with 1 * 10^3 oocysts; 12 chickens with 1 * 10^5 oocysts; 10 chickens with 1 * 10^6 oocysts) or brains of chronically infected mice (16 chickens), or intravenously with *in vitro*-cultivated tachyzoites (12 chickens with 1 * 10^6 tachyzoites). At the end of the observation periods, the infection state of the inoculated chickens was assessed. Detailed results of these examinations have been reported elsewhere (Schares et al., 2018). In addition to using $TgSAG1_{bio}$ as antigen to test for *T. gondii* infections, chicken serum albumin and anti-IgY antibody were included as negative and positive controls, respectively.

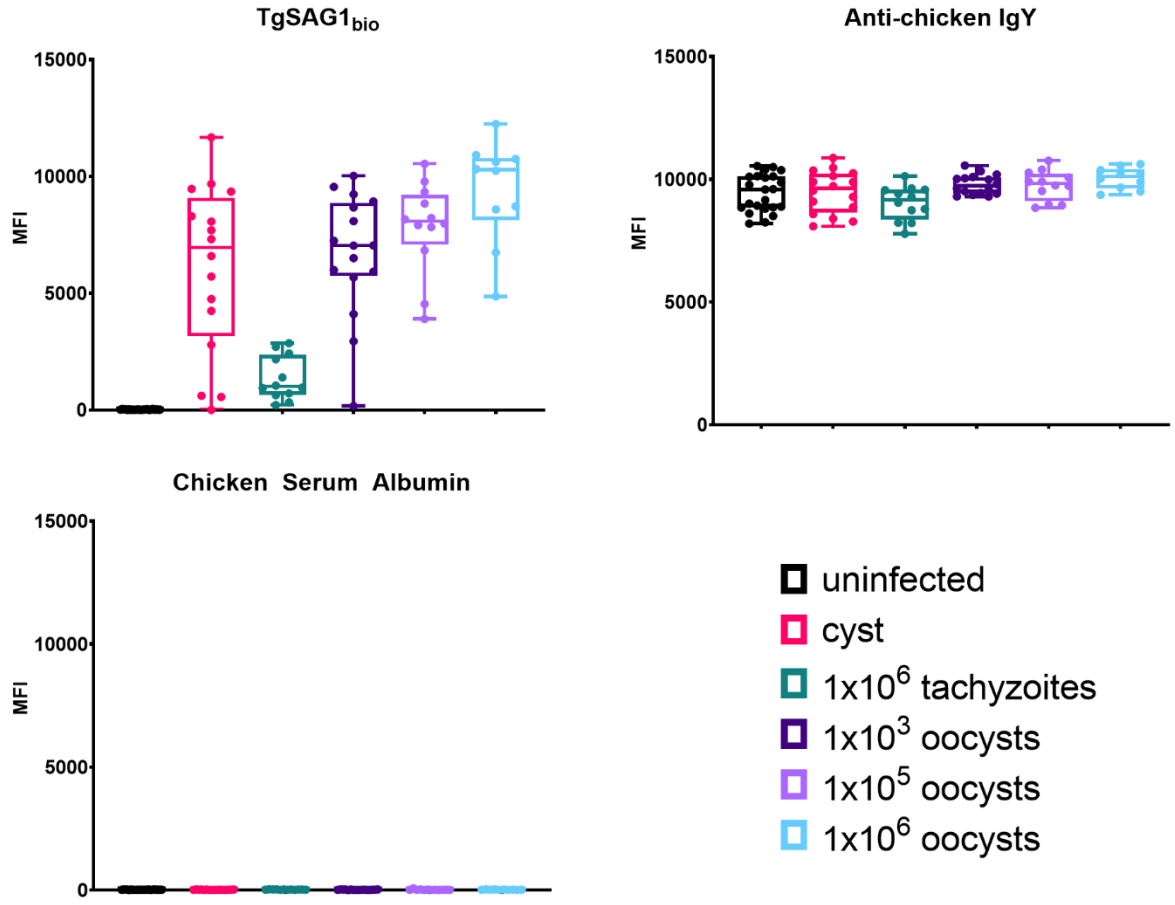

Figure 34: Luminex assay is well suited to detect T. gondii infections in chickens. The graphs show observed signal when testing sera from differently infected chickens with $TgSAG1_{bio}$, Anti-chicken IgY as positive control and chicken serum albumin as negative control. Signals for all sera were comparable within the respective controls. Sera from tachyzoite infected chickens (green) exhibited only low signal against $TgSAG1_{bio}$, whereas sera from all other infected groups were similarly high, albeit with high variability in the cyst infected and low oocyst dosage groups.

The anti-IgY control determined one sample to be an outlier which was therefore excluded from further analyses. All remaining sera exhibited high median fluorescence intensity (MFI) values slightly lower than 10,000. In the chicken serum albumin control, all samples resulted in very low MFI values. Using $TgSAG1_{bio}$ as antigen, all sera from noninfected chickens

resulted in MFI values comparable to those of the chicken serum albumin control. However, all sera from infected chickens exhibited MFI values of > 1,300 (see Figure 34).

Signal for sera from chickens infected by tissue cyst exhibited a wide range, reaching from 7 to > 11,500 MFI. From all infected chickens, those infected by tachyzoites resulted in the lowest overall MFI values of around 1,300. Sera from chickens given the lowest number of oocysts ($1 * 10^3$) gave MFI values similar to those of chickens infected by tissue cysts. Most importantly, sera from chickens that were infected by higher numbers of oocysts resulted in higher MFI values. Accordingly, chickens that were infected by $1 * 10^6$ oocysts resulted in the highest overall MFI values, comparable to the anti-IgY antibody control.

3.3.3 TgLEAs are not suited for ELISA testing against *T. gondii* infections

From the previous mentioned 89 chicken sera from experimentally infected animals, a robust panel of 33 sera in total was designed, accounting for several factors such as infection type, infection dose and strain type (see Table 6). All samples were taken five weeks after infection.

Table 6: Serum panel constructed from 33 sera from experimentally infected chickens.

Uninfected			Oocyst infected			Tissue cyst infected		
dosage	strain	sample	dosage	strain	sample	dosage	strain	sample
not infected	-	1.01	10^3 oocysts	CZ-Tiger	2.01	1 mouse brain	CZ-Tiger	3.01
not infected	-	1.02	10^3 oocysts	CZ-Tiger	2.02	1 mouse brain	CZ-Tiger	3.02
not infected	-	1.03	10^5 oocysts	CZ-Tiger	2.03	1 mouse brain	CZ-Tiger	3.03
not infected	-	1.04	10^5 oocysts	CZ-Tiger	2.04	1 mouse brain	CZ-Tiger	3.04
not infected	-	1.05	10^6 oocysts	CZ-Tiger	2.05	1 mouse brain	CZ-Tiger	3.05
not infected	-	1.06	10^6 oocysts	CZ-Tiger	2.06	1 mouse brain	CZ-Tiger	3.06
not infected	-	1.07	10^3 oocysts	ME49	2.07	1 mouse brain	ME49	3.07
not infected	-	1.08	10^3 oocysts	ME49	2.08	1 mouse brain	ME49	3.08
not infected	-	1.09	10^5 oocysts	ME49	2.09	1 mouse brain	ME49	3.09
not infected	-	1.10	10^5 oocysts	ME49	2.10	1 mouse brain	ME49	3.10
not infected	-	1.11	10^6 oocysts	ME49	2.11	1 mouse brain	ME49	3.11

This serum panel was used to assess suitability of TgLEAs in ELISA tests to specifically identify oocyst-caused infections. To ensure optimal antigenicity of the TgLEAs, a sandwich-ELISA-approach was established. MediSorp plates were precoated with anti-his-antibody prior to the ELISA procedure and afterwards the his-tagged TgLEAs were incubated within the precoated wells to anchor the his-tagged terminus of the protein on the antibody coated well surface. As a positive control, antibodies against TgLEAs-850 and -860 that were generated in immunized rabbits were used.

All 11 sera from chickens that were infected with oocysts resulted in equally high signal against $TgSAG1_{bio}$, while chickens that were infected with tissue cysts resulted in lower but still elevated signal that was in addition more variable. All sera from uninfected chickens resulted

in very low signal, albeit some background activity could be observed (Figure 35). In contrast, signal from all 33 chicken sera tested against TgLEA-850 was consistently lower than that of the uninfected chickens against $TgSAG1_{bio}$, regardless of infection type. Similarly, no differentiation between infection type could be observed with TgLEA-860 as antigen. Here, the signal for sera from chickens infected by oocysts was slightly higher than against TgLEA-850, however the signal was not higher than that of uninfected chickens or chickens infected by tissue cysts.

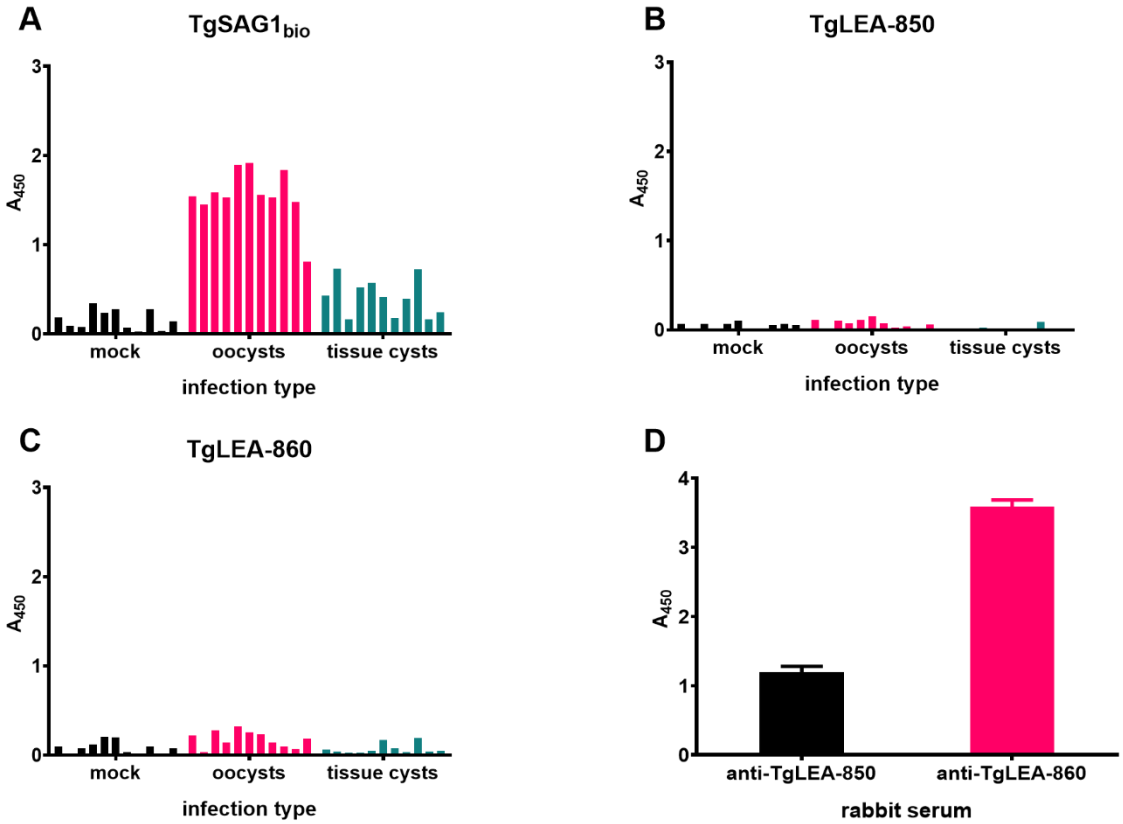

Figure 35: ELISA analysis indicates that TgLEAs are not suited for differentiation of infection sources. Reactivity of 11 sera each from chickens that were either not infected (mock), infected with different numbers of oocysts (oocysts) or one brain of mice infected with T. gondii (tissue cysts) was measured against $TgSAG1_{bio}$ (A), TgLEA-850 (B) or TgLEA-860 (C). As a control for antigenicity of TgLEAs, sera from rabbits immunized either with TgLEA-850 or -860 (three technical replicates each) were tested against the respective proteins (D).

Using purified IgG from rabbits immunized with recombinant TgLEAs as control confirmed that both TgLEAs result in a measurable signal if antibodies against them are present in the serum. Both rabbit sera resulted in pronounced signal that was much higher than any serum from uninfected chickens in the ELISA. However, the signal resulting from TgLEA-860 as antigen was nearly three times higher than that of TgLEA-850 although the plates were prepared with different amounts of protein to account for their differences in size.

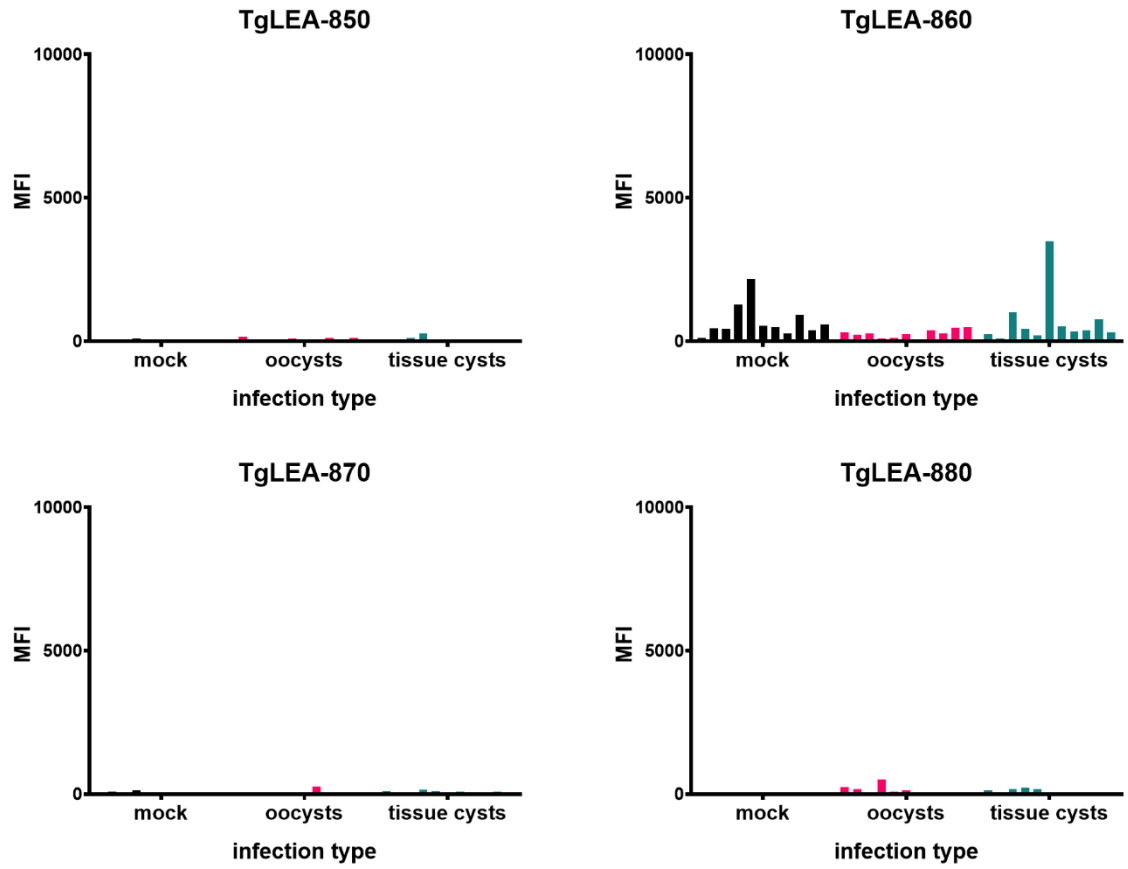

Figure 36: TgLEAs do not identify sera from oocyst infected chickens at a dilution of 1:200. The graphs depict observed signal of sera from noninfected chickens ("mock", black), oocyst infected chickens (magenta) and tissue cyst infected chickens (green). Except for TgLEA-860, almost no signal was observed for any TgLEA, regardless of infection type. Some signal was observed with TgLEA-860 as antigen, but the values observed in oocyst infected chickens were lower than those of noninfected or tissue cyst infected chickens.

3.3.4 TgLEAs do not result in a specific serological response in the Luminex assay

Luminex analysis of the same serum panel of 33 experimentally infected chickens using all four TgLEAs as antigens did not yield a reliable differentiation between infection routes. Figure 36 shows that no TgLEA lead to a clear MFI signal that allowed determination of an infection. If at all, sera reacted slightly more to TgLEA-860, however, in this particular case, MFI results of the 11 oocyst infected sera samples were all lower than the MFI values from sera of tissue cyst or even non infected chickens. In the case of the three other TgLEAs, MFI values of all sera samples were equally low. In addition to the four tested antigens, the assay included biotinylated TgSAG1$_{bio}$ as a known antigen control as well as chicken serum albumin and goat-anti-chicken IgY as negative and positive controls, respectively. Figure 37 shows the results of the Luminex analysis for these molecules. TgSAG1$_{bio}$ as antigen allowed clear discrimination of infected chicken sera from not infected chicken sera, as MFI values of these sera ranged from 5,000 to 10,000 as compared to the low hundreds of "mock" samples. CSA as negative

control resulted in similar MFI values to the TgLEAs and the anti-chicken IgY as positive control resulted in high MFI values of up to 5,000 for all 33 serum samples.

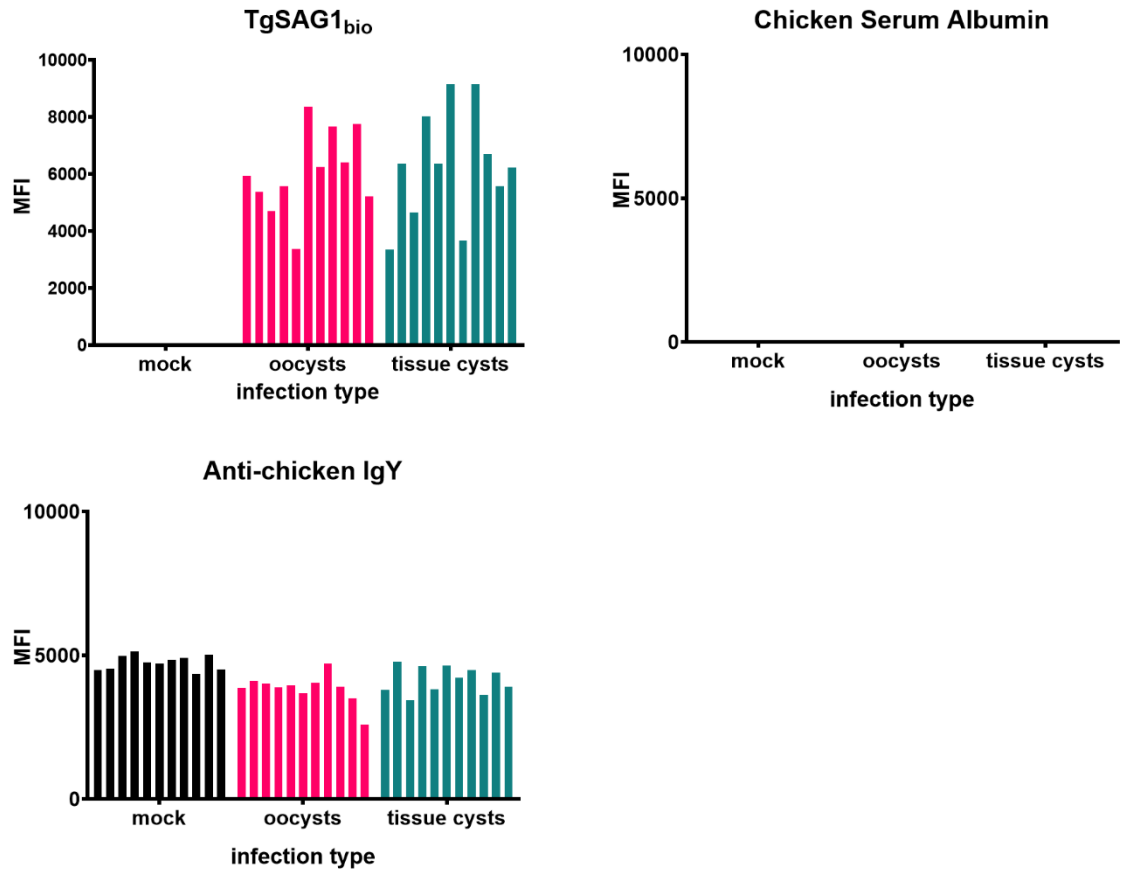

Figure 37: Controls confirm Luminex findings of chicken sera diluted 1:200. Graphs of control antigens confirm presence of T. gondii specific antibodies only in the groups of infected chickens (TgSAG1$_{bio}$), no background signal (chicken serum albumin) and presence of chicken IgY in all 33 sera (anti-chicken IgY).

3.3.5 A lower serum dilution does not result in better differentiation

For better comparison to previous publications, Luminex testing was repeated on the 33 chicken sera at a dilution of 1:25, otherwise, testing conditions remained unchanged. The results of the previous Luminex testing were confirmed, as no difference in MFI values could be observed in relation to any specific TgLEA (Figure 38). When using TgLEA-860 as antigen, all 33 sera resulted in similar values with two outliers, one in the group of tissue cyst infected chickens and one in the uninfected group. Both were already apparent at a serum dilution of 1:200. The decreased dilution resulted in elevated MFI values when using TgLEA-870 as antigen, however, all 33 sera resulted in indistinguishable, low values. An exception was TgLEA-880. Here, for each group of the infected chickens, six samples were distinguishable from the group of uninfected chickens due to higher MFI values (see chapter 3.3.6). Comparing both groups of infected chickens however revealed no difference that allowed clear determination of oocyst infected chickens from tissue cyst infected chickens.

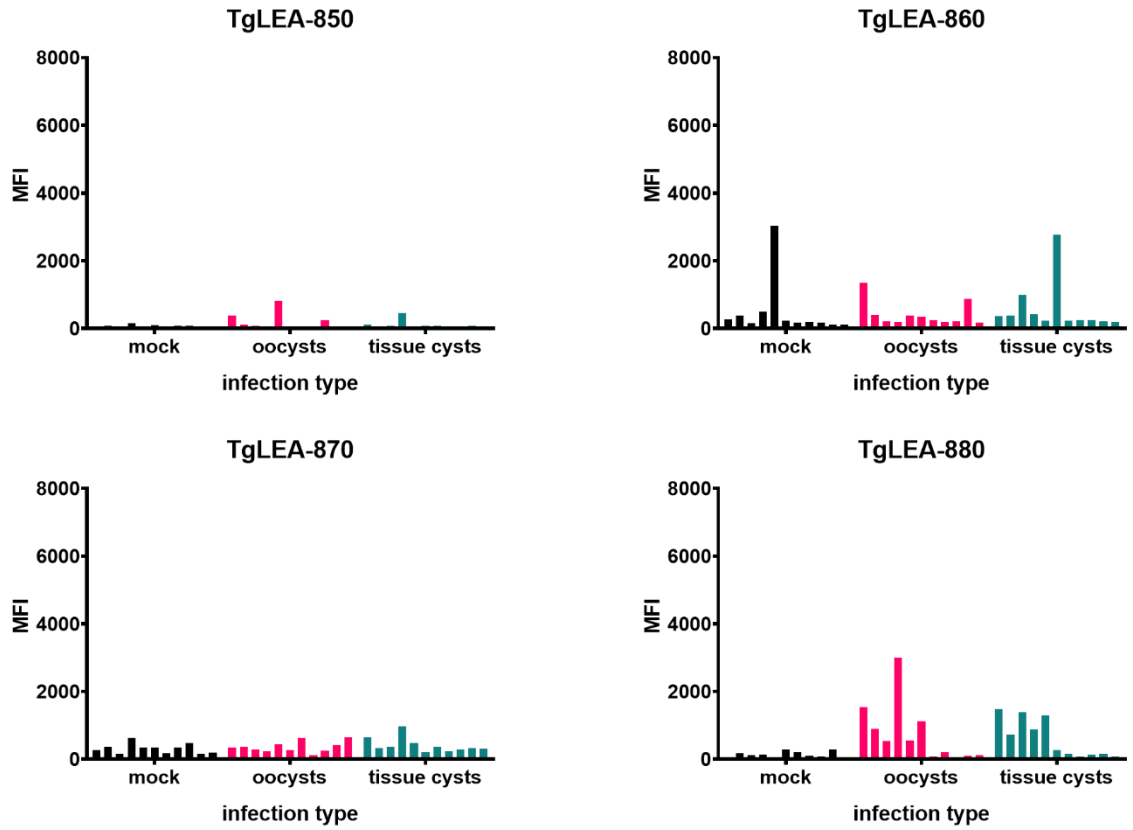

Figure 38: At a lower serum dilution of 1:25, TgLEAs do not detect infections resulting from oocyst ingestion in chickens. As above, the graphs depict observed signal of sera from noninfected chickens ("mock", black), oocyst infected chickens (magenta) and tissue cyst infected chickens (green). Again, almost no signal was observed for TgLEA-850 with a few peaks in the oocyst infected group and one in the tissue cyst infected group. Observed signal in TgLEA-870 was slightly elevated but similar in all serum groups. As before, higher signal occurred for TgLEA-860 with the highest values in noninfected and tissue cyst infected groups. For TgLEA-880, the signal observed in noninfected chickens was distinctively lower than in oocyst and tissue cyst infected chickens.

The same controls as in the previous assay were used ($TgSAG1_{bio}$, CSA, anti-chicken IgY). Slightly higher values for the anti-chicken IgY control confirmed the decreased serum dilution and low MFI values for the CSA control excluded any background activity.

The values for the $TgSAG1_{bio}$ control appeared to be highly variable. Upon closer inspection it became apparent that the bead count for $TgSAG1_{bio}$ conjugated beads was much lower than in all other assays, in some instance no beads were detected and in others the number of counted beads was too low to give a representative signal (see Table 8 in the appendix for the raw data). No further instances of reduced bead count were observed in all other assays. Therefore, the $TgSAG1_{bio}$ control cannot be considered for comparisons of values obtained for TgLEAs. However, since the remaining controls showed no significant background signal and anti-chicken IgY activity the obtained results can still be considered as valid.

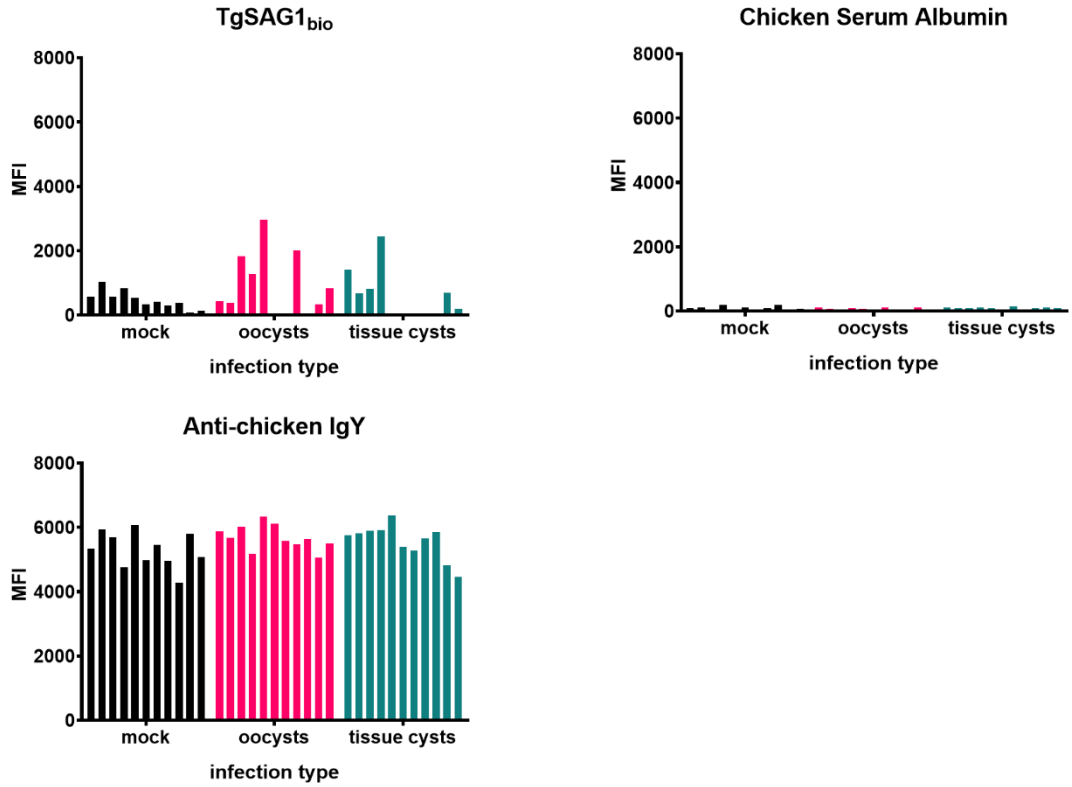

Figure 39: Controls confirm Luminex findings of chicken sera diluted 1:25. Graphs of control antigens confirm presence of T. gondii specific antibodies only in the groups of infected chickens (TgSAG1$_{bio}$), no background signal (chicken serum albumin) and presence of chicken IgY in all 33 sera (anti-chicken IgY).

3.3.6 Differences in antibody response of sera of different strains for TgLEA-880

Remarkably, using TgLEA-880 as antigen seemed to allow differentiation between different *T. gondii* strains. While sera from the control group of chickens that were not infected with *T. gondii* resulted in overall low observed MFI values, six sera from both groups of chickens infected either with oocysts or tissue cysts exhibited elevated FI values. Differentiating both groups of chickens further with regards to the strain of *T. gondii* from which the infective stages were derived, the six sera that were infected with the CZ-Tiger strain of *T. gondii* resulted in higher MFI as compared to five sera from chicken that were infected with the ME49 strain (see Figure 40). As mentioned above, comparisons to values obtained with TgSAG1$_{bio}$ as antigen are impeded by the reduced observed count of TgSAG1$_{bio}$ conjugated beads.

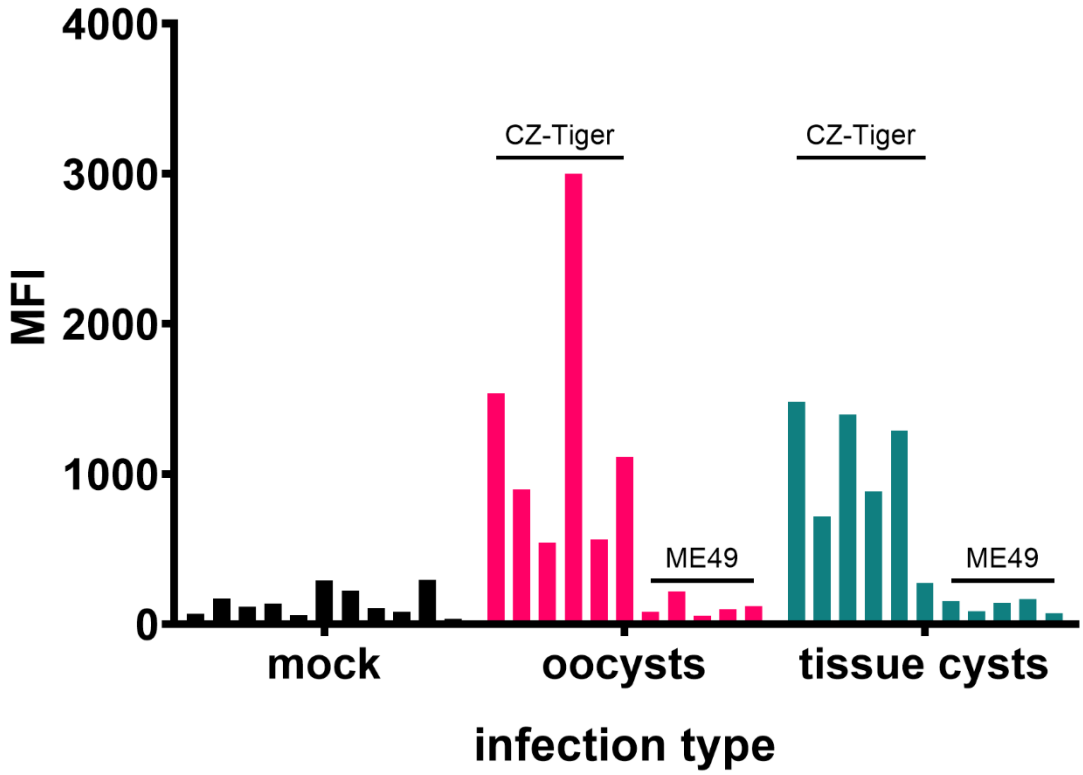

Figure 40: Detailed analysis of immune response to TgLEA-880 as an antigen. Sera from non infected chickens as controls result in low MFI values indicating no binding of antibodies to TgLEA-880 (black bars). Sera from chickens infected either with oocysts (magenta) or tissue cysts (green) of T. gondii vary in antibody response to TgLEA-880. Indicated are the different T. gondii strains from which the infective stages were derived.

Chapter 4: Discussion

4.1 Molecules binding to the oocyst wall

4.1.1 Advantages of the AEO-IFA

The reason why *T. gondii*'s sexual reproduction is limited exclusively to felids, remained unknown for several decades. In 2019 it was discovered that linoleic acid is the factor limiting sexual reproduction to the felid intestine. Cats lack enzymes to convert linoleic acid to arachidonic acid, resulting in a much higher linoleic acid concentration in the intestinal epithelium (Rivers et al., 1975; Sinclair et al., 1979). Further research demonstrated generation of *T. gondii* oocysts in intestinal organoids and mice when specific enzymatic activity was inhibited and linoleic acid was supplemented (Di Genova et al., 2019), although only few, fragile oocysts were detected. This again emphasizes the dire need for methods allowing the generation of robust results with reduced numbers of oocysts. Therefore, the agarose-based IFA technique presented here was established, building upon previously published methods using low-melt agarose for cell immobilization (Vartdal et al., 1986; Aufderheide, 2008; Hunt and Grover, 2010). The chemical and physical inertness of agarose (Zucca et al., 2016) provides the opportunity to study effects of fixating agents like methanol on oocyst integrity more closely as conventional methods would allow. The adverse effects of fixatives on oocysts due to water loss and the subsequent collapse has so far prevented high resolution electron microscopy imaging (Duszynski and Gardner, 1991). Still, the possibility to use acetone as a means to permeabilize oocysts embedded in agarose was investigated as other fixatives like methanol or Triton X-100 seem to be disadvantageous, based on reports of poor antigenicity retention (Salman et al., 2017) or no apparent effect on oocyst survival and thus permeabilization (Dubey, 2004), respectively. Nevertheless, acetone treatment of oocysts must be applied with care and requires proper controls, such as a comparison with no or alternative fixation methods. It is known to have profound effects on the detection of cellular structures, in particular membrane-associated antigens (Hoetelmans et al., 2001) as indicated by the different binding patterns of the 3G4 antibody with or without antibody binding (see Figure 13). Another advantage of low-melt agarose is its low melting and gelling temperatures, allowing experiments with viable oocysts, as temperatures below the melting point of regular agarose were shown to cause inactivate oocysts (Kuticic and Wikerhauser, 1996). Taken together, the AEO-IFA method was successfully demonstrated to drastically reduce the numbers of *T. gondii* oocysts required for robust immunofluorescence experiments and opens up new opportunities to acquire new insights into the understudied oocyst stage. This is best illustrated by visualization of the sutures in the sporocyst wall which has never been reported using light microscopy (see Figure 13). In line with detailed images of these structures obtained via scanning electron microscopy (Ferguson et al., 1982; Freppel et al., 2019), the plates can

be oriented either along a straight longitudinal line or in a staggered manner (see Figure 13Aj and Bj).

4.1.2 Implications of unsuccessful VHH isolation

The presence of antibodies to whole *T. gondii* oocysts after the alpaca immunization is a promising result as the immunogenic potential of oocysts is widely unknown. While antibodies against proteins of the oocyst wall have been produced (Possenti et al., 2010), the oocyst is considered to remain intact in a newly infected host only for a short period (Delgado Betancourt et al., 2019). Therefore, the development of a detectable antibody titer against whole oocysts has been doubted (see chapter 1.5). To overcome this issue and possibly increase the immune response, in both immunization schemes oocysts were applied subcutaneously. In addition, for the second immunization scheme, oocysts were disrupted to allow access to the inner part of the oocyst wall. This, in combination with higher doses of oocysts likely contributed to a detectable antibody response. The high signal for antibodies directed against glycan side chains of the GPI anchor indicates that antibodies were also generated against structures other than the oocyst wall, since the majority of GPI-anchored proteins are present on the extracellular surface (Kinoshita, 2016). Since the oocyst wall lacks a bilayered lipid membrane, the presence of GPI-anchored proteins seems unlikely. However, because the presence of specific carbohydrate structures in the oocyst wall was demonstrated via binding of several lectins, there is the possibility that the observed antibody response resulted from such carbohydrate structures in the wall.

Although isolation of intact RNA sequences should not present a major obstacle, it is still worthwhile to consider alternative approaches to compensate for problems regarding isolation of VHH sequences from the immunized alpaca. Especially modern techniques that harness the advantages of next-generation sequencing represent promising approaches. One proposed approach uses transcriptomic analysis to facilitate selection of candidate sequences and reduce the need for high amounts of immunization material (Deschaght et al., 2017). This technique however still relies on a cDNA library built from RNA as does the concept from another publication that uses cultured alpaca lymphocytes to forego the need for immunization of the animal and subsequently builds a phages display library from these immunized lymphocytes (Comor et al., 2017). To avoid reliance on PBMC and subsequent RNA isolation altogether, other methods seem more promising and worth further investigation, as they would allow easy and facile nanobody identification fully *in vitro*. One such method includes usage of a yeast display libraries in which certain regions of the nanobody sequence have been synthetically altered, namely the complementary-defining regions. This results in presentation of a wide range of nanobodies with slight differences in their affinity to possible ligands on the yeasts' surface (McMahon et al., 2017). This library comprises at least $1 * 10^8$ unique nanobodies (McMahon et al., 2018).

4.1.3 Implications of CLR and lectin binding to the oocyst wall

The visualization of the sporocyst sutures documented for the first time by fluorescence microscopy warranted further investigation. MPA-FITC preabsorbed with 100 mM of the specific ligand N-acetyl-galactosamine or N-acetyl-glucosamine as control did not result in an observable signal reduction of stained sporocyst structures such as walls and sutures. This lack of binding competition seems contradictory, however, there are studies that support ineffective lectin competition by carbohydrates (Gauthier et al., 2004) while others propose an inhibiting effect in other protozoa (De Stefano et al., 1992; Fuller and McDougald, 2002). Under physiological conditions, MPA forms tetramers and its structure hints at possible lattice formation, implying interactions of higher complexity with other molecules like amino acids (Lee et al., 1998; Huang et al., 2010) are possible. This would expand the array of potential ligands beyond carbohydrates. Therefore, further studies into MPA binding to the sporocyst wall are necessary and promising, since especially the characterization of interactions with noncarbohydrate ligands would aid in better understanding of sporocyst wall composition.

In contrast to MPA, CLRs are receptor molecules with a carbohydrate binding lectin domain, that depend on calcium for ligand binding. CLRs are involved in many immunity related processes, especially as PRRs in pathogen detection and their ligand specificity can aid in detection of new pathogen molecules (Bushkin et al., 2012). However, many CLRs have more than one specific ligand or not all ligands have been discovered this far. Nevertheless, using a previously published library comprised of a variety of related CLRs (Mayer et al., 2018) promised easy identification of new molecules binding to the oocyst wall. The identification of three CLRs interacting with the oocyst wall opens up several interesting aspects. Like in CLEC7A, the cytosolic domain of CLEC1B carries a tyrosine-based activation motif, suggesting a similar physiological function upon ligand binding. Using affinity chromatography studies, initial findings located CLEC1B primarily on the surface of platelets (Suzuki-Inoue et al., 2006). Recent findings suggest a more widespread expression, as CLEC1B was also shown to be expressed in neutrophils where it seems to be involved in phagocytosis and the expression of tumor necrosis factor alpha (TNF-α) (Kerrigan et al., 2009). However, a possible ligand on *T. gondii* oocysts with similarities to the CLEC1B ligands rhodocytin or podoplanin is so far unknown and not apparent in published proteome data in the ToxoDB. Additionally, BLAST searches did not yield evidence for a sulfotransferase gene (Ho, 2015), the enzyme required for sulfated glycan synthesis, making it unlikely that fucoidan is present in the oocyst wall and acting as a CLEC1B ligand.

The second newly identified CLR, CLEC9A, is expressed on BDCA3$^+$ dendritic cells as well as subsets of monocytes. Ablation of CLEC9A$^+$ dendritic cells resulted in much fewer brain CD8$^+$

T-cells during *Plasmodium falciparum* infections, which seemed to confer resistance to cerebral malaria (Piva et al., 2012). Like CLEC1B, CLEC9A carries an activating cytosolic domain. F-actin is the only known ligand so far, which, when exposed in dead cells is detected by CLEC9A (Zhang et al., 2012; Hanc et al., 2015). Thus, the main role of CLEC9A in the context of necrotic cells is the cross presentation of antigens (Sancho et al., 2009; Zelenay et al., 2012; Vu Manh et al., 2015), which seemingly can be amplified via myosin II activity (Schulz et al., 2018). The oocyst wall of the close relative of *T. gondii*, *Eimeria maxima,* was shown to incorporate F-actin underneath the outer wall layer (Frölich and Wallach, 2015). However, probing the presence of exposed F-actin in the *T. gondii* oocyst wall with labeled phalloidin, a cyclic peptide with high affinity to actin filaments forming the cytoskeleton (Wehland et al., 1978), no binding was observed, indicating that CLEC9A binding is not due to exposed F-actin in the oocyst wall (data not shown).

CLEC12A, the third identified CLR, has also been shown to be involved in *Plasmodium* infections, binding to the heme degradation product hemozoin, a molecule specific to this parasite. Binding of hemozoin to CLEC12A results in $CD8^+$ T-cell-mediated cross-priming (Raulf et al., 2019). Possible ligands of CLEC12A on *T. gondii* oocysts remain unknown. However, binding due to contaminating uric acid crystals was ruled out. This is an important finding, since sulfuric acid is routinely used as a stabilizing agent for sporulation and storage of oocysts (Fritz et al., 2012) and was shown to facilitate uric acid crystal formation (Chrom, 1909; Kanbara et al., 2010). Whether the observed binding of CLEC12A is caused by a specific ligand or a result of other contaminating agents remains elusive and must be further investigated. This will be facilitated by further insight into possible CLEC12A ligands gained through other interaction studies.

Like many CLRs, CLEC12A and CLEC7A are expressed on the surface of several cell types, myeloid dendritic cells and macrophages, amongst others. CLEC7A preferably binds particulate over soluble β-glucans and subsequently stimulates immune cell activation (Goodridge et al., 2011). This leads to inflammasome activation and generation of reactive oxygen species as well as the induction of the phagocytosis machinery (Brown et al., 2018). Previously, murine macrophages were demonstrated to phagocytose *T. gondii* oocysts, followed by observation of oocyst wall rupture within the macrophages and sporadic release of sporozoites in addition to stage conversion into tachyzoites (Freppel et al., 2016; Ndao et al., 2020). Subsequently it was speculated if phagocytized oocysts could contribute to the parasite's dissemination in the host if oocysts entered the body not via the fecal-oral-route, for example when inhaled and phagocytized by alveolar macrophages. Studies confirming airborne oocyst transmission are scarce, however (Wadhawan et al., 2018; Lass et al., 2019), although some cases of laboratory-acquired infections are known (Herwaldt, 2001).

Interestingly, CLEC7A and CLEC12A are expressed on the surface of alveolar macrophages (Reid et al., 2004; Álvarez et al., 2020). This presents an interesting aspect into alternative infection routes of *T. gondii* oocysts that calls for further investigation.

The main entry route of oocysts into the host is the intestinal tract. In the intestinal epithelium, sporozoites convert to tachyzoites, which invade the surrounding tissue and disseminate throughout the body (Delgado Betancourt et al., 2019). As described above, antibody responses against oocyst proteins have been reported (Hill et al., 2011; Santana et al., 2015; Liu et al., 2019), although an immunological explanation for the presentation of short-lived oocyst components to immune effector cells is still lacking. In this context, the coexpression of CLEC12A and the fractalkine receptor CX3CR1 on several dendritic cells and macrophages/monocytes (Dicken et al., 2013; Lund et al., 2018; Brown et al., 2019; Kolter et al., 2019) might provide an interesting point of approach, since $CXCCR1^{+}$ intestinal macrophages have been shown to extrude transepithelial dendrites (TEDs) into the intestinal lumen enabling antigen sampling, without compromising the epithelium's integrity (Man et al., 2017; Regoli et al., 2017; Kelsall, 2020). Corroborating this, inhibition of TED extrusion in mice lead to reduced antibody responses and immunity against bacterial infections (Morita et al., 2019). Taken together, these findings call for further investigation into the uptake of oocyst wall fragments, mediated by CLEC12A in $CX3CR1^{+}$ macrophages.

In conclusion, the successful development of the material-saving AEO-IFA enabled the identification of three new molecules binding to *T. gondii* oocysts as well as more insights into the binding patterns of MPA, a previously known lectin binding to *T. gondii* oocysts. Although the ligands for CLEC1B, CLEC9A, and CLEC12A on this parasite stage remain unknown, they provide a useful tool in further studies to deepen the understanding of the composition of the oocyst wall and its resilience to harsh environmental conditions. Furthermore, the variety of processes these CLRs are involved in, such as phagocytosis, antigen cross-presentation, and immune cell activation, provoke exciting new hypotheses regarding early immune responses against the short-lived oocyst stage.

4.2 Molecules contributing to stress tolerance inside the oocyst

4.2.1 TgLEAs are IDPRs rather than IDPs

Although TgLEAs have been known for several years, they are not well categorized due to their presumed exclusivity to the oocyst stage (Fritz et al., 2012; Possenti et al., 2013). This means that studies on their biological function are not trivial and almost always would require cat infections to conduct functional analysis in gene knockout experiments. Thus, existing data on TgLEAs today is limited to predictions based on sequence. Therefore, to facilitate TgLEA characterization, *in vitro* experiments with recombinant TgLEAs and gain-of-function investigations in bacteria and yeast represent valid options to corroborate *in silico* findings. As

described in chapter 1.4, preliminary *in silico* analyses via MobiDB suggest LEA-like characteristics, as the observed high disordered content represents a hallmark of LEA proteins (Wise and Tunnacliffe, 2004; Tunnacliffe and Wise, 2007). Furthermore, the CIDER classification of context dependent structure in all TgLEAs indicates their involvement in stress responses, as conformational change upon stress is an often observed mechanism in IDPs and LEAs (Artur et al., 2019). Experimental confirmation of IDP characteristics of the TgLEAs was achieved by showing their tolerance to high temperatures. The ability to successfully purify functional protein after boiling the bacterial lysate for 10 minutes strengthens the assumption that TgLEAs are IDPs. In fact, boiling lysate prior to purification is recommended as an easy and feasible method to separate IDPs from unwanted globular proteins during purification (Kalthoff, 2003). Additionally, the occurrence of aberrant band patterns in the western blots of LEA-proteins are not uncommon (Boswell et al., 2014; Warner et al., 2016). However, as of yet, the cause of these aberrant band patterns is unknown. Several aspects could be the reason for this. LEA-proteins have been shown to form oligomers that are resistant to dissociation by SDS (Goyal et al., 2003) and could thus result in occurrence of multiple, seemingly oligomeric bands in western blot. Another factor influencing these band patterns could be yet unclear characteristics in the translational process of LEA-proteins (Warner et al., 2016). Lastly, the sensitivity of LEA-proteins to proteolysis resulting from their intrinsic disorder could also cause such multifold band patterns in western blot.

Most IDPs are known to be very sensitive to proteolytic enzymes due to their unfolded structure that allows easy access to proteases (Fontana et al., 2004; Fontana et al., 2012). Hence, the TgLEAs' observed sensitivity to protease digestion further confirms their IDP characteristics. Furthermore, it could be shown that addition of even low concentrations of TFE induces resistance to proteolytic digestion of TgLEAs. TFE is often used in IDP studies since it is well known to induce formation of secondary structures in proteins (Shiraki et al., 1995). The exact cause of this effect is unknown, however one interesting proposed mode of action is the reinforcement of hydrogen bonds between carbonyl and amidic NH groups by removal of water molecules in proximity (Luo and Baldwin, 1997), thus simulating desiccation effects on a molecular level. While trypsin and the similarly structured α-chymotrypsin seem to be sensitive to co-solvents such as TFE (Rezaei-Ghaleh et al., 2008; Ataei and Hosseinkhani, 2015), thermolysin is a protease that is supposedly resistant to the effects of TFE as indicated by limited changes in the UV spectra even at concentrations of 50 % (Polverino de Laureto et al., 1998). However, in the literature there are conflicting findings on this topic with some reporting interesting effects on thermolysin activity at a 50 % TFE concentration. More specifically, it seems the broad substrate specificity of thermolysin (Heinrikson, 1977) is lost, as cleavage was only observed at the amino sides of isoleucine, leucine and phenylalanine and furthermore seems to only cleave at few select sites (Fontana et al., 1997). Considering that these three

amino acids occur relatively rarely in each of the four respective TgLEAs (maximum abundance 5 %, see Table 7 in the appendix), this could yield an explanation for the observed reduction of proteolytic activity in presence of TFE. Similarly, in control experiments to exclude effects of TFE on thermolysin activity, even small concentrations of TFE fully inhibited the thermolysin catalyzed hydrolysis of FAGLA. This observation could either be caused by TFE directly influencing the enzymatic activity of thermolysin or via induced changes in conformation of the FAGLA molecule. It is unclear what exactly caused this, and nothing could be found in the literature regarding the effect of TFE on FAGLA. Still, as an amino side of leucine is present in the dipeptidic FAGLA molecule (see Figure 51 in the appendix), a cleavage site for thermolysin in its TFE state would be present. As stated above though, TFE state thermolysin seems to exhibit a strong preference for select leucine sites in a given protein, as it was shown to cleave hen egg lysozyme, which contains eight possible leucine cleavage sites, only at the Lys97-Ile98 position (Polverino de Laureto et al., 1995). While this increase in cleavage site specificity can be attributed to conformational changes in the substrate, there is sufficient evidence that TFE might have adverse effects on thermolysin activity, assuming that TFE like other organic co-solvents might contribute to increased rigidity (Affleck et al., 1992; Hartsough and Merz, 1992; Polverino de Laureto et al., 1998), hampering the catalytic activity that requires chain mobility to a certain degree (Welch et al., 1982). Given these data, it is recommended to not consider TFE mediated resistance to thermolysin as a confirmation of IDP characteristic due to the profound effects of TFE on disordered and well-structured proteins alike, which has also been observed elsewhere (Povey et al., 2007). Consequently, TFE has already been disregarded for studying dehydration effects (Boothby and Pielak, 2017). A better indicator of putative IDP characteristics of the TgLEAs is the observed high sensitivity to low concentrations of proteases. In a similar manner, the lack of distinct melting points of all TgLEAs in TSAs underlines the proposed IDP characteristics, as similar melting curves to those of the TgLEAs have been observed in other potential IDPs in a similar experimental context (Hamdi et al., 2017). The initially observed apparent melting points in earlier TSAs using not-boiled bacterial lysate are most likely due to contamination with folded proteins that were subsequently eliminated when the bacterial lysate was boiled prior to loading onto the column, as has been proposed previously (Kalthoff, 2003).

Unequivocal conformation of IDP characteristics of the TgLEAs was achieved via CD spectroscopy, a method often used in the characterization of putative disordered proteins (Uversky, 2002). The CD analysis showed disordered regions ranging from one-third to half of the whole molecule for all four TgLEAs. Next to mainly disordered regions, all TgLEAs showed a high proportion of beta sheet formation in their structures. Similarly, other publications reported a high percentage of beta sheets and unordered region as well as some observed alpha-helices and turn motifs in their characterization of LEA proteins from

Arabidopsis thaliana using Fourier-transform infrared (FTIR) and CD spectroscopy (Nakayama et al., 2007; Dang et al., 2014), highlighting structural similarities between known LEA proteins and the analyzed TgLEAs. Receveur-Brechot et al. described three pronounced characteristics observable in CD spectra of disordered proteins: (1) a molar ellipticity close to zero at and around 185 nm, (2) a largely negative molar ellipticity at 200 nm and (3) negligible molar ellipticity at 222 nm (Receveur-Brechot et al., 2006). These criteria are illustrated in Figure 41, using the CD spectrum of domain I from pig calpastatin, a known IDP with high similarity to hCD1 (Asada et al., 1989). Comparing the TgLEAs' CD spectra to this spectrum of a known IDP and applying the criteria defined above, it becomes obvious that all TgLEAs exhibit CD spectra indicative of disordered regions, with molar ellipticity close to zero at 190 nm and a highly negative molar ellipticity at 200 nm, especially in the case of TgLEA-860, although the CD spectra at higher wavelengths are probably also influenced by the observed alpha-helix and beta-sheet formations, as the molar ellipticity is not as close to zero around the 220 nm mark (see Figure 28). Comparing the TgLEAs' spectra to instances where alpha-helix and particularly beta-sheet formation was artificially induced, confirms this assumption, as the induction of alpha-helices was demonstrated to be accompanied by a decrease in the negative band at 222 nm and beta-sheets resulted in a broadening of the maximum negative intensity and a slight shift towards higher wavelengths (Chemes et al., 2012). Together with the CD analyses of a known LEA protein from *A. thaliana* mentioned above, which exhibited similar curves with an extended negative band at the 220 nm wavelength (Nakayama et al., 2007), these findings indicate that all four TgLEAs, while exhibiting similarities to LEA proteins, are not fully IDPs but rather hybrid proteins carrying both IDPRs and structured regions. In such proteins the structured regions are often linked by long, flexible, unstructured regions. This could mean that the TgLEAs are involved in signal cascade complexes as has been shown for other IDPR carrying proteins (Peng et al., 2013; Fonin et al., 2019; Popelka, 2020), as their increased flexibility could allow for more diverse ligand interactions (Wright and Dyson, 2015).

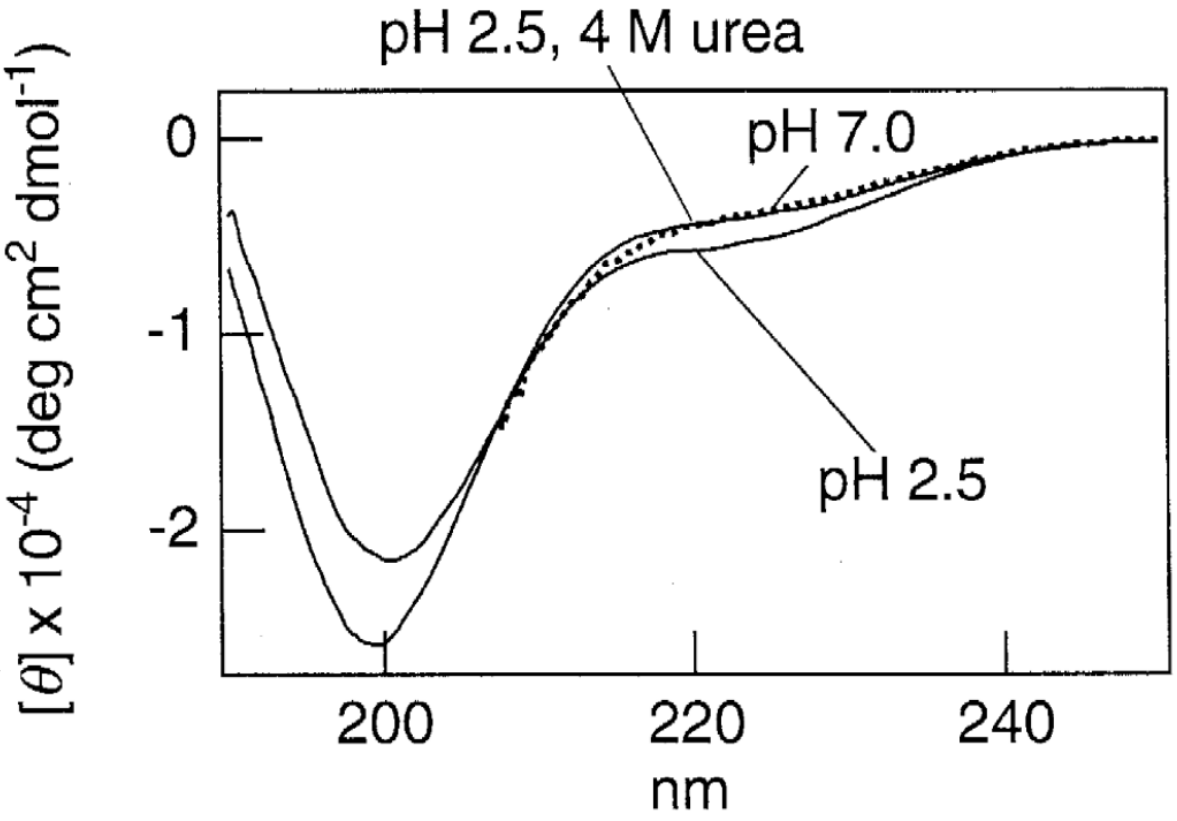

Figure 41: CD spectrum of domain I of pig calpastatin under different conditions. Of interest is the curve at pH 7, indicative of a typical IDP CD spectrum with molar elipticity close to zero at approx. 190 nm, pronounced negative molar ellipticity at 200 nm and negligible molar ellipticity at 222 nm. Figure adapted from (Konno et al., 1997).

Still, the implications of the observed hybrid characteristic of structured regions and IDPRs in the TgLEAs needs further investigation, as the extent of the IDPRs remains unclear. However, this is a defining feature for hybrid proteins as many short, disordered regions would overall reduce the unfolded nature of such proteins as compared to small, ordered regions linked by long flexible domains (Dunker et al., 2013). Corroborating the latter assumption that the TgLEAs exhibit IDP characteristic due to long IDPRs is their observed resistance to high temperature-mediated aggregation as well as sequence-based bioinformatical predictions. Interestingly, the observed disordered content by CD spectroscopy differs from the predicted disorder content by MobiDB. These discrepancies in prediction and observation are a known problem and shortcoming of IDP prediction algorithms and mainly based on the fact that most prediction methods still need to rely on data from already characterized IDPs. Since the number of well-known and characterized IDPs is very small compared to the actual prevalence of IDPs and IDPRs in nature, these datasets don't necessarily give a good representation of the actual diversity amongst IDPs (He et al., 2009). Still, as interest and research on IDPs increases, more information becomes readily available, allowing improvement of existing prediction methods, which in turn will lead to more interest and research on the topic, resulting

in a kind of positive feedback-loop, allowing increasingly accurate predictions (Necci et al., 2021). For example, while early version 2 of the IDP database DisProt included 179 IDPs and 290 IDPRs in 2005, the most recent version 8.2 from June 2021 includes data from more than 2,000 IDPs and 4,400 IDPRs (Hatos et al., 2020), indicating the rapidly increasing knowledge on IDPs.

Accordingly, CD spectroscopy represents only one of a vast array of different experimental methods used to analyze disorder in proteins which all yield slightly differing insights. Methods such as nuclear magnetic resonance spectroscopy (NMR), light scattering and small-angle X-ray scattering, amongst others, would aid in achieving more detailed information on the disordered characteristic of a protein, but are not always readily available (He et al., 2009; Necci et al., 2021). Hence, knowledge on the TgLEAs' disordered regions derived from CD spectroscopy should be considered as a promising, ground-laying but preliminary indication of their disordered characteristics. Therefore, further CD experiments to investigate conformational changes in TgLEAs in different contexts are essential to a more detailed characterization (Artur et al., 2019). In addition, more extensive analyses, especially NMR spectroscopy experiments would contribute to a more definite assessment of the TgLEAs' disorder character, as NMR data can be used to calculate the Chemical shift Z-score for quantitative protein Order and Disorder assessment (CheZOD (Nielsen and Mulder, 2016)) which in turn would allow for more reliable disorder predictions, as algorithms purely relying on a given amino acid sequence have been reported to underperform compared to prediction methods that rely on using CheZOD values amongst others (Nielsen and Mulder, 2019). To mitigate the issue of cost and labor-intensive NMR experiments, a prediction method that applies extensive neural networking to better predict disordered and ordered regions in a given protein based on its amino acid sequence, has been developed recently, called Prediction of Order and Disorder by evaluation of NMR data (ODiNPred (Dass et al., 2020)). ODiNPred uses a dataset of over 1,000 protein sequences that includes their CheZOD and NMR data to yield more accurate disorder predictions. Preliminary analysis of TgLEAs and TgSAG1 and hCD1 controls indeed indicates the presence of scattered disordered regions in the TgLEAs. In comparison, TgSAG1 mainly seems to contain ordered regions and hCD1 seems to almost exclusively contain disordered regions. While these data somewhat compensate for as of yet missing NMR data, at the same time they highlight how additional NMR data would strengthen the holistic characterization of IDP candidate proteins, especially in order to distinct between IDPs and IDPRs.

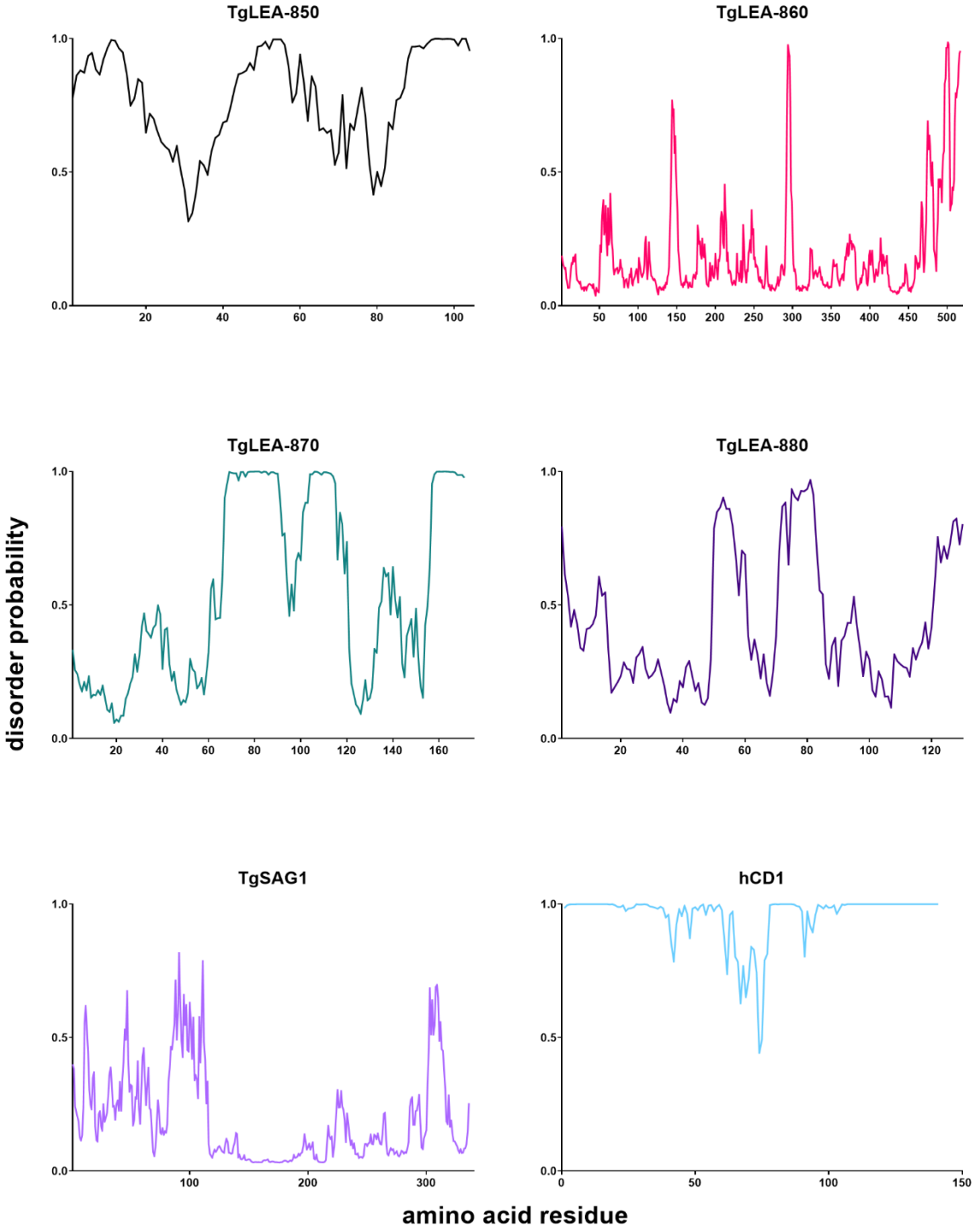

Figure 42: Predicted disordered regions in TgLEAs and control proteins using ODiNPred. The machine learning based prediction approach of ODiNPred that also considers Z-scores based on available NMR spectra reveals a large divergence in disorder content for TgLEAs. TgLEA-860 is predicted to be even less disordered than TgSAG1, while the other TgLEAs contain relatively more and longer regions of high disorder more similar to hCD1 with the highest disorder content of all analyzed proteins.

4.2.2 TgLEA mediated stress resistance in bacteria is equivocal

Preliminary analysis showed that all TgLEAs are categorized as class_6 LEA proteins. The LEA proteins of this class are predicted to have several different functions, such as response to desiccation, response to hyperosmotic stress and response to temperature stimuli (Bhattacharya et al., 2019). The assessment of beneficial effects of TgLEAs on *E. coli* growth under stress revealed equivocal effects on stress tolerance, as in several cases expression of TgLEAs resulted in inhibited growth, while in other cases, e.g., upon freezing in a cold sensitive bacterial strain, TgLEAs-870 and -880 mediated improved growth while the other TgLEAs caused reduced growth even after relatively harmless stress of 7 days at 4 °C. Furthermore, while initial growth experiments under desiccating conditions to assess optimal IPTG concentration for induction indicated a beneficial effect of TgLEA-850, repetition of these experiments under more controlled desiccation conditions did not confirm a beneficial effect of any TgLEA on desiccation resistance (data not shown). One reason for this could be that the TgLEAs target one or more specific proteins that are absent in *E. coli*, thus resulting in no observable effect. Accordingly, *S. cerevisiae* as a eucaryotic model was transformed with TgLEAs. *S. cerevisiae* was shown to achieve tolerance to desiccation stress via trehalose (Tapia and Koshland, 2014), although the relevance of trehalose for stress resistance is still debated (Ratnakumar and Tunnacliffe, 2006; Tapia et al., 2015). Interestingly, key enzymes of the trehalose pathway have been discovered in other apicomplexan parasites like *C. parvum* , where trehalose has also been detected in oocysts (Yu et al., 2010). This suggests a similar protective role of trehalose against stress induced damage to important oocyst molecules. Moreover, trehalose and LEAs are proposed to act synergistically in conveying stress resistance (Iturriaga, 2008), as particularly in the case of heat-induced stress, the protective effect of LEAs only was observed in presence of trehalose (Goyal et al., 2005). However, preliminary growth experiments with *S. cerevisiae* revealed similarly equivocal results (data not shown). An interesting aspect of the TgLEAs' genetic location is their adjacent arrangement on the chromosome. The localization of functionally similar genes in close proximity is seldom observed in *T. gondii*, suggesting that this particular gene locus warrants further looking into, especially since a recent publication postulates that nuclear proximity of genes that share a protein interaction is enforced by evolution (Tarbier et al., 2020). Thus, it seems promising to test whether a beneficial effect on growth under stress is mediated if all TgLEAs are expressed simultaneously. Preliminary research looking into this via knockout experiments in *T. gondii* has been conducted and is ongoing. The observed growth reduction of bacteria upon TgLEA expression during the stress experiments certainly provides an intriguing aspect that warrants further investigation regarding potential antimicrobial effects. In contrast, the bacterial growth during TgLEA expression when no stress was applied to the bacteria was largely unaffected, except in the case of TgLEA-860. Still, LEA proteins have previously been shown to provide varying antimicrobial effects, from increased tolerance to *Pseudomonas* infections

in plants (Liu et al., 2013) to bacterial growth inhibition (Campos et al., 2006) and antibacterial and antifungal effects (Zhai et al., 2011; Drira et al., 2015). In addition, it has become clear that drought events substantially affect the microbiota surrounding different, sub-surface plant tissues (Santos-Medellín et al., 2017; Xie et al., 2021) and it has subsequently been hypothesized that extensive drought events contribute to a rise in opportunistic pathogen infections, which is mitigated by LEA activity (Battaglia and Covarrubias, 2013). Supportive of this claim and strongly corroborating the above described observations of TgLEA effects on the growth of stressed and non-stressed bacteria are observations in *A. thaliana*, demonstrating that plants exposed to drought stress exhibited increased pathogen resistance, as the count of *Pseudomonas* bacteria residing in stressed plant was lower than that in non-stressed specimens (Gupta et al., 2016). The reason why *T. gondii* oocysts would possess similarly sophisticated machinery to combat settings of mixed biotic and abiotic stressors is currently unknown and awaits exploration.

4.2.3 TgLEAs protect an abundant oocyst protein from stress induced damage

In vitro characterization of (putative) LEA proteins often includes analysis of their ability to preserve the enzymatic activity of LDH upon different stressors, as LDH provides an easy experimental setup with quick read outs and the enzyme is sensitive to damages LEA proteins are known to protect against, such as high temperatures or freezing (Goyal et al., 2005; Thalhammer et al., 2014). Furthermore, other class 6 LEA proteins have previously been shown to prevent aggregation of LDH (Goyal et al., 2005; Popova et al., 2015). Findings of protection from general aggregate formation upon repeated freezing in pLDH by the TgLEAs were corroborated by observed preservation of enzymatic activity after repeatedly freezing pLDH. This is particularly interesting, since fast freezing was shown to be much more deleterious to LDH activity than slow freezing (Park et al., 2021), underlining the significance of TgLEAs preserving almost 100 % activity after repeated fast freezing at – 196 °C. The observed effects occurred at a molar LDH:protectant ratio of 1:25. It is worth noting that ratios reported in the literature for similar characterizations vary greatly from much higher ratios of 1:500 (Hatanaka et al., 2013) to a similar range (Dang et al., 2014), and even a lower ratio of 1:10 (Goyal et al., 2005), while other studies don't report a molar ratio at all and only state a given concentration that was investigated (Sasaki et al., 2013). Moreover, in some cases, plant LEA proteins even in nanomolar range were sufficient to protect LDH (Honjoh et al., 2000), while in other cases no beneficial effect surpassing BSA was observable (Boswell et al., 2014). Given the reasonable assumption that the molecular composition inside *T. gondii* oocysts and plant embryos vastly differ as would the implications of a certain stressor on a molecular level, there is no reason to assume that this seemingly high molar ratio necessary to protect LDH is indicative of a weaker or stronger protective effect than in other known LEA proteins. Supporting this is the reported large diversity in different modes of action by which LEA proteins

are proposed to protect cellular components, attributed to the different classes of LEA proteins (Hundertmark and Hincha, 2008). These proposed modes of action range from chaperone-like activity through direct interaction to formation of molecular shields that form electrostatic barriers, protecting sensitive proteins without direct interaction (Chakrabortee et al., 2010; Olvera-Carrillo et al., 2011; Chakrabortee et al., 2012; Kovacs and Tompa, 2012). The latter is also the proposed mode of action for at least some class_6 LEA proteins, as they have been found to prevent liposomes from fusing upon desiccation by adhering to the phospholipid membrane, thus shielding the liposomes from each other (Furuki and Sakurai, 2014). But because LEA proteins have been discovered in many distinctly different organisms and due to the large structural diversity among LEA proteins, research on them is still fragmented (Hundertmark and Hincha, 2008). Therefore, it is still unclear how a LEA protein's characteristics and its mode of action are related, not least due to their wide variety of stress protecting abilities and different subcellular localizations (Saucedo et al., 2017).

Finally, the importance of pLDH damage protection by TgLEAs was confirmed by observing similar effects on recombinant TgLDH1 and as such in a physiologically more relevant context. TgLDH1 was found to be an important pathogenesis factor for *T. gondii* that is vital for stage conversion and cyst formation in infected hosts (Al-Anouti et al., 2004; Abdelbaset et al., 2017; Xia et al., 2018; Xia et al., 2018). Accordingly, it is important to note that TgLEAs were even shown to preserve TgLDH1 activity in a system not using its preferred co-factor APAD but rather NADH, since although TgLDH1 was shown to favor APAD as cofactor, at the same time it was shown that pyruvate is still the preferred substrate, regarding catalytic efficiency (Dando et al., 2001; Kavanagh et al., 2004). Further analysis to shed light on the TgLEAs protective effect on the reversely catalyzed TgLDH1 reaction would be highly interesting and could potentially reveal new insights also into oocyst physiology.

Interestingly, for both LDH variants, a much lower LDH:TgLEA molar ratio of 1:2 was sufficient for drastic reduction of aggregate formation as compared to the molar ratio of 1:25 necessary to preserve enzymatic activity. A factor at play could be that freezing, and thus reduction of liquid water content, permanently damages the tertiary structure of LDH. Such effects have been observed before, as well as the protective effect of additives like glycerol to freezing solutions (Gabellieri and Strambini, 2003). Therefore, it could be argued that low concentrations TgLEAs are sufficient to prevent aggregation of denatured proteins, but in order to preserve activity through stabilization of the enzyme's structure, a higher concentration is necessary.

Taken together, these findings clearly determine the TgLEAs as proteins that contain IDPRs and exhibit similarities to other previously characterized LEA proteins. Accordingly, their ability to potently protect TgLDH1 as an important pathogenesis factor against stress induced

damage coupled with their exclusivity to the oocyst stage in which they are among the most abundant proteins (Fritz et al., 2012; Possenti et al., 2013; Wang et al., 2017) identifies them as promising candidates for further studies on targeted measures against oocyst contaminations in the environment.

4.3 Molecules as antigens for identification of oocyst-mediated infections

4.3.1 The need for new test methods against *T. gondii*

Although since the first description of *T. gondii* many highly sensitive and specific tests have been described, there is substantial demand for development of new testing methods against this parasite. Some of the shortcomings of established tests are the limited potential for high throughput testing of large numbers of samples or the missing ability to differentiate infection sources. The latter would be highly beneficial especially in the prevention of disease outbreaks as identification of specific infection sources would allow immediate action and prevent further rise in infection numbers thus inhibiting the parasites spread (Dubey, 1996; Opsteegh et al., 2014).

One way to mitigate this issue somewhat could be the use of suitable sentinels. This means that certain species that exhibit a specific type of feeding behavior could serve as markers for infections sources themselves. More specifically, chickens pose a well-suited opportunity to determine the presence of oocysts in the environment, as they are ground feeders and thus most likely acquired a *T. gondii* infection by ingestion of oocysts (Dubey et al., 2020). Therefore, if a test method allowed routinely high throughput serological supervision of large numbers of chickens this would allow early discovery of potential oocyst contamination in certain areas. Using chickens as sentinels on meat producing farms has been proposed as a method for early identification of infection sources to allow a timely response to prevent introduction of infective parasites into the food chain (Dubey et al., 2015). This approach however needs to consider the delayed serological response, as chickens fed oocysts developed detectable antibody titers only at 12 days after infection (Biancifiori et al., 1986).

The bead based Luminex assay provides a reliable method to regularly assay large numbers of serum samples and has already been shown to be a good alternative to established test methods in humans (Klein et al., 2020). As is shown here and more in depth in a recent publication (Fabian et al., 2020), testing chicken sera with the Luminex technique yielded promising results. As detailed in the publication, the assay exhibited the highest diagnostic sensitivity as compared to ELISA, MAT and IFA and showed the same diagnostic specificity as all other methods during the analysis of sera from experimentally infected chickens. Moreover, in the analysis of sera from naturally exposed chickens conducted in that publication, the Luminex assay continued to show promising results with the second highest

diagnostic sensitivity of all compared methods and the highest diagnostic specificity. The diagnostic sensitivity was only surpassed by an ELISA that used a less stringent cut-off value and was thus determined to have lower specificity. Likewise, the high diagnostic specificity of the Luminex assay was only shared by the MAT, which in turn had the lowest diagnostic sensitivity of all methods. This underlines the potential the Luminex assay possesses for future serological monitoring.

In addition to the results indicating similar to superior performance of the Luminex assay in comparison to established test methods, one key advantage is the multiplexing ability. Having the opportunity to test one sample from one individual for antibodies against several different pathogens in parallel would be highly beneficial. An important group of pathogens in chickens is the genus of close relatives of *T. gondii* called *Eimeria sp.* To date, there is no publication indicating establishment of a Luminex based method to test for *Eimeria* parasites in chickens. Therefore, a combined Luminex assay against *T. gondii* and *Eimeria* infections would drastically reduce sampling material from animals and ensure closer surveillance, since due to reduced need for sample material, more animals could be monitored simultaneously. Moreover, the multiplexing would allow for reduced cost of labor and handling time. These advantages become more distinct, the more samples are analyzed in parallel (Graham et al., 2019).

4.3.2 The need for specific infection markers

For a molecule to be considered a suitable antigen in serological assays, there are certain criteria that must be met. It must be highly specific, readily available, cause an antibody response that results in detectable antibody titers and the antibody binding should be highly affine (Sela, 1998; Reverberi and Reverberi, 2007).

Most established test methods to detect *T. gondii* infections rely on SAG1 as antigen, a protein expressed on the surface of tachyzoites. Therefore, all test methods using this protein as antigen are only suited to confirm that an infection has taken place without being able to determine whether the tested individual is chronically infected or undergoing acute infection. This is due to *T. gondiis* ability to revert back to the tachyzoite stage even in chronic infections. There are methods however, that allow specific determination of IgM levels to detect acute infections. Until now, there are no established tests that use a bradyzoite specific antigen to investigate chronic infections. Still, there are some candidate proteins that are specific to the bradyzoite stage and could be used as bradyzoite specific infection markers in serological tests or as vaccine candidates (Gross et al., 2004; Döşkaya et al., 2018; Rezaei et al., 2019; Asghari et al., 2021). This lack of established tests for detection of chronic infections is probably a result of the limited need for such specific tests, as in most cases (e.g. pregnant women,

immunocompromised individuals such as organ donor recipients or HIV patients) a test method that confirms an infection took place at some point in the past is sufficient.

One case however, where a bradyzoite specific marker would be advantageous, is in the tracing of sources of infections. Hosts of *T. gondii* can be infected via all three life stages of the parasite. Until now it is unclear which infection route predominantly contributes to the parasites spread (Tenter et al., 2000). Tissue cysts used to be considered as the main route of infections (Dubey et al., 2000). However, data covering the second half of the 20th century suggest that prevalence of *T. gondii* in meat producing pigs steadily declined since the 1960s to below 1 % in several parts of the EU, including Germany (Van Knapen et al., 1995; Edelhofer and Aspöck, 1996; Tenter et al., 1999). Somewhat contradictory, the most recent serological data on *T. gondii* infections in Germany suggests an overall constant incidence in toxoplasmosis cases (Krings et al., 2021), although reliable data on incidence and seroprevalence in Germany is scarce (Wilking et al., 2016; Pleyer et al., 2019). Nevertheless, this reported constant incidence rate in combination with an observed decline of prevalence in meat products hints at other factors contributing more heavily to *T. gondii* transmission than previously thought. In addition, this is helped by an increased number of reports on *T. gondii* presence in diverse environmental settings such as coastal regions and even aquatic environments (Shapiro et al., 2019), substantiating this possible paradigm shift in how *T. gondii* infections are thought to be transmitted, as it at least suggests that the main cause of the parasite's transmission might not be tissue cysts in contaminated meat products but rather oocysts contaminating the environment. Thus, the need for development of test methods to determine the source of *T. gondii* infections becomes more apparent, as it would help to answer this question more clearly, eventually contributing to development of suitable counter measures to prevent the parasite's spread.

Since bradyzoites as well as sporozoites differ in their respective transcriptome and proteome from each other and from tachyzoites (Fritz et al., 2012; Fritz et al., 2012) there is reason to assume that all three of the parasites' stages should possess a molecule that can serve as a specific infection marker. For oocysts several have been proposed and used, such as TgOWP1, CCp5A or TgLEA-850. For bradyzoites, in addition to above mentioned candidates, a recent publication proposes BCLA/MAG2 as a protein confined to the bradyzoite stage of the parasite (Dard et al., 2021). However, it remains unclear if this marker would be suitable to detect infections that were caused by tissue cysts or rather only confirms the presence of latent parasite stages in the patient.

4.3.3 TgLEAs as specific markers for infections caused by oocysts

As described above, TgLEA-850 has previously been suggested as a marker antibody eliciting antigen for infections caused by oocysts. Data implies that individuals showed detectable

TgLEA-850-specific antibody titers up to six months after a known *T. gondii* infection caused by oocysts. The fact that proteins rich in disordered, flexible regions like TgLEA-850 could elicit such distinct immune responses seemed questionable to the scientific community. As such, the ability of IDPs and IDPRs to trigger an immune response has been doubted (Dunker et al., 2002) and their disorder has even been proposed as a key feature in intracellular parasites and viruses to evade immune response (Anders, 1986; Schofield, 1991; Kwong et al., 2002). In contrast, the important role IDPs and IDPRs play in metabolic and cellular processes through diverse interactions that are enabled by their molecular flexibility have long since been unveiled (Wright and Dyson, 2015; Bondos et al., 2021). Only in recent years did the research effort into possible links between protein disorder and antigenic potential increase and some publications have since yielded substantial evidence that IDPs might in fact be well suited as immunogenic molecules and could even be prime candidates for vaccine design. Their flexible and unorganized structure could contribute to an increased variety of possible interaction partners or ensure an increased affinity through more efficient antibody interaction (Guy et al., 2015; MacRaild et al., 2016; Krishnarjuna et al., 2018; MacRaild et al., 2018).

Accordingly, the two IDPR candidate proteins investigated herein, TgLEA-850 and -860, resulted in detectable antibody titers in the two immunized rabbits in ELISA tests. Similar successes have been made in previous studies, where antibodies against candidate LEA proteins were successfully developed for characterization purposes (Olvera-Carrillo et al., 2010; Boswell et al., 2014; Saucedo et al., 2017). These findings highlight the general suitability of LEA proteins to elicit an antibody response.

Interestingly, the TgLEAs did not enable specific detection of oocyst-borne infections in chickens when analyzing a larger serum panel from 33 animals. Regardless of the investigated 1:200 or 1:25 sample dilution, the reported signals were much lower than any positive controls. One factor at play might be the differences in antigen presentation to the organism. The rabbits were presented recombinant TgLEAs. The chickens were fed a varying numbers of whole oocysts, ranging from 10^3 to 10^6. For one, the amount of TgLEAs resulting from the fixed number of oocysts could be significantly lower compared to the amount of recombinant protein presented to the rabbits, resulting in a reduced immune reaction, although there are contradictory data on the relationship between antigen dose and antibody response, some supporting the assumption that higher antigen doses lead to higher antibody responses (Romstad et al., 2013), others reporting no difference in antibody titers comparing two different antigen doses (Frey et al., 1999).

Generally, chickens rarely show manifestations of clinical toxoplasmosis. Experimental infections often times failed to replicate symptoms of clinical toxoplasmosis (Dubey, 2010). Especially experimental inoculation of chickens with oocysts mostly remained asymptomatic

(Biancifiori et al., 1986; Dubey et al., 1993; Kaneto et al., 1997). These findings could be indicative of particular differences between the gastrointestinal tracts of chickens and mammals that affect the severity of *T. gondii* infections. Namely, in contrast to mammals, chickens, like other birds, possess a gizzard, an organ to aid digestion by mechanical shredding of food through strong muscular contractions and previously ingested small stones (Gionfriddo and Best, 1999). In the case of coccidian parasites, the gizzard might play a role in oocyst excystation as indicated by the observation that oocyst shedding in chickens challenged with *Eimeria* was lower in animals with a normally developed gizzard than in animals with an underdeveloped gizzard (Cumming, 1992; Evans et al., 2005). Such developmental issues within the gizzard can be the result of diets deficient of whole grain (Amerah and Ravindran, 2014). Subsequently, it is worth noting that there is functional similarity between the avian gizzard and recommended excystation protocols to extract sporocysts from coccidian oocysts that recommend to incorporate small glass beads into the procedure to facilitate excystation by mechanical means (Kurth and Entzeroth, 2008; Sokol et al., 2020). Interestingly, data from such excystation experiments suggests that prolonged exposure to mechanical strain negatively influences the number of viable sporocysts retrieved. This is likely due to sporocysts being more susceptible to further mechanical strain the earlier they are released from oocysts during such excystation procedures as their cumulative wall layers only equal two whereas in whole oocysts these layers' sum equals 4 (Freyre and Falcón, 2004). This could mean that the gizzard disrupts oocysts relatively early in the gastrointestinal tract, exposing unprotected sporozoites to stomach acid and digestive enzymes, as the shredded food can be passed back to the regular stomach from the gizzard for further enzymatic digestion. This could then lead to reduced numbers of sporocyst that eventually can infect the host, resulting in relatively mild infection courses.

Still, the MFI values observed in the Luminex analysis suggest that even if only lower numbers of sporozoites or bradyzoites survived gizzard and stomach, there were sufficient parasites to infect the host. This is indicated by the observed elevated levels of antibodies against the tachyzoite exclusive antigen TgSAG1. Comparing two different sample dilutions, the lower dilution allowed a more refined look at the TgLEA-performance. As before, neither of the TgLEAs resulted in high MFI values for any of the infected chicken samples that allowed clear classification of infection route. Values for TgLEA-850 rarely were higher than those of the CSA control and while the values for TgLEA-870 were slightly higher than at 1:200 dilution, overall, the MFI values from each of the groups were not distinctly different from each other. In contrast though, TgLEA-880 exhibited distinctly higher MFI values for at least some of the sera from the two groups of infected chickens, allowing to determine a limited number of chickens correctly as infected. Closer analysis revealed that those animals which yielded higher MFI values had been infected by the CZ-Tiger strain of *T. gondii* while those whose MFI

values were comparable to that of uninfected animals were infected by the ME49 strain. However, promising this looks at first glance, a clear contradictions here is as above that animals who had been infected with a life stage of the parasite that does not appear to express TgLEA-880 seem to have developed antigens to this protein.

It has been shown that different strains of *T. gondii* exhibit differences in the expressed proteins. More specifically, a recent publication showed that TgLEA-870 was more abundant in oocysts of the PRU strain (type II) compared to oocysts of the PYS strain (atypical) (Zhou et al., 2017). While CZ-Tiger and ME49 are both type II strains, not much is known in regard to the abundance of TgLEAs in oocysts of these strains. The existence of TgLEAs was reported based on studies on oocysts of the M4 strain of *T. gondii*, also a type II strain. Therefore, it could be possible that TgLEAs are more abundant in certain strains and less abundant in others, further contradicting their suitability as infection markers. However, the differences in protein abundance were reported between oocysts of different types, hence it is not known how strains of the same type differ in the expression of proteins.

Another argument that is often brought forward generally against specific infection markers for the oocyst stage is the fact that oocysts are quite short lived if ingested by a new host. Sporozoites have been observed to invade enterocytes as early as 30 minutes after ingestion and have been observed in the lamia propria 2 hours after infection (Delgado Betancourt et al., 2019). However, newer results suggest reliable detection of sporozoites in intestinal tissue after 3 to 5 days after ingestion of oocysts by the host (Coombes et al., 2013; Gregg et al., 2013). In order for the immune system to mount an efficient response against an invading pathogen, it is assumed that antigens need to be present in the infected organism for an extended time above a certain threshold to develop detectable levels of antibodies against the pathogen. General assumption is that since most infectious agents enter the body in smaller numbers, a detectable immune response is only mounted against pathogens that can multiply to a level where the antigen dose threshold is exceeded (Marois et al., 2012; Handel et al., 2018). However, research suggests that hosts infected with *T. gondii* tachyzoites develop tissue cysts as early as 3 days after inoculation (Lindsay et al., 1991). Still, infected hosts regularly develop detectable antibody titers against SAG1, an exclusive tachyzoite protein as early as two weeks after infection (Dubey, 2016). It is likely that the robust antibody response to SAG1 is based on regular presentation of this protein to the immune system due to repeated stage conversion of bradyzoites to the tachyzoite stage. It cannot be excluded that the hosts immune system would be able to develop antibodies against a molecule of the short-lived oocyst stage. As detailed in chapter 4.1.3 for example, TED presenting macrophages in the intestinal tract represent a possibility for the hosts immune system to act against this short-lived parasite life-stage. Another interesting aspect in this regard concerns the possibility of

antibodies directed against oocysts in feline hosts. Since cats can shed oocysts for up to two weeks, it would be reasonable to assume that during this process enough antigen would be present in the body to exceed the antigen dose threshold and result in production of detectable levels of antibodies specifically targeting epitopes unique to the oocyst, which mediate immunity to oocyst infections. This is supported by the observation that cats rarely shed oocysts repeatedly in their life. However, this idea is challenged by observations in cats considered immune that were challenged with *T. gondii* tissue cysts. Upon histological examination of the intestine, asexual stages of the parasite were found even after 5 days post infection, indicating partially successful *T. gondii* development (Davis and Dubey, 1995). Still, immune cats did not shed oocysts again upon challenge. In contrast, reshedding of *T. gondii* oocysts in cats was shown to be the result of infections by a different *T. gondii* strain than the one causing the previous infection (Zulpo et al., 2018), corroborating the observation of differential protein expression in different *T. gondii* strains.

Taking together the observations in this thesis, no TgLEA was able to correctly identify exclusively infections that were caused by oocysts, neither in ELISA nor in Luminex assays, indicating they are not suitable as antigens for specific infection markers. However, there is reason to assume that such antigens could exist and further research into this topic is highly relevant. Differences in expression patterns of individual strains need to be taken into account, however.

Summary

Toxoplasmosis is a disease that affects one third of the world's population. It is caused by *T. gondii*, an obligate intracellular parasite, that spreads via the ingestion of meat contaminated with tissue cysts from infected animals or via the environmental oocyst stage. While the infection route via tissue cysts was long thought to be the most relevant, the discovery of the oocyst as transmissible infectious agent and the subsequently growing number of reports on environmental resistance, widespread prevalence in various environmental matrices and contribution to infections is increasingly hinting that a reevaluation of factors contributing to *T. gondii*'s transmission might be called for. To prevent further spread of the disease, methods for robust quantification of environmental oocyst contamination are needed. To facilitate oocyst enrichment from environmental samples, potential molecules binding to oocyst walls were investigated. In this thesis, three CLRs were newly identified to bind to the oocyst wall. They were characterized to bind sporulated and unsporulated oocysts but not sporocysts. Their discovery bears several implications regarding the oocyst wall composition as well as immunological processes. Determination of oocyst contaminated areas followed by efficient inactivation measures could further curb the spread of *T. gondii*. Therefore, the role of four oocyst specific proteins, called TgLEAs, regarding the oocyst's increased environmental resilience was investigated. The four proteins were bioinformatically analyzed and shown to have a moderately high content of disordered regions that exhibit context dependent structure. The *in-silico* findings were confirmed via CD spectroscopy. *In vivo* characterization showed no clear beneficial effect on bacterial growth under stress. Functional *in vitro* characterization however further confirmed IDPR characteristics of these proteins as well as their ability to protect a key enzyme of *T. gondii* which represents an important pathogenesis factor from damage induced by freezing and also preserve enzyme activity. Effective countermeasures against infections caused by oocysts would be complemented by unequivocal determination of infection sources. Optimally, serological methods would allow differentiation of meat borne from oocyst mediated infections and enable early identification of infection clusters. As one of the TgLEAs is proposed to enable this, all TgLEAs were investigated in this thesis. Since the TgLEAs were shown to possess regions of high disorder, their potential to elicit antibody responses was doubted, but immunization procedures in rabbits confirmed antigenicity of the TgLEAs in principle. Serological analysis of a serum panel from experimentally infected chickens however led to the eventual conclusion none of the TgLEAs is suited to identify specific infection sources. Taken together, the presented thesis expands the knowledge on a vastly understudied but highly relevant life cycle stage of *T. gondii* in several cellular und structural aspects and opens up opportunities for promising further research approaches.

Zusammenfassung

Toxoplasmose ist eine Krankheit, von der ein Drittel der Weltbevölkerung betroffen ist. Sie wird durch *T. gondii*, ein obligat intrazellulärer Parasit, verursacht, der durch den Verzehr von Fleisch von infizierten Tieren, das mit Gewebezysten kontaminiert ist oder über das in der Umwelt prävalente Oozystenstadium verbreitet. Während der Infektionsweg über Gewebezysten lange Zeit als der wichtigste angesehen wurde, deuten die Entdeckung der Oozysten als übertragbare Infektionserreger und die daraufhin wachsende Zahl von Berichten über deren Umweltresistenz, die weite Verbreitung in verschiedenen Umgebungen und den Beitrag zu Infektionen zunehmend darauf hin, dass eine Neubewertung der Faktoren, die zur Übertragung von *T. gondii* beitragen, erforderlich ist. Um eine weitere Ausbreitung der Krankheit zu verhindern, werden Methoden zur zuverlässigen Quantifizierung der Oozystenkontamination der Umwelt benötigt. Um die Anreicherung von Oozysten aus Umweltproben zu erleichtern, wurden potenzielle Moleküle, die an die Oozystenwände binden, untersucht. In dieser Arbeit wurden drei CLRs neu identifiziert, die an die Oozystenwand binden. Diese CLRs binden sporulierte und nicht sporulierte Oozysten, nicht aber Sporozysten. Diese Entdeckung hat vielfältigen Einfluss auf das Wissen über die Zusammensetzung der Oozystenwand und auf immunologische Prozesse. Die Bestimmung von mit Oozysten kontaminierten Gebieten, gefolgt von wirksamen Inaktivierungsmaßnahmen, könnte die Verbreitung von *T. gondii* weiter eindämmen. Daher wurde die Rolle von vier oozystenspezifischen Proteinen, den so genannten TgLEAs, in Bezug auf die erhöhte Widerstandsfähigkeit der Oozysten in der Umwelt untersucht. Die vier Proteine wurden bioinformatisch analysiert und es zeigte sich, dass sie einen hohen Gehalt an ungeordneten Regionen aufweisen, die eine kontextabhängige Struktur besitzen. Die *in-silico*-Ergebnisse wurden durch CD-Spektroskopie bestätigt. Die *in-vivo*-Charakterisierung zeigte keine eindeutige positive Wirkung auf das Wachstum unter Stress von Bakterien, die TgLEA-Proteine exprimieren. Die funktionelle in vitro-Charakterisierung bestätigte jedoch die IDPR-Eigenschaften dieser Proteine sowie ihre Fähigkeit, ein Schlüsselenzym von *T. gondii*, das einen wichtigen Pathogenesefaktor darstellt, vor Schäden durch Einfrieren zu schützen und darüber hinaus die Enzymaktivität zu erhalten. Wirksame Gegenmaßnahmen gegen durch Oozysten verursachte Infektionen würden durch die eindeutige Bestimmung von Infektionsquellen ergänzt. Optimalerweise würden serologische Methoden die Unterscheidung zwischen durch Fleisch übertragenen und durch Oozysten vermittelten Infektionen ermöglichen und eine frühzeitige Identifizierung von Infektionsclustern erlauben. Da eines der TgLEAs dies ermöglichen soll, wurden in dieser Arbeit alle TgLEAs dahingehend untersucht. Da die TgLEAs nachweislich Regionen mit hoher Unordnung aufweisen, wurde ihr Potenzial

zur Auslösung von Antikörperreaktionen bezweifelt, doch die erfolgreiche Immunisierung von Kaninchen bestätigten die grundlegende Antigenität der TgLEAs. Die serologische Analyse eines Serum-Panels von experimentell infizierten Hühnern führte jedoch zu dem Schluss, dass keines der TgLEAs geeignet ist, spezifische Infektionsquellen zu identifizieren. Insgesamt hat die vorliegende Arbeit somit das Wissen über ein bisher wenig erforschtes, aber hochrelevantes Lebenszyklusstadium von *T. gondii* in mehreren zellulären und strukturellen Aspekten erweitert und eröffnet Möglichkeiten für vielversprechende weitere Forschungsansätze.

Chapter 5: Appendix

5.1 Figures

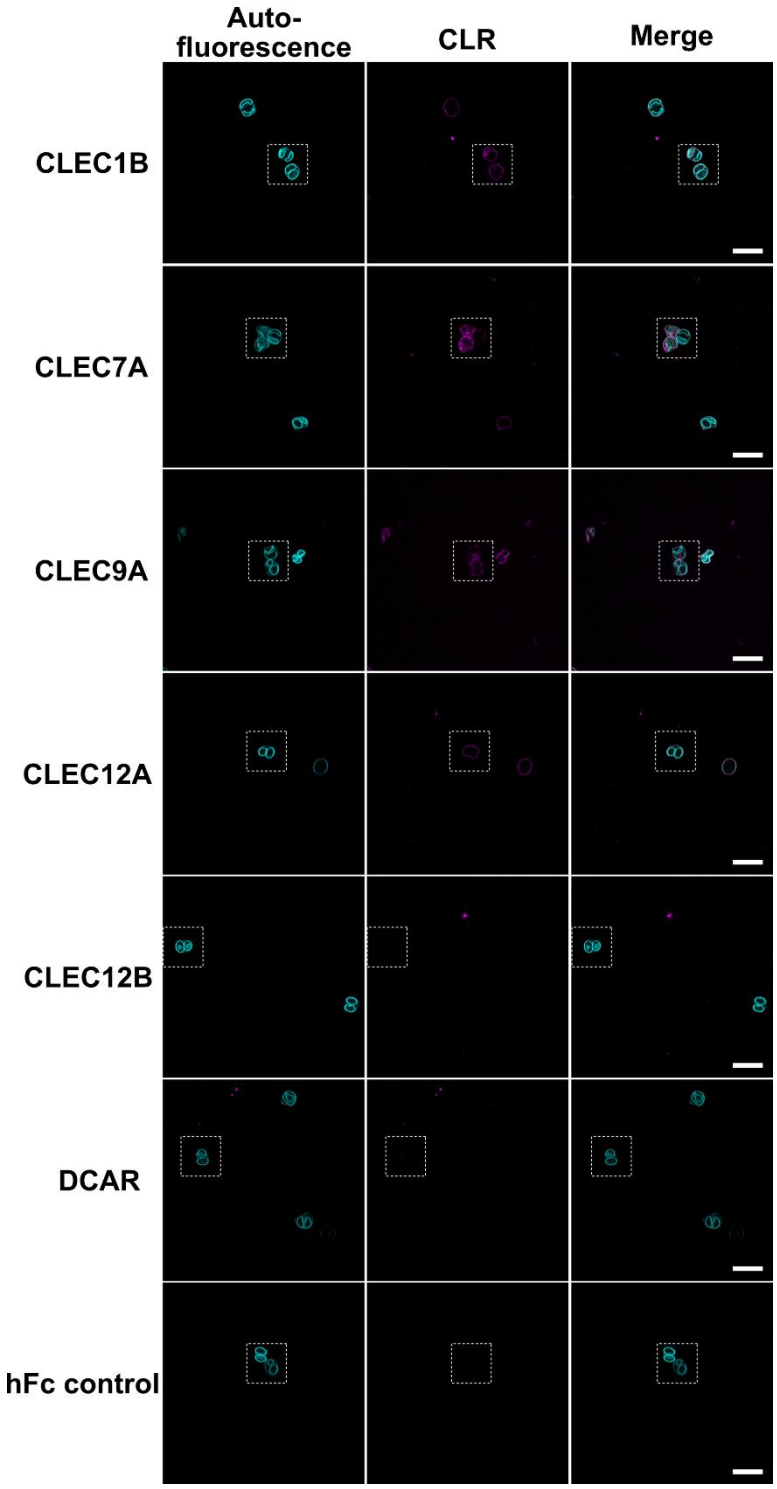

Figure 43: Montage of original images used to obtain cut-outs for Figure 14. Stippled boxes indicate areas from which detailed oocyst representations were taken. Details as described there. Scale bar = 20 µm.

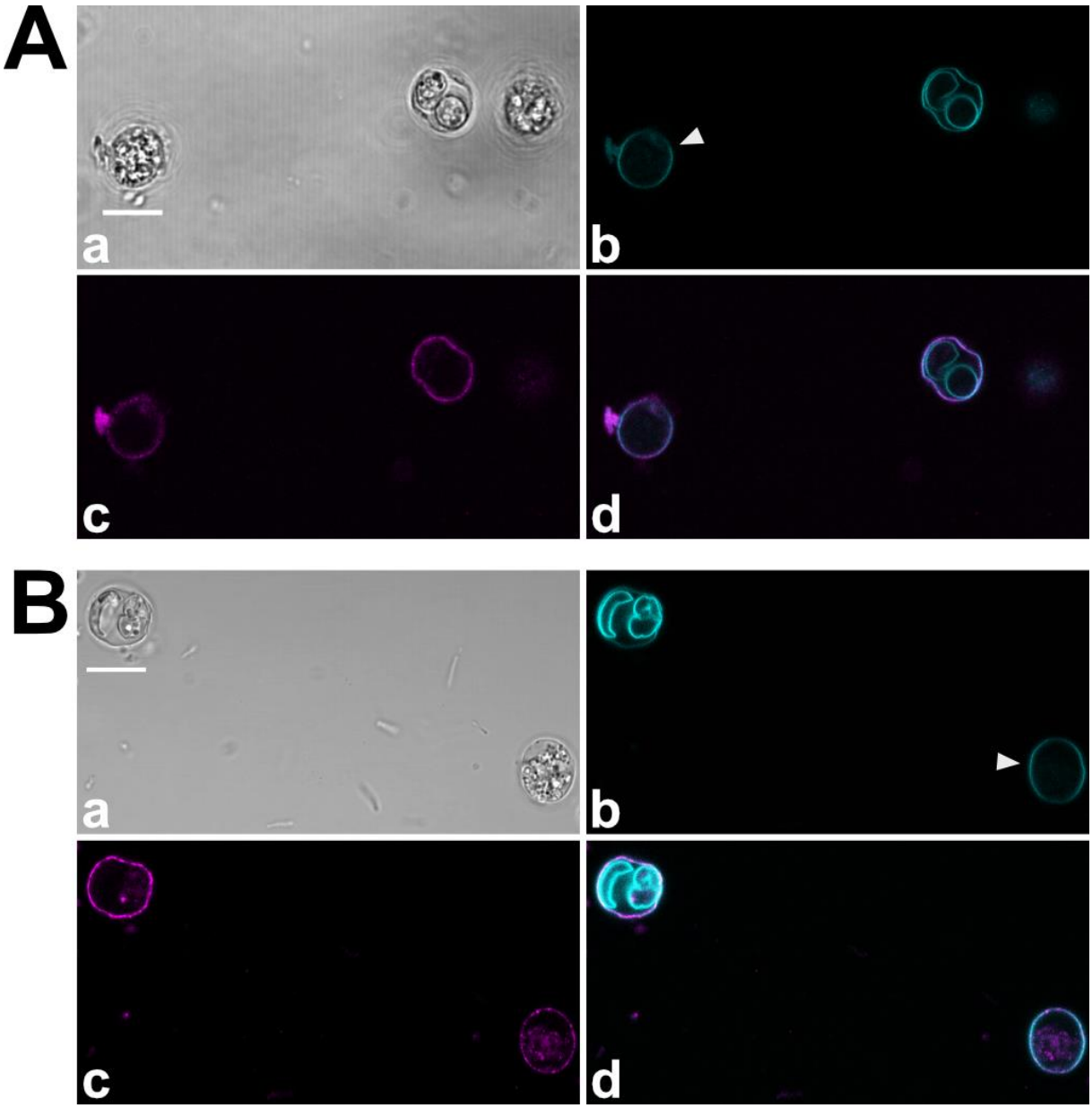

Figure 44: CLRs bind to sporulated and unsporulated oocysts of T. gondii. *Montage of original images used to compose Figure 15. (A) CLEC9A (B) CLEC12A (a) BF (b) oocyst autofluorescence (c) CLR detected by secondary AB (d) merge; arrowheads = unsporulated oocysts.*

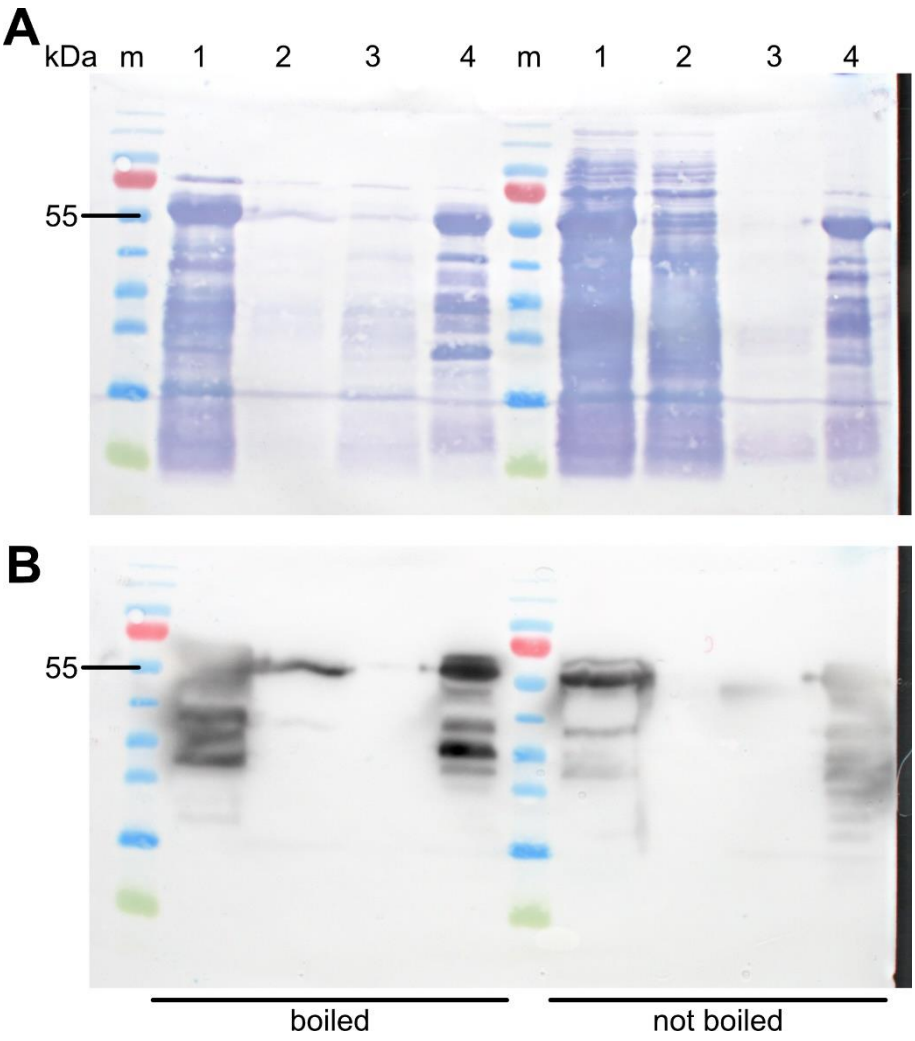

Figure 45: Western blot analysis of recombinantly expressed TgLEA-860. Pictured are total protein staining via DB71 (A) and ECL staining of his-tagged TgLEA-860 (B) of the same western blot membrane, comparing two protein preparation procedures (boiled vs. not boiled). (A) The total protein stain reveals that boiling the bacterial lysate prior to loading onto the column for purification reduces contamination with unwanted proteins during purification as indicated by overall reduction of signal in all fractions. (B) Specific ECL staining of his-tagged TgLEA-860 shows no difference with regards to concentration of the purified protein as there is no obvious signal difference in the eluate fractions. m = molecular marker, 1 = lysate prior to loading, 2 = lysate after running over column, 3 = washing fraction, 4 = pool of eluted fractions.

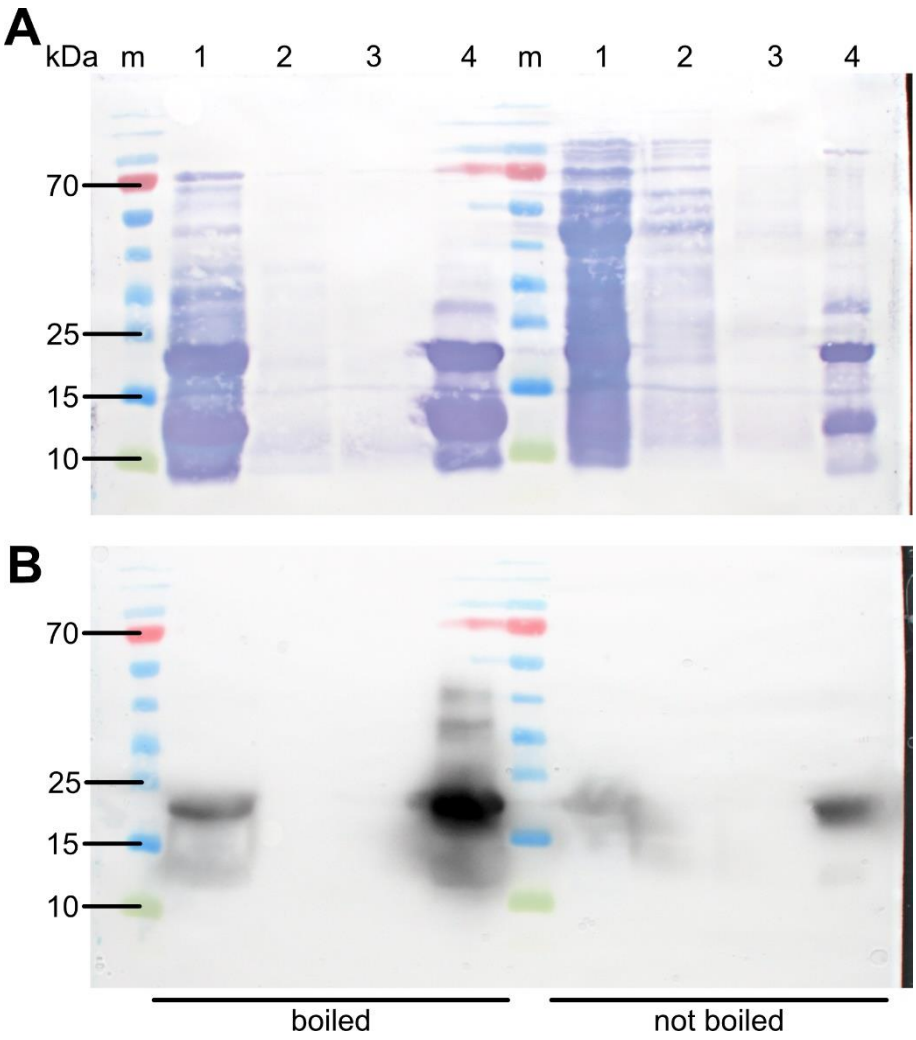

Figure 46: Western blot analysis of recombinantly expressed TgLEA-870. Pictured are total protein staining via DB71 (A) and ECL staining of his-tagged TgLEA-870 (B) of the same western blot membrane, comparing two protein preparation procedures (boiled vs. not boiled). (A) The total protein stain reveals that boiling the bacterial lysate prior to loading onto the column for purification reduces contamination with unwanted proteins during purification as indicated by overall reduction of signal in all fractions. (B) Specific ECL staining of his-tagged TgLEA-870 shows no difference with regards to concentration of the purified protein as there is no obvious signal difference in the eluate fractions. M = molecular marker, 1 = lysate prior to loading, 2 = lysate after running over column, 3 = washing fraction, 4 = pool of eluted fractions.

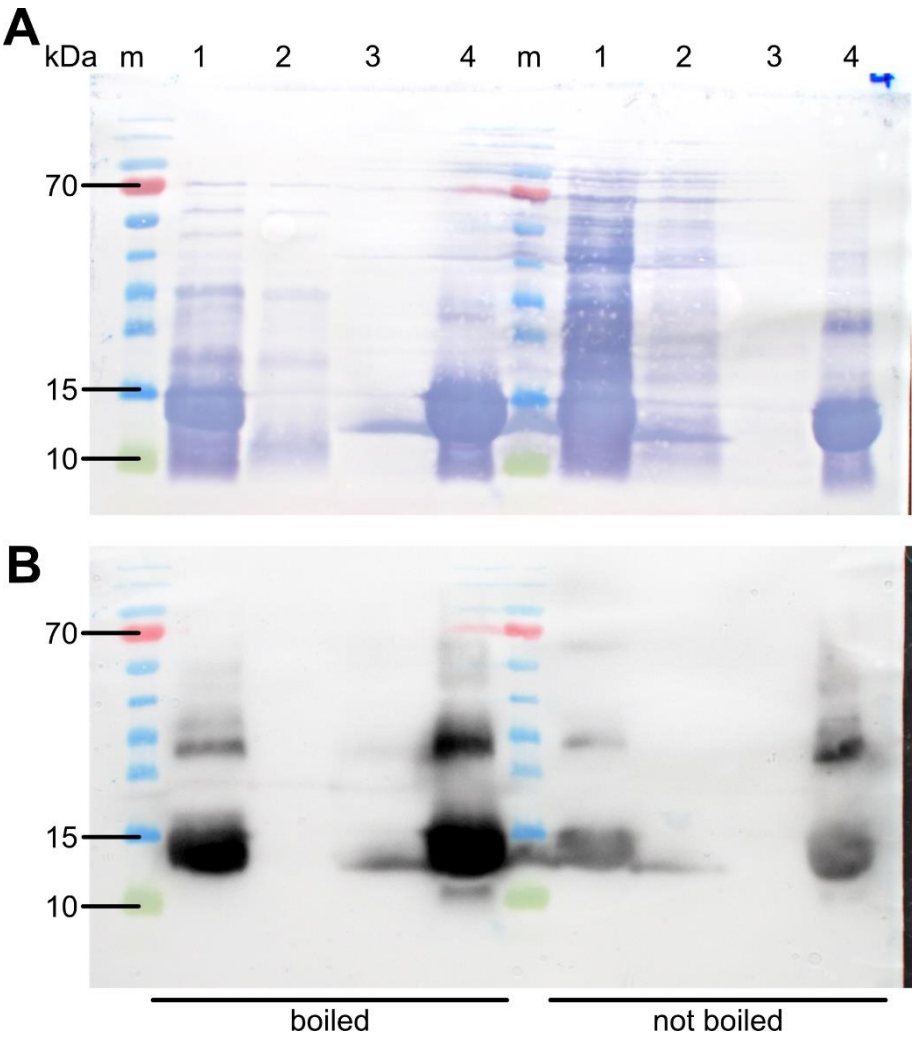

Figure 47: Western blot analysis of recombinantly expressed TgLEA-880. Pictured are total protein staining via DB71 (A) and ECL staining of his-tagged TgLEA-880 (B) of the same western blot membrane, comparing two protein preparation procedures (boiled vs. not boiled). (A) The total protein stain reveals that boiling the bacterial lysate prior to loading onto the column for purification reduces contamination with unwanted proteins during purification as indicated by overall reduction of signal in all fractions. (B) Specific ECL staining of his-tagged TgLEA-880 shows no difference with regards to concentration of the purified protein as there is no obvious signal difference in the eluate fractions. M = molecular marker, 1 = lysate prior to loading, 2 = lysate after running over column, 3 = washing fraction, 4 = pool of eluted fractions.

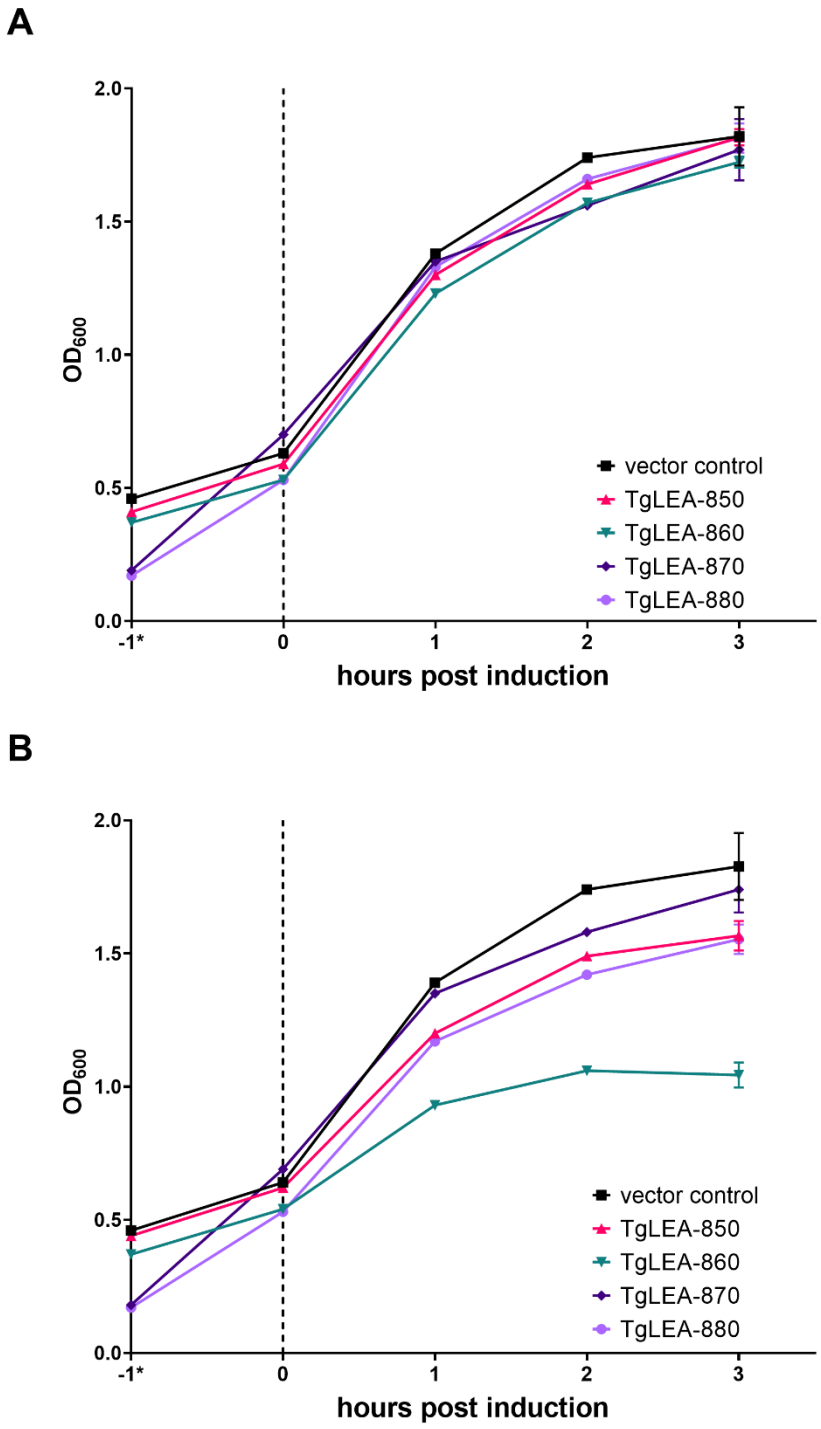

*Figure 48: Bacterial growth during TgLEA expression. Depicted is the growth of bacteria over time derived from OD_{600} without (A) or with (B) addition of 0.5 mM IPTG to induce expression of TgLEAs. *: First OD_{600} measurement was performed 1 hour after inoculation but not necessarily 1 hour before induction, which was performed when OD_{600} was between 0.5 and 0.6 for each individual culture. Error bars at 3 hours post induction indicate SD of three individual experiments.*

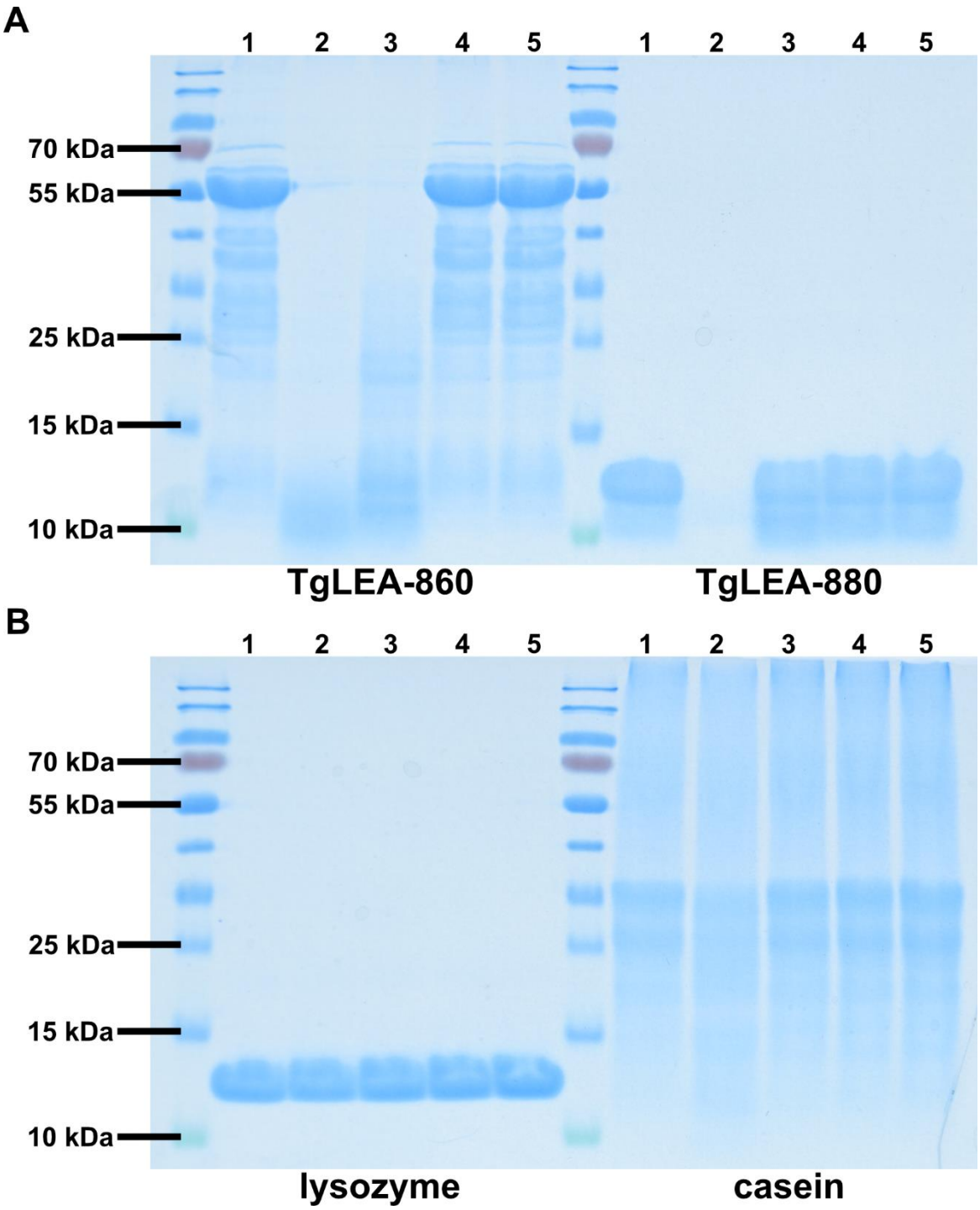

Figure 49: TgLEAs are susceptible to trypsin digestion which can be prevented by TFE. Blot (A) depicts effects of trypsin and TFE on TgLEAs, while blot (B) details the effects under the same conditions on a globular protein (lysozyme) and an IDP (casein). In absence of trypsin all proteins were detected (lane 1). TgLEAs were rapidly digested by trypsin while casein exhibited less distinct bands, indicating proteolytic activity, whereas lysozyme was still unaffected (lane 2). With increasing TFE concentrations, the amount of digested TgLEAs and the IDP control decreased (lanes 3 to 5). 1: no trypsin; 2: only trypsin; 3: trypsin + 10 % TFE; 4: trypsin + 20 % TFE; 5: trypsin + 30 % TFE.

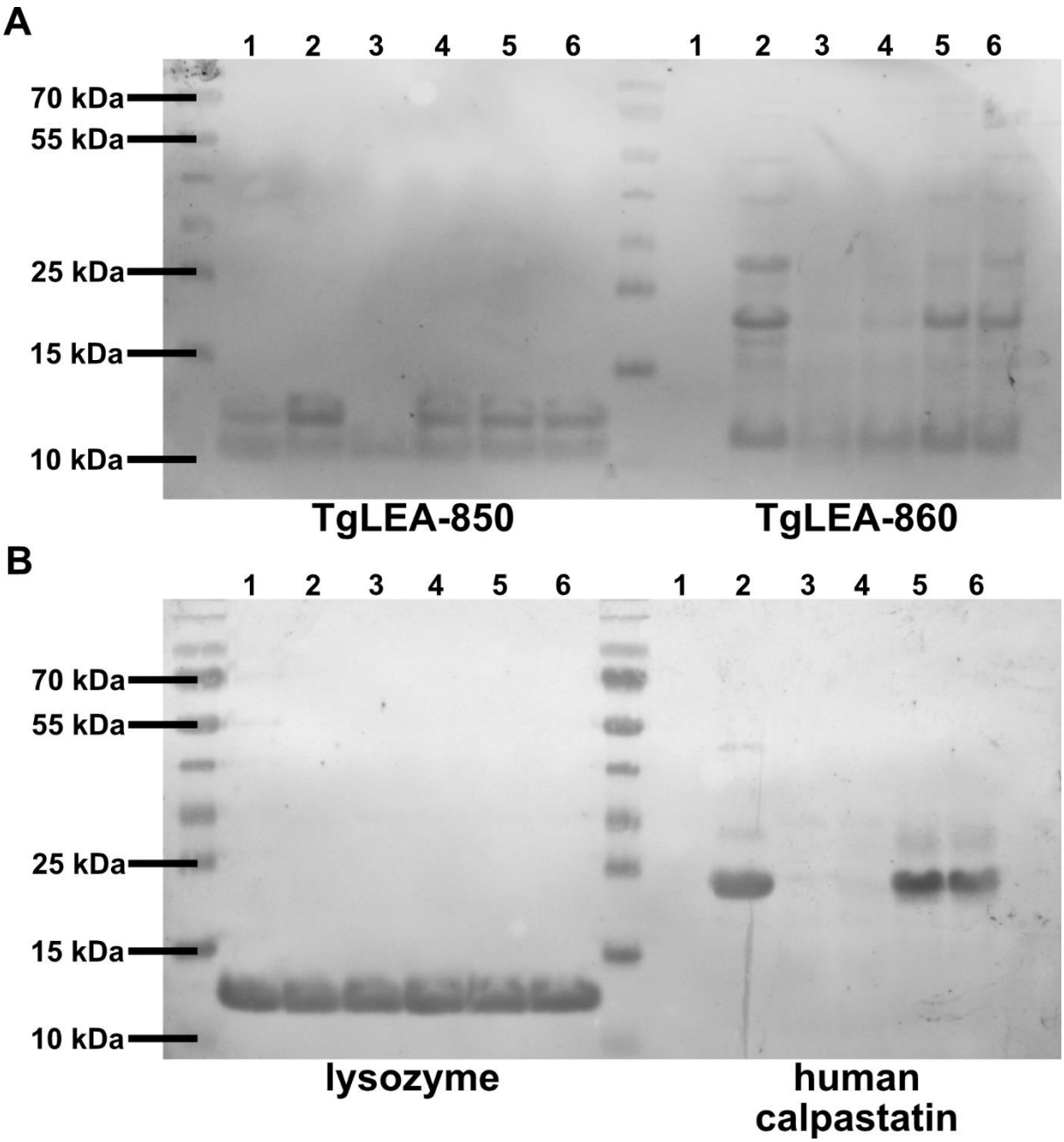

Figure 50: TgLEAs are susceptible to thermolysin digestion which can be prevented by TFE. Blot (A) depicts effects of thermolysin and TFE on TgLEAs, while blot (B) details the effects under the same conditions on a globular protein (lysozyme) and an IDP (hCD1). TgLEAs and the IDP were rapidly digested by thermolysin while lysozyme was still unaffected (lane 1). In absence of thermolysin all proteins were detected (lane 2). With increasing TFE concentrations, the amount of digested TgLEAs and the IDP control decreased (lanes 3 to 6). 1: only thermolysin; 2: no thermolysin; 3: thermolysin + 10 % TFE; 4: thermolysin + 15 % TFE; 5: thermolysin + 20 % TFE; 6: thermolysin + 25 % TFE.

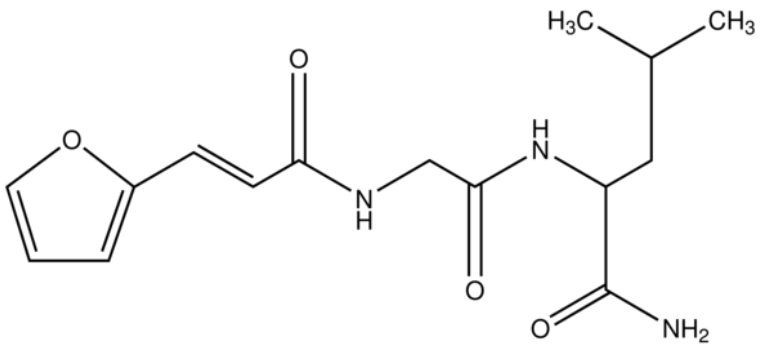

Figure 51: Structure of FAGLA. Image adapted from the manufacturer's website.

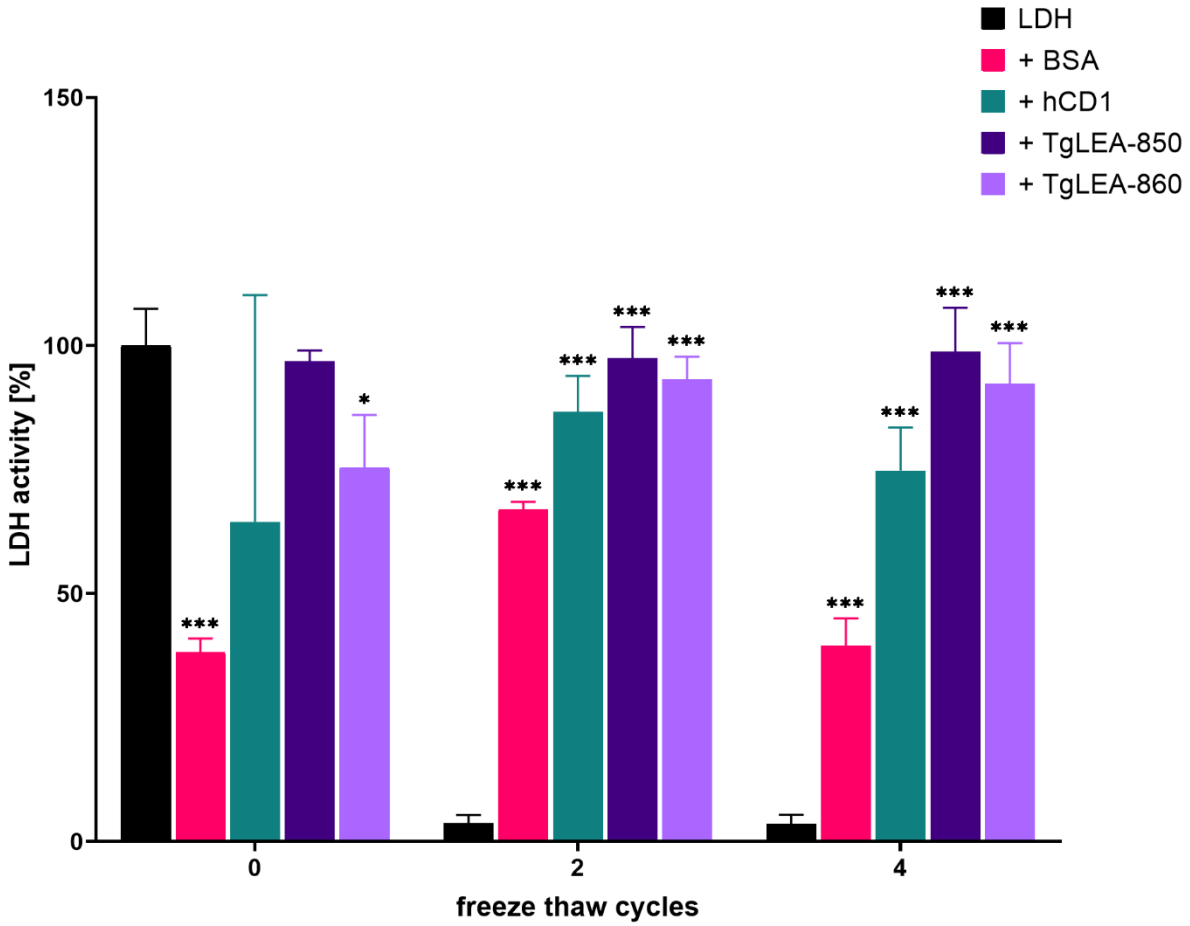

*Figure 52: Preservation of pLDH activity upon freeze-thaw-stress by TgLEAs at molar ratio of 1:100. Depicted is relative pLDH activity in presence of TgLEAs and control proteins after repeated freeze-thawing. Alone, pLDH activity is reduced to almost 0 % after four freeze-thaw-cycles. Remarkably, before freezing, pLDH activity was significantly reduced in presence of BSA and TgLEA-860. Initially, activity increased after the first freezing in all samples, but dropped to activity levels prior to freezing in the case of BSA. Still, the high concentrations of TgLEAs or control proteins preserved at least approx. 50 % of initial pLDH activity after four freeze-thaw-cycles. * = P < 0.05, ** = P < 0.01 and *** = P < 0.001 shown above the bar indicate results significantly different from those for LDH alone. n = three replicates.*

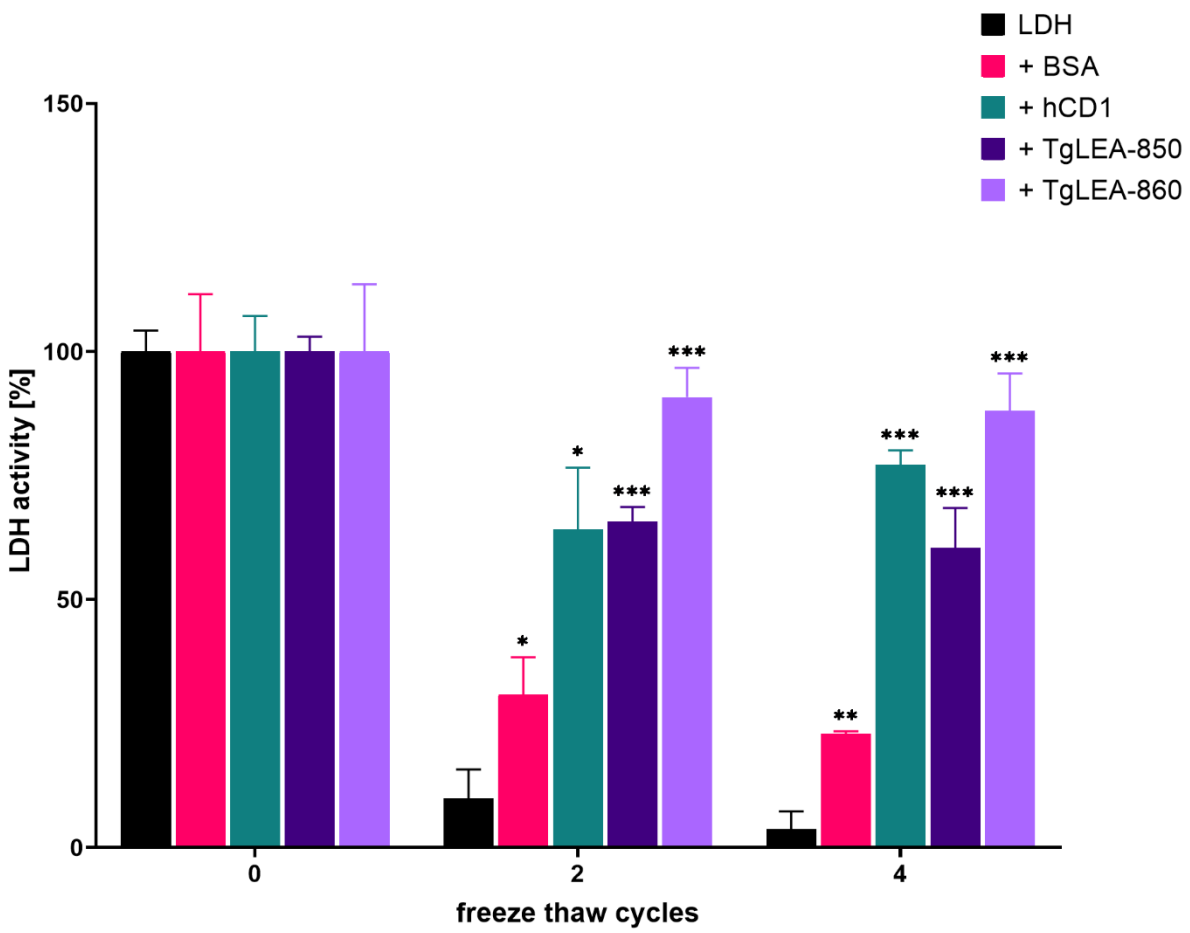

*Figure 53: Preservation of pLDH activity upon freeze-thaw-stress by TgLEAs at molar ratio of 1:50. Depicted is relative pLDH activity in presence of TgLEAs and control proteins after repeated freeze-thawing. Alone, pLDH activity is reduced to almost 0 % after four freeze-thaw-cycles. Significant effects on pLDH activity after freeze-thawing is observed for all tested proteins, although at a molar ratio of 1:50, BSA only preserves 25 % of the initially observed pLDH activity, while the TgLEAs and the hCD1 control preserve more than 50 % of the initial pLDH activity even after four freeze-thaw-cycles. * = P < 0.05, ** = P < 0.01 and *** = P < 0.001 shown above the bar indicate results significantly different from those for LDH alone. n = three replicates.*

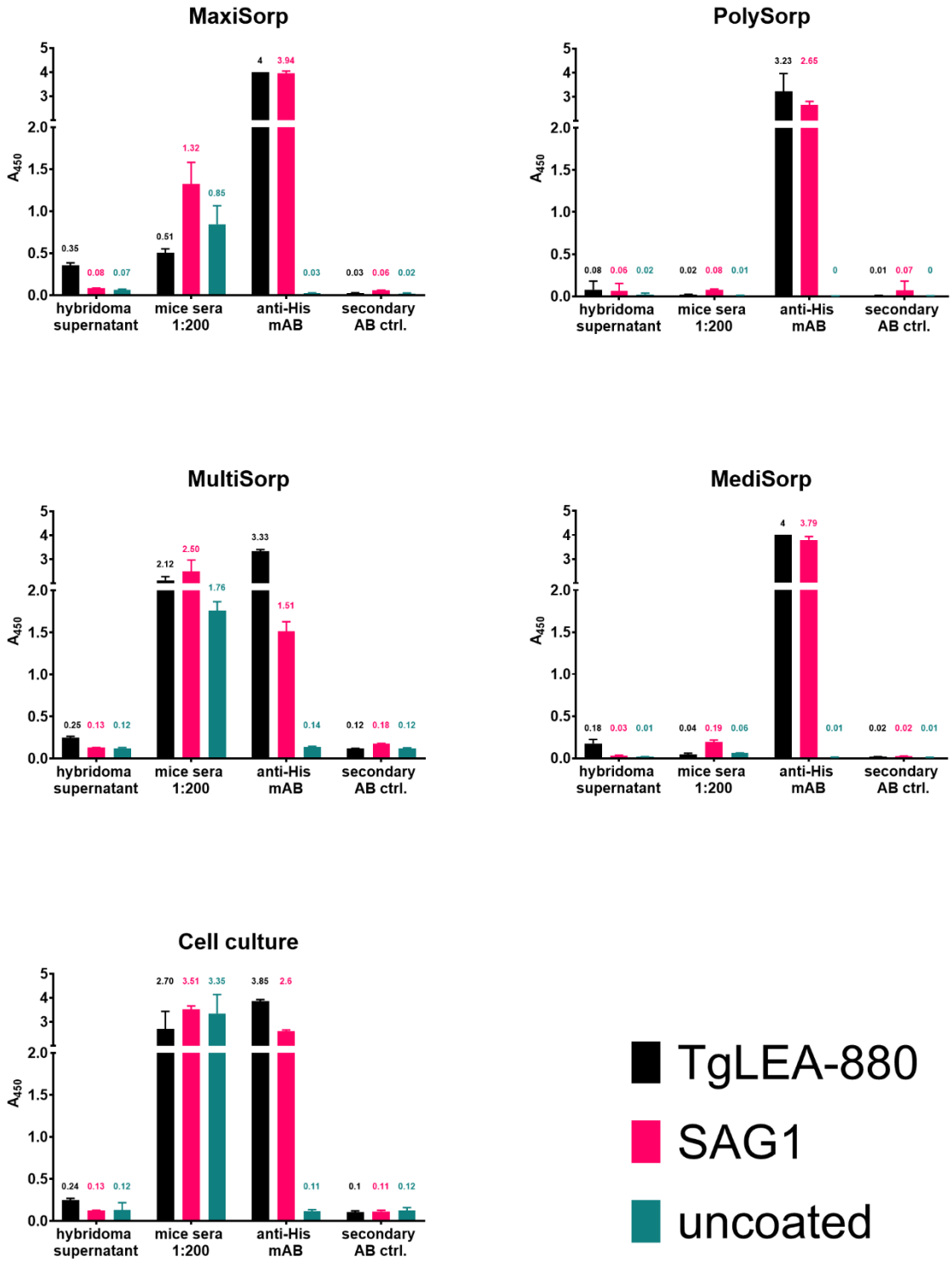

Figure 54: ELISA results of all tested plate types using BSA as blocking agent. MaxiSorp, MultiSorp and regular cell culture plates exhibit high unspecific signal in sera from uninfected mice. PolySorp exhibits no unspecific binding but reduced signal in the anti-his antibody as compared to MediSorp plates. n = three replicates

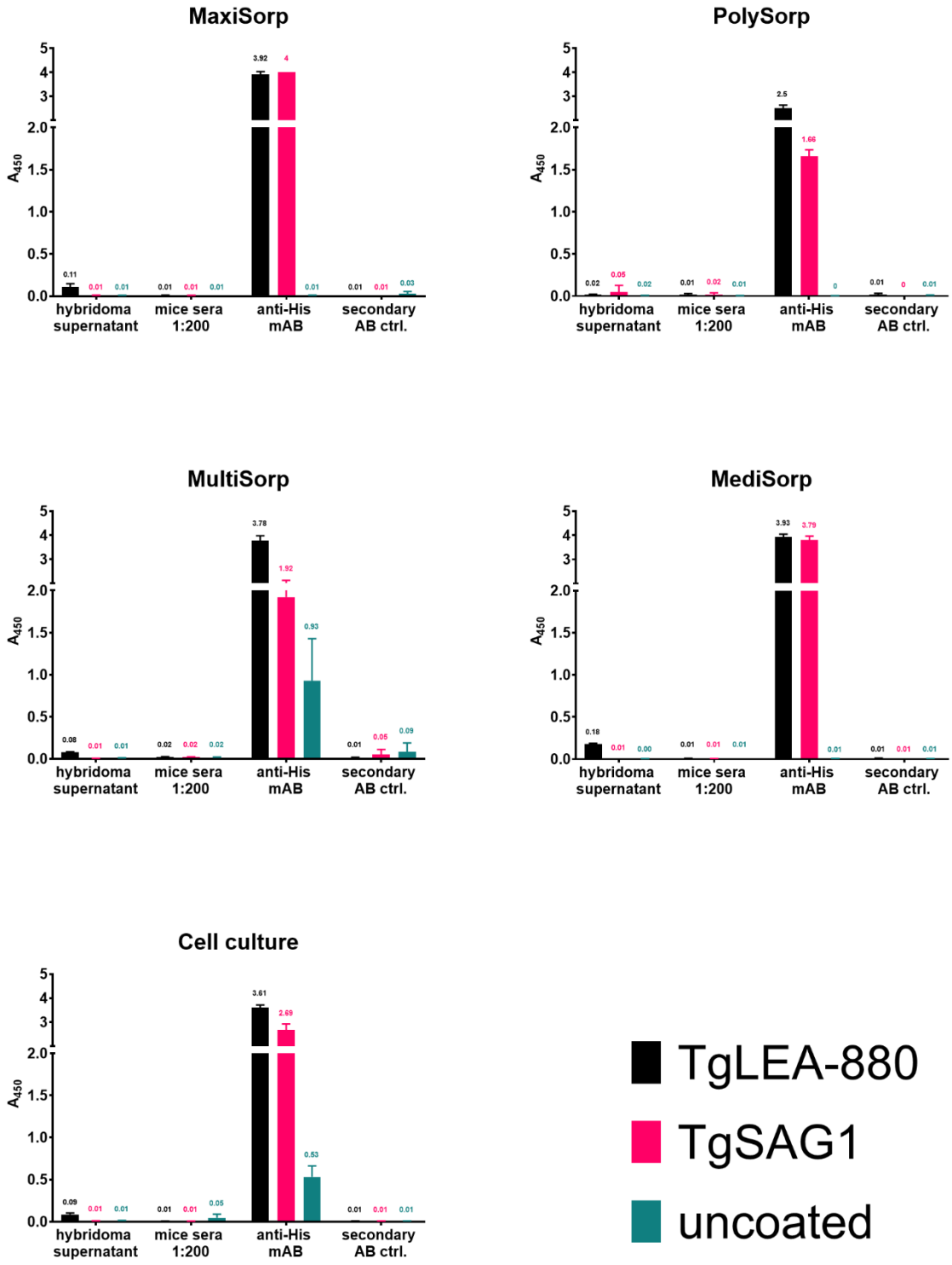

Figure 55: ELISA results of all tested plate types using milk as blocking agent. MaxiSorp plates performed similarly well to MediSorp plates with slightly lower signal of the hybridoma supernatant. PolySorp plates exhibited lower signal of the anti-his antibody, while MultiSorp and regular cell culture plates exhibited in addition high background signal for the secondary anti-his antibody. n = three replicates.

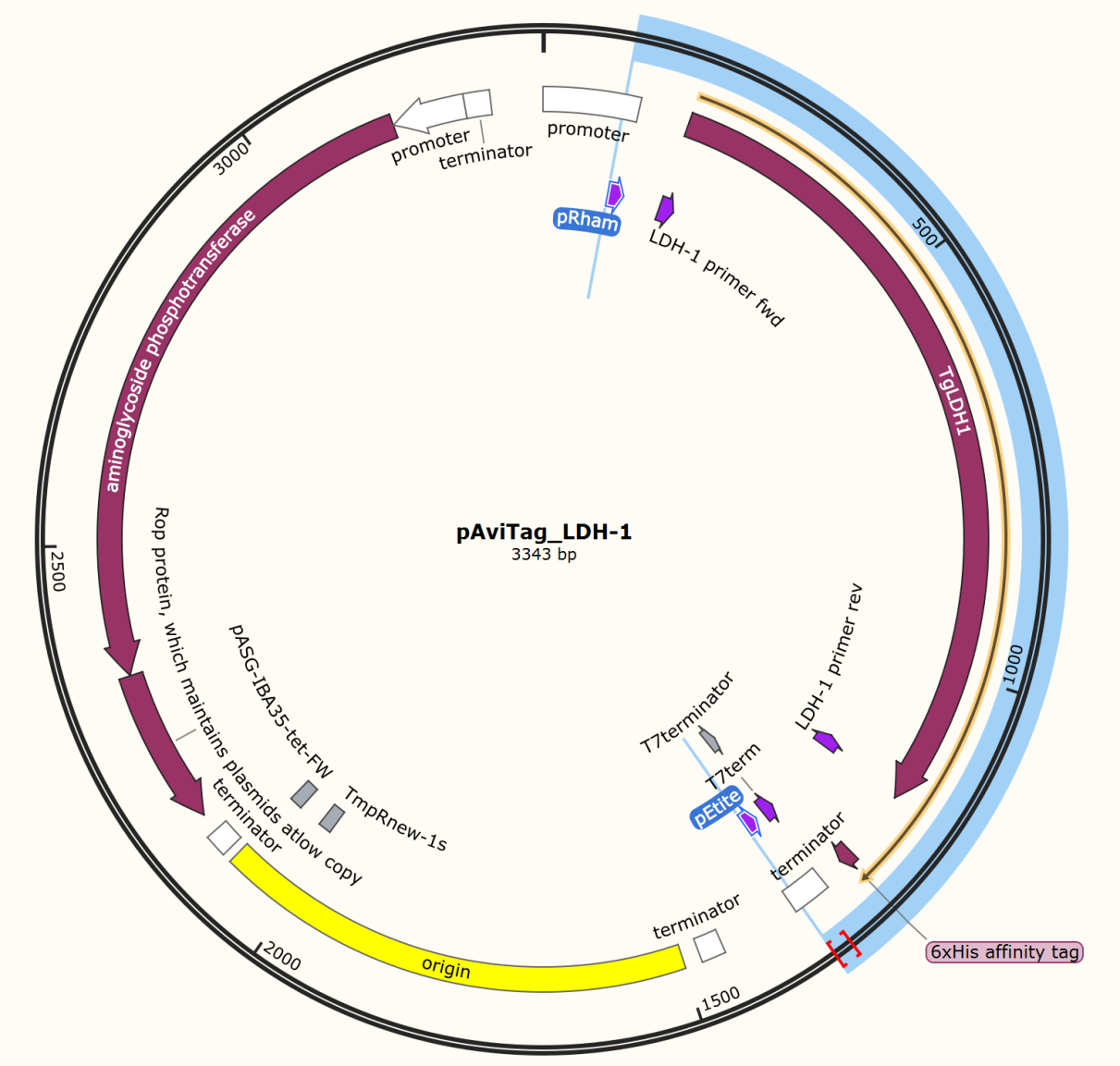

Figure 56: Plasmid map of pAviTag_TgLDH1. TgLDH1 is cloned in frame with the 6His-tag. Binding sites of primers pRham-fwd and pEtite-rev are indicated in blue.

5.2 Tables

Table 7: Abundance of amino acids in TgLEAs. Absolute numbers, select amino acids also in relative abundance [in brackets].

Amino acid	TgLEA-850	TgLEA-860	TgLEA-870	TgLEA-880
Alanine	21	91	29	30
Arginine	3	19	6	2
Asparagine	3	17	3	5
Aspartic acid	5	40	15	10
Cysteine	0	0	0	1
Glutamic acid	12	49	8	9
Glutamine	3	21	9	4
Glycine	9 [9 %]	35 [7 %]	11 [6 %]	11 [8 %]
Histidine	4	4	2	1
Isoleucine	3 [3 %]	14 [3 %]	4 [2 %]	4 [3 %]
Leucine	3 [3 %]	18 [3 %]	8 [5 %]	1 [1 %]
Lysine	10	58	19	13
Methionine	2	3	7	6
Phenylalanine	0 [0 %]	3 [1 %]	4 [2 %]	0 [0 %]
Proline	1	2	8	0
Serine	10	49	15	15
Threonine	6	35	8	10
Tryptophan	0	24	0	0
Tyrosine	2	2	1	3
Valine	7	33	14	5

Table 8: Number of counted beads and MFI values obtained with $TgSAG1_{bio}$ as antigen per sample from chicken sera diluted 1:25.

infection type	sample number	beads counted	MFI
mock	1.01	4	583,5
	1.02	1	1042,0
	1.03	25	564,0
	1.04	22	832,0
	1.05	30	526,0
	1.06	23	337,0
	1.07	5	420,0
	1.08	20	301,5
	1.09	39	366,0
	1.10	9	70,0
	1.11	50	127,5
oocyst	2.01	11	444,0
	2.02	24	375,0
	2.03	2	1822,0
	2.04	3	1277,0
	2.05	1	2960,0
	2.06	-	-
	2.07	-	-
	2.08	3	2012,0
	2.09	-	-
	2.10	22	339,5
	2.11	1	824,0
tissue cyst	3.01	9	1403,0
	3.02	1	669,0
	3.03	8	809,0
	3.04	2	2444,0
	3.05	-	-
	3.06	-	-
	3.07	-	-
	3.08	-	-
	3.09	-	-
	3.10	6	690,5
	3.11	7	200,0

5.3 List of figures

5.4 List of tables

5.5 *Curriculum vitae*

Education

2017 to 2021	PhD, Biology, Robert Koch-Institute Berlin, Thesis: Expanding the Knowledge on Oocyst molecules of *Toxoplasma gondii*
2014 to 2017	Master of Science, Biology, Freie Universität Berlin, Thesis: Etablierung eines Multiplex-basierten Verfahrens zur Detektion von Masernvirus-spezifischen IgG im menschlichen Serum
2011 to 2014	Bachelor of Science, Biology, Ruhr Universität Bochum, Thesis: Funktionelle Charakterisierung des putativen Transkriptionsfaktors SMAC_02413 in *Sordaria macrospora*

Professional experience

Since November 2021	Vaccines and Pandemic Preparedness at the Association of Research-based Pharmaceutical Companies (vfa e.V.)
2017 to 2021	PhD student at the Robert Koch-Institute
2015 to 2017	Student employee in the department Research, Development and Innovation at vfa e.V. and vfa bio

Presentations (selection)

May 2020	LiveTalk at the Naturkundemuseum Berlin within the lecture series „Parasiten - Life undercover“ Berlin, Germany
June 2019	15th International Toxoplasma Conference Armenia, Colombia
October 2018 & 2019	International Symposia on zoonoses research Berlin, Germany
March 2018	28th Annual Meeting of the German Society for Parasitology Berlin, Germany

5.6 List of publications

1. B. T. Fabian, B. Lepenies, G. Schares, J. P. Dubey, F. Spano and F. Seeber (2021). "Expanding the Known Repertoire of C-Type Lectin Receptors Binding to *Toxoplasma gondii* Oocysts Using a Modified High-Resolution Immunofluorescence Assay." mSphere 6(2): e01341-20.
   ➔ BTF, FSe, BL and GS designed the study. BL, JPD and FSp provided the CLR library, Oocysts and antibodies, respectively. BTF and FSp performed experiments. BTF, FSe, GS and BL interpreted the Data. BTF wrote the manuscript, FSe made major contributions. All authors read, provided input on and approved of the final manuscript.

2. B. T. Fabian, F. Hedar, M. Koethe, B. Bangoura, P. Maksimov, F. J. Conraths, I. Villena, D. Aubert, F. Seeber and G. Schares (2020). "Fluorescent bead-based serological detection of *Toxoplasma gondii* infection in chickens." Parasites & Vectors 13(1): 388.
   ➔ GS and FS designed the study. BTF, FH, BB and GS collected the data. BTF, FH, FS, MK, PM, BB, GS, IV and DA performed experiments and analyzed the samples. GS, BTF and MK statistically analyzed the data. BTF, FS, MK, BB and GS interpreted the data. GS, FS, FJC and BTF made major contributions to the writing of the manuscript. All authors read and approved the fnal manuscript

3. E. Delgado Betancourt, B. Hamid, B. T. Fabian, C. Klotz, S. Hartmann and F. Seeber (2019). "From Entry to Early Dissemination-*Toxoplasma gondii*'s Initial Encounter With Its Host." Front Cell Infect Microbiol 9: 46.
   ➔ ED provided parts of Figure 1A and Figures 1B–D. BH provided parts of Figure 1A. All authors contributed to the text and approved its final version.

5.7 References

Abdelbaset, A. E., Fox, B. A., Karram, M. H., Abd Ellah, M. R., Bzik, D. J. and Igarashi, M. (2017). Lactate Dehydrogenase in *Toxoplasma Gondii* Controls Virulence, Bradyzoite Differentiation, and Chronic Infection. PloS one **12**(3): e0173745-e0173745.

Affleck, R., Haynes, C. A. and Clark, D. S. (1992). Solvent Dielectric Effects on Protein Dynamics. Proc Natl Acad Sci U S A **89**(11): 5167-5170.

Al-Anouti, F., Tomavo, S., Parmley, S. and Ananvoranich, S. (2004). The Expression of Lactate Dehydrogenase Is Important for the Cell Cycle of *Toxoplasma Gondii*. J Biol Chem **279**(50): 52300-52311.

Altschul, S. F., Madden, T. L., Schäffer, A. A., Zhang, J., Zhang, Z., Miller, W. and Lipman, D. J. (1997). Gapped Blast and Psi-Blast: A New Generation of Protein Database Search Programs. Nucleic Acids Res **25**(17): 3389-3402.

Álvarez, B., Nieto-Pelegrín, E., Martínez de la Riva, P., Toki, D., Poderoso, T., Revilla, C., Uenishi, H., Ezquerra, A. and Domínguez, J. (2020). Characterization of the Porcine Clec12a and Analysis of Its Expression on Blood Dendritic Cell Subsets. Front Immunol **11**: 863.

Amerah, A. M. and Ravindran, V. (2014). Chapter 3 - Effect of Whole Wheat Feeding on Gut Function and Nutrient Utilization in Poultry. Wheat and Rice in Disease Prevention and Health. R. R. Watson, V. R. Preedy and S. Zibadi. San Diego, Academic Press**:** 35-40.

Amores, A., Force, A., Yan, Y. L., Joly, L., Amemiya, C., Fritz, A., Ho, R. K., Langeland, J., Prince, V., Wang, Y. L., Westerfield, M., Ekker, M. and Postlethwait, J. H. (1998). Zebrafish Hox Clusters and Vertebrate Genome Evolution. Science **282**(5394): 1711-1714.

Anders, R. F. (1986). Multiple Cross-Reactivities Amongst Antigens of *Plasmodium Falciparum* Impair the Development of Protective Immunity against Malaria. Parasite Immunology **8**(6): 529-539.

Andersen, K. R., Leksa, N. C. and Schwartz, T. U. (2013). Optimized *E. Coli* Expression Strain Lobstr Eliminates Common Contaminants from His-Tag Purification. Proteins **81**(11): 1857-1861.

Angeloni, S., Cordes, R., Dunbar, S., Garcia, C., Gibson, G., Martin, C. and Stone, V. (2016). Xmap Cookbook: A Collection of Methods and Protocols for Developing Multiplex Assays with Xmap Technology. Luminex, Austin, TX.

Artur, M. A. S., Rienstra, J., Dennis, T. J., Farrant, J. M., Ligterink, W. and Hilhorst, H. (2019). Structural Plasticity of Intrinsically Disordered Lea Proteins from *Xerophyta Schlechteri* Provides Protection in Vitro and in Vivo. Front Plant Sci **10**(1272).

Asada, K., Ishino, Y., Shimada, M., Shimojo, T., Endo, M., Kimizuka, F., Kato, I., Maki, M., Hatanaka, M. and Murachi, T. (1989). Cdna Cloning of Human Calpastatin: Sequence Homology among Human, Pig, and Rabbit Calpastatins. Journal of Enzyme Inhibition **3**(1): 49-56.

Asghari, A., Majidiani, H., Fatollahzadeh, M., Nemati, T., Shams, M. and Azizi, E. (2021). Insights into the Biochemical Features and Immunogenic Epitopes of Common Bradyzoite Markers of the Ubiquitous *Toxoplasma Gondii*. Infection, Genetics and Evolution: 105037.

Ataei, F. and Hosseinkhani, S. (2015). Impact of Trifluoroethanol-Induced Structural Changes on Luciferase Cleavage Sites. Journal of Photochemistry and Photobiology B: Biology **144**: 1-7.

Aufderheide, K. J. (2008). An Overview of Techniques for Immobilizing and Viewing Living Cells. Micron (Oxford, England : 1993) **39**(2): 71-76.

Baba, T., Ara, T., Hasegawa, M., Takai, Y., Okumura, Y., Baba, M., Datsenko, K. A., Tomita, M., Wanner, B. L. and Mori, H. (2006). Construction of *Escherichia Coli* K-12 in-Frame, Single-Gene Knockout Mutants: The Keio Collection. Mol Syst Biol **2**: 2006.0008.

Battaglia, M. and Covarrubias, A. (2013). Late Embryogenesis Abundant (Lea) Proteins in Legumes. Front Plant Sci **4**(190).

Battaglia, M., Olvera-Carrillo, Y., Garciarrubio, A., Campos, F. and Covarrubias, A. A. (2008). The Enigmatic Lea Proteins and Other Hydrophilins. Plant physiology **148**(1): 6-24.

Belli, S. I., Smith, N. C. and Ferguson, D. J. (2006). The Coccidian Oocyst: A Tough Nut to Crack! Trends Parasitol **22**(9): 416-423.

Bermejo-Jambrina, M., Eder, J., Helgers, L. C., Hertoghs, N., Nijmeijer, B. M., Stunnenberg, M. and Geijtenbeek, T. B. H. (2018). C-Type Lectin Receptors in Antiviral Immunity and Viral Escape. Frontiers in Immunology **9**(590).

Bhattacharya, S., Dhar, S., Banerjee, A. and Ray, S. (2019). Structural, Functional, and Evolutionary Analysis of Late Embryogenesis Abundant Proteins (Lea) in *Triticum Aestivum*: A Detailed Molecular Level Biochemistry Using in Silico Approach. Comput Biol Chem **82**: 9-24.

Biancifiori, F., Rondini, C., Grelloni, V. and Frescura, T. (1986). Avian Toxoplasmosis: Experimental Infection of Chicken and Pigeon. Comparative Immunology, Microbiology and Infectious Diseases **9**(4): 337-346.

Birch-Andersen, A., Ferguson, D. J. and Pontefract, R. D. (1976). A Technique for Obtaining Thin Sections of Coccidian Oocysts. Acta Pathol Microbiol Scand B **84**(4): 235-239.

Blumenthal, T. (1998). Gene Clusters and Polycistronic Transcription in Eukaryotes. Bioessays **20**(6): 480-487.

Blumenthal, T., Evans, D., Link, C. D., Guffanti, A., Lawson, D., Thierry-Mieg, J., Thierry-Mieg, D., Chiu, W. L., Duke, K., Kiraly, M. and Kim, S. K. (2002). A Global Analysis of *Caenorhabditis Elegans* Operons. Nature **417**(6891): 851-854.

Bondos, S. E., Dunker, A. K. and Uversky, V. N. (2021). On the Roles of Intrinsically Disordered Proteins and Regions in Cell Communication and Signaling. Cell Communication and Signaling **19**(1): 88.

Boonham, N., Kreuze, J., Winter, S., van der Vlugt, R., Bergervoet, J., Tomlinson, J. and Mumford, R. (2014). Methods in Virus Diagnostics: From Elisa to Next Generation Sequencing. Virus Research **186**: 20-31.

Boothby, T. C. and Pielak, G. J. (2017). Intrinsically Disordered Proteins and Desiccation Tolerance: Elucidating Functional and Mechanistic Underpinnings of Anhydrobiosis. BioEssays **39**(11): 1700119-1700119.

Boothby, T. C., Tapia, H., Brozena, A. H., Piszkiewicz, S., Smith, A. E., Giovannini, I., Rebecchi, L., Pielak, G. J., Koshland, D. and Goldstein, B. (2017). Tardigrades Use Intrinsically Disordered Proteins to Survive Desiccation. Molecular Cell **65**(6): 975-984.e975.

Boswell, L. C., Menze, M. A. and Hand, S. C. (2014). Group 3 Late Embryogenesis Abundant Proteins from Embryos of *Artemia Franciscana*: Structural Properties and Protective Abilities During Desiccation. Physiological and Biochemical Zoology **87**(5): 640-651.

Boswell, L. C., Moore, D. S. and Hand, S. C. (2014). Quantification of Cellular Protein Expression and Molecular Features of Group 3 Lea Proteins from Embryos of *Artemia Franciscana*. Cell Stress and Chaperones **19**(3): 329-341.

Brenner, N., Mentzer, A. J., Butt, J., Braband, K. L., Michel, A., Jeffery, K., Klenerman, P., Gärtner, B., Schnitzler, P., Hill, A., Taylor, G., Demontis, M. A., Guy, E., Hadfield, S. J., Almond, R., Allen, N., Pawlita, M. and Waterboer, T. (2019). Validation of Multiplex Serology for Human Hepatitis Viruses B and C, Human T-Lymphotropic Virus 1 and *Toxoplasma Gondii*. PLOS ONE **14**(1): e0210407.

Brown, C. C., Gudjonson, H., Pritykin, Y., Deep, D., Lavallee, V. P., Mendoza, A., Fromme, R., Mazutis, L., Ariyan, C., Leslie, C., Pe'er, D. and Rudensky, A. Y. (2019). Transcriptional Basis of Mouse and Human Dendritic Cell Heterogeneity. Cell **179**(4): 846-863.e824.

Brown, G. D., Willment, J. A. and Whitehead, L. (2018). C-Type Lectins in Immunity and Homeostasis. Nat Rev Immunol **18**(6): 374-389.

Browne, J., Tunnacliffe, A. and Burnell, A. (2002). Plant Desiccation Gene Found in a Nematode. Nature **416**(6876): 38-38.

Brudner, M., Karpel, M., Lear, C., Chen, L., Yantosca, L. M., Scully, C., Sarraju, A., Sokolovska, A., Zariffard, M. R., Eisen, D. P., Mungall, B. A., Kotton, D. N., Omari, A., Huang, I. C., Farzan, M., Takahashi, K., Stuart, L., Stahl, G. L., Ezekowitz, A. B., Spear, G. T., Olinger, G. G., Schmidt, E. V. and Michelow, I. C. (2013). Lectin-Dependent Enhancement of Ebola Virus Infection Via Soluble and Transmembrane C-Type Lectin Receptors. PLoS One **8**(4): e60838.

Burrells, A., Opsteegh, M., Pollock, K. G., Alexander, C. L., Chatterton, J., Evans, R., Walker, R., McKenzie, C.-A., Hill, D., Innes, E. A. and Katzer, F. (2016). The Prevalence and Genotypic Analysis of *Toxoplasma Gondii* from Individuals in Scotland, 2006-2012. Parasites & vectors **9**(1): 324-324.

Bushkin, G. G., Motari, E., Carpentieri, A., Dubey, J. P., Costello, C. E., Robbins, P. W. and Samuelson, J. (2013). Evidence for a Structural Role for Acid-Fast Lipids in Oocyst Walls of *Cryptosporidium*, *Toxoplasma*, and *Eimeria*. mBio **4**(5): e00387-00313.

Bushkin, G. G., Motari, E., Magnelli, P., Gubbels, M.-J., Dubey, J. P., Miska, K. B., Bullitt, E., Costello, C. E., Robbins, P. W. and Samuelson, J. (2012). B-1,3-Glucan, Which Can Be Targeted by Drugs, Forms a Trabecular Scaffold in the Oocyst Walls of *Toxoplasma* and *Eimeria*. mBio **3**(5).

Campos, F., Zamudio, F. and Covarrubias, A. A. (2006). Two Different Late Embryogenesis Abundant Proteins from *Arabidopsis Thaliana* Contain Specific Domains That Inhibit *Escherichia Coli* Growth. Biochemical and Biophysical Research Communications **342**(2): 406-413.

Chakrabortee, S., Meersman, F., Kaminski Schierle, G. S., Bertoncini, C. W., McGee, B., Kaminski, C. F. and Tunnacliffe, A. (2010). Catalytic and Chaperone-Like Functions in an Intrinsically Disordered Protein Associated with Desiccation Tolerance. Proc Natl Acad Sci U S A **107**(37): 16084-16089.

Chakrabortee, S., Tripathi, R., Watson, M., Kaminski Schierle, G. S., Kurniawan, D. P., Kaminski, C. F., Wise, M. J. and Tunnacliffe, A. (2012). Intrinsically Disordered Proteins as Molecular Shields. Mol. BioSyst. **8**(1): 210-219.

Chatterjee, A., Banerjee, S., Steffen, M., O'Connor, R. M., Ward, H. D., Robbins, P. W. and Samuelson, J. (2010). Evidence for Mucin-Like Glycoproteins That Tether Sporozoites of *Cryptosporidium Parvum* to the Inner Surface of the Oocyst Wall. Eukaryotic Cell **9**(1): 84-96.

Chavali, S., Gunnarsson, A. and Babu, M. M. (2017). Intrinsically Disordered Proteins Adaptively Reorganize Cellular Matter During Stress. Trends in Biochemical Sciences **42**(6): 410-412.

Chemes, L. B., Alonso, L. G., Noval, M. G. and de Prat-Gay, G. (2012). Circular Dichroism Techniques for the Analysis of Intrinsically Disordered Proteins and Domains. Methods Mol Biol **895**: 387-404.

Chrom, J. P. (1909). A Study of Uric Acid. Dublin Journal of Medical Science (1872-1920) **128**(1): 63-66.

Colman, P. M. (1997). Virus Versus Antibody. Structure **5**(5): 591-593.

Comor, L., Dolinska, S., Bhide, K., Pulzova, L., Jiménez-Munguía, I., Bencurova, E., Flachbartova, Z., Potocnakova, L., Kanova, E. and Bhide, M. (2017). Joining the in Vitro Immunization of Alpaca Lymphocytes and Phage Display: Rapid and Cost Effective Pipeline for Sdab Synthesis. Microbial cell factories **16**(1): 13-13.

Coombes, J. L., Charsar, B. A., Han, S. J., Halkias, J., Chan, S. W., Koshy, A. A., Striepen, B. and Robey, E. A. (2013). Motile Invaded Neutrophils in the Small Intestine of *Toxoplasma Gondii*-Infected Mice Reveal a Potential Mechanism for Parasite Spread. Proc Natl Acad Sci U S A **110**(21): E1913-1922.

Cumming, R. (1992). The Biological Control of Coccidiosis by Choice Feeding. Proc. 19th World's Poult. Cong: 20-24.

Dando, C., Schroeder, E. R., Hunsaker, L. A., Deck, L. M., Royer, R. E., Zhou, X., Parmley, S. F. and Vander Jagt, D. L. (2001). The Kinetic Properties and Sensitivities to Inhibitors of Lactate Dehydrogenases (Ldh1 and Ldh2) from *Toxoplasma Gondii*: Comparisons with Pldh from *Plasmodium Falciparum*. Mol Biochem Parasitol **118**(1): 23-32.

Dang, N. X. and Hincha, D. K. (2011). Identification of Two Hydrophilins That Contribute to the Desiccation and Freezing Tolerance of Yeast (*Saccharomyces Cerevisiae*) Cells. Cryobiology **62**(3): 188-193.

Dang, N. X., Popova, A. V., Hundertmark, M. and Hincha, D. K. (2014). Functional Characterization of Selected Lea Proteins from *Arabidopsis Thaliana* in Yeast and in Vitro. Planta **240**(2): 325-336.

Dard, C., Swale, C., Brenier-Pinchart, M.-P., Farhat, D. C., Bellini, V., Robert, M. G., Cannella, D., Pelloux, H., Tardieux, I. and Hakimi, M.-A. (2021). A Brain Cyst Load-Associated Antigen Is a *Toxoplasma Gondii* Biomarker for Serodetection of Persistent Parasites and Chronic Infection. BMC Biology **19**(1): 25.

Dass, R., Mulder, F. A. A. and Nielsen, J. T. (2020). Odinpred: Comprehensive Prediction of Protein Order and Disorder. Sci Rep **10**(1): 14780.

Datsenko, K. A. and Wanner, B. L. (2000). One-Step Inactivation of Chromosomal Genes in *Escherichia Coli* K-12 Using Pcr Products. Proc Natl Acad Sci U S A **97**(12): 6640-6645.

Dattoli, V. C., Veiga, R. V., Cunha, S. S., Pontes-de-Carvalho, L., Barreto, M. L. and Alcantara-Neves, N. M. (2011). Oocyst Ingestion as an Important Transmission Route of *Toxoplasma Gondii* in Brazilian Urban Children. J Parasitol **97**(6): 1080-1084.

Davis, S. W. and Dubey, J. P. (1995). Mediation of Immunity to *Toxoplasma Gondii* Oocyst Shedding in Cats. The Journal of Parasitology **81**(6): 882-886.

De Stefano, J. A., Trinkle, L. S., Walzer, P. D. and Cushion, M. T. (1992). Flow Cytometric Analyses of Lectin Binding to *Pneumocystis Carinii* Surface Carbohydrates. J Parasitol **78**(2): 271-280.

Delgado Betancourt, E., Hamid, B., Fabian, B. T., Klotz, C., Hartmann, S. and Seeber, F. (2019). From Entry to Early Dissemination-*Toxoplasma Gondii*'s Initial Encounter with Its Host. Front Cell Infect Microbiol **9**: 46.

Deschaght, P., Vintem, A. P., Logghe, M., Conde, M., Felix, D., Mensink, R., Goncalves, J., Audiens, J., Bruynooghe, Y., Figueiredo, R., Ramos, D., Tanghe, R., Teixeira, D., Van de Ven, L., Stortelers, C. and Dombrecht, B. (2017). Large Diversity of Functional Nanobodies from a Camelid Immune Library Revealed by an Alternative Analysis of Next-Generation Sequencing Data. Front Immunol **8**: 420-420.

Desmonts, G. and Remington, J. S. (1980). Direct Agglutination Test for Diagnosis of *Toxoplasma* Infection: Method for Increasing Sensitivity and Specificity. Journal of clinical microbiology **11**(6): 562-568.

Di Genova, B. M., Wilson, S. K., Dubey, J. P. and Knoll, L. J. (2019). Intestinal Delta-6-Desaturase Activity Determines Host Range for *Toxoplasma* Sexual Reproduction. PLOS Biology **17**(8): e3000364.

Dicken, J., Mildner, A., Leshkowitz, D., Touw, I. P., Hantisteanu, S., Jung, S. and Groner, Y. (2013). Transcriptional Reprogramming of Cd11b+Esam(Hi) Dendritic Cell Identity and Function by Loss of Runx3. PLoS One **8**(10): e77490.

Dickhut, C., Feldmann, I., Lambert, J. and Zahedi, R. P. (2014). Impact of Digestion Conditions on Phosphoproteomics. J Proteome Res **13**(6): 2761-2770.

Djurkovic-Djakovic, O., Dupouy-Camet, J., Van der Giessen, J. and Dubey, J. P. (2019). Toxoplasmosis: Overview from a One Health Perspective. Food and Waterborne Parasitology: e00054.

Döşkaya, M., Liang, L., Jain, A., Can, H., İz, G., Felgner, P. L., Değirmenci Döşkaya, A., Davies, D. H. and Gürüz, A. Y. (2018). Discovery of New *Toxoplasma Gondii* Antigenic Proteins Using a High Throughput Protein Microarray Approach Screening Sera of Murine Model Infected Orally with Oocysts and Tissue Cysts. Parasites & Vectors.

Drira, M., Saibi, W., Amara, I., Masmoudi, K., Hanin, M. and Brini, F. (2015). Wheat Dehydrin K-Segments Ensure Bacterial Stress Tolerance, Antiaggregation and Antimicrobial Effects. Applied Biochemistry and Biotechnology **175**(7): 3310-3321.

Dubey, J. P. (1993). *Toxoplasma*, *Neospora*, *Sarcocystis*, and Other Tissue Cyst-Forming Coccidia of Humans and Animals. Parasitic Protozoa (Second Edition). J. P. Kreier. San Diego, Academic Press**:** 1-158.

Dubey, J. P. (1995). Duration of Immunity to Shedding of *Toxoplasma Gondii* Oocysts by Cats. The Journal of Parasitology **81**(3): 410-410.

Dubey, J. P. (1996). Strategies to Reduce Transmission of *Toxoplasma Gondii* to Animals and Humans. Veterinary Parasitology **64**(1): 65-70.

Dubey, J. P. (1998). Advances in the Life Cycle of *Toxoplasma Gondii*. Int J Parasitol **28**(7): 1019-1024.

Dubey, J. P. (2001). Oocyst Shedding by Cats Fed Isolated Bradyzoites and Comparison of Infectivity of Bradyzoites of the Veg Strain *Toxoplasma Gondii* to Cats and Mice Source Journal of Parasitology J. Parasitol **87**(871): 215-219.

Dubey, J. P. (2004). Toxoplasmosis - a Waterborne Zoonosis. Vet Parasitol **126**(1-2): 57-72.

Dubey, J. P. (2006). Comparative Infectivity of Oocysts and Bradyzoites of *Toxoplasma Gondii* for Intermediate (Mice) and Definitive (Cats) Hosts. Veterinary Parasitology **140**(1): 69-75.

Dubey, J. P. (2010). *Toxoplasma Gondii* Infections in Chickens (*Gallus Domesticus)*: Prevalence, Clinical Disease, Diagnosis and Public Health Significance. Zoonoses Public Health **57**(1): 60-73.

Dubey, J. P. (2016). Toxoplasmosis of Animals and Humans, CRC press.

Dubey, J. P. and Crutchley, C. (2008). Toxoplasmosis in Wallabies (*Macropus Rufogriseus* and *Macropus Eugenii*): Blindness, Treatment with Atovaquone, and Isolation of *Toxoplasma Gondii*. J Parasitol **94**(4): 929-933.

Dubey, J. P. and Desmonts, G. (1987). Serological Responses of Equids Fed *Toxoplasma Gondii* Oocysts. Equine Vet J **19**(4): 337-339.

Dubey, J. P. and Frenkel, J. K. (1974). Immunity to Feline Toxoplasmosis: Modification by Administration of Corticosteroids. Veterinary Pathology **11**(4): 350-379.

Dubey, J. P., Lehmann, T., Lautner, F., Kwok, O. C. and Gamble, H. R. (2015). Toxoplasmosis in Sentinel Chickens (*Gallus Domesticus*) in New England Farms: Seroconversion, Distribution of Tissue Cysts in Brain, Heart, and Skeletal Muscle by Bioassay in Mice and Cats. Vet Parasitol **214**(1-2): 55-58.

Dubey, J. P., Lunney, J. K., Shen, S. K., Kwok, O. C., Ashford, D. A. and Thulliez, P. (1996). Infectivity of Low Numbers of *Toxoplasma Gondii* Oocysts to Pigs. J Parasitol **82**(3): 438-443.

Dubey, J. P., Pena, H. F. J., Cerqueira-Cézar, C. K., Murata, F. H. A., Kwok, O. C. H., Yang, Y. R., Gennari, S. M. and Su, C. (2020). Epidemiologic Significance of *Toxoplasma Gondii* Infections in Chickens (*Gallus Domesticus*): The Past Decade. Parasitology **147**(12): 1263-1289.

Dubey, J. P., Petersen, E. and Ambroise-Thomas, P. (2000). Congenital Toxoplasmosis: Scientific Background, Clinical Management and Control.

Dubey, J. P., Ruff, M. D., Camargo, M. E., Shen, S. K., Wilkins, G. L., Kwok, O. C. and Thulliez, P. (1993). Serologic and Parasitologic Responses of Domestic Chickens after Oral Inoculation with *Toxoplasma Gondii* Oocysts. Am J Vet Res **54**(10): 1668-1672.

Dubey, J. P., Speer, C. A., Shen, S. K., Kwok, O. C. and Blixt, J. A. (1997). Oocyst-Induced Murine Toxoplasmosis: Life Cycle, Pathogenicity, and Stage Conversion in Mice Fed *Toxoplasma Gondii* Oocysts. J Parasitol **83**(5): 870-882.

Dubey, J. P., Thayer, D. W., Speer, C. A. and Shen, S. K. (1998). Effect of Gamma Irradiation on Unsporulated and Sporulated *Toxoplasma Gondii* Oocysts. International Journal for Parasitology **28**(3): 369-375.

Dumètre, A. and Dardé, M. L. (2005). Immunomagnetic Separation of *Toxoplasma Gondii* Oocysts Using a Monoclonal Antibody Directed against the Oocyst Wall. Journal of Microbiological Methods **61**(2): 209-217.

Dumètre, A., Dardé, M. L., Dumetre, A. and Darde, M. L. (2003). How to Detect *Toxoplasma Gondii* Oocysts in Environmental Samples? FEMS Microbiology Reviews **27**(5): 651-661.

Dumètre, A., Dubey, J. P., Ferguson, D. J. P., Bongrand, P., Azas, N. and Puech, P.-H. (2013). Mechanics of the *Toxoplasma Gondii* Oocyst Wall. Proceedings of the National Academy of Sciences of the United States of America **110**(28): 11535-11540.

Dumetre, A., Le Bras, C., Baffet, M., Meneceur, P., Dubey, J. P., Derouin, F., Duguet, J. P., Joyeux, M. and Moulin, L. (2008). Effects of Ozone and Ultraviolet Radiation Treatments on the Infectivity of *Toxoplasma Gondii* Oocysts. Vet Parasitol **153**(3-4): 209-213.

Dunker, A. K., Babu, M. M., Barbar, E., Blackledge, M., Bondos, S. E., Dosztányi, Z., Dyson, H. J., Forman-Kay, J., Fuxreiter, M., Gsponer, J., Han, K.-H., Jones, D. T., Longhi, S., Metallo, S. J., Nishikawa, K., Nussinov, R., Obradovic, Z., Pappu, R. V., Rost, B., Selenko, P., Subramaniam, V., Sussman, J. L., Tompa, P. and Uversky, V. N. (2013). What's in a Name? Why These Proteins Are Intrinsically Disordered: Why These Proteins Are Intrinsically Disordered. Intrinsically Disord Proteins **1**(1): e24157-e24157.

Dunker, A. K., Brown, C. J., Lawson, J. D., Iakoucheva, L. M. and Obradović, Z. (2002). Intrinsic Disorder and Protein Function. Biochemistry **41**(21): 6573-6582.

Dure, L., Greenway, S. C. and Galau, G. A. (1981). Developmental Biochemistry of Cottonseed Embryogenesis and Germination: Changing Messenger Ribonucleic Acid Populations as Shown by in Vitro and in Vivo Protein Synthesis. Biochemistry **20**(14): 4162-4168.

Duszynski, D. W. and Gardner, S. L. (1991). Fixing Coccidian Oocysts Is Not an Adequate Solution to the Problem of Preserving Protozoan Type Material. J Parasitol **77**(1): 52-57.

Edelhofer, R. and Aspöck, H. (1996). Infektionsquellen Und Infektionswege Aus Der Sicht Des Toxoplasmose-Screenings Der Schwangeren in Österreich. Mitt Osterr Ges Tropenmed Parasitol **18**: 59-70.

El-Nawawi, F., Tawfik, M. and Shaapan, R. (2008). Methods for Inactivation of *Toxoplasma Gondii* Cysts in Meat and Tissues of Experimentally Infected Sheep. Foodborne pathogens and disease **5**: 687-690.

Erlich, H. A., Rodgers, G., Vaillancourt, P., Araujo, F. G. and Remington, J. S. (1983). Identification of an Antigen-Specific Immunoglobulin M Antibody Associated with Acute *Toxoplasma* Infection. Infection and immunity **41**(2): 683-690.

Evans, M., Singh, D., Trappet, P. and Nagle, T. (2005). Investigations into the Effect of Feeding Laying Hens Complete Diets with Wheat in Whole or Ground Form and Zeolite Presented in Powdered or Grit Form, on Performance and Oocyst Output after Being Challenged with Coccidiosis. Proceedings of the 17th Australian Poultry Science Symposium, Sydney, New South Wales, Australia, 7-9 February 2005, Poultry Research Foundation.

Ezemaduka, A. N., Yu, J., Shi, X., Zhang, K., Yin, C.-C., Fu, X. and Chang, Z. (2014). A Small Heat Shock Protein Enables *Escherichia Coli* to Grow at a Lethal Temperature of 50°C

Conceivably by Maintaining Cell Envelope Integrity. Journal of bacteriology **196**(11): 2004-2011.

Fabian, B. T., Hedar, F., Koethe, M., Bangoura, B., Maksimov, P., Conraths, F. J., Villena, I., Aubert, D., Seeber, F. and Schares, G. (2020). Fluorescent Bead-Based Serological Detection of *Toxoplasma Gondii* Infection in Chickens. Parasites & Vectors **13**(1): 388.

Feder, J. (1968). A Spectrophotometric Assay for Neutral Protease. Biochemical and Biophysical Research Communications **32**(2): 326-332.

Ferguson, D. J., Birch-Andersen, A., Siim, J. C. and Hutchison, W. M. (1982). Scanning Electron Microscopy of the Oocyst and Sporocyst of *Toxoplasma Gondii*. Acta Pathol Microbiol Immunol Scand B **90**(4): 269-272.

Ferguson, D. J., Hutchison, W. M. and Siim, J. C. (1975). The Ultrastructural Development of the Macrogamete and Formation of the Oocyst Wall of *Toxoplasma Gondii*. Acta Pathol Microbiol Scand B **83**(5): 491-505.

Ferguson, D. J. P., Birch-Andersen, A., Siim, J. C. and Hutchison, W. M. (1979). Ultrastructural Studies on the Sporulation of Oocysts of *Toxoplasma Gondii* Ii. Formation of the Sporocyst and Structure of the Sporocyst Wall. Acta Pathologica Microbiologica Scandinavica Section B Microbiology **87B**(1-6): 183-190.

Fischer, E. (1894). Einfluss Der Configuration Auf Die Wirkung Der Enzyme. Berichte der deutschen chemischen Gesellschaft **27**(3): 2985-2993.

Fonin, A. V., Darling, A. L., Kuznetsova, I. M., Turoverov, K. K. and Uversky, V. N. (2019). Multi-Functionality of Proteins Involved in Gpcr and G Protein Signaling: Making Sense of Structure–Function Continuum with Intrinsic Disorder-Based Proteoforms. Cellular and Molecular Life Sciences **76**(22): 4461-4492.

Fontana, A., de Laureto, P. P., Spolaore, B. and Frare, E. (2012). Identifying Disordered Regions in Proteins by Limited Proteolysis. Methods Mol Biol **896**: 297-318.

Fontana, A., de Laureto, P. P., Spolaore, B., Frare, E., Picotti, P. and Zambonin, M. (2004). Probing Protein Structure by Limited Proteolysis. Acta Biochim Pol **51**(2): 299-321.

Fontana, A., Polverino de Laureto, P., De Filippis, V., Scaramella, E. and Zambonin, M. (1997). Probing the Partly Folded States of Proteins by Limited Proteolysis. Folding and Design **2**(2): R17-R26.

Frenkel, J. K. (1981). False-Negative Serologic Tests for *Toxoplasma* in Birds. J Parasitol **67**(6): 952-953.

Frenkel, J. K. and Dubey, J. P. (1973). Effects of Freezing on the Viability of *Toxoplasma* Oocysts. J Parasitol **59**(3): 587-588.

Freppel, W., Ferguson, D. J. P., Shapiro, K., Dubey, J. P., Puech, P.-H. and Dumètre, A. (2019). Structure, Composition, and Roles of the *Toxoplasma Gondii* Oocyst and Sporocyst Walls. The Cell Surface **5**: 100016.

Freppel, W., Puech, P.-H., Ferguson, D. J. P., Azas, N., Dubey, J. P. and Dumètre, A. (2016). Macrophages Facilitate the Excystation and Differentiation of *Toxoplasma Gondii* Sporozoites into Tachyzoites Following Oocyst Internalisation. Scientific Reports **6**: 33654-33654.

Frey, S. E., Harrison, C., Pass, R. F., Yang, E., Boken, D., Sekulovich, R. E., Percell, S., Izu, A. E., Hirabayashi, S., Burke, R. L. and Duliège, A.-M. (1999). Effects of Antigen Dose and

Immunization Regimens on Antibody Responses to a Cytomegalovirus Glycoprotein B Subunit Vaccine. The Journal of Infectious Diseases **180**(5): 1700-1703.

Freyre, A. and Falcón, J. (2004). Massive Excystation of *Toxoplasma Gondii* Sporozoites. Experimental Parasitology **107**(1): 72-77.

Fridy, P. C., Li, Y., Keegan, S., Thompson, M. K., Nudelman, I., Scheid, J. F., Oeffinger, M., Nussenzweig, M. C., Fenyo, D., Chait, B. T. and Rout, M. P. (2014). A Robust Pipeline for Rapid Production of Versatile Nanobody Repertoires. Nat Methods **11**(12): 1253-1260.

Fritz, H., Barr, B., Packham, A., Melli, A. and Conrad, P. A. A. (2012). Methods to Produce and Safely Work with Large Numbers of *Toxoplasma Gondii* Oocysts and Bradyzoite Cysts. Journal of Microbiological Methods **88**(1): 47-52.

Fritz, H. M., Bowyer, P. W., Bogyo, M., Conrad, P. A. and Boothroyd, J. C. (2012). Proteomic Analysis of Fractionated *Toxoplasma* Oocysts Reveals Clues to Their Environmental Resistance. PLoS One **7**(1): e29955-e29955.

Fritz, H. M., Buchholz, K. R., Chen, X., Durbin-Johnson, B., Rocke, D. M., Conrad, P. A. and Boothroyd, J. C. (2012). Transcriptomic Analysis of *Toxoplasma* Development Reveals Many Novel Functions and Structures Specific to Sporozoites and Oocysts. PLoS One **7**(2): e29998-e29998.

Frölich, S. and Wallach, M. (2015). F-Actin Distribution and Function During Sexual Development in *Eimeria Maxima*. Parasitology **142**(7): 855-864.

Fuller, A. L. and McDougald, L. R. (2002). Lectin-Binding by Sporozoites of *Eimeria Tenella*. Parasitol Res **88**(2): 118-125.

Furuki, T. and Sakurai, M. (2014). Group 3 Lea Protein Model Peptides Protect Liposomes During Desiccation. Biochimica et Biophysica Acta (BBA) - Biomembranes **1838**(11): 2757-2766.

Gabellieri, E. and Strambini, G. B. (2003). Perturbation of Protein Tertiary Structure in Frozen Solutions Revealed by 1-Anilino-8-Naphthalene Sulfonate Fluorescence. Biophysical journal **85**(5): 3214-3220.

Gal, T. Z., Glazer, I. and Koltai, H. (2004). An Lea Group 3 Family Member Is Involved in Survival of *C. Elegans* During Exposure to Stress. FEBS Letters **577**(1-2): 21-26.

Galau, G. A., Hughes, D. W. and Dure, L. (1986). Abscisic Acid Induction of Cloned Cotton Late Embryogenesis-Abundant (Lea) Mrnas. Plant Molecular Biology **7**(3): 155-170.

Gao, J. and Lan, T. (2016). Functional Characterization of the Late Embryogenesis Abundant (Lea) Protein Gene Family from *Pinus Tabuliformis* (Pinaceae) in *Escherichia Coli*. Scientific reports **6**: 19467-19467.

Garay-Arroyo, A., Colmenero-Flores, J. M., Garciarrubio, A. and Covarrubias, A. A. (2000). Highly Hydrophilic Proteins in Prokaryotes and Eukaryotes Are Common During Conditions of Water Deficit. The Journal of biological chemistry **275**(8): 5668-5674.

Gauthier, J. D., Jenkins, J. A. and La Peyre, J. F. (2004). Flow Cytometric Analysis of Lectin Binding to in Vitro-Cultured *Perkinsus Marinus* Surface Carbohydrates. J Parasitol **90**(3): 446-454.

Gionfriddo, J. P. and Best, L. B. (1999). Grit Use by Birds. Current Ornithology. V. Nolan, E. D. Ketterson and C. F. Thompson. Boston, MA, Springer US**:** 89-148.

Goodridge, H. S., Reyes, C. N., Becker, C. A., Katsumoto, T. R., Ma, J., Wolf, A. J., Bose, N., Chan, A. S., Magee, A. S., Danielson, M. E., Weiss, A., Vasilakos, J. P. and Underhill, D. M. (2011). Activation of the Innate Immune Receptor Dectin-1 Upon Formation of a 'Phagocytic Synapse'. Nature **472**(7344): 471-475.

Goyal, K., Tisi, L., Basran, A., Browne, J., Burnell, A., Zurdo, J. and Tunnacliffe, A. (2003). Transition from Natively Unfolded to Folded State Induced by Desiccation in an Anhydrobiotic Nematode Protein. J Biol Chem **278**(15): 12977-12984.

Goyal, K., Walton, L. J. and Tunnacliffe, A. (2005). Lea Proteins Prevent Protein Aggregation Due to Water Stress. The Biochemical journal **388**(Pt 1): 151-157.

Graham, H., Chandler, D. J. and Dunbar, S. A. (2019). The Genesis and Evolution of Bead-Based Multiplexing. Methods **158**: 2-11.

Gregg, B., Taylor, B. C., John, B., Tait-Wojno, E. D., Girgis, N. M., Miller, N., Wagage, S., Roos, D. S. and Hunter, C. A. (2013). Replication and Distribution of *Toxoplasma Gondii* in the Small Intestine after Oral Infection with Tissue Cysts. Infect Immun **81**(5): 1635-1643.

Griffin, S. M., Chen, I. M., Fout, G. S., Wade, T. J. and Egorov, A. I. (2011). Development of a Multiplex Microsphere Immunoassay for the Quantitation of Salivary Antibody Responses to Selected Waterborne Pathogens. J Immunol Methods **364**(1-2): 83-93.

Gross, U., Holpert, M. and Goebel, S. (2004). Impact of Stage Differentiation on Diagnosis of Toxoplasmosis. Ann Ist Super Sanita **40**(1): 65-70.

Gupta, A., Dixit, S. K. and Senthil-Kumar, M. (2016). Drought Stress Predominantly Endures *Arabidopsis Thaliana* to *Pseudomonas Syringae* Infection. Front Plant Sci **7**(808).

Guy, A. J., Irani, V., MacRaild, C. A., Anders, R. F., Norton, R. S., Beeson, J. G., Richards, J. S. and Ramsland, P. A. (2015). Insights into the Immunological Properties of Intrinsically Disordered Malaria Proteins Using Proteome Scale Predictions. PLoS One **10**(10): e0141729.

Hachim, A., Kavian, N., Cohen, C. A., Chin, A. W. H., Chu, D. K. W., Mok, C. K. P., Tsang, O. T. Y., Yeung, Y. C., Perera, R. A. P. M., Poon, L. L. M., Peiris, J. S. M. and Valkenburg, S. A. (2020). Orf8 and Orf3b Antibodies Are Accurate Serological Markers of Early and Late Sars-Cov-2 Infection. Nature Immunology **21**(10): 1293-1301.

Hamdi, K., Salladini, E., O'Brien, D. P., Brier, S., Chenal, A., Yacoubi, I. and Longhi, S. (2017). Structural Disorder and Induced Folding within Two Cereal, Aba Stress and Ripening (Asr) Proteins. Scientific Reports **7**(1): 15544.

Hamers-Casterman, C., Atarhouch, T., Muyldermans, S., Robinson, G., Hammers, C., Songa, E. B., Bendahman, N. and Hammers, R. (1993). Naturally Occurring Antibodies Devoid of Light Chains. Nature **363**(6428): 446-448.

Hanc, P., Fujii, T., Iborra, S., Yamada, Y., Huotari, J., Schulz, O., Ahrens, S., Kjaer, S., Way, M., Sancho, D., Namba, K. and Reis e Sousa, C. (2015). Structure of the Complex of F-Actin and Dngr-1, a C-Type Lectin Receptor Involved in Dendritic Cell Cross-Presentation of Dead Cell-Associated Antigens. Immunity **42**(5): 839-849.

Handel, A., Li, Y., McKay, B., Pawelek, K. A., Zarnitsyna, V. and Antia, R. (2018). Exploring the Impact of Inoculum Dose on Host Immunity and Morbidity to Inform Model-Based Vaccine Design. PLOS Computational Biology **14**(10): e1006505.

Harb, O. S. and Roos, D. S. (2020). Toxodb: Functional Genomics Resource for *Toxoplasma* and Related Organisms. Methods Mol Biol **2071**: 27-47.

Harito, J. B., Campbell, A. T., Prestrud, K. W., Dubey, J. P. and Robertson, L. J. (2016). Surface Binding Properties of Aged and Fresh (Recently Excreted) *Toxoplasma Gondii* Oocysts. Exp Parasitol **165**: 88-94.

Harito, J. B., Campbell, A. T., Tysnes, K. R., Dubey, J. P. and Robertson, L. J. (2017). Lectin-Magnetic Separation (Lms) for Isolation of *Toxoplasma Gondii* Oocysts from Concentrated Water Samples Prior to Detection by Microscopy or Qpcr. Water Res **114**: 228-236.

Harito, J. B., Campbell, A. T., Tysnes, K. R. and Robertson, L. J. (2017). Use of Lectin-Magnetic Separation (Lms) for Detecting *Toxoplasma Gondii* Oocysts in Environmental Water Samples. Water Research **127**: 68-76.

Hartsough, D. S. and Merz, K. M. (1992). Protein Flexibility in Aqueous and Nonaqueous Solutions. Journal of the American Chemical Society **114**(26): 10113-10116.

Hatanaka, R., Hagiwara-Komoda, Y., Furuki, T., Kanamori, Y., Fujita, M., Cornette, R., Sakurai, M., Okuda, T. and Kikawada, T. (2013). An Abundant Lea Protein in the Anhydrobiotic Midge, Pvlea4, Acts as a Molecular Shield by Limiting Growth of Aggregating Protein Particles. Insect Biochemistry and Molecular Biology **43**(11): 1055-1067.

Hatos, A., Hajdu-Soltész, B., Monzon, A. M., Palopoli, N., Álvarez, L., Aykac-Fas, B., Bassot, C., Benítez, G. I., Bevilacqua, M., Chasapi, A., Chemes, L., Davey, N. E., Davidović, R., Dunker, A. K., Elofsson, A., Gobeill, J., Foutel, N. S. G., Sudha, G., Guharoy, M., Horvath, T., Iglesias, V., Kajava, A. V., Kovacs, O. P., Lamb, J., Lambrughi, M., Lazar, T., Leclercq, J. Y., Leonardi, E., Macedo-Ribeiro, S., Macossay-Castillo, M., Maiani, E., Manso, J. A., Marino-Buslje, C., Martínez-Pérez, E., Mészáros, B., Mičetić, I., Minervini, G., Murvai, N., Necci, M., Ouzounis, C. A., Pajkos, M., Paladin, L., Pancsa, R., Papaleo, E., Parisi, G., Pasche, E., Barbosa Pereira, P. J., Promponas, V. J., Pujols, J., Quaglia, F., Ruch, P., Salvatore, M., Schad, E., Szabo, B., Szaniszló, T., Tamana, S., Tantos, A., Veljkovic, N., Ventura, S., Vranken, W., Dosztányi, Z., Tompa, P., Tosatto, S. C. E. and Piovesan, D. (2020). Disprot: Intrinsic Protein Disorder Annotation in 2020. Nucleic Acids Res **48**(D1): D269-d276.

Havakhah, Y., Esmaeili Rastaghi, A. R., Amiri, S., Babaie, J., Aghighi, Z. and Golkar, M. (2014). Prevalence of *Toxoplasma Gondii* in Sheep and Goats in Three Counties of Gilan Province, North of Iran the More Humid Climate the Higher Prevalence. Journal of Medical Microbiology and Infectious Diseases **2**(2): 80-83.

He, B., Wang, K., Liu, Y., Xue, B., Uversky, V. N. and Dunker, A. K. (2009). Predicting Intrinsic Disorder in Proteins: An Overview. Cell Research **19**(8): 929-949.

Heinrikson, R. L. (1977). [20] Applications of Thermolysin in Protein Structural Analysis. Methods in Enzymology, Academic Press. **47:** 175-189.

Herwaldt, B. L. (2001). Laboratory-Acquired Parasitic Infections from Accidental Exposures. Clin Microbiol Rev **14**(4): 659-688.

Hill, D., Coss, C., Dubey, J. P., Wroblewski, K., Sautter, M., Hosten, T., Muñoz-Zanzi, C., Mui, E., Withers, S., Boyer, K., Hermes, G., Coyne, J., Jagdis, F., Burnett, A., McLeod, P., Morton, H., Robinson, D., McLeod, R. and Group, T. S. (2011). Identification of a Sporozoite-Specific Antigen from *Toxoplasma Gondii*. Journal of Parasitology **97**(2): 328-337.

Hincha, D. K. and Thalhammer, A. (2012). Lea Proteins: Idps with Versatile Functions in Cellular Dehydration Tolerance. Biochemical Society transactions **40**(5): 1000-1003.

Ho, C. L. (2015). Phylogeny of Algal Sequences Encoding Carbohydrate Sulfotransferases, Formylglycine-Dependent Sulfatases, and Putative Sulfatase Modifying Factors. Front Plant Sci **6**: 1057.

Hoetelmans, R. W., Prins, F. A., Cornelese-ten Velde, I., van der Meer, J., van de Velde, C. J. and van Dierendonck, J. H. (2001). Effects of Acetone, Methanol, or Paraformaldehyde on Cellular Structure, Visualized by Reflection Contrast Microscopy and Transmission and Scanning Electron Microscopy. Applied immunohistochemistry & molecular morphology : AIMM **9**(4): 346-351.

Hofhuis, A., van Pelt, W., van Duynhoven, Y. T., Nijhuis, C. D., Mollema, L., van der Klis, F. R., Havelaar, A. H. and Kortbeek, L. M. (2011). Decreased Prevalence and Age-Specific Risk Factors for *Toxoplasma Gondii* Igg Antibodies in the Netherlands between 1995/1996 and 2006/2007. Epidemiol Infect **139**(4): 530-538.

Holehouse, A. S., Ahad, J., Das, R. K. and Pappu, R. V. (2015). Cider: Classification of Intrinsically Disordered Ensemble Regions. Biophysical Journal **108**(2): 228a.

Hong, H. Y., Yoo, G. S. and Choi, J. K. (2000). Direct Blue 71 Staining of Proteins Bound to Blotting Membranes. Electrophoresis **21**(5): 841-845.

Honjoh, K.-i., Matsumoto, H., Shimizu, H., Ooyama, K., Tanaka, K., Oda, Y., Takata, R., Joh, T., Suga, K., Miyamoto, T., Iio, M. and Hatano, S. (2000). Cryoprotective Activities of Group 3 Late Embryogenesis Abundant Proteins from *Chlorella Vulgaris* C-27. Bioscience, Biotechnology, and Biochemistry **64**(8): 1656-1663.

Huang, J., Xu, Z., Wang, D., Ogata, C. M., Palczewski, K., Lee, X. and Young, N. M. (2010). Characterization of the Secondary Binding Sites of *Maclura Pomifera* Agglutinin by Glycan Array and Crystallographic Analyses. Glycobiology **20**(12): 1643-1653.

Hundertmark, M. and Hincha, D. K. (2008). Lea (Late Embryogenesis Abundant) Proteins and Their Encoding Genes in *Arabidopsis Thaliana*. BMC genomics **9**: 118-118.

Hunt, N. C. and Grover, L. M. (2010). Cell Encapsulation Using Biopolymer Gels for Regenerative Medicine. Biotechnology letters **32**(6): 733-742.

Hutchison, W. (1965). Experimental Transmission of *Toxoplasma Gondii*. Nature **206**(4987): 961-962.

Inoue, H., Nojima, H. and Okayama, H. (1990). High Efficiency Transformation of *Escherichia Coli* with Plasmids. Gene **96**(1): 23-28.

Ito, S., Tsunoda, K., Shimada, K., Taki, T. and Matsui, T. (1975). Disinfectant Effects of Several Chemicals against *Toxoplasma* Oocysts. Nihon Juigaku Zasshi **37**(3): 229-234.

Iturriaga, G. (2008). The Lea Proteins and Trehalose Loving Couple: A Step Forward in Anhydrobiotic Engineering. The Biochemical journal **410**(2): e1-2.

Jackson, M. H. and Hutchison, W. M. (1989). The Prevalence and Source of *Toxoplasma* Infection in the Environment. Adv Parasitol **28**: 55-105.

Jani, I. V., Janossy, G., Brown, D. W. and Mandy, F. (2002). Multiplexed Immunoassays by Flow Cytometry for Diagnosis and Surveillance of Infectious Diseases in Resource-Poor Settings. Lancet Infect Dis **2**(4): 243-250.

Jaspard, E., Macherel, D. and Hunault, G. (2012). Computational and Statistical Analyses of Amino Acid Usage and Physico-Chemical Properties of the Twelve Late Embryogenesis Abundant Protein Classes. PLOS ONE **7**(5): e36968.

Jones, J. L. and Dubey, J. P. (2010). Waterborne Toxoplasmosis – Recent Developments. Experimental Parasitology **124**(1): 10-25.

Kalani, H., Daryani, A., Sharif, M., Ahmadpour, E., Alizadeh, A., Nasrolahei, M., Sarvi, S., Kalani, F. and Faridnia, R. (2016). Comparison of Eight Cell-Free Media for Maintenance of *Toxoplasma Gondii* Tachyzoites. Iran J Parasitol **11**(1): 104-109.

Kalthoff, C. (2003). A Novel Strategy for the Purification of Recombinantly Expressed Unstructured Protein Domains. **786**: 247-254.

Kanbara, A., Hakoda, M. and Seyama, I. (2010). Urine Alkalization Facilitates Uric Acid Excretion. Nutr J **9**: 45-45.

Kaneto, C. N., Costa, A. J., Paulillo, A. C., Moraes, F. R., Murakami, T. O. and Meireles, M. V. (1997). Experimental Toxoplasmosis in Broiler Chicks. Vet Parasitol **69**(3-4): 203-210.

Kavanagh, K. L., Elling, R. A. and Wilson, D. K. (2004). Structure of *Toxoplasma Gondii* Ldh1: Active-Site Differences from Human Lactate Dehydrogenases and the Structural Basis for Efficient Apad+ Use. Biochemistry **43**(4): 879-889.

Kelsall, B. L. (2020). Chapter 3 - Mucosal Antigen Sampling across the Villus Epithelium by Epithelial and Myeloid Cells. Mucosal Vaccines (Second Edition). H. Kiyono and D. W. Pascual, Academic Press**:** 55-69.

Kerkhof, K., Sluydts, V., Willen, L., Kim, S., Canier, L., Heng, S., Tsuboi, T., Sochantha, T., Sovannaroth, S., Ménard, D., Coosemans, M. and Durnez, L. (2016). Serological Markers to Measure Recent Changes in Malaria at Population Level in Cambodia. Malaria Journal **15**(1): 529.

Kerrigan, A. M., Dennehy, K. M., Mourao-Sa, D., Faro-Trindade, I., Willment, J. A., Taylor, P. R., Eble, J. A., Reis e Sousa, C. and Brown, G. D. (2009). Clec-2 Is a Phagocytic Activation Receptor Expressed on Murine Peripheral Blood Neutrophils. J Immunol **182**(7): 4150-4157.

Kinoshita, T. (2016). Glycosylphosphatidylinositol (Gpi) Anchors: Biochemistry and Cell Biology: Introduction to a Thematic Review Series. J Lipid Res **57**(1): 4-5.

Klein, S., Stern, D. and Seeber, F. (2020). Expression of in Vivo Biotinylated Recombinant Antigens Sag1 and Sag2a from *Toxoplasma Gondii* for Improved Seroepidemiological Bead-Based Multiplex Assays. BMC biotechnology **20**(1): 53.

Kolter, J., Feuerstein, R., Zeis, P., Hagemeyer, N., Paterson, N., d'Errico, P., Baasch, S., Amann, L., Masuda, T., Losslein, A., Gharun, K., Meyer-Luehmann, M., Waskow, C., Franzke, C. W., Grun, D., Lammermann, T., Prinz, M. and Henneke, P. (2019). A Subset of Skin Macrophages Contributes to the Surveillance and Regeneration of Local Nerves. Immunity **50**(6): 1482-1497.e1487.

Konno, T., Tanaka, N., Kataoka, M., Takano, E. and Maki, M. (1997). A Circular Dichroism Study of Preferential Hydration and Alcohol Effects on a Denatured Protein, Pig Calpastatin Domain I. Biochimica et Biophysica Acta (BBA) - Protein Structure and Molecular Enzymology **1342**(1): 73-82.

Kovacs, D. and Tompa, P. (2012). Diverse Functional Manifestations of Intrinsic Structural Disorder in Molecular Chaperones. Biochem Soc Trans **40**(5): 963-968.

Krings, A., Jacob, J., Seeber, F., Pleyer, U., Walker, J., Stark, K. and Wilking, H. (2021). Estimates of Toxoplasmosis Incidence Based on Healthcare Claims Data, Germany, 2011–2016. Emerging Infectious Disease journal **27**(8): 2097.

Krishnarjuna, B., Sugiki, T., Morales, R. A. V., Seow, J., Fujiwara, T., Wilde, K. L., Norton, R. S. and MacRaild, C. A. (2018). Transient Antibody-Antigen Interactions Mediate the Strain-Specific Recognition of a Conserved Malaria Epitope. Communications Biology **1**(1): 58.

Kurth, M. and Entzeroth, R. (2008). Improved Excystation Protocol for *Eimeria Nieschulzi* (Apikomplexa, Coccidia). Parasitol Res **102**(4): 819-822.

Kuticic, V. and Wikerhauser, T. (1996). Studies of the Effect of Various Treatments on the Viability of *Toxoplasma Gondii* Tissue Cysts and Oocysts. Curr Top Microbiol Immunol **219**: 261-265.

Kwong, P. D., Doyle, M. L., Casper, D. J., Cicala, C., Leavitt, S. A., Majeed, S., Steenbeke, T. D., Venturi, M., Chaiken, I., Fung, M., Katinger, H., Parren, P. W., Robinson, J., Van Ryk, D., Wang, L., Burton, D. R., Freire, E., Wyatt, R., Sodroski, J., Hendrickson, W. A. and Arthos, J. (2002). Hiv-1 Evades Antibody-Mediated Neutralization through Conformational Masking of Receptor-Binding Sites. Nature **420**(6916): 678-682.

Kyte, J. and Doolittle, R. F. (1982). A Simple Method for Displaying the Hydropathic Character of a Protein. Journal of Molecular Biology **157**(1): 105-132.

Lass, A., Ma, L., Kontogeorgos, I., Zhang, X., Li, X. and Karanis, P. (2019). First Molecular Detection of *Toxoplasma Gondii* in Vegetable Samples in China Using Qualitative, Quantitative Real-Time Pcr and Multilocus Genotyping. Scientific Reports **9**(1): 17581.

Lathe, G. H. and Ruthven, C. R. (1955). The Separation of Substances on the Basis of Their Molecular Weights, Using Columns of Starch and Water. Biochem J **60**(4): xxxiv.

Lee, J. M. and Sonnhammer, E. L. L. (2003). Genomic Gene Clustering Analysis of Pathways in Eukaryotes. Genome Res **13**(5): 875-882.

Lee, X., Thompson, A., Zhang, Z., Ton-that, H., Biesterfeldt, J., Ogata, C., Xu, L., Johnston, R. A. Z. and Young, N. M. (1998). Structure of the Complex of *Maclura Pomifera* Agglutinin and the T-Antigen Disaccharide, Galβ1,3galnac *. Journal of Biological Chemistry **273**(11): 6312-6318.

Lekutis, C., Ferguson, D. J., Grigg, M. E., Camps, M. and Boothroyd, J. C. (2001). Surface Antigens of *Toxoplasma Gondii*: Variations on a Theme. Int J Parasitol **31**(12): 1285-1292.

Lélu, M., Villena, I., Dardé, M.-L., Aubert, D., Geers, R., Dupuis, E., Marnef, F., Poulle, M.-L., Gotteland, C., Dumètre, A. and Gilot-Fromont, E. (2012). Quantitative Estimation of the Viability of *Toxoplasma Gondii* Oocysts in Soil. Applied and environmental microbiology **78**(15): 5127-5132.

Li, S., Chakraborty, N., Borcar, A., Menze, M. A., Toner, M. and Hand, S. C. (2012). Late Embryogenesis Abundant Proteins Protect Human Hepatoma Cells During Acute Desiccation. Proc Natl Acad Sci U S A **109**(51): 20859-20864.

Lima-Junior, D. S., Mineo, T. W. P., Calich, V. L. G. and Zamboni, D. S. (2017). Dectin-1 Activation During *Leishmania Amazonensis* Phagocytosis Prompts Syk-Dependent Reactive

Oxygen Species Production to Trigger Inflammasome Assembly and Restriction of Parasite Replication. J Immunol **199**(6): 2055-2068.

Lindsay, D. S. and Dubey, J. P. (2009). Long-Term Survival of *Toxoplasma Gondii* Sporulated Oocysts in Seawater. J Parasitol **95**(4): 1019-1020.

Lindsay, D. S., Dubey, J. P., Blagburn, B. L. and Toivio-Kinnucan, M. (1991). Examination of Tissue Cyst Formation by *Toxoplasma Gondii* in Cell Cultures Using Bradyzoites, Tachyzoites, and Sporozoites. J Parasitol **77**(1): 126-132.

Lindsay, D. S. and Todd, K. S. (1993). Chapter 2 - Coccidia of Mammals. Parasitic Protozoa (Second Edition). J. P. Kreier. San Diego, Academic Press**:** 89-131.

Liu, X.-Y., Wang, Z.-D., El-Ashram, S. and Liu, Q. (2019). *Toxoplasma Gondii* Oocyst-Driven Infection in Pigs, Chickens and Humans in Northeastern China. BMC Veterinary Research **15**(1): 366.

Liu, Y., Wang, L., Xing, X., Sun, L., Pan, J., Kong, X., Zhang, M. and Li, D. (2013). Zmlea3, a Multifunctional Group 3 Lea Protein from Maize (*Zea Mays* L.), Is Involved in Biotic and Abiotic Stresses. Plant and Cell Physiology **54**(6): 944-959.

Lund, H., Pieber, M., Parsa, R., Han, J., Grommisch, D., Ewing, E., Kular, L., Needhamsen, M., Espinosa, A., Nilsson, E., Overby, A. K., Butovsky, O., Jagodic, M., Zhang, X. M. and Harris, R. A. (2018). Competitive Repopulation of an Empty Microglial Niche Yields Functionally Distinct Subsets of Microglia-Like Cells. Nature communications **9**(1): 4845.

Luo, P. and Baldwin, R. L. (1997). Mechanism of Helix Induction by Trifluoroethanol: A Framework for Extrapolating the Helix-Forming Properties of Peptides from Trifluoroethanol/Water Mixtures Back to Water. Biochemistry **36**(27): 8413-8421.

MacRaild, C. A., Anders, R. F., Foley, M. and Norton, R. S. (2011). Apical Membrane Antigen 1 as an Anti-Malarial Drug Target. Curr Top Med Chem **11**(16): 2039-2047.

MacRaild, C. A., Richards, J. S., Anders, R. F. and Norton, R. S. (2016). Antibody Recognition of Disordered Antigens. Structure **24**(1): 148-157.

MacRaild, C. A., Seow, J., Das, S. C. and Norton, R. S. (2018). Disordered Epitopes as Peptide Vaccines. Pept Sci (Hoboken) **110**(3): e24067-e24067.

Maglinao, M., Eriksson, M., Schlegel, M. K., Zimmermann, S., Johannssen, T., Götze, S., Seeberger, P. H. and Lepenies, B. (2014). A Platform to Screen for C-Type Lectin Receptor-Binding Carbohydrates and Their Potential for Cell-Specific Targeting and Immune Modulation. Journal of Controlled Release **175**(1): 36-42.

Mai, K., Sharman, P. A., Walker, R. A., Katrib, M., de Souza, D., McConville, M. J., Wallach, M. G., Belli, S. I., Ferguson, D. J. P. and Smith, N. C. (2009). Oocyst Wall Formation and Composition in Coccidian Parasites. Memorias do Instituto Oswaldo Cruz **104**(2): 281-289.

Man, A. L., Gicheva, N., Regoli, M., Rowley, G., De Cunto, G., Wellner, N., Bassity, E., Gulisano, M., Bertelli, E. and Nicoletti, C. (2017). Cx3cr1+ Cell-Mediated *Salmonella* Exclusion Protects the Intestinal Mucosa During the Initial Stage of Infection. J Immunol **198**(1): 335-343.

Mangiavacchi, B. M., Vieira, F. P., Bahia-Oliveira, L. M. G. and Hill, D. (2016). Salivary Iga against Sporozoite-Specific Embryogenesis-Related Protein (Tgerp) in the Study of Horizontally Transmitted Toxoplasmosis Via *T. Gondii* Oocysts in Endemic Settings. Epidemiology and Infection **144**(12): 2568-2577.

Marino, A. M. F., Giunta, R. P., Salvaggio, A., Castello, A., Alfonzetti, T., Barbagallo, A., Aparo, A., Scalzo, F., Reale, S., Buffolano, W. and Percipalle, M. (2019). *Toxoplasma Gondii* in Edible Fishes Captured in the Mediterranean Basin. Zoonoses and Public Health **0**(0).

Markwalter, C. F., Davis, K. M. and Wright, D. W. (2016). Immunomagnetic Capture and Colorimetric Detection of Malarial Biomarker *Plasmodium Falciparum* Lactate Dehydrogenase. Anal Biochem **493**: 30-34.

Marois, I., Cloutier, A., Garneau, É. and Richter, M. V. (2012). Initial Infectious Dose Dictates the Innate, Adaptive, and Memory Responses to Influenza in the Respiratory Tract. Journal of Leukocyte Biology **92**(1): 107-121.

Mayer, S., Moeller, R., Monteiro, J. T., Ellrott, K., Josenhans, C. and Lepenies, B. (2018). C-Type Lectin Receptor (Clr)-Fc Fusion Proteins as Tools to Screen for Novel Clr/Bacteria Interactions: An Exemplary Study on Preselected *Campylobacter Jejuni* Isolates. Front Immunol **9**: 213.

McMahon, C., Baier, A. S., Pascolutti, R., Wegrecki, M., Zheng, S., Ong, J. X., Erlandson, S. C., Hilger, D., Rasmussen, S. G. F., Ring, A. M., Manglik, A. and Kruse, A. C. (2018). Yeast Surface Display Platform for Rapid Discovery of Conformationally Selective Nanobodies. Nature Structural & Molecular Biology.

McMahon, C., Baier, A. S., Zheng, S., Pascolutti, R., Ong, J. X., Erlandson, S. C., Hilger, D., Ring, A. M., Manglik, A. and Kruse, A. C. (2017). Platform for Rapid Nanobody Discovery in Vitro. bioRxiv.

Metcalf, C. J., Farrar, J., Cutts, F. T., Basta, N. E., Graham, A. L., Lessler, J., Ferguson, N. M., Burke, D. S. and Grenfell, B. T. (2016). Use of Serological Surveys to Generate Key Insights into the Changing Global Landscape of Infectious Disease. Lancet **388**(10045): 728-730.

Milne, G., Webster, J. P. and Walker, M. (2020). Towards Improving Interventions against Toxoplasmosis by Identifying Routes of Transmission Using Sporozoite-Specific Serological Tools. Clin Infect Dis.

Mistry, J., Chuguransky, S., Williams, L., Qureshi, M., Salazar, Gustavo A., Sonnhammer, E. L. L., Tosatto, S. C. E., Paladin, L., Raj, S., Richardson, L. J., Finn, R. D. and Bateman, A. (2020). Pfam: The Protein Families Database in 2021. Nucleic Acids Research **49**(D1): D412-D419.

Montoya, J. G. and Liesenfeld, O. (2004). Toxoplasmosis. Lancet **363**(9425): 1965-1976.

Moreno-Hagelsieb, G., Treviño, V., Pérez-Rueda, E., Smith, T. F. and Collado-Vides, J. (2001). Transcription Unit Conservation in the Three Domains of Life: A Perspective from *Escherichia Coli*. Trends Genet **17**(4): 175-177.

Morita, N., Umemoto, E., Fujita, S., Hayashi, A., Kikuta, J., Kimura, I., Haneda, T., Imai, T., Inoue, A., Mimuro, H., Maeda, Y., Kayama, H., Okumura, R., Aoki, J., Okada, N., Kida, T., Ishii, M., Nabeshima, R. and Takeda, K. (2019). Gpr31-Dependent Dendrite Protrusion of Intestinal Cx3cr1(+) Cells by Bacterial Metabolites. Nature **566**(7742): 110-114.

Murphy, K. and Weaver, C. (2018). Janeway Immunologie, Springer-Verlag.

Muyldermans, S. (2013). Nanobodies: Natural Single-Domain Antibodies. Annu Rev Biochem **82**: 775-797.

Nagae, M., Morita-Matsumoto, K., Kato, M., Kaneko, M. K., Kato, Y. and Yamaguchi, Y. (2014). A Platform of C-Type Lectin-Like Receptor Clec-2 for Binding O-Glycosylated Podoplanin and Nonglycosylated Rhodocytin. Structure **22**(12): 1711-1721.

Nagaraju, M., Kumar, S. A., Reddy, P. S., Kumar, A., Rao, D. M. and Kavi Kishor, P. B. (2019). Genome-Scale Identification, Classification, and Tissue Specific Expression Analysis of Late Embryogenesis Abundant (Lea) Genes under Abiotic Stress Conditions in *Sorghum Bicolor* L. PloS one **14**(1): e0209980-e0209980.

Nakayama, K., Okawa, K., Kakizaki, T., Honma, T., Itoh, H. and Inaba, T. (2007). *Arabidopsis* Cor15am Is a Chloroplast Stromal Protein That Has Cryoprotective Activity and Forms Oligomers. Plant Physiology **144**(1): 513-523.

Naot, Y., Desmonts, G. and Remington, J. S. (1981). Igm Enzyme-Linked Immunosorbent Assay Test for the Diagnosis of Congenital *Toxoplasma* Infection. J Pediatr **98**(1): 32-36.

Naot, Y. and Remington, J. S. (1980). An Enzyme-Linked Immunosorbent Assay for Detection of Igm Antibodies to *Toxoplasma Gondii*: Use for Diagnosis of Acute Acquired Toxoplasmosis. J Infect Dis **142**(5): 757-766.

Ndao, O., Puech, P. H., Bérard, C., Limozin, L., Rabhi, S., Azas, N., Dubey, J. P. and Dumètre, A. (2020). Dynamics of *Toxoplasma Gondii* Oocyst Phagocytosis by Macrophages. Front Cell Infect Microbiol **10**: 207.

Necci, M., Piovesan, D., Hoque, M. T., Walsh, I., Iqbal, S., Vendruscolo, M., Sormanni, P., Wang, C., Raimondi, D., Sharma, R., Zhou, Y., Litfin, T., Galzitskaya, O. V., Lobanov, M. Y., Vranken, W., Wallner, B., Mirabello, C., Malhis, N., Dosztányi, Z., Erdős, G., Mészáros, B., Gao, J., Wang, K., Hu, G., Wu, Z., Sharma, A., Hanson, J., Paliwal, K., Callebaut, I., Bitard-Feildel, T., Orlando, G., Peng, Z., Xu, J., Wang, S., Jones, D. T., Cozzetto, D., Meng, F., Yan, J., Gsponer, J., Cheng, J., Wu, T., Kurgan, L., Promponas, V. J., Tamana, S., Marino-Buslje, C., Martínez-Pérez, E., Chasapi, A., Ouzounis, C., Dunker, A. K., Kajava, A. V., Leclercq, J. Y., Aykac-Fas, B., Lambrughi, M., Maiani, E., Papaleo, E., Chemes, L. B., Álvarez, L., González-Foutel, N. S., Iglesias, V., Pujols, J., Ventura, S., Palopoli, N., Benítez, G. I., Parisi, G., Bassot, C., Elofsson, A., Govindarajan, S., Lamb, J., Salvatore, M., Hatos, A., Monzon, A. M., Bevilacqua, M., Mičetić, I., Minervini, G., Paladin, L., Quaglia, F., Leonardi, E., Davey, N., Horvath, T., Kovacs, O. P., Murvai, N., Pancsa, R., Schad, E., Szabo, B., Tantos, A., Macedo-Ribeiro, S., Manso, J. A., Pereira, P. J. B., Davidović, R., Veljkovic, N., Hajdu-Soltész, B., Pajkos, M., Szaniszló, T., Guharoy, M., Lazar, T., Macossay-Castillo, M., Tompa, P., Tosatto, S. C. E., Predictors, C. and DisProt, C. (2021). Critical Assessment of Protein Intrinsic Disorder Prediction. Nature Methods **18**(5): 472-481.

Neumann, K., Castineiras-Vilarino, M., Hockendorf, U., Hannesschlager, N., Lemeer, S., Kupka, D., Meyermann, S., Lech, M., Anders, H. J., Kuster, B., Busch, D. H., Gewies, A., Naumann, R., Gross, O. and Ruland, J. (2014). Clec12a Is an Inhibitory Receptor for Uric Acid Crystals That Regulates Inflammation in Response to Cell Death. Immunity **40**(3): 389-399.

Nicolle, C. and Manceaux, L. H. (1908). On a Leishman Body Infection (or Related Organisms) of the Gondi. Int J Parasitol **39**(8): 863-864.

Nielsen, J. T. and Mulder, F. A. A. (2016). There Is Diversity in Disorder-"in All Chaos There Is a Cosmos, in All Disorder a Secret Order". Frontiers in molecular biosciences **3**: 4-4.

Nielsen, J. T. and Mulder, F. A. A. (2019). Quality and Bias of Protein Disorder Predictors. Scientific Reports **9**(1): 5137.

Nogareda, F., Le Strat, Y., Villena, I., De Valk, H. and Goulet, V. (2014). Incidence and Prevalence of *Toxoplasma Gondii* Infection in Women in France, 1980-2020: Model-Based Estimation. Epidemiol Infect **142**(8): 1661-1670.

Olvera-Carrillo, Y., Campos, F., Reyes, J. L., Garciarrubio, A. and Covarrubias, A. A. (2010). Functional Analysis of the Group 4 Late Embryogenesis Abundant Proteins Reveals Their Relevance in the Adaptive Response During Water Deficit in *Arabidopsis*. Plant Physiology **154**(1): 373-390.

Olvera-Carrillo, Y., Luis Reyes, J. and Covarrubias, A. A. (2011). Late Embryogenesis Abundant Proteins: Versatile Players in the Plant Adaptation to Water Limiting Environments. Plant Signal Behav **6**(4): 586-589.

Opsteegh, M., Kortbeek, T. M., Havelaar, A. H. and van der Giessen, J. W. B. (2014). Intervention Strategies to Reduce Human *Toxoplasma Gondii* Disease Burden. Clinical Infectious Diseases **60**(1): 101-107.

Pardon, E., Laeremans, T., Triest, S., Rasmussen, S. G. F., Wohlkönig, A., Ruf, A., Muyldermans, S., Hol, W. G. J., Kobilka, B. K., Steyaert, J., Wohlkonig, A., Ruf, A., Muyldermans, S., Hol, W. G. J., Kobilka, B. K. and Steyaert, J. (2014). A General Protocol for the Generation of Nanobodies for Structural Biology. Nature Protocols **9**(3): 674-693.

Park, H., Park, J.-Y., Park, K.-M. and Chang, P.-S. (2021). Effects of Freezing Rate on Structural Changes in L-Lactate Dehydrogenase During the Freezing Process. Scientific Reports **11**(1): 13643.

Peng, Z., Xue, B., Kurgan, L. and Uversky, V. N. (2013). Resilience of Death: Intrinsic Disorder in Proteins Involved in the Programmed Cell Death. Cell Death & Differentiation **20**(9): 1257-1267.

Pinto-Ferreira, F., Caldart, E. T., Pasquali, A. K. S., Mitsuka-Breganó, R., Freire, R. L. and Navarro, I. T. (2019). Patterns of Transmission and Sources of Infection in Outbreaks of Human Toxoplasmosis. Emerging infectious diseases **25**(12): 2177-2182.

Piovesan, D., Necci, M., Escobedo, N., Monzon, A. M., Hatos, A., Mičetić, I., Quaglia, F., Paladin, L., Ramasamy, P., Dosztányi, Z., Vranken, W. F., Davey, N. E., Parisi, G., Fuxreiter, M. and Tosatto, S. C. E. (2021). Mobidb: Intrinsically Disordered Proteins in 2021. Nucleic Acids Res **49**(D1): D361-d367.

Piva, L., Tetlak, P., Claser, C., Karjalainen, K., Renia, L. and Ruedl, C. (2012). Cutting Edge: Clec9a+ Dendritic Cells Mediate the Development of Experimental Cerebral Malaria. J Immunol **189**(3): 1128-1132.

Plato, A., Willment, J. A. and Brown, G. D. (2013). C-Type Lectin-Like Receptors of the Dectin-1 Cluster: Ligands and Signaling Pathways. Int Rev Immunol **32**(2): 134-156.

Pleyer, U., Groß, U., Schlüter, D., Wilking, H. and Seeber, F. (2019). Toxoplasmose in Deutschland. Dtsch Arztebl International **116**(25): 435-444.

Polverino de Laureto, P., De Filippis, V., Scaramella, E., Zambonin, M. and Fontana, A. (1995). Limited Proteolysis of Lysozyme in Trifluoroethanol. European journal of biochemistry **230**(2): 779-787.

Polverino de Laureto, P., Scaramella, E., Zambonin, M., Filippis, V. D. and Fontana, A. (1998). Limited Proteolysis of Proteins by Thermolysin in Trifluoroethanol. Progress in Biotechnology. A. Ballesteros, F. J. Plou, J. L. Iborra and P. J. Halling, Elsevier. **15:** 381-392.

Popelka, H. (2020). Chapter Seven - Dancing While Self-Eating: Protein Intrinsic Disorder in Autophagy. Progress in Molecular Biology and Translational Science. V. N. Uversky, Academic Press. **174:** 263-305.

Popova, A. V., Rausch, S., Hundertmark, M., Gibon, Y. and Hincha, D. K. (2015). The Intrinsically Disordered Protein Lea7 from *Arabidopsis Thaliana* Protects the Isolated Enzyme Lactate Dehydrogenase and Enzymes in a Soluble Leaf Proteome During Freezing and Drying. Biochimica et biophysica acta **1854**(10 Pt A): 1517-1525.

Possenti, A., Cherchi, S., Bertuccini, L., Pozio, E., Dubey, J. P. and Spano, F. (2010). Molecular Characterisation of a Novel Family of Cysteine-Rich Proteins of *Toxoplasma Gondii* and Ultrastructural Evidence of Oocyst Wall Localisation. International Journal for Parasitology **40**(14): 1639-1649.

Possenti, A., Fratini, F., Fantozzi, L., Pozio, E., Dubey, J. P., Ponzi, M., Pizzi, E. and Spano, F. (2013). Global Proteomic Analysis of the Oocyst/Sporozoite of *Toxoplasma Gondii* Reveals Commitment to a Host-Independent Lifestyle. BMC genomics **14**: 183-183.

Povey, J. F., Smales, C. M., Hassard, S. J. and Howard, M. J. (2007). Comparison of the Effects of 2,2,2-Trifluoroethanol on Peptide and Protein Structure and Function. J Struct Biol **157**(2): 329-338.

Priest, J. W., Jenks, M. H., Moss, D. M., Mao, B., Buth, S., Wannemuehler, K., Soeung, S. C., Lucchi, N. W., Udhayakumar, V., Gregory, C. J., Huy, R., Muth, S. and Lammie, P. J. (2016). Integration of Multiplex Bead Assays for Parasitic Diseases into a National, Population-Based Serosurvey of Women 15-39 Years of Age in Cambodia. PLOS Neglected Tropical Diseases **10**(5): e0004699.

Priest, J. W., Moss, D. M., Arnold, B. F., Hamlin, K., Jones, C. C. and Lammie, P. J. (2015). Seroepidemiology of *Toxoplasma* in a Coastal Region of Haiti: Multiplex Bead Assay Detection of Immunoglobulin G Antibodies That Recognize the Sag2a Antigen. Epidemiol Infect **143**(3): 618-630.

Proc, J. L., Kuzyk, M. A., Hardie, D. B., Yang, J., Smith, D. S., Jackson, A. M., Parker, C. E. and Borchers, C. H. (2010). A Quantitative Study of the Effects of Chaotropic Agents, Surfactants, and Solvents on the Digestion Efficiency of Human Plasma Proteins by Trypsin. Journal of proteome research **9**(10): 5422-5437.

Ratnakumar, S. and Tunnacliffe, A. (2006). Intracellular Trehalose Is Neither Necessary nor Sufficient for Desiccation Tolerance in Yeast. FEMS Yeast Research **6**(6): 902-913.

Raulf, M. K., Johannssen, T., Matthiesen, S., Neumann, K., Hachenberg, S., Mayer-Lambertz, S., Steinbeis, F., Hegermann, J., Seeberger, P. H., Baumgartner, W., Strube, C., Ruland, J. and Lepenies, B. (2019). The C-Type Lectin Receptor Clec12a Recognizes Plasmodial Hemozoin and Contributes to Cerebral Malaria Development. Cell Rep **28**(1): 30-38.e35.

Receveur-Brechot, V., Bourhis, J. M., Uversky, V. N., Canard, B. and Longhi, S. (2006). Assessing Protein Disorder and Induced Folding. Proteins **62**(1): 24-45.

Regoli, M., Bertelli, E., Gulisano, M. and Nicoletti, C. (2017). The Multifaceted Personality of Intestinal Cx3cr1(+) Macrophages. Trends in immunology **38**(12): 879-887.

Reid, D. M., Montoya, M., Taylor, P. R., Borrow, P., Gordon, S., Brown, G. D. and Wong, S. Y. C. (2004). Expression of the B-Glucan Receptor, Dectin-1, on Murine Leukocytes in Situ Correlates with Its Function in Pathogen Recognition and Reveals Potential Roles in Leukocyte Interactions. J Leukoc Biol **76**(1): 86-94.

Remington, J., McLeod, R., Thulliez, P. and Desmonts, G. (2011). Toxoplasmosis. Infectious Diseases of the Fetus and Newborn Infant. K. G. Remington J, Wilson C, Baker C. Philadelphia, WB Saunders**:** 918-1041.

Remington, J. S. and Klein, J. O. (1983). Infectious Diseases of the Fetus and Newborn Infant, WB Saunders Company.

Reverberi, R. and Reverberi, L. (2007). Factors Affecting the Antigen-Antibody Reaction. Blood Transfus **5**(4): 227-240.

Revets, H., De Baetselier, P. and Muyldermans, S. (2005). Nanobodies as Novel Agents for Cancer Therapy. Expert Opinion on Biological Therapy **5**(1): 111-124.

Rezaei-Ghaleh, N., Amininasab, M. and Nemat-Gorgani, M. (2008). Conformational Changes of Alpha-Chymotrypsin in a Fibrillation-Promoting Condition: A Molecular Dynamics Study. Biophys J **95**(9): 4139-4147.

Rezaei, F., Sarvi, S., Sharif, M., Hejazi, S. H., Pagheh, A. S., Aghayan, S. A. and Daryani, A. (2019). A Systematic Review of *Toxoplasma Gondii* Antigens to Find the Best Vaccine Candidates for Immunization. Microb Pathog **126**: 172-184.

Rivers, J. P. W., Sinclair, A. J. and Crawford, M. A. (1975). Inability of the Cat to Desaturate Essential Fatty Acids. Nature **258**(5531): 171-173.

Romstad, A. B., Reitan, L. J., Midtlyng, P., Gravningen, K. and Evensen, Ø. (2013). Antibody Responses Correlate with Antigen Dose and in Vivo Protection for Oil-Adjuvanted, Experimental Furunculosis (*Aeromonas Salmonicida Subsp. Salmonicida*) Vaccines in Atlantic Salmon (*Salmo Salar* L.) and Can Be Used for Batch Potency Testing of Vaccines. Vaccine **31**(5): 791-796.

Rutishauser, U. and Sachs, L. (1975). Cell-to-Cell Binding Induced by Different Lectins. J Cell Biol **65**(2): 247-257.

Salman, D., Okuda, L. H., Ueno, A., Dautu, G., Zhang, F. and Igarashi, M. (2017). Evaluation of Novel Oocyst Wall Protein Candidates of *Toxoplasma Gondii*. Parasitology International **66**(5): 643-651.

Sancho, D., Joffre, O. P., Keller, A. M., Rogers, N. C., Martinez, D., Hernanz-Falcon, P., Rosewell, I. and Reis e Sousa, C. (2009). Identification of a Dendritic Cell Receptor That Couples Sensing of Necrosis to Immunity. Nature **458**(7240): 899-903.

Sanders, J. L., Zhou, Y., Moulton, H. M., Moulton, Z. X., McLeod, R., Dubey, J. P., Weiss, L. M. and Kent, M. L. (2015). The Zebrafish, *Danio Rerio*, as a Model for *Toxoplasma Gondii*: An Initial Description of Infection in Fish. J Fish Dis **38**(7): 675-679.

Santana, S. S., Gebrim, L. C., Carvalho, F. R., Barros, H. S., Barros, P. C., Pajuaba, A. C., Messina, V., Possenti, A., Cherchi, S., Reiche, E. M., Navarro, I. T., Garcia, J. L., Pozio, E., Mineo, T. W., Spano, F. and Mineo, J. R. (2015). Ccp5a Protein from *Toxoplasma Gondii* as a Serological Marker of Oocyst-Driven Infections in Humans and Domestic Animals. Front Microbiol **6**: 1305-1305.

Santos-Medellín, C., Edwards, J., Liechty, Z., Nguyen, B. and Sundaresan, V. (2017). Drought Stress Results in a Compartment-Specific Restructuring of the Rice Root-Associated Microbiomes. mBio **8**(4).

Sasaki, K., Christov, N. K., Tsuda, S. and Imai, R. (2013). Identification of a Novel Lea Protein Involved in Freezing Tolerance in Wheat. Plant and Cell Physiology **55**(1): 136-147.

Saucedo, A. L., Hernández-Domínguez, E. E., de Luna-Valdez, L. A., Guevara-García, A. A., Escobedo-Moratilla, A., Bojorquéz-Velázquez, E., del Río-Portilla, F., Fernández-Velasco, D. A. and Barba de la Rosa, A. P. (2017). Insights on Structure and Function of a Late Embryogenesis Abundant Protein from Amaranthus Cruentus: An Intrinsically Disordered Protein Involved in Protection against Desiccation, Oxidant Conditions, and Osmotic Stress. Front Plant Sci **8**(497).

Schares, G., Koethe, M., Bangoura, B., Geuthner, A. C., Randau, F., Ludewig, M., Maksimov, P., Sens, M., Bärwald, A., Conraths, F. J., Villena, I., Aubert, D., Opsteegh, M. and Van der Giessen, J. (2018). *Toxoplasma Gondii* Infections in Chickens – Performance of Various Antibody Detection Techniques in Serum and Meat Juice Relative to Bioassay and DNA Detection Methods. International Journal for Parasitology **48**(9): 751-762.

Schmidt, M., Sonneville, R., Schnell, D., Bigé, N., Hamidfar, R., Mongardon, N., Castelain, V., Razazi, K., Marty, A., Vincent, F., Dres, M., Gaudry, S., Luyt, C. E., Das, V., Micol, J. B., Demoule, A. and Mayaux, J. (2013). Clinical Features and Outcomes in Patients with Disseminated Toxoplasmosis Admitted to Intensive Care: A Multicenter Study. Clin Infect Dis **57**(11): 1535-1541.

Schofield, L. (1991). On the Function of Repetitive Domains in Protein Antigens of *Plasmodium* and Other Eukaryotic Parasites. Parasitology Today **7**(5): 99-105.

Schoonooghe, S., Laoui, D., Van Ginderachter, J. A., Devoogdt, N., Lahoutte, T., De Baetselier, P. and Raes, G. (2012). Novel Applications of Nanobodies for in Vivo Bio-Imaging of Inflamed Tissues in Inflammatory Diseases and Cancer. Immunobiology **217**(12): 1266-1272.

Schulz, O., Hanč, P., Böttcher, J. P., Hoogeboom, R., Diebold, S. S., Tolar, P. and Reis e Sousa, C. (2018). Myosin Ii Synergizes with F-Actin to Promote Dngr-1-Dependent Cross-Presentation of Dead Cell-Associated Antigens. Cell Rep **24**(2): 419-428.

Sela, M. (1998). Antigens. Encyclopedia of Immunology (Second Edition). P. J. Delves. Oxford, Elsevier**:** 201-207.

Shapiro, K., Bahia-Oliveira, L., Dixon, B., Dumètre, A., de Wit, L. A., VanWormer, E. and Villena, I. (2019). Environmental Transmission of *Toxoplasma Gondii*: Oocysts in Water, Soil and Food. Food and Waterborne Parasitology: e00049.

Shapiro, K., Mazet, J. A. K., Schriewer, A., Wuertz, S., Fritz, H., Miller, W. A., Largier, J. and Conrad, P. A. (2010). Detection of *Toxoplasma Gondii* Oocysts and Surrogate Microspheres in Water Using Ultrafiltration and Capsule Filtration. Water Research **44**(3): 893-903.

Shiraki, K., Nishikawa, K. and Goto, Y. (1995). Trifluoroethanol-Induced Stabilization of the A-Helical Structure of B-Lactoglobulin: Implication for Non-Hierarchical Protein Folding. Journal of Molecular Biology **245**(2): 180-194.

Sinclair, A. J., McLean, J. G. and Monger, E. A. (1979). Metabolism of Linoleic Acid in the Cat. Lipids **14**(11): 932-936.

Smith, G. P. (1985). Filamentous Fusion Phage: Novel Expression Vectors That Display Cloned Antigens on the Virion Surface. Science **228**(4705): 1315-1317.

Sokol, S. L., Wong, Z. S., Boyle, J. P. and Dubey, J. P. (2020). Generation of *Toxoplasma Gondii* and *Hammondia Hammondi* Oocysts and Purification of Their Sporozoites for Downstream Manipulation. Methods in molecular biology **2071**: 81-98.

Sousa, S., Almeida, A., Delgado, L., Conceição, A., Marques, C., da Costa, J. M. C. and Castro, A. (2020). Rtgowp1-F, a Specific Biomarker for *Toxoplasma Gondii* Oocysts. Scientific Reports **10**(1): 7947.

Speer, C. A., Clark, S. and Dubey, J. P. (1998). Ultrastructure of the Oocysts, Sporocysts, and Sporozoites of *Toxoplasma Gondii*. The Journal of parasitology **84**(3): 505-512.

Speer, C. A. and Dubey, J. P. (1998). Ultrastructure of Early Stages of Infections in Mice Fed *Toxoplasma Gondii* Oocysts. Parasitology **116 (Pt 1**: 35-42.

Sun, T., Chance, R. R., Graessley, W. W. and Lohse, D. J. (2004). A Study of the Separation Principle in Size Exclusion Chromatography. Macromolecules **37**(11): 4304-4312.

Suzuki-Inoue, K., Fuller, G. L., García, A., Eble, J. A., Pöhlmann, S., Inoue, O., Gartner, T. K., Hughan, S. C., Pearce, A. C., Laing, G. D., Theakston, R. D., Schweighoffer, E., Zitzmann, N., Morita, T., Tybulewicz, V. L., Ozaki, Y. and Watson, S. P. (2006). A Novel Syk-Dependent Mechanism of Platelet Activation by the C-Type Lectin Receptor Clec-2. Blood **107**(2): 542-549.

Tapia, H. and Koshland, Douglas E. (2014). Trehalose Is a Versatile and Long-Lived Chaperone for Desiccation Tolerance. Current Biology **24**(23): 2758-2766.

Tapia, H., Young, L., Fox, D., Bertozzi, C. R. and Koshland, D. (2015). Increasing Intracellular Trehalose Is Sufficient to Confer Desiccation Tolerance to *Saccharomyces Cerevisiae*. Proceedings of the National Academy of Sciences **112**(19): 6122-6127.

Tarbier, M., Mackowiak, S. D., Frade, J., Catuara-Solarz, S., Biryukova, I., Gelali, E., Menéndez, D. B., Zapata, L., Ossowski, S., Bienko, M., Gallant, C. J. and Friedländer, M. R. (2020). Nuclear Gene Proximity and Protein Interactions Shape Transcript Covariations in Mammalian Single Cells. Nature communications **11**(1): 5445.

Tenter, A., Seineke, P., Simon, K., Heckerozh, A., Damriyasa, I., Bauer, C. and Zahner, H. (1999). Aktuelle Studien Zur Epidemiologie Von *Toxoplasma*-Infektionen. Proc. German Vet. Med. Soc: 247-264.

Tenter, A. M., Heckeroth, A. R. and Weiss, L. M. (2000). *Toxoplasma Gondii*: From Animals to Humans. International journal for parasitology **30**(12-13): 1217-1258.

Thalhammer, A., Bryant, G., Sulpice, R. and Hincha, D. K. (2014). Disordered Cold Regulated15 Proteins Protect Chloroplast Membranes During Freezing through Binding and Folding, but Do Not Stabilize Chloroplast Enzymes in Vivo. Plant Physiology **166**(1): 190-201.

Tone, K., Stappers, M. H. T., Willment, J. A. and Brown, G. D. (2019). C-Type Lectin Receptors of the Dectin-1 Cluster: Physiological Roles and Involvement in Disease. European journal of immunology **49**(12): 2127-2133.

Tunnacliffe, A. and Wise, M. J. (2007). The Continuing Conundrum of the Lea Proteins. Naturwissenschaften **94**(10): 791-812.

Uemori, T., Shimojo, T., Asada, K., Asano, T., Kimizuka, F., Kato, I., Maki, M., Hatanaka, M., Murachi, T., Hanzawa, H. and Arata, Y. (1990). Characterization of a Functional Domain of Human Calpastatin. Biochemical and Biophysical Research Communications **166**(3): 1485-1493.

Uversky, V. N. (2002). Natively Unfolded Proteins: A Point Where Biology Waits for Physics. Protein Sci **11**(4): 739-756.

Uversky, V. N. (2019). Intrinsically Disordered Proteins and Their “Mysterious” (Meta)Physics. Frontiers in Physics **7**(10).

van der Lee, R., Buljan, M., Lang, B., Weatheritt, R. J., Daughdrill, G. W., Dunker, A. K., Fuxreiter, M., Gough, J., Gsponer, J., Jones, D. T., Kim, P. M., Kriwacki, R. W., Oldfield, C. J., Pappu, R. V., Tompa, P., Uversky, V. N., Wright, P. E. and Babu, M. M. (2014). Classification of Intrinsically Disordered Regions and Proteins. Chem Rev **114**(13): 6589-6631.

Van Knapen, F., Kremers, A., Franchimont, J. and Narucka, U. (1995). Prevalence of Antibodies to *Toxoplasma Gondii* in Cattle and Swine in the Netherlands: Towards an Integrated Control of Livestock Production. Veterinary Quarterly **17**(3): 87-91.

Vanlandschoot, P., Stortelers, C., Beirnaert, E., Ibanez, L. I., Schepens, B., Depla, E. and Saelens, X. (2011). Nanobodies(R): New Ammunition to Battle Viruses. Antiviral Res **92**(3): 389-407.

VanWormer, E., Fritz, H., Shapiro, K., Mazet, J. A. K. and Conrad, P. A. (2013). Molecules to Modeling: *Toxoplasma Gondii* Oocysts at the Human–Animal–Environment Interface. Comparative Immunology, Microbiology and Infectious Diseases **36**(3): 217-231.

Vartdal, F., Vandvik, B. and Lea, T. (1986). Immunofluorescence Staining of Agarose-Embedded Cells: A New Technique Developed for Immunological Characterization of Markers on a Small Number of Cells. Journal of Immunological Methods **92**(1): 125-129.

Vieira, F. P., Alves, M. d. G., Martins, L. M., Rangel, A. L. P., Dubey, J. P., Hill, D. and Bahia-Oliveira, L. M. G. (2015). Waterborne Toxoplasmosis Investigated and Analysed under Hydrogeological Assessment: New Data and Perspectives for Further Research. Memorias do Instituto Oswaldo Cruz **110**(7): 929-935.

Vu Manh, T. P., Bertho, N., Hosmalin, A., Schwartz-Cornil, I. and Dalod, M. (2015). Investigating Evolutionary Conservation of Dendritic Cell Subset Identity and Functions. Front Immunol **6**: 260.

Wadhawan, A., Hill, D. E., Dagdag, A., Mohyuddin, H., Donnelly, P., Jones, J. L. and Postolache, T. T. (2018). No Evidence for Airborne Transmission of *Toxoplasma Gondii* in a Very High Prevalence Area in Lancaster County. Pteridines **29**(1): 172.

Wadman, M. (2019). Closure of U.S. *Toxoplasma* Lab Draws Ire. Science **364**(6436): 109.

Wagener, M., Hoving, J. C., Ndlovu, H. and Marakalala, M. J. (2018). Dectin-1-Syk-Card9 Signaling Pathway in Tb Immunity. Front Immunol **9**: 225.

Walker, R. (1985). The Use of Lectins in Histopathology. Histopathology **9**(10): 1121-1124.

Wang, Y., Hedman, L., Perdomo, M. F., Elfaitouri, A., Bölin-Wiener, A., Kumar, A., Lappalainen, M., Söderlund-Venermo, M., Blomberg, J. and Hedman, K. (2016). Microsphere-Based Antibody Assays for Human Parvovirus B19v, Cmv and *T. Gondii*. BMC Infect Dis **16**: 8-8.

Wang, Z.-X., Zhou, C.-X., Elsheikha, H. M., He, S., Zhou, D.-H. and Zhu, X.-Q. (2017). Proteomic Differences between Developmental Stages of *Toxoplasma Gondii* Revealed by Itraq-Based Quantitative Proteomics. Frontiers in Microbiology **8**(985).

Warner, A. H., Guo, Z.-h., Moshi, S., Hudson, J. W. and Kozarova, A. (2016). Study of Model Systems to Test the Potential Function of Artemia Group 1 Late Embryogenesis Abundant (Lea) Proteins. Cell Stress and Chaperones **21**(1): 139-154.

Watson, A. A., Eble, J. A. and O'Callaghan, C. A. (2008). Crystal Structure of Rhodocytin, a Ligand for the Platelet-Activating Receptor Clec-2. Protein Sci **17**(9): 1611-1616.

Wehland, J., Stockem, W. and Weber, K. (1978). Cytoplasmic Streaming in *Amoeba Proteus* Is Inhibited by the Actin-Specific Drug Phalloidin. Exp Cell Res **115**(2): 451-454.

Weiss, L. M. and Kim, K. (2020). *Toxoplasma Gondii*: The Model Apicomplexan-Perspectives and Methods, Academic Press.

Welch, G. R., Somogyi, B. and Damjanovich, S. (1982). The Role of Protein Fluctuations in Enzyme Action: A Review. Progress in Biophysics and Molecular Biology **39**: 109-146.

WHO (2017). The Burden of Foodborne Diseases in the Who European Region, WHO Regional Office for Europe.

Wilking, H., Thamm, M., Stark, K., Aebischer, T. and Seeber, F. (2016). Prevalence, Incidence Estimations, and Risk Factors of *Toxoplasma Gondii* Infection in Germany: A Representative, Cross-Sectional, Serological Study. Sci Rep **6**: 22551-22551.

Wise, M. J. and Tunnacliffe, A. (2004). Popp the Question: What Do Lea Proteins Do? Trends in Plant Science **9**(1): 13-17.

Wong, B. (2011). Points of View: Avoiding Color. Nat Methods **8**(7): 525.

Wright, P. E. and Dyson, H. J. (2015). Intrinsically Disordered Proteins in Cellular Signalling and Regulation. Nature Reviews Molecular Cell Biology **16**(1): 18-29.

Xia, N., Yang, J., Ye, S., Zhang, L., Zhou, Y., Zhao, J., David Sibley, L. and Shen, B. (2018). Functional Analysis of *Toxoplasma* Lactate Dehydrogenases Suggests Critical Roles of Lactate Fermentation for Parasite Growth in Vivo. Cell Microbiol **20**(1).

Xia, N., Zhou, T., Liang, X., Ye, S., Zhao, P., Yang, J., Zhou, Y., Zhao, J. and Shen, B. (2018). A Lactate Fermentation Mutant of *Toxoplasma* Stimulates Protective Immunity against Acute and Chronic Toxoplasmosis. Front Immunol **9**: 1814.

Xie, J., Dawwam, G. E., Sehim, A. E., Li, X., Wu, J., Chen, S. and Zhang, D. (2021). Drought Stress Triggers Shifts in the Root Microbial Community and Alters Functional Categories in the Microbial Gene Pool. Frontiers in Microbiology **12**(3066).

Xue, B., Dunker, A. K. and Uversky, V. N. (2012). Orderly Order in Protein Intrinsic Disorder Distribution: Disorder in 3500 Proteomes from Viruses and the Three Domains of Life. Journal of biomolecular structure & dynamics **30**(2): 137-149.

Yan, C., Liang, L.-J., Zheng, K.-Y. and Zhu, X.-Q. (2016). Impact of Environmental Factors on the Emergence, Transmission and Distribution of *Toxoplasma Gondii*. Parasites & vectors **9**: 137-137.

Yang, S. and Parmley, S. F. (1997). *Toxoplasma Gondii* Expresses Two Distinct Lactate Dehydrogenase Homologous Genes During Its Life Cycle in Intermediate Hosts. Gene **184**(1): 1-12.

Yilmaz, S. M. and Hopkins, S. H. (1972). Effects of Different Conditions on Duration of Infectivity of *Toxoplasma Gondii* Oocysts. J Parasitol **58**(5): 938-939.

Yoshida, N., Domart, M. C., Peddie, C. J., Yakimovich, A., Mazon-Moya, M. J., Hawkins, T. A., Collinson, L., Mercer, J., Frickel, E. M. and Mostowy, S. (2020). The Zebrafish as a Novel

Model for the in Vivo Study of *Toxoplasma Gondii* Replication and Interaction with Macrophages. Dis Model Mech **13**(7).

Yu, Y., Zhang, H. and Zhu, G. (2010). Plant-Type Trehalose Synthetic Pathway in *Cryptosporidium* and Some Other Apicomplexans. PLOS ONE **5**(9): e12593.

Zelenay, S., Keller, A. M., Whitney, P. G., Schraml, B. U., Deddouche, S., Rogers, N. C., Schulz, O., Sancho, D. and Reis e Sousa, C. (2012). The Dendritic Cell Receptor Dngr-1 Controls Endocytic Handling of Necrotic Cell Antigens to Favor Cross-Priming of Ctls in Virus-Infected Mice. J Clin Invest **122**(5): 1615-1627.

Zhai, C., Lan, J., Wang, H., Li, L., Cheng, X. and Liu, G. (2011). Rice Dehydrin K-Segments Have in Vitro Antibacterial Activity. Biochemistry (Mosc) **76**(6): 645-650.

Zhang, J. G., Czabotar, P. E., Policheni, A. N., Caminschi, I., Wan, S. S., Kitsoulis, S., Tullett, K. M., Robin, A. Y., Brammananth, R., van Delft, M. F., Lu, J., O'Reilly, L. A., Josefsson, E. C., Kile, B. T., Chin, W. J., Mintern, J. D., Olshina, M. A., Wong, W., Baum, J., Wright, M. D., Huang, D. C., Mohandas, N., Coppel, R. L., Colman, P. M., Nicola, N. A., Shortman, K. and Lahoud, M. H. (2012). The Dendritic Cell Receptor Clec9a Binds Damaged Cells Via Exposed Actin Filaments. Immunity **36**(4): 646-657.

Zhang, L., Ohta, A., Takagi, M. and Imai, R. (2000). Expression of Plant Group 2 and Group 3 Lea Genes in *Saccharomyces Cerevisiae* Revealed Functional Divergence among Lea Proteins. Journal of biochemistry **127**(4): 611-616.

Zhang, Y., Werling, U. and Edelmann, W. (2014). Seamless Ligation Cloning Extract (Slice) Cloning Method. Methods in molecular biology (Clifton, N.J.) **1116**: 235-244.

Zhou, D. H., Wang, Z. X., Zhou, C. X., He, S., Elsheikha, H. M. and Zhu, X. Q. (2017). Comparative Proteomic Analysis of Virulent and Avirulent Strains of *Toxoplasma Gondii* Reveals Strain-Specific Patterns. Oncotarget **8**(46): 80481-80491.

Zucca, P., Fernandez-Lafuente, R. and Sanjust, E. (2016). Agarose and Its Derivatives as Supports for Enzyme Immobilization. Molecules **21**(11): 1577.

Zulpo, D. L., Sammi, A. S., dos Santos, J. R., Sasse, J. P., Martins, T. A., Minutti, A. F., Cardim, S. T., de Barros, L. D., Navarro, I. T. and Garcia, J. L. (2018). *Toxoplasma Gondii*: A Study of Oocyst Re-Shedding in Domestic Cats. Veterinary Parasitology **249**(51): 17-20.

Acknowledgements

First and foremost, I'd like to thank Prof. Lothar H. Wieler for providing me with the opportunity work within the German One Health Initiative at the Robert Koch-Institute on this exciting topic.

Next, my thanks go to Toni Aebischer and all staff of Unit 16 and junior group 2 at the RKI. It was a pleasure to work with you, discuss and learn from you. Always friendly and inspiring, never boring. I'll always look back happily on my time with you.

Prof. Frank Seeber deserves a special thank you for his supervision, his ongoing support, scientific input and his patience. He managed to keep me critical and curious and nudge me in the right direction when needed. So, thank you Frank, for helping me on this journey. You've taught me a lot!

I thank Prof. Monika Hilker from the Dahlem Centre for Plant Sciences at the Freie Universität Berlin for being my 2nd supervisor and her valuable scientific support during this dissertation.

I'd also like to thank Dr. Gereon Schares and all colleagues in his group at the Friedrich Loeffler-Institute in Greifswald for his extensive support and scientific input!

The next, big THANK YOU is addressed to the RTG2046 for allowing me to be associated with my project. Without it, I would have missed out on some of the most significant scientific experiences of my career. The things I learned and especially the friends I made, I'll always cherish.

Furthermore, I'd like to thank the following people (in no particular order), without whom the presented thesis would not have been possible: JP Dubey, Bernd Lepenies, Furio Spano, Aurelien Dumetre, David Ferguson, Jonnel Jaurigue, Oren Moscovitz, Andreas Rummel, Totta Ehret, Celine Christiansen, Francesca Torelli, Stephanie Henkel and Deborah Maus.

I thank my family for their continuous support and belief in me.

And lastly but most importantly, I'd like to thank Sabrina. You truly are my resting place. Thank you!

Selbstständigkeitserklärung

Hiermit erkläre ich, dass ich die vorliegende Doktorarbeit selbstständig verfasst und keine anderen als die angegebenen Quellen und Hilfsmittel benutzt habe. Ich erkläre ausdrücklich, dass ich sämtliche in der oben genannten Arbeit enthaltenen Bezüge auf fremde Quellen (einschließlich Tabellen, Grafiken u. Ä.) nach bestem Wissen als solche kenntlich gemacht habe.

Berlin, den 17. Dezember 2021

_____

Benedikt Fabian